CEREAL NON-STARCH POLYSACCHARIDE DEGRADATION BY DIETARY ENZYMES IN BROILERS

DIMITRIOS KOUZOUNIS

Propositions

1. Establishing beneficial effects of dietary non-starch polysaccharide-active enzymes for animal growth requires the characterization of their degradation products formed *in vivo*.

   (this thesis)

2. Xylanase-mediated stimulation of fiber fermentation contributes to sustainable poultry nutrition.

   (this thesis)

3. Meat analogues are a "green" trojan horse serving the perpetuation of an unhealthy lifestyle.

4. The slogan "stay home, stay safe" launched during intervention campaigns to combat COVID-19 presents a myopic view of safety.

   (Mazza et al., Psychiatry Research, 2020; 289: 113046)

5. The metaverse will radically change internationalization in higher education.

6. Lab work is often considered to require strict orchestration, as practiced in classical music, while in fact it resembles more jazz and the blues.

Propositions belonging to the thesis, entitled:

Cereal non-starch polysaccharide degradation by dietary enzymes in broilers

Dimitrios Kouzounis

Wageningen, 16 September 2022

Cereal non-starch polysaccharide degradation by dietary enzymes in broilers

Dimitrios Kouzounis

Thesis committee

Promotor
Prof. Dr H.A. Schols
Personal chair at the Laboratory of Food Chemistry
Wageningen University & Research

Co-promotor
Dr M.A. Kabel
Associate professor, Laboratory of Food Chemistry
Wageningen University & Research

Other members
Prof. Dr C.M. Courtin, Katholieke Universiteit Leuven, Belgium
Prof. Dr H.-G. Jansen, Wageningen University & Research
Dr F.J. Vilaplana Domingo, Royal Institute of Technology, Sweden
Dr S. de Vries, Wageningen University & Research

Cereal non-starch polysaccharide degradation by dietary enzymes in broilers

Dimitrios Kouzounis

To my family.

Abstract

Our understanding of the role of cereal non-starch polysaccharides (NSP) in animal nutrition has drastically improved in the past decades. Moreover, the necessary shift to more sustainable, antibiotic-free animal production stresses the need for harnessing the full potential of NSPs in feed. Hereto, feed supplementation with NSP-degrading enzymes has been a successful strategy to offset the anti-nutritive effect of NSP, leading to improved broiler performance. Although enzyme supplementation has been linked with improved nutrient digestibility and fiber fermentability, the underlying mechanisms of action were not clear yet. Therefore, this PhD thesis aims at further exploring, at a molecular level, the impact of enzyme supplementation on NSP structure and its implications for nutrient digestion and hindgut fermentation in broilers.

In this thesis, it was demonstrated that endo-xylanase and endo-glucanase supplementation improved the growth of broilers fed a wheat diet. This coincided with improved starch and protein digestibility, and with increased hindgut fermentation of arabinoxylan (AX) to short-chain fatty acids. Furthermore, *in vivo* AX degradation to arabinoxylo-oligosaccharides (AXOS) by dietary endo-xylanase was first demonstrated by MALDI-TOF-MS, for broilers fed a wheat diet. The complex maize AX structure most likely limited the impact of dietary enzymes in broilers fed a maize diet. The impact of cereal type and enzyme supplementation on NSP fermentation was highlighted by the different bacterial communities (beta diversity) residing in the ceca of broilers fed wheat-based and maize-based diets. The abundance of beneficial bacteria in wheat diets was partly associated with presence of fermentable AX and AXOS. AXOS formed *in vivo* by endo-xylanase, being relevant for hindgut fermentation, were isolated from digesta samples and further characterized by a currently developed analytical strategy to identify $NaBH_4$-reduced AXOS using hydrophilic-interaction liquid chromatography coupled to tandem mass spectrometry (HILIC-MS^n). This strategy was set-up with model AXOS isomers with a degree of polymerization of 3-7, separated in HILIC, and identified based on distinct MS^2 and MS^3 fragmentation patterns. It was determined that AX depolymerization began in the gizzard and that the xylanase-mediated release of readily fermentable, lowly-substituted AXOS proceeded in the small intestine and increased AX utilization in the hindgut. Lastly, determination of AX-to-lignin ratios in digesta suggested different transit patterns of insoluble, unfermented cereal cell wall fractions along the gastrointestinal tract. In particular, the associations between cell wall components appeared unaffected by dietary enzymes, suggesting that besides AXOS release, enzyme action might not promote nutrient digestion by further loosening the cell wall architecture. The present findings demonstrate that dietary enzymes improve NSP fermentation in broilers and contribute to the more complete utilization of the diet.

Table of contents

Chapter

1

General Introduction

1   Relevance of this research

The increase in meat consumption globally has, alongside the necessary shift to a more sustainable, antibiotic-free livestock production, placed the stakeholders under unprecedented strain. To address this, the development of new strategies enhancing feed utilization and livestock production has been undertaken. For instance, feed supplementation with enzymes degrading non-starch polysaccharides (NSP) has been introduced with success in poultry and swine nutrition. Such enzymes have been found to offset the anti-nutritive effect of NSP, leading to improved nutrient digestion in broilers. Additionally, enzymatic breakdown of NSP may further promote hindgut fermentation. Ultimately, NSP degrading enzymes are envisaged to function as natural growth promotors increasing the feeding efficiency of livestock. Although enzyme supplementation is common practice in animal nutrition, the underlying mechanisms of action have not been fully elucidated. Therefore, this PhD thesis research aimed at further exploring, at a molecular level, the impact of enzyme supplementation on NSP structure and its implications for nutrient digestion and hindgut fermentation in broilers.

2   Poultry production and nutrition in the 21st century

Poultry is widely consumed by humans due to its well-regarded nutritional profile (1). It is indicative that 92.7 million tons of poultry were produced globally in 2017 (2), following the upward trend in meat consumption observed in the past thirty years (3). The global poultry production is projected to increase to 103 million tons by 2021 to keep up with the soaring demand (2). Broilers (*Gallus gallus domesticus*) are the poultry intended for meat production and have been specifically bred to serve the consumption demands. With a population estimated at 22.7 billion, the broilers are considered a vivid example of human intervention in the biosphere (4). It is indicative that currently, broilers are four to five times larger than their ancestor, the red junglefowl, and broilers bred in 1957 (Fig. 1) (4–6).

Modern broilers are expected to increase approximately ten times in size until they reach their slaughter age, that being between 5 to 8 weeks (6,7). At the same time, genetic breeding of broilers has resulted in tremendous reduction in the feed conversion ratio in the past fifty years (6,8). This implies that contemporary broiler breeds can reach a desired weight, while consuming less feed. Such goal is of utmost importance as feed-related costs are the main source of expenses in broiler production (8). More importantly than cutting costs, reduction of the ecological and physical footprint of livestock production has become necessary, if not imperative, to curb its contribution to climate change (9,10). Cereal grains are the major feed ingredients, corresponding to 58% of the dry matter consumed by poultry (10). Therefore, enhancing broiler performance while reducing the amount of cereal consumed is integral for the cost-effective production and sustainability of poultry meat (8,10,11).
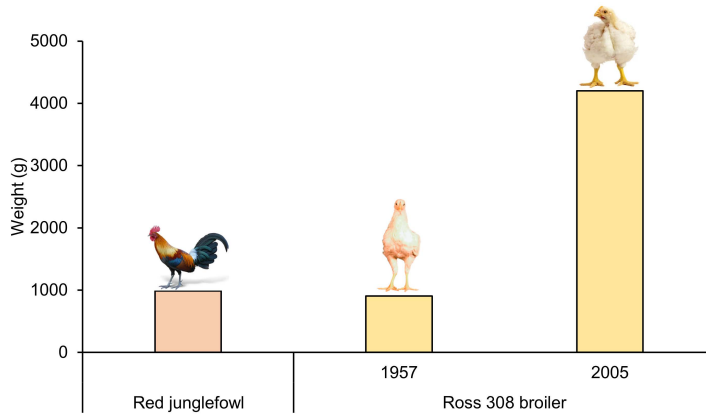
Fig. 1. Body weight (g) of adult Red junglefowl (i.e., ancestor of Ross broilers), and 56 days-old Ross 308 broilers from 1957 and 2005 (5,6).

3   Nutritional value of cereal grains for broilers

Cereal grains provide broilers with starch (Table 1), which accounts for approximately half of the metabolizable energy (12). Still, broilers require well-rounded diets providing the energy and nutrients needed to sustain their rapid growth (7). Next to starch, poultry diets typically include protein, fat, fiber, vitamins, calcium, phosphorus and other minerals, as well as water (13).

Wheat and maize are the main cereal grains used for broiler feed (11). Barley, oats, rye and sorghum can be used as well, depending on local availability (14,15). Apart from starch, cereal grains are also a considerable dietary source of protein as well as non-starch polysaccharides (NSP), the latter representing the main dietary fiber fraction of cereal.

Table 1. Digestible energy (MJ/kg dry matter (DM)), starch, protein and non-starch polysaccharides (NSP) content (% DM) of whole cereal grains used in poultry nutrition (Data from: 13,15–20).

Grain type	Digestible energy (MJ/kg)	Starch (% DM)	Protein[1] (% DM)	NSP (% DM)
Wheat *Triticum aestivum*	13.9	65.1	11.4	11.9
Maize *Zea mays*	16.9	69.0	8.5	9.7
Barley *Hordeum vulgare*	14.3	58.7	11.5	18.6
Oat *Avena sativa*	13.6	46.8	11.8	23.2
Rye *Secale cereale*	ND	61.3	12.0	14.7
Sorghum *Sorghum bicolor*	15.9	60.2	10.9[2]	5.4

[1]N conversion factor not specified. [2]% in grain (17)

3.1 **Starch**

Starch is the main form of dietary energy that is being used by broilers for muscle growth (21). Starch is a plant storage polysaccharide located in the endosperm of cereal grains, and comprises ~75% of the endosperm weight (15,22) (Fig. 2). Starch is composed of two glucans: amylose and amylopectin. Amylose is a linear polysaccharide and consists of α-(1→4)-linked D-glucosyl residues (23). Amylopectin is a branched glucan, with side-chains linked by α-(1→6) linkages to the α-(1→4) linked glucosyl (Glc) backbone (23). Typically, cereal starches contain 20-30% amylose and 70-80% amylopectin (24). Amylose and amylopectin are ordered into a supramolecular, semicrystalline structure within starch granules (23,24).
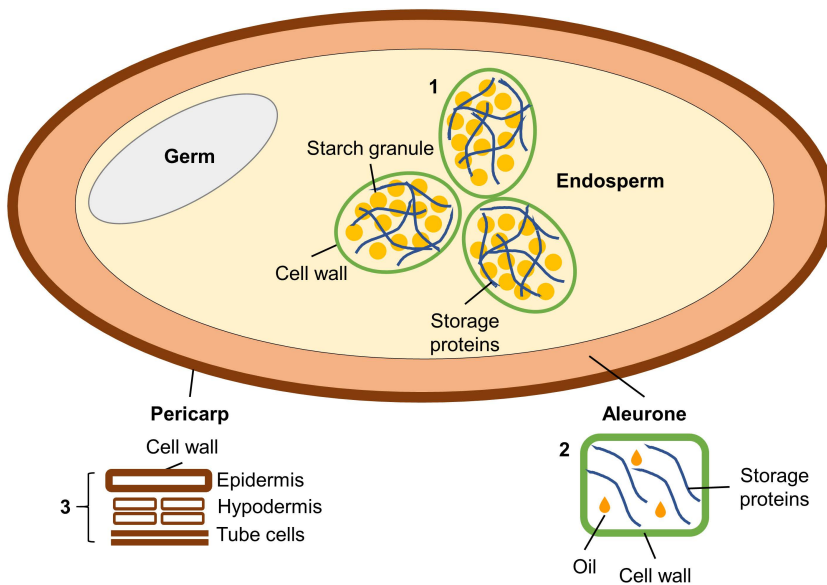
Fig. 2. Schematic overview of a wheat kernel, according to Burton & Fincher (2014), Tervilä-Wilo et al. (1996) and Belitz, Grosch & Schieberle (2009) (23,30,31). Cells from endosperm (**1**) and aleurone layer (**2**), and pericarp cell walls (**3**) are drawn out of proportion.

The specific starch properties, such as amylose *versus* amylopectin ratio, granule morphology and crystallinity differ between cereals and impact starch digestibility and physical properties (24,25). For example, isolated wheat starch was digested ~1.3 and ~2.2 times faster than barley and maize isolated starch, respectively, while all starches exhibited digestibility values above 75%, as reported during *in vitro* experiments (25,26). However, starch digestion *in vivo* is not only governed by aforementioned intrinsic starch properties, but by extrinsic factors as well (i.e., feed particle size and form, presence of anti-nutritive factors, (12,21)). Generally, starch digestibility above 94% is observed for broilers for the majority of cereals

fed (12). In spite of these high digestibility values, there is still a starch fraction that escapes digestion in the small intestine and is termed resistant starch (RS) (27). For instance, starch that is physically entrapped by the cell wall matrix, and therefore inaccessible to digestive enzymes, is termed RS type 1 (27). Fermentation of RS by gut microbiota in the hindgut can still provide energy to the animal, although to a lower degree than digestible starch (11,28). Therefore, improvement of starch digestibility (> 94%) through feed interventions is of major interest for livestock production (29).

3.2 Protein

Next to starch, cereal grains contain around 10% proteins (DM based; Table 1). Storage proteins like gliadins and glutelins in wheat and zein in maize are located primarily in the endosperm, but proteins may also be found in the aleurone tissues (Fig. 2) (32,33). The protein content is higher in endosperm cells closer to the aleurone layer than in cells closer to the center of the grain (33). It is accepted that inside the cells, storage proteins form a continuous, independent network that encloses other constituents, such as the starch granules (33).

Cereal proteins account for 25-40% of the total protein content in poultry diets (32). However, cereal proteins alone cannot provide all essential amino acids needed to sustain growth (34). Lysine is the main limiting amino acid across cereals, followed by threonine, tryptophan and methionine (32). For that reason, feed formulations typically combine cereal grains with legume seeds or their byproducts. For example, soybean meal is rich in lysine, and when combined with cereal proteins, can add up to a more complete amino acid profile for broilers (32).

3.3 Lipids, vitamins, minerals and phytochemicals

Cereal grains contain a low amount of lipids, primarily found in the germ and to a lesser degree in the aleurone layer (Fig. 2) (22,30). The lipid content in wheat is between 1-3%, while in maize it is higher, between 4-10% (DM basis) (34,35). Additionally, cereal grains contain B vitamins and minerals such as potassium, iron and zinc (34). More importantly, cereal grains contain calcium and phosphorus, with the latter being part of phytic acid. Both minerals are highly important for the skeletal and muscular growth of broilers (34,36). However, the amount and bioavailability of cereal-derived minerals is not sufficient, and diets are typically supplemented with minerals from other sources (36). Finally, cereals contain low amounts of bioactive phytochemicals, such as tocopherols and lignans (34).

4 Cereal cell wall components in broiler diets

Apart from the nutrients discussed above, cereal grains contain a significant amount of undigestible compounds mainly present in the cell walls (Fig. 2). Namely, the cereal cell walls are composed of three main macromolecule types: non-starch polysaccharides (NSP) lignin and proteins (30).

4.1 Non-starch polysaccharides (NSP) in cereal grains

Arabinoxylan

Arabinoxylan (AX) is the main NSP present in cereal grains (Table 2: 2% DM) and represents 64-70% of the cell wall dry matter (37). AX is a heteroxylan composed of a β-(1→4)-linked D-xylosyl (Xyl) backbone, mainly substituted by L-arabinofuranosyl (Ara) units at the *O*-2- and/or *O*-3-positions of the Xyl units (Fig. 3). Additional backbone substitution by 4-*O*-D-methyl-glucuronosyl and acetyl moieties may also occur, while Ara units might be further *O*-5-linked to feruloyl units (38,39). Particularly complex AX from maize and sorghum can present oligomeric Ara side chains, as well as Xyl and galactosyl residues (Gal) as decorations (38–40; Fig. 3).

The type, number and distribution of substituents over the xylan backbone in AX differs per type of cereal grain and type of grain tissues (37,42–44). In this thesis, we focus on the structure and properties of wheat and maize AX (Table 2), because of the high prevalence of wheat and maize in broiler nutrition. Wheat endosperm AX has a low degree of substitution (Fig. 3A), with approximately 66% of all Xyl residues being unsubstituted. Monosubstituted Xyl, mainly by *O*-3-linked Ara, account for 21%, while doubly substituted Xyl at both *O*-2 and *O*-3 account for 13% of total backbone Xyl residues. Albeit in low amounts, *O*-2-linked Ara may also be present (37,39,45). AX in the wheat aleurone and pericarp tissues is more heavily decorated by Ara (Ara/Xyl = 0.7) compared to endosperm AX (Ara/Xyl = 0.6), and is further substituted by 4-*O*-methyl-D-glucuronosyl, acetyl and/or feruloyl and coumaroyl units (37,39). Maize grains contain heavily substituted AX molecules, whose structural complexity is exemplified in Fig. 3B. In particular, maize AX exhibits a much higher Ara/Xyl-ratio than wheat AX (1.1 *vs* 0.6) in the endosperm. Moreover, AX from maize bran comprises a higher number of ferulic acid (FA) and glucuronic acid (GlcA) substituents, as judged from the higher FA (2% *vs* 0.6% DM) and GlcA (4% *vs* 3% DM) contents compared to AX originating from wheat bran (Table 2).

Table 2. Main cell wall components and chemical characteristics of arabinoxylan (AX) in endosperm and bran of wheat and maize grains (15,37,46–50). Values are expressed on DM basis of the endosperm or bran, unless stated otherwise.

Cell wall component	Wheat		Maize	
(% DM)	Endosperm	Bran[3]	Endosperm	Bran
AX	2	23	1	21
Cellulose	0.3	29	0	23
Klason lignin	N.A.[2]	7	0.4	3
Ferulic acid	<0.01	0.6	0.4	2
Glucuronic acid	N.A.	3[4]	N.A.	4
AX-structural features				
Ratio Ara/Xyl[1]	0.6	0.7	1.1	0.7

[1]Ara/ Xyl ratio in mol. [2]Data not available. [3]Includes aleurone and pericarp. [4]Determined as total uronic acids (50).

AX structural features, such as the degree of substitution and the distribution of Ara branches over the Xyl backbone, greatly determine its physicochemical properties (39,51). For instance, soluble AX populations account for 21% of AX in wheat endosperm and exhibit an average Mw of 300 kDa and an Ara/Xyl ratio of 0.5 (37,45). When present in solution, AX generally increases the viscosity (37,39). In comparison, water insoluble AX populations from wheat endosperm and bran typically exhibit higher Mw and a broader degree of Ara-substitution (Ara/Xyl: 0.5-0.8) than soluble AX (37,44,50,52). These structural differences, in addition to association with other cell wall components all contribute to the insolubility of these AX populations (37,51,53). The influence of AX structure and physicochemical properties like viscosity and solubility on nutrient digestion, fermentation and susceptibility by enzymes will be discussed in the following sections.

Fig. 3. Typical structural motifs (including glycosidic linkages) (**A**) of cereal heteroxylans. Proposed structural models (**B**) for water-insoluble wheat endosperm AX (44) and maize bran AX (40).

Cellulose

Cellulose is a β-(1→4)-linked D-glucan composed of 6000-14000 Glc units, and is considered as the most abundant biopolymer on earth (54,55). Nevertheless, cellulose is only present at low quantities in cereal endosperm (<0.3% DM) and aleurone (3% DM), while it is more abundant in bran cell walls (23-29%; Table 2) (15,30,56,57). Cellulose is self-assembled into microfibrils that act as scaffold for the organization of other plant cell wall constituents (54,55).

Other NSP

Apart from AX and cellulose, other NSP are minorly present in cereal grains. Of these, β-glucan (BG) stands out. BG is a β-(1→3,1→4)-linked D-glucan that is

highly abundant in barley and oat grains (4-10% DM), but is present to a lesser extent in wheat and maize grains (0.5-2% DM) (15,56). Glucomannan, xyloglucan and pectin are considered minor cereal polysaccharides and account for less than 7% of total cell wall NSP (15,56). Additionally, β-D-fructans are soluble carbohydrates present in cereals in variable amounts (56). For instance, the fructan content in wheat and maize grains is approximately 2% and 0.2% DM, respectively (16).

4.2   Lignin and cell wall proteins

Next to carbohydrates, cereal cell walls are also composed of lignin and proteins. Lignin is an alkyl-aromatic polymer composed of aromatic monomers that is integral for the function of xylem in plants (58). Lignin is only present in low amounts in cereal grains (< 2% DM) (15). It is mainly found in the pericarp, where it contributes to the rigidity and strength of the cell wall and accounts for 3-10% DM of the bran (15,50,56,58,59).

In contrast to storage proteins present inside the endosperm and aleurone cells (see 3.2), (glyco)proteins can also be present in the cell wall and account for less than 10% of its dry matter (54,56). They consist of diverse molecules that have signaling function (arabinogalactan proteins) or can form an independent network, thus contributing to the cell wall architecture (54,56).

4.3   The cereal cell wall matrix

The different cell wall components discussed in 3.1 and 3.2 associate via covalent and non-covalent interactions into a three-dimensional matrix, whose main role is to provide the plant cells with structural integrity (30,54,60). The four main macrostructures involved are presented in Fig. 4 and are: the cellulose microfibril scaffold, the protein network, the lignin network (if present) and the hemicellulose (i.e., majorly AX) matrix (54). It should be noted that lignin is not found in primary cell walls present in the endosperm, but is a structural component of secondary cell walls found in the bran (Fig. 4) (61,62).

AX molecules can associate with each other non-covalently via hydrogen bonds by the formation of junction zones (Fig. 4) (54). Moreover, AX can associate by hydrogen bonding with cellulose fibrils (54). Covalent cross-links can occur between AX polymers, between AX and lignin, between AX and protein as well as between lignin and protein (53,54). AX polymers can be covalently linked with each other mainly by dehydrodiferulate cross-links (54). Additionally, AX-lignin interactions have been suggested to occur via ester-ether ferulate and diferulate bridges, as well as direct ester linkages involving uronic acids (53). Therefore, AX plays an important role in tethering the cell wall matrix of cereals (54). The cell wall shaped by aforementioned interactions encapsulates nutrients needed for plant growth (Fig. 2) (63,64). Consequently, the cell wall may pose a barrier for nutrient digestion in broilers (11,15,65). In other words, the complex cell wall

architecture might influence digestive enzyme efficiency and can be expected to determine NSP recalcitrance to NSP-active enzymes.
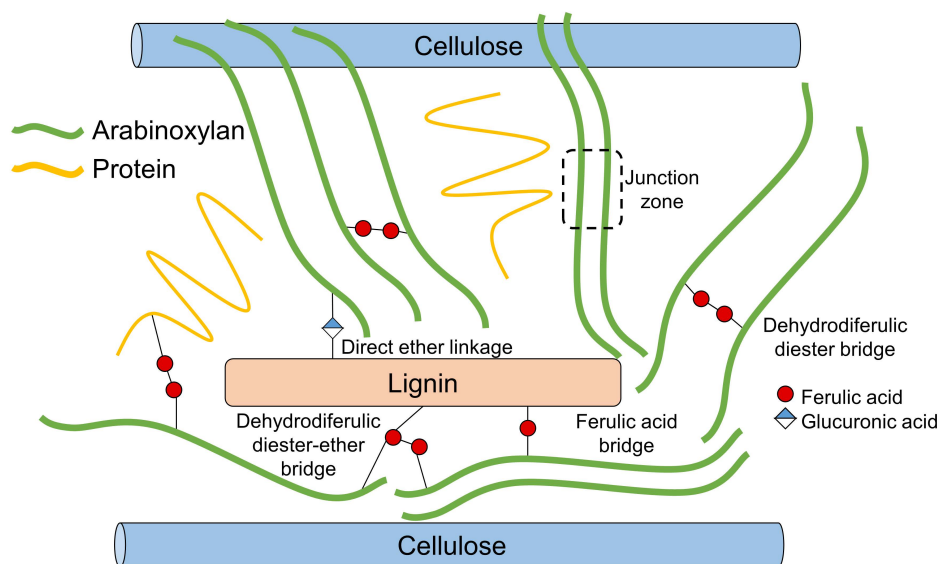

Fig. 4. Schematic representation of covalent and non-covalent interactions between plant cell wall components in secondary cell walls of monocots, including grasses, according to Iiyama, Lam & Stone (1994) and Harris & Stone (2008) (53,54).

5   Legumes and legume NSP in feed formulations

As mentioned in the above text, cereal-based diets require supplementation of an additional protein source in order to provide broilers with a well-rounded diet. Legume seeds and their by-products are used as main protein sources for poultry. Among these, soybean (*Glycine max*) stands out as the most used protein source (32). Usually, defatted soybean meal (SBM) contain 44-48% protein (32). Next to protein, SBM contains about 15-21% NSP, predominantly pectin that accounts for more than 60% of the total NSP in SBM (15,66). The main chelating agent-extractable soy pectins are described as rhamnogalacturonan with arabinan and arabinogalactan side-chains as well as xylogalacturonan (67). Additionally, SBM contains low amounts of xyloglucan (< 2%) and cellulose (< 3 %) (67). It is worth mentioning that soybean hull contains acetylated pectin and xylan (15). Finally, SBM contains considerable amounts of sucrose (5% DM) and non-digestible raffinose-family oligosaccharides (6% DM) (66). Overall, cereal-soybean feed formulations contain a complex and diverse carbohydrate profile. NSP influence on nutrient digestion by poultry, as well as NSP manipulation by enzyme supplementation will be elaborated in the following sections.

6   Feed digestion and fermentation in poultry

6.1   The avian gastrointestinal tract

Poultry are omnivores and, therefore, have a versatile digestive system able to adapt to different diets (Fig. 5) (68). The gastrointestinal tract (GIT) of broilers is tasked with handling large quantities of grain-based diets daily, sometimes as high as 10% of the bird's body weight (69).
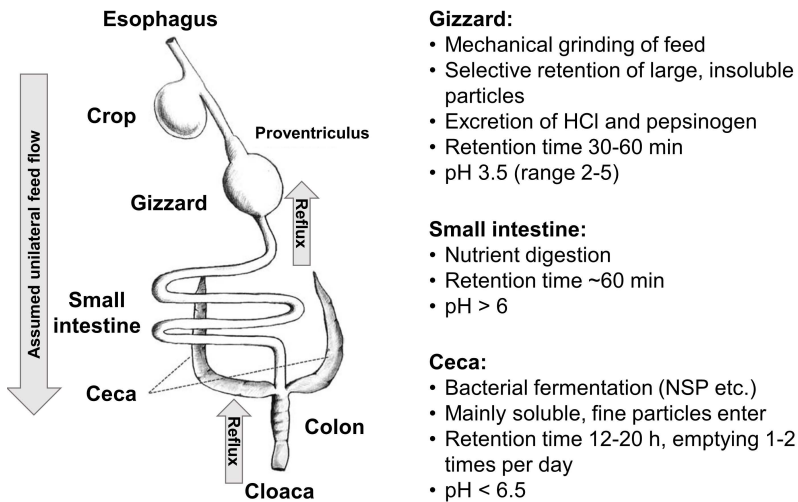

Gizzard:
- Mechanical grinding of feed
- Selective retention of large, insoluble particles
- Excretion of HCl and pepsinogen
- Retention time 30-60 min
- pH 3.5 (range 2-5)

Small intestine:
- Nutrient digestion
- Retention time ~60 min
- pH > 6

Ceca:
- Bacterial fermentation (NSP etc.)
- Mainly soluble, fine particles enter
- Retention time 12-20 h, emptying 1-2 times per day
- pH < 6.5

Fig. 5. Schematic overview of the avian digestive tract (70) and main characteristics of principal digestive organs (69).

Upon ingestion, feed components enter the crop where they are being moisturized before moving along the GIT. Nevertheless, when chicken are fed *ad libitum*, which means that they have free access to feed, the crop is essentially by-passed (69). Next, feed passes rapidly through the proventriculus (chemical stomach) where it is coated with hydrochloric acid and pepsinogen, ending up in the gizzard (mechanical stomach) (71,72). The main function of the gizzard is to reduce feed particle size by grinding, and to regulate feed flow (72). In specific, coarse, insoluble feed particles are selectively retained in this organ, to be ground down to smaller, more easily digestible ones (69,73).

Following gastric digestion, feed components are being released in the small intestine. Although usually a unilateral digesta flow is assumed, gastroduodenal reflux can occur at the gizzard-duodenal junction (74). Nutrient digestion (starch, protein, lipid) takes place in the proximal part of the small intestine (i.e., duodenum, jejunum) accompanied by a rapid elevation of pH value (pH > 6) and the secretion of pancreatic enzymes. Nutrient absorption and digestion continues until the distal part of the small intestine, the ileum. As an indication, more than

93% of starch, 78% of protein and 80% of lipids, accounting for more than 70% of energy provided, are being digested in the broiler small intestine (75,76).

Nutrients escaping digestion and non-digestible feed components (i.e., NSP) reach the hindgut (i.e., ceca, colon). To some extent, insoluble material is refluxed in the ileum via the ileocecal junction (77). Furthermore, soluble and insoluble components reach the cloaca, where they are separated. Soluble molecules and fine particles can enter the ceca via antiperistalsis, while the insoluble fraction will be excreted (77–79). Components entering the ceca are being fermented by gut microbiota to short chain fatty acids (SCFAs) (69,79).

6.2 The importance of cereal NSP in poultry nutrition

NSP are intrinsic feed components that are not digestible by poultry due to the lack of the necessary enzymes. Although indigestible, NSP are far from inert and play important roles during feed digestion by acting as anti-nutritive factors, stimulating grinding in the gizzard and acting as substrates for hindgut fermentation.

NSP as anti-nutritive factors

NSP are widely regarded as anti-nutritional factors for poultry (65,80). The anti-nutritive effect of soluble NSP (i.e., AX, β-glucan) has been attributed to their ability to increase digesta viscosity, thereby limiting the diffusion of digestive enzymes and nutrients (81–84). Additionally, swelling of insoluble cell wall material due to water adsorption can also contribute to elevated viscosity (85). As a consequence of impaired digestion and longer retention of nutrients, increased digesta viscosity has been related to pathogen growth in the small intestine (81,86,87). Another anti-nutritive effect of insoluble cell wall components such as NSP (i.e. AX, cellulose) and lignin, relates to their ability to encapsulate nutrients, rendering these nutrients less accessible to digestive enzymes (65,88).

Gizzard stimulation by insoluble fiber

Despite their potential anti-nutritive effects, NSP have also been indicated to play a beneficial role in poultry nutrition. Several studies showed that inclusion of whole wheat, oat hulls and wood shavings increased feed retention and grinding activity in the gizzard, which was associated with improved nutrient digestibility (72,89,90). Overall, feeding of coarse fibers > 1 mm and at relatively high inclusion levels (above 5%) has been recently reviewed to be advantageous for broiler growth (91).

The role of dietary carbohydrates in hindgut fermentation

A second beneficial role for NSP relates to their fermentation by potentially health-promoting gut bacteria. As mentioned in 6.1, mainly soluble feed components and a minor fraction of small particles can enter the ceca were they can be fermented by bacteria to short chain fatty acids (SCFAs) (77–79,92). Examples of feed-derived, fermentable carbohydrates are: resistant starch, partially digested

maltodextrins, various raffinose-family oligosaccharides from soy, fructans and water-soluble NSP (e.g., AX, β-glucan, pectin) (92–94). Additionally, fermentable oligosaccharides enzymatically produced from AX, such as arabinoxylo-oligosaccharides (AXOS), xylo-oligoaccharides (XOS), alongside fructo-, manno- and galacto-oligosaccharides (FOS, MOS, GOS) can be supplemented to poultry diets (85,92,95).

The ceca are two blind pouches (Fig. 5) that are colonized predominantly by anaerobic bacteria (92). In the ceca, a diversity of microbes have been found (10^{10} CFU/g), mainly composed by the phyla Firmicutes and Bacteroidetes (96). For comparison, the ileum contains a much lower amount of microbes (10^5 CFU/g) and is mainly colonized by *Lactobacillus* genera (96). Hence, fermentation is expected to mainly occur in the ceca. Carbohydrate fermentation in monogastrics (e.g., humans, poultry, swine) is typically conducted by members of bacterial families such as Lachnospiraceae, Ruminococaceae, Bacteroidaceae, Bifidobacteriaceae and Lactobacilaceae (92,96–98). Bacterial metabolism produces SCFAs, predominantly acetate, butyrate and propionate, which are very important for the health of the host. For instance, SCFAs can provide additional energy and decrease pathogen growth by controlling and lowering the cecal pH value (92). Overall, a well-balanced microbial ecology has been linked with improved broiler health and growth (92,96,99).

Table 3. Impact of type, degree and distribution of substituents on *in vitro* fermentation of AX and associated oligosaccharides. Abbreviations are shown below.

Structural feature*	Impact on fermentation	Ref.
Degree of polymerization (DP)	Propionate formation and *Bacteroides* spp. growth decreased by increased DP of fermented AX	(100) (101) (105)
Ara/Xyl	Not correlated with fermentation rate of polymeric AX	(103)
Ara substitution pattern	Presence of contiguous Xyl residues increased fermentation rate; Disubstituted AXOS were less fermented than monosubstituted AXOS by *Bacteroides cellulosilyticus*	(100) (101)
Oligosaccharide class*	**Impact on fermentation**	
AXOS	Limited *Bacteroides* spp. growth compared to XOS	(100)
AcXOS	Lower SCFAs formation compared to AXOS and XOS	(102)
GlcA$_{me}$XOS	Lower SCFAs formation compared to AXOS and XOS	(102)
FAXOS	Lower butyrate and propionate formation compared to AXOS	(105)

*Abbreviations: Ara: arabinosyl substituents, Xyl: xylosyl backbone residues, Ara/Xyl: molar based arabinose-to-xylose ratio, XOS: linear xylo-oligosaccharides, AXOS: arabinoxylo-oligosaccharides, AcXOS: acetylated XOS, GlcA$_{me}$XOS: 4-*O*-methyl-glucuronosylated XOS, FAXOS: feruloylated AXOS.

The extent to which AX and AXOS are fermented in the hindgut has been demonstrated to be linked to their chemical structure by several *in vitro* studies (Table 3) (93,100–104). For example, the presence of Ara substituents was found

to hinder fermentation of AXOS compared to XOS by *Bacteroides* spp. Likewise, the presence of unsubstituted regions in wheat bran AX contributed to a more rapid fermentation compared to more complex maize bran AX (101). Furthermore, AXOS as well as acetylated, 4-*O*-methyl-glucuronosylated and feruloylated (A)XOS produced 1.3-10 times lower SCFAs amounts compared to XOS (102,105). In the same line, AXs with complex substitution patterns presented 2-6 times slower fermentation rates by human fecal inocula compared to 'simpler' AXs or FOS (103).

The impact of AX and AX-derived oligosaccharides on their fermentation in poultry is less studied compared to their fermentation in humans. In specific, colonic fermentation of AX and (A)XOS in the human gut is performed by a consortium of bacterial communities, via a cross-feeding mechanism (93). For instance, *Roseburia* spp. and *Bacteroides* spp. extracellularly and enzymatically depolymerize AX and (A)XOS. The resulting hydrolytic products (e.g. monosaccharides, oligosaccharides) are then utilized as substrates by *Bifidobacterium* spp. In turn, the metabolic products of the latter (lactate) can be used as a substrate by other bacteria (93).

For broilers, soluble AX, AXOS and XOS were shown to promote *Bifidobacterium* spp. growth in the ceca, with the impact of oligosaccharides being more pronounced than that of the polymer (106). Similarly, AX hydrolysis by endo-xylanase and debranching enzymes was found to promote SCFAs during *in vitro* fermentation by cecal broiler inoculum (107). Further research is warranted to determine the mechanisms of AX and (A)XOS utilization in the poultry GIT.

7 The application of NSP-active enzymes in poultry nutrition

Cereal NSP play an important role in poultry nutrition with both negative and positive implications, as explained in 6.2. Consequently, fiber manipulation in order to reduce the negative effect of NSP for nutrient digestion and increase the positive effect of NSP on fermentation is of particular interest in order to improve animal health and growth, while minimizing costs. The main means of achieving this is the dietary supplementation of NSP-active enzymes (NSPases; see section 8 for further details on effect of NSPases on broiler performance). The main commercial NSPase preparations consist of glycoside hydrolases (GH) of fungal origin, able to depolymerize plant polysaccharides. Therefore, in this section we focus on introducing only fungal GHs, in the context of NSP degradation.

7.1 Endo-β-1,4-xylanases (EC 3.2.1.8)

Endo-xylanases depolymerize (hetero)xylans by hydrolysis of the β-(1→4) linkages between two Xyl residues of the backbone (108,109). Endo-xylanases are produced by fungi, yeasts, bacteria and plants, and play an important role in (hetero)xylan decomposition and degradation in nature (110,111). Fungal endo-xylanases find many applications in food (e.g., bread-making), paper manufacturing, biorefinery and animal feed. The most commonly used microorganisms to produce commercial

enzyme cocktails are *Aspergillus* and *Trichoderma* spp. (110,111). The application of endo-xylanases as animal feed supplements is linked to their capability of hydrolyzing AX from cereal (Fig. 6A). AX depolymerization by endo-xylanase mainly releases substituted AXOS and linear XOS (108,109). Commercially applied xylanases are members of the GH families 10 and 11 (CAZy.org (112)).
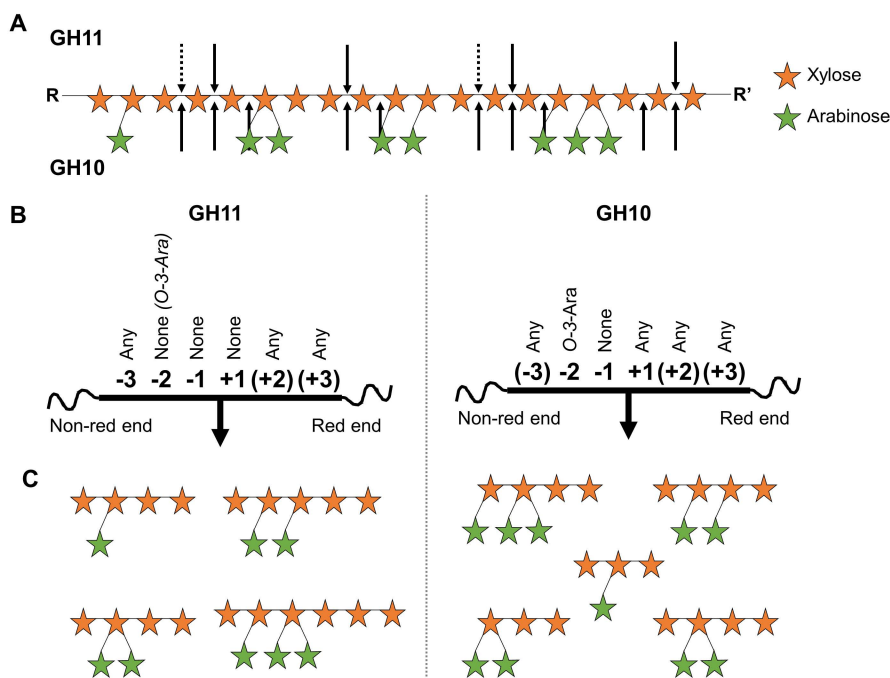

Fig. 6. Mode of action of GH11 and GH10 family endo-xylanases on a hypothetical AX structure from wheat flour (**A**). Subsite model (**B**) of GH11 and GH10 family endo-xylanases. The active site is located between -1 and +1 subsites. The ability of different subsites to accommodate no substitutions, any type or only *O*-3-linked Ara substitutions is specified. Arrows indicate the cleavage sites along the AX backbone. Examples of structurally different AXOS (**C**) released by GH10 and GH11 endo-xylanases (108,109,113,118). R = non-reducing end terminus. R' = reducing end terminus.

GH11 endo-xylanases present a Mw close to 20 kDa while their pI can vary greatly (3.5-10.0) (111,113). GH11 endo-xylanases have been described to hydrolyze the linkage between two unsubstituted Xyl (uXyl) residues and typically require the presence of at least one additional uXyl next to the cleavage site (-2 position; Fig. 6B) (109,113,114). Although several GH11 xylanases have been found to efficiently degrade insoluble AX (114–116), such property may not be extrapolated to all members of the GH11 family. Conversely, GH10 endo-xylanases are larger (> 30 kDa), have a more acidic pI and are more tolerant to substitutions than GH11 xylanases (108,113,114,116,117). In specific, GH10 endo-xylanases can accommodate Xyl residues having single and double Ara substitutions at the +1

position, but only having single *O*-3-linked Ara at the -2 position (Fig. 6B) (109,110,117). GH10 endo-xylanases exhibit a preference for soluble AX over insoluble AX compared to GH11 ones (110,114–116).

Due to their different catalytic sites and consequently different mode of action, GH11 endo-xylanases mainly yield larger DP AXOS than GH10 xylanases. In addition, GH11 endo-xylanases release (A)XOS having an unsubstituted non-reducing end (Fig. 6C), while GH10 xylanases can release (A)XOS substituted at the non-reducing terminus (108,109,113,118). Although enzymes from both families can efficiently degrade soluble AX, GH11 endo-xylanases are more efficient than GH10 ones when it comes to insoluble AX (110,114–116) that is associated with or embedded in the cell wall matrix (Fig. 4) and represents the major AX fraction in cereal grains (Table 2).

7.2   Accessory enzymes for AX degradation

The enzymatic arsenal required for the complete hydrolysis of AX to monosaccharides is described in the text below and schematically indicated in Fig. 7. Nevertheless, supplementation with such enzymes is not very common in broiler studies (107,119,120).
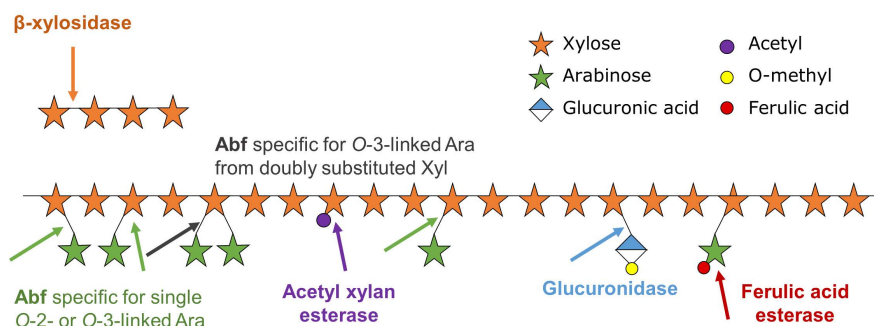

Fig. 7. Accessory xylanolytic enzymes, and corresponding cleavage sites of a hypothetical heteroxylan structure (121,122).

Arabinofuranosidases (EC 3.2.1.55)

Fungal arabinofuranosidases (Abfs) belong to the GH families 43, 51, 54 and 62 (CAZy.org (112,123,124)) and hydrolyze the α-(1→2,3)-linkages between Ara side chains and Xyl backbone residues of AX (Fig. 7; 121). Abfs are accessory to endo-xylanases in deconstructing AX (122,125). Different Abfs can exhibit distinct modes of action towards AX, AXOS or both. For instance, certain Abfs, such as GH43 Abf from *Humicola insolens* specifically cleave *O*-3-linked Ara from doubly substituted Xyl (124,126). Conversely, other Abfs such as GH51 Abfs from *H. insolens* and *Meripilus giganteus* cleave single *O*-2- and *O*-3-linked Ara units (126). As a result of their debranching action, Abfs have been shown to assist endo-xylanases in degrading AX (119,126).

Glucuronidases (EC 3.2.1.139)

Glucuronidases from fungi belong to the GH67 and 115 families (CAZy.org (112,123)) and hydrolyze the α-(1→2)-linkage between Xyl residue and (4-*O*-methyl-) glucuronosyl substituents (121,122). These enzymes are required for the degradation of glucuronoarabinoxylan (GAX), and have shown synergy with endo-xylanases, Abfs and β-xylosidases (122,127).

Esterases

The cleavage of acetyl, feruloyl and coumaroyl substituents of AX is catalyzed by acetyl xylan esterases (EC 3.1.1.72) and ferulic/coumaric acid esterases (EC 3.1.1.73), respectively (122). Fungal esterase members belong to the carbohydrate esterase (CE) family 1 (CAZy.org (112)). The removal of such substituents has been shown to improve the activity of other xylanolytic enzymes, such as xylanases and glucuronidases (122,128,129).

β-xylosidases (EC 3.2.1.37)

The complete saccharification of XOS, released by a combination of xylanolytic enzymes, to monomeric Xyl requires the action of β-xylosidases (111,122). Fungal xylosidases belong to the GH families 3, 30 and 43 (CAZy.org (112,123)). Although such enzymes are of interest for biorefinery applications where monosaccharides release is aimed at (111,125,127), this is not the case for animal nutrition due to the negative impact of xylose on animal performance (130).

7.3   Endo-β-1,4-glucanases (EC 3.2.1.4)

Endo-β-1,4-glucanases hydrolyze the β-(1→4) linkage between two consecutive Glc residues of cellulose and BG. Fungal endo-glucanases belong to the GH families 5, 7, 12, and 45 (CAZy.org (112,123)). So far, commercial endo-glucanases are mainly included in barley-based diets to offset the viscosity increase by polymeric β-glucan, and their use as feed supplements historically preceded that of xylanases (65,131). Endo-glucanases are part of the catalytic machinery responsible for cellulose and β-glucan degradation (132). For complete cellulose conversion to Glc, the synergistic action of various enzymes is required. In brief, first endo-glucanases and oxidative lytic polysaccharide mono-oxygenases (LPMOs) generate new glucan chain ends. LPMOs oxidatively cleave crystalline and amorphous regions of cellulose (133). Next, cellobiohydrolases (CBHs) act on the resulting new chain ends releasing cellobiose, which can be further degraded to Glc by β-glucosidases (132,134). Other cellulases than endo-glucanases are not further discussed here as glucose release from NSP was not aimed at in the current research, due to the negative impact of monosaccharide provision to animal health and performance (130,135). Finally, to the best of our knowledge, no reports regarding the influence of cellobiose for broilers have been published.

Still, the use of endo-glucanases alone is of interest as they can release of gluco-oligosaccharides (GlcOS) from single chains of (soluble) β-(1→3,1→4)-linked

glucan (136–138). For example, *in vitro* studies have demonstrated the ability of glucanases to solubilize Glc-containing carbohydrates from wheat grains (31,139). Moreover, it was observed that a combination of endo-xylanase and endo-glucanase resulted in higher release of Glc units and protein from wheat grains than endo-glucanase alone, suggesting an additive or synergistic effect of both enzyme activities regarding cereal cell wall degradation (31,139).

7.4   Other NSP-active and non NSP-active enzymes

Endo-xylanases and endo-glucanases are the predominantly used NSPases in broiler nutrition to address the anti-nutritive effect of AX and β-glucan from cereal (65). Nevertheless, the presence of various NSPs in feed means that supplementation of broiler feed with other NSPases might be of interest as well. For example, pectinase supplementation in maize-rapeseed meal diet was reported to improve arabinan fermentability (140). In another study, supplementation of a mixture of xylanase, glucanase, pectinase, mannanase and galactanase was shown to improve NSP fermentability in maize-soybean and maize-pea diets (141).

Apart for NSPases, also other enzymes have been tested as growth promotors in broilers. Phytases stand out as they are the most widely used enzymes in poultry nutrition (142). Phytases of fungal or bacterial origin (EC 3.1.3.8) are supplemented in poultry and swine diets to break down phytate and increase phosphorus bioavailability and digestibility (143). Additional improvements in calcium, zinc and amino acid bioavailability, as well as in metabolizable energy, clearly showcase the significance of phytases for poultry (143).

Next to NSPases and phytases, the use of exogenous digestive enzymes in poultry has also been studied (144). For example, the use of xylanase in combination with amylase and protease improved protein digestibility and energy uptake, but not starch digestibility (76,145). Such other NSPases, phytases and dietary supplemented amylases and proteases, fall outside the scope of this thesis, and, hence, are not discussed in further detail.

8   NSP-active enzymes promote poultry performance

The use of NSP-active enzymes (NSPases) in poultry nutrition dates back to the 1950's (65). Since then, several studies have demonstrated that supplementation of NSPases, especially endo-xylanase, led to improved broiler performance (Table 4).

In particular, the dietary supplementation of endo-xylanase alone or in combination with endo-glucanase and other NSPases has been widely shown to lower the feed conversion ratio (FCR) for wheat-fed and maize-fed broilers (75,141,146–150). The beneficial impact of endo-xylanase and other NSPases for broiler performance has been narrowed down to three distinct mechanisms, as previously summarized by Bedford (2018) (65). These three mechanisms are: 1)

viscosity reduction, 2) release of prebiotic oligosaccharides and 3) de-encapsulation of nutrients entrapped by the cell wall matrix.

Table 4. Overview of the effect of NSP-active enzymes on broiler performance, nutrient digestibility, NSP content, SCFAs formation and cecal microbiota reported in representative studies spanning between 2004-2018; ↑ indicates significant increase, ↓ indicates significant decrease and – indicates no significant change (significance threshold set at $p<0.05$) in response to enzyme addition. Empty cells indicate that corresponding parameters were not measured.

	Wheat-soybean diets							Maize-soybean diets[13]						
Xylanase	GH11	NS[7]	NS	NS	NS	NS	NS	NS	NS	NS	NS	NS	NS	GH11
Other enzymes	–	G[8]	–	–	–	–	A[9]+F[10]	G	M[12]	G	–	–	–	A
Duration (days)	42	21	21	49	24	31	36	42	18	21	21	49	39	29
Perf.[1] BW	–		↑	–	↑	–	↑				–	–	–	↑
Perf.[1] WG	–	↑		–		↑	↑	–	↑	↑		–	–	↑
Perf.[1] FCR	–	↓	↓	↓	↓	↓	↓	↓	↓	↓	–	↓	–	↓
Perf.[1] FI		–	–	↑	–	–	–	–	–	–	–	↑	–	–
Ileal Viscosity	↓	↓	↓		↓	↓	↓			↓	↓		–	
Digest.[2] Sta		↑							↑	–		–		
Digest.[2] Pro		–	↑	–	–			↑	↑	–	↑	–		–
Digest.[2] DM			↑	↑	–			–				–	↑	
Digest.[2] Ene				↑	↑			↑				↑	–	
SCFAs[3]	↑		↑	↑		–	↑[11]				↑	↑		↑
Sol.NSP[4]	↑					↑		↑						
Ins.NSP[5]						–		↓						↓
Microb.[6]	↑	–									–		↑	–
Ref.	(152)	(146)	(75)	(147)	(148)	(149)	(107)	(150)	(141)	(146)	(75)	(147)	(154)	(119)

[1]Animal performance: Body weight (BW), body weight gain (WG), feed conversion ratio (FCR), feed intake (FI). [2]Ileal nutrient digestibility of starch (Sta), protein or nitrogen (Pro), dry matter (DM) and energy (Ene). [3]Short chain fatty acids (SCFAs) content in the ceca. [4]Soluble NSP content in the ileum. [5]Insoluble NSP content in the ileum. [6]Cecal microbiota composition evaluated by different methodologies, further elaborated in 7.2. [7]Not specified. [8]Glucanase. [9]Arabinofuranosidase. [10]Ferulic acid esterase. [11]Determined *in vitro*. [12]Mixture of glucanase, pectinase, mannanase and galactanase. [13]Maize-based diets containing distiller dried grains with solubles from maize (mDDGS) were used in (75,119,146).

8.1   Viscosity reduction

As mentioned earlier (see 6.2), solubilization of high Mw polysaccharides such as AX and β-glucan, during feed digestion results in increased intestinal viscosity.

Several studies documented the decrease of ileal viscosity upon NSPase supplementation (75,83,107,146,148,149,151,152), as summarized in Table 4. Decreased digesta viscosity coincided with pronounced nutrient digestibility and broiler performance (75,107,149,151). In particular, this relationship has been documented when endo-xylanase was supplemented in wheat-based diets (Table 4). Endo-glucanase supplementation in barley-based diet also resulted in viscosity decrease and coincided with an increase in nutrient digestibility (131,153). Overall, viscosity reduction is considered to be a result of soluble NSP depolymerization by enzymes. This is widely accepted as a main mechanism by which endo-xylanases and other NSPases promote broiler growth in viscous diets (65).

However, inhibition of digestion by viscosity increase is not a concern in maize-based diets due to the low amount of soluble AX (154,155). Consequently, in maize-based diets the impact of endo-xylanase in terms of viscosity decrease is expected to be limited. Furthermore, it has been shown that higher starch digestibility was achieved in maize diets than in wheat diets, even when the viscosity of maize diets was increased by guar gum addition at a level comparable to that of wheat diets (155). Such observations revealed that in addition to viscosity, there are additional factors governing feed assimilation, and therefore, impacting the influence of exogenous enzymes in broilers.

8.2 Prebiotic oligosaccharide release

Microbial fermentation of non-digestible feed components such as NSP, maltodextrins, low Mw carbohydrates and proteins occurs in the broiler ceca (78,79). Therefore, the provision of cecal microbial communities with soluble and fermentable carbohydrates is of interest (see 6.2).

Several studies have demonstrated that endo-xylanase supplementation in wheat diets coincided with an increase in soluble arabinosyl and xylosyl units measured in the water soluble fraction of ileal digesta for broilers and pigs (149,152,156). These observations suggested the solubilization of AX structures due to the degradation of insoluble AX. Such *in vivo* reports are consistent with the ability of both GH11 and GH10 endo-xylanases to degrade and solubilize AX from wheat grains *in vitro* (109,114,157,158). Furthermore, xylanase supplementation in wheat diets has been found to increase SCFAs (i.e., acetate, butyrate, propionate) formation in the ceca (75,147,152). At the same time, qPCR analysis of targeted bacteria indicated that dietary endo-xylanase improved *Bifidobacterium* spp. growth in broiler ceca (152). However, determination of cecal gut microbiota by 16S rRNA sequencing did not reveal differences between broilers fed control and xylanase/glucanase-supplemented wheat diets (146). In comparison, the provision of AXOS and XOS in broilers resulted in similar increase in bifidobacteria counts in the ceca for wheat diets (95,106). Xylanase supplementation in maize diets has also been found to increase acetate, propionate and butyrate formation in the broiler and coincided with increased counts of fiber-fermenting Clostridia in the ceca (75,147,154). All the above studies point towards the *in vivo* release of AXOS

in the small intestine by endo-xylanase. However, AXOS detection in animal digesta has not yet been achieved and, therefore, direct evidence of their formation remains elusive.

8.3   Nutrient de-encapsulation

Apart from reducing digesta viscosity and enhancing hindgut fermentation, NSPases may promote animal growth by offsetting nutrient encapsulation (see 6.2) by the cell wall matrix (65,88). Similar to viscosity reduction, this mechanism concerns nutrient digestibility in the small intestine. Similar to the prebiotic mechanism, nutrient de-encapsulation is also focused on (insoluble) NSP degradation. To date, most scientific evidence regarding this mechanism is derived from *in vitro* studies. In particular, several studies describing *in vitro* experiments documented that NSPase treatment of wheat grains was accompanied by NSP solubilization, protein and starch release as well as structural changes in the cell walls (31,139,158–160). Nevertheless, *in vitro* studies typically involve high enzyme doses and prolonged incubation times compared to *in vivo* conditions (65). On top of that, such observations have not been validated by *in vivo* studies yet.

9   Practices and challenges of evaluating the NSPase effect on NSP fate and structure in the animal GIT

9.1   Digestibility markers

Currently, having widely demonstrated the impact of NSPases in terms of animal performance and nutrient digestibility, research in the field is paying more attention to the effect of supplemented enzymes on the fate and structure of NSP throughout the GIT. First and foremost, the fate of nutrients and fiber in the small intestine and hindgut of animals can be followed by the use of digestibility markers (73,161,162). Such markers are considered to be inert, undigestible and non-toxic compounds that follow the flow of feed components along the GIT (162). Insoluble markers, such as metal oxides (Cr_2O_3, TiO_2) and acid insoluble ash (AIA), are added to the feed and are used to evaluate the transit, retention time and digestibility of the main feed fraction, assuming a unilateral flow of digesta in the GIT (161,162). Nevertheless, research has shown that this assumption is not always valid, especially in broilers. For example, insoluble markers have been found to be retained less in the gizzard than coarse feed particles (73). Additionally, the reflux of insoluble feed components in the ileum from the ileocecal junction may lead to overestimation of ileal digestibility (77). Lastly, insoluble markers are not able to enter the ceca (77,78). Instead, the use of soluble markers (e.g. Cr-, Co-EDTA) is considered more suitable to follow the fermentation of soluble feed components in the ceca (162).

9.2   Carbohydrate analysis in digesta

Carbohydrate analysis in animal digesta typically begins by determining the neutral monosaccharide composition, according to Englyst & Cummings (163). In this

approach, carbohydrates are being subjected to pre-hydrolysis by 72% H_2SO_4, followed by acid hydrolysis (1M H_2SO_4) to their constituent monosaccharides, and by their subsequent analysis by gas chromatography (after derivatization to alditol acetates) or liquid chromatography. In parallel, uronic acids such as glucuronic and galacturonic acid present in pectin or in hemicellulosic material can be identified and measured (164,165). Although this methodology can provide an overview of carbohydrate content and composition in digesta, it cannot discriminate between the various carbohydrate species present. For example, starch, β-glucan and cellulose will all contribute to the measured glucose content. Additionally, the presence of different carbohydrate sources in the diet (i.e., cereal and soybean) means that a broad range of distinct NSP structures will contribute to the measured monosaccharide contents.

A more detailed analysis of individual carbohydrates requires laborious procedures such as digestion by specific enzymes and glycosidic linkage analysis (27,140,166). Another common procedure of characterization is to fractionate carbohydrates present in digesta to water soluble and insoluble ones. This is typically carried out by non-standardized procedures that can result in considerable differences in composition and yield of extracted NSP between studies (119,149,152,156,163,167–169). Following their separation, soluble and insoluble carbohydrates are being subjected to sugar composition analysis, as described above. Alternatively, the sugar composition of soluble carbohydrates can be determined by more rapid hydrolysis procedures suitable to hydrolyze soluble carbohydrates, but not insoluble ones. For example, this can be achieved by trifluoroacetic acid (TFA) hydrolysis with or without a preceding methanolysis step (170,171). Next, the amount of NSP (total, soluble, insoluble) recovered or 'digested' in the ileum or total tract can be estimated by combining the carbohydrate contents analyzed and compared to the recovery of the digestibility markers (140,141,149,171). Although this approach can provide insights about the fate and fermentability of NSP components in a quantitative manner, it is not informative about the structure of NSP present in digesta. Therefore, the potential NSP degradation by NSPases *in vivo* remains poorly characterized.

9.3   Bridging the gap between analysis of (complex) digesta matrices and sophisticated analytical tools

In spite of the plethora of evidence regarding the beneficial effect of endo-xylanase for broilers, its ability to release AXOS *in vivo* has not yet been confirmed, mainly due to the lack of proper analytical tools and methodologies. In this view, the comprehensive investigation of carbohydrate species in digesta seems to be the missing piece potentially linking the enzymological properties of endo-xylanase, as observed *in vitro*, with its *in vivo* function as a feed additive.

The enzymatic degradation of plant polysaccharides such as AX is typically followed by three main analytical techniques (Table 6): high performance size-exclusion chromatography with refractive index detection (HPSEC-RI), high performance

anion exchange chromatography with pulsed amperometric detection (HPAEC-PAD) and matrix-assisted laser desorption/ionization time-of-flight mass spectrometry (MALDI-TOF-MS).

Table 5. Overview of sophisticated analytical techniques applied to characterize enzymatically-derived oligosaccharides across disciplines (172,180–186).

Analytical technique*	Main applications	Main drawbacks
HPSEC-RI	Molecular weight distribution of poly- oligosaccharides	Unspecific
HPAEC-PAD	Profiling, identification and quantification of oligosaccharides	Loss of alkali-labile substituents; Identification depends on availability of analytical standards; Low MS compatibility
MALDI-TOF-MS	Identification, determination of DP	Quantification not always possible; Does not separate isomers
^{1}H NMR, ^{13}C NMR	Identification of individual oligosaccharides	High sample purity and amount required
UPLC-MS^{n}	Identification of individual oligosaccharides	Pre-column derivatization often needed; Chromatographic separation and MS-based identification need further development
CE	Profiling, identification and quantification of oligosaccharides	Pre-column derivatization often needed; Low MS compatibility
IM-MS	Identification of individual oligosaccharides	Still at an early development stage

*Abbreviations: HPSEC-RI; high performance size-exclusion chromatography with refractive index detection, HPAEC-PAD; high performance anion exchange chromatography with pulsed amperometric detection, MALDI-TOF-MS; matrix-assisted laser desorption/ionization time-of-flight mass spectrometry, NMR; nuclear resonance spectroscopy, UPLC-MS^{n}; utlra-high performance liquid chromatography coupled to tandem mass spectrometry, CE; capillary electrophoresis, IM-MS; ion mobility MS

Such techniques can provide valuable information regarding the size distribution, degree of polymerization (DP) range and oligosaccharide profile of enzymatic digests (41,172–174). However, they require relatively pure matrices and have been mainly used to characterize enzymatic digests prepared *in vitro* from polysaccharides that were either well-defined or previously extracted from plant material. Therefore, analysis of more complex samples such as digesta, fermentation broths or waste streams requires sample clean-up. This can be achieved by techniques such as preparative chromatography or solid-phase extraction (SPE), among others (175). For example, reverse phase and graphitized carbon SPE have been successful in extracting oligosaccharides from complex matrices (175–179).

Capillary electrophoresis (CE) has been applied in the analysis of mainly acidic glycans, although it is used less frequently than the three main analytical techniques mentioned above (183,187). Ion mobility-MS (IM-MS) is an emerging new technique that shows more promise in separating isomeric glycans than direct infusion MS (184). Nevertheless, IM-MS is still not widely used. In contrast, nuclear magnetic resonance spectroscopy (^{1}H NMR, ^{13}C NMR) has been widely applied to elucidate the fine structure of oligosaccharides, such as AXOS, after extensive purification steps (188,189). In spite of its ability to provide precise structural information, the high requirements in analyte purity and amount limit its applicability in the study of digesta.

Ultra-high performance chromatography coupled to tandem MS (UPLC-MS^n) has been a more robust technique for glycan analysis. In particular, different separation modes, such as reverse phase (RP), normal phase (NP), porous graphitized carbon (PGC) and hydrophilic interaction (HILIC) chromatography have been applied for glycan oligomer separation (180,186,190). Overall, UPLC hyphenation to MS^n is considered a powerful tool for oligosaccharide analysis, and has been applied to study AXOS structures (191–193). To date, such research has mainly focused on studying the behavior during MS^n of previously purified and well-defined by ^{1}H-NMR oligosaccharides. More recently, the separation and identification of alginate oligosaccharides by HILIC-MS in pig digesta, after SPE, showcases the potential of such approaches for oligosaccharide characterization in digesta samples (194). Still, further research is warranted to address the complexity of digesta matrices, while at the same time being able to elucidate the chemical structure of target oligosaccharides.

10   Aim and outline of the thesis

This project aims at elucidating the impact of dietary endo-xylanase on NSP fate and fermentability in the broiler GIT at a molecular level. Therefore, it is hypothesized that endo-xylanase releases AXOS of diverse structure *in vivo*, leading to i) pronounced AX (and AXOS) fermentation to SCFAs, ii) alterations in cecal microbial ecology and iii) ultimately to pronounced nutrient digestion and animal growth by (partly) offsetting the hypothetical encapsulation of nutrients by NSP ('de-caging')(Fig. 8).

In **Chapter 1**, the background and aim of this project is presented. In particular, bibliography dating back to the start of the project (2018) or earlier is taken into account, regarding the structure and chemical properties of feed components, the broiler GIT, the dietary enzymes and their hypothesized mechanisms of action *in vivo*.

In **Chapter 2**, the impact of xylanase and glucanase on broiler growth, nutrient digestion and NSP fermentation is described for wheat-based and maize-based diets. This chapter further focuses on the release of AXOS *in vivo* upon enzyme supplementation and on AX fermentation to SCFAs.

In **Chapter 3**, the impact of enzyme supplementation on gut microbial communities in the ileum and ceca of broilers is described further. In this part, associations between AX/AXOS fermentation and proliferation of beneficial gut microbiota that are known to ferment NSP to SCFAs are evaluated.

In **Chapter 4**, the development of a strategy to identify individual AXOS present in mixtures is described. In particular, separation and identification of (NaBH$_4$-reduced) AXOS produced by GH11 and GH10 endo-xylanases is carried out by HILIC-MS^n.
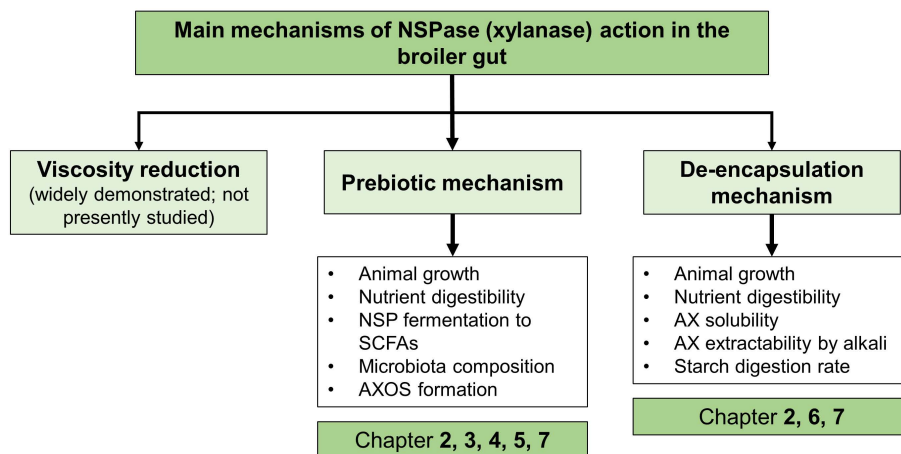
Fig. 8. Overview of the three main mechanisms by which dietary xylanase may promote animal growth. The widely demonstrated viscosity reduction mechanism will not be elaborated in this thesis. However, the less well-demonstrated potential mechanisms (prebiotic, de-caging) shall be further explored. The boxes at the bottom of the scheme demonstrate the main parameters that will be investigated experimentally and elaborated in this thesis.

In **Chapter 5**, AXOS release by endo-xylanase *in vivo* is delineated. Here, a procedure to extract AX/AXOS from complex digesta matrices by SPE is described. Next, AX/AXOS extracted from digesta are being analyzed using established chromatographic methods as well as the method developed in Chapter 4, in order to portray the structural variability and to follow the utilization of AXOS in the broiler hindgut.

In **Chapter 6**, the investigation of the widely overlooked insoluble NSP fraction of broiler digesta is described. Here the transit behavior of cell wall components such as insoluble AX and lignin as well as the alkali extractability of AX along the broiler GIT are elaborated in order to obtain a better understanding on cell wall NSP degradation *in vivo* by supplemented enzymes.

In **Chapter 7**, the relevance of this research on future study and application of dietary enzymes in broilers and beyond, is being discussed. The findings of this thesis are discussed further with additional (*in vitro*) experimental data and recent literature.

References

1. Marangoni F, Corsello G, Cricelli C, Ferrara N, Ghiselli A, Lucchin L, Poli A. Role of poultry meat in a balanced diet aimed at maintaining health and wellbeing: An Italian consensus document. Food Nutr Res. 2015;59:27606.

2. U.S. Department Of Agricilture. Livestock and poultry: world markets and trade [Internet]. 2022 [cited 2022 Jan 15]. p. 16. Available from: https://www.fas.usda.gov/data/livestock-and-poultry-world-markets-and-trade

3. Dean RW. Agronomic and political factors influencing feedstuff use. In: McNab JM, Boorman KN, editors. Poultry feedstuffs: supply, composition and nutritive value. Wallingford: CABI; 2002. p. 3–13.

4. Bennett CE, Thomas R, Williams M, Zalasiewicz J, Edgeworth M, Miller H, Coles B, Foster A, Burton EJ, Marume U. The broiler chicken as a signal of a human reconfigured biosphere. R Soc Open Sci. 2018;5(12).

5. Endo H, Tsunekawa N, Kudo K, Oshida T, Motokawa M, Sonoe M, Wanghongsa S, Tirawattanawanich C, Phimphachanhvongsod V, Sasaki T, Yonezawa T, Akishinonomiya F. Comparative morphological study of skeletal muscle weight among the red jungle fowl (*Gallus gallus*) and various fowl breeds (*Gallus domesticus*). J Exp Zool Part B Mol Dev Evol. 2021:1–10.

6. Zuidhof MJ, Schneider BL, Carney VL, Korver DR, Robinson FE. Growth, efficiency, and yield of commercial broilers from 1957, 1978, and 2005. Poult Sci. 2014;93(12):2970–82.

7. Tallentire CW, Leinonen I, Kyriazakis I. Breeding for efficiency in the broiler chicken: A review. Agron Sustain Dev. 2016;36(4).

8. Donohue M, Cunningham DL. Effects of grain and oilseed prices on the costs of US poultry production. J Appl Poult Res. 2009;18(2):325–37.

9. Giller KE, Delaune T, Silva JV, Descheemaeker K, van de Ven G, Schut AGT, van Wijk M, Hammond J, Hochman Z, Taulya G, Chikowo R, Narayanan S, Kishore A, Bresciani F, Teixeira HM, Andersson JA, van Ittersum MK. The future of farming: Who will produce our food? Food Secur. 2021;13(5):1073–99.

10. Mottet A, Tempio G. Global poultry production: Current state and future outlook and challenges. Worlds Poult Sci J. 2017;73(2):245–56.

11. Black JL. Cereal grains as animal feed. In: Wrigley CW, Corke H, Seetharaman K, Faubion J, editors. Encyclopedia of food grains. 2nd ed. Amsterdam: Elsevier Inc.; 2016. p. 215–22.

12. Zaefarian F, Abdollahi MR, Ravindran V. Starch digestion in broiler chickens fed cereal diets. Anim Feed Sci Technol. 2015;209:16–29.

13. National Research Council. Nutrient Requirements of Poultry. Washington, D.C.: National Academies Press; 1994.

14. Svihus B, Gullord M. Effect of chemical content and physical characteristics on nutritional value of wheat, barley and oats for poultry. Anim Feed Sci Technol. 2002;102(1–4):71–92.

15. Bach Knudsen KE. Fiber and nonstarch polysaccharide content and variation in common crops used in broiler diets. Poult Sci. 2014;93(9):2380–93.

16. Bach Knudsen KE. Carbohydrate and lignin contents of plant materials used in animal feeding. Anim Feed Sci Technol. 1997;67(4):319–38.

17. Liu SY, Truong HH, Khoddami A, Moss AF, Thomson PC, Roberts TH, Selle, PH. Comparative performance of broiler chickens offered ten equivalent diets based on three grain sorghum

varieties as determined by response surface mixture design. Anim Feed Sci Technol. 2016;218:70–83.

18.   Black JL, Ratanpaul V, Williams BA, Diffey S, Gidley MJ. Variability in cereal grain composition and nutritional value: the importance of fibre. In: González-Ortiz G, Bedford MR, Knudsen KEB, Courtin CM, Classen HL, editors. The value of fibre. Wageningen: Wageningen Academic Publishers; 2019. p. 47–59.

19.   Morris CF, Rose SP. Wheat. In: Henry RJ, Kettlewell PS, editors. Cereal grain quality. 1st ed. Dordrecht: Springer Netherlands; 1996. p. 3–54.

20.   Wankhede DB, Deshpande HW, Gunjal BB, Bhosale MB, Patil HB, Gahilod AT, Sawate AR, Walde SG. Studies on physicochemical, pasting characteristics and amylolytic susceptibility of starch from sorghum (*Sorghum bicolor* L. Moench) grains. Starch - Stärke. 1989;41(4):123–7.

21.   Svihus B, Uhlen AK, Harstad OM. Effect of starch granule structure, associated components and processing on nutritive value of cereal starch: A review. Anim Feed Sci Technol. 2005;122(3–4):303–20.

22.   Grundas S, Wrigley CW. Ultrastructure of the wheat grain, flour, and dough. In: Wrigley CW, Corke H, Seetharaman K, Faubion J, editors. Encyclopedia of food grains. 2nd ed. Amsterdam: Elsevier Inc.; 2016. p. 384–95.

23.   Belitz HD, Grosch W, Schieberle P. Carbohydrates. In: Food chemistry. 4th ed. Leipzig: Springer-Verlag Berlin Heidelberg; 2009. p. 316.

24.   Pérez S, Bertoft E. The molecular structures of starch components and their contribution to the architecture of starch granules: A comprehensive review. Starch - Stärke. 2010;62(8):389–420.

25.   Martens BMJ, Gerrits WJJ, Bruininx EMAM, Schols HA. Amylopectin structure and crystallinity explains variation in digestion kinetics of starches across botanic sources in an *in vitro* pig model. J Anim Sci Biotechnol. 2018;9:91.

26.   van Kempen T, Pujol S, Tibble S, Balfagon A. *In vitro* characterization of starch digestion and its implications for pigs. In: Wiseman J, Varley MA, McOrist S, Kemp B, editors. Paradigms in pig science. Nottingham: Nottingham University Press; 2007. p. 515–25.

27.   Englyst HN, Kingman SM, Hudson GJ, Cummings JH. Measurement of resistant starch *in vitro* and *in vivo*. Br J Nutr. 1996 May 9;75(5):749–55.

28.   Gerrits WJJ, Bosch MW, van den Borne JJGC. Quantifying resistant starch using novel, *in vivo* methodology and the energetic utilization of fermented starch in pigs. J Nutr. 2012;142(2):238–44.

29.   Bedford MR, Apajalahti JH. The role of feed enzymes in maintaining poultry intestinal health. J Sci Food Agric. 2021

30.   Burton RA, Fincher GB. Evolution and development of cell walls in cereal grains. Front Plant Sci. 2014;51–15.

31.   Tervilä-Wilo A, Parkkonen T, Morgan A, Hopeakoski-Nurminen M, Poutanen K, Heikkinen P, Autio K. *In vitro* digestion of wheat microstructure with xylanase and cellulase from *Trichoderma reesei*. J Cereal Sci. 1996;24(3):215–25.

32.   Elkin RG. Nutritional components of feedstuffs: A qualitative chemical appraisal of protein. In: McNab JM, Boorman KN, editors. Poultry Feedstuffs: Supply, composition and nutritive value. New York, NY: CABI Publishing; 2002. p. 65–86.

33.   Shewry PR, Halford NG. Cereal seed storage proteins: Structures, properties and role in grain utilization. J Exp Bot. 2002;53(370):947–58.

34.   McKevith B. Nutritional aspects of cereals. Nutr Bull. 2004;29(2):111–42.

35. Scott MP, Emery M. Maize: Overview. In: Wrigley CW, Corke H, Seetharaman K, Faubion J, editors. Encyclopedia of food grains. 2nd ed. Amsterdam: Elsevier Inc; 2016. p. 99–104.

36. Coon C, Leske K, Seo S. The availability of calcium and phosphorus in feedstuffs. In: McNab J, Boorman KN, editors. Poultry feedstuffs: supply, composition and nutritive value. New York, NY: CABI Publishing; 2002. p. 151–79.

37. Saulnier L, Sado P-E, Branlard G, Charmet G, Guillon F. Wheat arabinoxylans: Exploiting variation in amount and composition to develop enhanced varieties. J Cereal Sci. 2007;46(3):261–81.

38. Fauré R, Courtin CM, Delcour JA, Dumon C, Faulds CB, Fincher GB, Sébastien F, Fry SC, Halila S, Kabel MA, Pouvreau L, Quemener B, Rivet A, Saulnier L, Schols HA, Driguez H, O'Donohue MJ. A brief and informationally rich naming system for oligosaccharide motifs of heteroxylans found in plant cell walls. Aust J Chem. 2009;62(6):533–7.

39. Izydorczyk MS, Biliaderis CG. Cereal arabinoxylans: Advances in structure and physicochemical properties. Carbohydr Polym. 1995;28(1):33–48.

40. Saulnier L, Marot C, Chanliaud E, Thibault JF. Cell wall polysaccharide interactions in maize bran. Carbohydr Polym. 1995;26(4):279–87.

41. Verbruggen MA, Spronk BA, Schols HA, Beldman G, Voragen AGJ, Thomas JR, Kamerling JP, Vliegenthart JFG. Structures of enzymically derived oligosaccharides from sorghum glucuronoarabinoxylan. Carbohydr Res. 1998;306(1–2):265–74.

42. Vinkx CJA, Delcour JA. Rye (*Secale cereale* L.) arabinoxylans: A critical review. J Cereal Sci. 1996;24(1):1–14.

43. Wang J, Bai J, Fan M, Li T, Li Y, Qian H, Wang L, Zhang H, Qi X, Rao Z. Cereal-derived arabinoxylans: Structural features and structure–activity correlations. Trends Food Sci Technol. 2020;96:157–65.

44. Gruppen H, Kormelink FJM, Voragen AGJ. Water-unextractable cell wall material from wheat flour. 3. A structural model for arabinoxylans. J Cereal Sci. 1993;18(2):111–28.

45. Gruppen H, Hamer RJ, Voragen AGJ. Water-unextractable cell wall material from wheat flour. 2. Fractionation of alkali-extracted polymers and comparison with water-extractable arabinoxylans. J Cereal Sci. 1992;16(1):53–67.

46. Fincher GB, Stone B. Chemistry of nonstarch polysaccharides. In: Wrigley C, editor. Encyclopedia of grain science. Amsterdam: Elsevier Academic Press; 2004. p. 206–23.

47. Marcotuli I, Hsieh YSY, Lahnstein J, Yap K, Burton RA, Blanco A, Fincher GB, Gadaleta A. Structural variation and content of arabinoxylans in endosperm and bran of durum wheat (*Triticum turgidum* L.). J Agric Food Chem. 2016;64(14):2883–92.

48. Vangsøe CT, Nørskov NP, Devaux MF, Bonnin E, Bach Knudsen KE. Carbohydrase complexes rich in xylanases and arabinofuranosidases affect the autofluorescence signal and liberate phenolic acids from the cell wall matrix in wheat, maize, and rice bran: An *in vitro* digestion study. J Agric Food Chem. 2020;68(37):9878–87.

49. Chateigner-Boutin AL, Ordaz-Ortiz JJ, Alvarado C, Bouchet B, Durand S, Verhertbruggen Y, Barrière Y, Saulnier L. Developing pericarp of maize: A model to study arabinoxylan synthesis and feruloylation. Front Plant Sci. 2016;7:1476.

50. Bergmans MEF, Beldman G, Gruppen H, Voragen AGJ. Optimisation of the selective extraction of (glucurono)arabinoxylans from wheat bran: Use of barium and calcium hydroxide solution at elevated temperatures. J Cereal Sci. 1996;23(3):235–45.

51. Gruppen H. Structural characteristics of wheat flour arabinoxylans (Doctoral Thesis). Wageningen University; 1992.

52. Gruppen H, Hamer RJ, Voragen AGJ. Barium hydroxide as a tool to extract pure arabinoxylans from water-insoluble cell wall material of wheat flour. J Cereal Sci. 1991;13(3):275–90.

53. Iiyama K, Lam T, Stone BA. Covalent cross-links in the cell wall. Plant Physiol. 1994;104(2):315–20.

54. Harris PJ, Stone B. Chemistry and molecular organization of plant cell walls. In: Himmel ME, editor. Biomass recalcitrance: Deconstructing the plant cell wall for bioenergy. Oxford: Blackwell Publishing Ltd.; 2008. p. 61–93.

55. Ding S-Y, Himmel ME. Anatomy and ultrastructure of maize cell walls: An example of energy plants. In: Himmel ME, editor. Biomass recalcitrance: Deconstructing the plant cell wall for bioenergy. Oxford: Blackwell Publishing Ltd.; 2008. p. 38–55.

56. Fincher GB. Cereals: Chemistry and physicochemistry of non-starchy polysaccharides. In: Wrigley CW, Corke H, Seetharaman K, Faubion J, editors. Encyclopedia of food grains. 2nd ed. Amsterdam: Elsevier Inc; 2016. p. 208–23.

57. Brouns F, Hemery Y, Price R, Anson NM. Wheat aleurone: Separation, composition, health aspects, and potential food use. Crit Rev Food Sci Nutr. 2012;52(6):553–68.

58. Donaldson LA. Lignification and lignin topochemistry - An ultrastructural view. Phytochemistry. 2001;57(6):859–73.

59. Chateigner-Boutin AL, Lapierre C, Alvarado C, Yoshinaga A, Barron C, Bouchet B, Bakan B, Saulnier L, Devaux MF, Girousse C, Guillon F. Ferulate and lignin cross-links increase in cell walls of wheat grain outer layers during late development. Plant Sci. 2018;276:199–207.

60. Scheller HV, Ulvskov P. Hemicelluloses. Annu Rev Plant Biol. 2010;61:263–89.

61. Carpita NC, Gibeaut DM. Structural models of primary cell walls in flowering plants: Consistency of molecular structure with the physical properties of the walls during growth. Plant J. 1993;3(1):1–30.

62. Burton RA, Fincher GB. Current challenges in cell wall biology in the cereals and grasses. Front Plant Sci. 2012;3:130.

63. MacNeill GJ, Mehrpouyan S, Minow MAA, Patterson JA, Tetlow IJ, Emes MJ. Starch as a source, starch as a sink: The bifunctional role of starch in carbon allocation. J Exp Bot. 2017;68(16):4433–53.

64. Andriotis VME, Rejzek M, Barclay E, Rugen MD, Field RA, Smith AM. Cell wall degradation is required for normal starch mobilisation in barley endosperm. Sci Rep. 2016;6:33215.

65. Bedford MR. The evolution and application of enzymes in the animal feed industry: the role of data interpretation. Br Poult Sci. 2018;59(5):486–93.

66. Huisman MMH, Schols HA, Voragen AGJ. Cell wall polysaccharides from soybean (*Glycine max.*) meal. Isolation and characterisation. Carbohydr Polym. 1998;37(1):87–95.

67. Huisman MH. Elucidation of the chemical fine structure of polysaccharides from soybean and maize kernel cell walls (Doctoral Thesis). Wageningen University; 2000.

68. Klasing KC. Poultry nutrition: A comparative approach. J Appl Poult Res. 2005;14(2):426–36.

69. Svihus B. Function of the digestive system. J Appl Poult Res. 2014;23(2):306–14.

70. Grond K, Sandercock BK, Jumpponen A, Zeglin LH. The avian gut microbiota: Community, physiology and function in wild birds. J Avian Biol. 2018 Nov;49(11).

71. Klasing KC. Avian gastrointestinal anatomy and physiology. Semin Avian Exot Pet Med. 1999;8(2):42–50.

1

72. Svihus B. The gizzard: Function, influence of diet structure and effects on nutrient availability. Worlds Poult Sci J. 2011;67(2):207–23.

73. Vergara P, Ferrando C, Jiménez M, Fernández E, Goñalons E. Factors determining gastrointestinal transit time of several markers in the domestic fowl. Q J Exp Physiol. 1989;74(6):867–74.

74. Sacranie A, Svihus B, Denstadli V, Moen B, Iji PA, Choct M. The effect of insoluble fiber and intermittent feeding on gizzard development, gut motility, and performance of broiler chickens. Poult Sci. 2012;91(3):693–700.

75. Kiarie E, Romero LF, Ravindran V. Growth performance, nutrient utilization, and digesta characteristics in broiler chickens fed corn or wheat diets without or with supplemental xylanase. Poult Sci. 2014;93(5):1186–96.

76. Romero LF, Sands JS, Indrakumar SE, Plumstead PW, Dalsgaard S, Ravindran V. Contribution of protein, starch, and fat to the apparent ileal digestible energy of corn- and wheat-based broiler diets in response to exogenous xylanase and amylase without or with protease. Poult Sci. 2014;93(10):2501–13.

77. De Vries S, Kwakkel RP, Pustjens AM, Kabel MA, Hendriks WH, Gerrits WJJ. Separation of digesta fractions complicates estimation of ileal digestibility using marker methods with Cr_2O_3 and cobalt-ethylenediamine tetraacetic acid in broiler chickens. Poult Sci. 2014;93(8):2010–7.

78. Duke GE. Relationship of cecal and colonic motility to diet, habitat, and cecal anatomy in several avian species. J Exp Zool. 1989;252(3 S):38–47.

79. Svihus B, Choct M, Classen HL. Function and nutritional roles of the avian caeca: A review. Worlds Poult Sci J. 2013;69(2):249–64.

80. Capuano E. The behavior of dietary fiber in the gastrointestinal tract determines its physiological effect. Crit Rev Food Sci Nutr. 2017;57(16):3543–64.

81. Choct M, Annison G. Anti-nutritive effect of wheat pentosans in broiler chickens: Roles of viscosity and gut microflora. Br Poult Sci. 1992;33(4):821–34.

82. Abdollahi MR, Ravindran V, Svihus B. Pelleting of broiler diets: An overview with emphasis on pellet quality and nutritional value. Anim Feed Sci Technol. 2013;179(1–4):1–23.

83. Bedford MR, Classen HL. Reduction of intestinal viscosity through manipulation of dietary rye and pentosanase concentration is effected through changes in the carbohydrate composition of the intestinal aqueous phase and results in improved growth rate and food conversion efficiency of broiler chicks. J Nutr. 1992;122(3):560–9.

84. Choct M, Annison G. The inhibition of nutrient digestion by wheat pentosans. Br J Nutr. 1992;67(1):123–32.

85. Svihus B, Hervik AK. The influence of fibre on gut physiology and feed intake regulation. In: González-Ortiz G, Bedford MR, Knudsen KEB, Courtin CM, Classen HL, editors. The value of fibre. Wageningen: Wageningen Academic Publishers; 2019. p. 127–39.

86. Choct M, Hughes RJ, Wang J, Bedford MR, Morgan AJ, Annison G. Increased small intestinal fermentation is partly responsible for the anti-nutritive activity of non-starch polysaccharides in chickens. Br Poult Sci. 1996;37(3):609–21.

87. Kiarie E, Romero LF, Nyachoti CM. The role of added feed enzymes in promoting gut health in swine and poultry. Nutr Res Rev. 2013;26(1):71–88.

88. Classen HL. Cereal grain starch and exogenous enzymes in poultry diets. Anim Feed Sci Technol. 1996;62(1):21–7.

89. Hetland H, Choct M, Svihus B. Role of insoluble non-starch polysaccharides in poultry nutrition. Worlds Poult Sci J. 2004;60(04):415–22.

90. Jiménez-Moreno E, González-Alvarado JM, González-Sánchez D, Lázaro R, Mateos GG. Effects of type and particle size of dietary fiber on growth performance and digestive traits of broilers from 1 to 21 days of age. Poult Sci. 2010;89(10):2197–212.

91. Röhe I, Zentek J. Lignocellulose as an insoluble fiber source in poultry nutrition: a review. J Anim Sci Biotechnol. 2021;12:82.

92. Pan D, Yu Z. Intestinal microbiome of poultry and its interaction with host and diet. Gut Microbes. 2013;5(1):108–19.

93. Broekaert WF, Courtin CM, Verbeke K, van de Wiele T, Verstraete W, Delcour JA. Prebiotic and other health-related effects of cereal-derived arabinoxylans, arabinoxylan-oligosaccharides, and xylooligosaccharides. Crit Rev Food Sci Nutr. 2011;51(2):178–94.

94. Flint HJ, Scott KP, Duncan SH, Louis P, Forano E. Microbial degradation of complex carbohydrates in the gut. Gut Microbes. 2012 Jul 14;3(4):289–306.

95. Ribeiro T, Cardoso V, Ferreira LMA, Lordelo MMS, Coelho E, Moreira ASP, Domingues MRM, Coimbra MA, Bedford MR, Fontes CMGA. Xylo-oligosaccharides display a prebiotic activity when used to supplement wheat or corn-based diets for broilers. Poult Sci. 2018;97(12):4330–41.

96. Rychlik I. Composition and function of chicken gut microbiota. Animals. 2020 Jan 8;10(1):103.

97. Crittenden R, Karppinen S, Ojanen S, Tenkanen M, Fagerström R, Mättö J, Saarela M, Mattila-Sandholm T, Poutanen K. *In vitro* fermentation of cereal dietary fibre carbohydrates by probiotic and intestinal bacteria. J Sci Food Agric. 2002;82(8):781–9.

98. Sergeant MJ, Constantinidou C, Cogan TA, Bedford MR, Penn CW, Pallen MJ. Extensive microbial and functional diversity within the chicken cecal microbiome. PLoS One. 2014;9(3).

99. Oakley BB, Lillehoj HS, Kogut MH, Kim WK, Maurer JJ, Pedroso A, Lee MD, Collett SR, Johnson TJ, Cox NA. The chicken gastrointestinal microbiome. FEMS Microbiol Lett. 2014;360(2):100–12.

100. Mendis M, Martens EC, Simsek S. How fine structural differences of xylooligosaccharides and arabinoxylooligosaccharides regulate differential growth of *Bacteroides* species. J Agric Food Chem. 2018;66(31):8398–405.

101. Rose DJ, Patterson JA, Hamaker BR. Structural differences among alkali-soluble arabinoxylans from maize (*Zea mays*), rice (*Oryza sativa*), and wheat (*Triticum aestivum*) brans influence human fecal fermentation profiles. J Agric Food Chem. 2010;58(1):493–9.

102. Kabel MA, Kortenoeven L, Schols HA, Voragen AGJ. *In vitro* fermentability of differently substituted xylo-oligosaccharides. J Agric Food Chem. 2002;50(21):6205–10.

103. Rumpagaporn P, Reuhs BL, Kaur A, Patterson JA, Keshavarzian A, Hamaker BR. Structural features of soluble cereal arabinoxylan fibers associated with a slow rate of *in vitro* fermentation by human fecal microbiota. Carbohydr Polym. 2015;130:191–7.

104. Grootaert C, Delcour JA, Courtin CM, Broekaert WF, Verstraete W, Van de Wiele T. Microbial metabolism and prebiotic potency of arabinoxylan oligosaccharides in the human intestine. Trends Food Sci Technol. 2007;18(2):64–71.

105. Snelders J, Olaerts H, Dornez E, Van de Wiele T, Aura AM, Vanhaecke L, Delcour JA, Courtin CM. Structural features and feruloylation modulate the fermentability and evolution of antioxidant properties of arabinoxylanoligosaccharides during *in vitro* fermentation by human gut derived microbiota. J Funct Foods. 2014;10:1–12.

106. Courtin CM, Swennen K, Broekaert WF, Swennen Q, Buyse J, Decuypere E, Michiels CW, De Ketelaere B, Delcour JA. Effects of dietary inclusion of xylooligo- saccharides, arabinoxylooligosaccha- rides and soluble arabinoxylan on the microbial composition of caecal contents of chickens. J Sci Food Agric. 2008;88(14):2517–22.

1

107. Lei Z, Shao Y, Yin X, Yin D, Guo Y, Yuan J. Combination of xylanase and debranching enzymes specific to wheat arabinoxylan improve the growth performance and gut health of broilers. J Agric Food Chem. 2016;64(24):4932–42.

108. Biely P, Vršanská M, Tenkanen M, Kluepfel D. Endo-β-1,4-xylanase families: differences in catalytic properties. J Biotechnol. 1997;57(1):151–66.

109. Kormelink FJM, Gruppen H, Viëtor RJ, Voragen AGJ. Mode of action of the xylan-degrading enzymes from *Aspergillus awamori* on alkali-extractable cereal arabinoxylans. Carbohydr Res. 1993;249(2):355–67.

110. Berrin JG, Juge N. Factors affecting xylanase functionality in the degradation of arabinoxylans. Biotechnol Lett. 2008;30(7):1139–50.

111. Polizeli MLTM, Rizzatti ACS, Monti R, Terenzi HF, Jorge JA, Amorim DS. Xylanases from fungi: Properties and industrial applications. Appl Microbiol Biotechnol. 2005;67(5):577–91.

112. Lombard V, Golaconda Ramulu H, Drula E, Coutinho PM, Henrissat B. The carbohydrate-active enzymes database (CAZy) in 2013. Nucleic Acids Res. 2014;42(D1):490–5.

113. Paës G, Berrin JG, Beaugrand J. GH11 xylanases: Structure/function/properties relationships and applications. Biotechnol Adv. 2012;30(3):564–92.

114. Bonnin E, Daviet S, Sorensen JF, Sibbesen O, Goldson A, Juge N, Saulnier L. Behaviour of family 10 and 11 xylanases towards arabinoxylans with varying structure. J Sci Food Agric. 2006;86(11):1618–22.

115. Beaugrand J, Chambat G, Wong VWKK, Goubet F, Rémond C, Paës G, Benamrouche S, Debeire P, O'Donohue M, Chabbert B. Impact and efficiency of GH10 and GH11 thermostable endoxylanases on wheat bran and alkali-extractable arabinoxylans. Carbohydr Res. 2004;339(15):2529–40.

116. Courtin CM, Delcour JA. Relative activity of endoxylanases towards water-extractable and water-unextractable arabinoxylan. J Cereal Sci. 2001;33(3):301–12.

117. Pell G, Taylor EJ, Gloster TM, Turkenburg JP, Fontes CMGA, Ferreira LMA, Nagy T, Clark SJ, Davies GJ, Gilbert HJ. The mechanisms by which family 10 glycoside hydrolases bind decorated substrates. J Biol Chem. 2004;279(10):9597–605.

118. Vardakou M, Dumon C, Murray JW, Christakopoulos P, Weiner DP, Juge N, Lewis RJ, Gilbert HJ, Flint JE. Understanding the structural basis for substrate and inhibitor recognition in eukaryotic GH11 xylanases. J Mol Biol. 2008;375(5):1293–305.

119. Ravn JL, Glitsø V, Pettersson D, Ducatelle R, Van Immerseel F, Pedersen NR. Combined endo-β-1,4-xylanase and α-L-arabinofuranosidase increases butyrate concentration during broiler cecal fermentation of maize glucurono-arabinoxylan. Vol. 236, Animal Feed Science and Technology. 2018. p. 159–69.

120. Cozannet P, Kidd MT, Neto RM, Geraert PA. Next-generation non-starch polysaccharide-degrading, multi-carbohydrase complex rich in xylanase and arabinofuranosidase to enhance broiler feed digestibility. Poult Sci. 2017;96(8):2743–50.

121. Biely P, Singh S, Puchart V. Towards enzymatic breakdown of complex plant xylan structures: State of the art. Biotechnol Adv. 2016;34(7):1260–74.

122. Dodd D, Cann IKO. Enzymatic deconstruction of xylan for biofuel production. GCB Bioenergy. 2009;1(1):2–17.

123. Van den Brink J, De Vries RP. Fungal enzyme sets for plant polysaccharide degradation. Appl Microbiol Biotechnol. 2011;91(6):1477–92.

124. Sørensen HR, Jørgensen CT, Hansen CH, Jørgensen CI, Pedersen S, Meyer AS. A novel GH43 α-L-arabinofuranosidase from *Humicola insolens*: Mode of action and synergy with GH51 α-L-arabinofuranosidases on wheat arabinoxylan. Appl Microbiol Biotechnol. 2006;73(4):850–61.

125. Lagaert S, Pollet A, Courtin CM, Volckaert G. β-Xylosidases and α-L-arabinofuranosidases: Accessory enzymes for arabinoxylan degradation. Biotechnol Adv. 2014;32(2):316–32.

126. Van den Broek LAM, Lloyd RM, Beldman G, Verdoes JC, McCleary B V., Voragen AGJ. Cloning and characterization of arabinoxylan arabinofuranohydrolase-D3 (AXHd3) from *Bifidobacterium adolescentis* DSM20083. Appl Microbiol Biotechnol. 2005;67(5):641–7.

127. McKee LS, Sunner H, Anasontzis GE, Toriz G, Gatenholm P, Bulone V, Vilaplana F, Olsson L. A GH115 α-glucuronidase from *Schizophyllum* commune contributes to the synergistic enzymatic deconstruction of softwood glucuronoarabinoxylan. Biotechnol Biofuels. 2016;9:2.

128. Vardakou M, Katapodis P, Topakas E, Kekos D, Macris BJ, Christakopoulos P. Synergy between enzymes involved in the degradation of insoluble wheat flour arabinoxylan. Innov Food Sci Emerg Technol. 2004;5(1):107–12.

129. Tong X, Lange L, Grell MN, Busk PK. Hydrolysis of wheat arabinoxylan by two acetyl xylan esterases from *Chaetomium thermophilum*. Appl Biochem Biotechnol. 2015;175(2):1139–52.

130. Huntley NF, Patience JF. Xylose: Absorption, fermentation, and post-absorptive metabolism in the pig. J Anim Sci Biotechnol. 2018;9:4.

131. Almirall M, Francesch M, Perez-Vendrell AM, Brufau J, Esteve-Garcia E. The differences in intestinal viscosity produced by barley and β-glucanase alter digesta enzyme activities and ileal nutrient digestibilities more in broiler chicks than in cocks. J Nutr. 1995;125(4):947–55.

132. Pérez J, Muñoz-Dorado J, De La Rubia T, Martínez J. Biodegradation and biological treatments of cellulose, hemicellulose and lignin: An overview. Int Microbiol. 2002;5(2):53–63.

133. Frommhagen M, Westphal AH, van Berkel WJH, Kabel MA. Distinct substrate specificities and electron-donating systems of fungal lytic polysaccharide monooxygenases. Front Microbiol. 2018;9:1080.

134. Horn SJ, Vaaje-Kolstad G, Westereng B, Eijsink VG. Novel enzymes for the degradation of cellulose. Biotechnol Biofuels. 2012;5:45.

135. Jiang KJ, Jiao HC, Song ZG, Yuan L, Zhao JP, Lin H. Corticosterone administration and dietary glucose supplementation enhance fat accumulation in broiler chickens. Br Poult Sci. 2008;49(5):625–31.

136. Lazaridou A, Chornick T, Biliaderis CG, Izydorczyk MS. Composition and molecular structure of polysaccharides released from barley endosperm cell walls by sequential extraction with water, malt enzymes, and alkali. J Cereal Sci. 2008;48(2):304–18.

137. Lafond M, Navarro D, Haon M, Couturier M, Berrin JG. Characterization of a broad-specificity β-glucanase acting on β-(1,3)-, β-(1,4)-, and β-(1,6)-glucans that defines a new glycoside hydrolase family. Appl Environ Microbiol. 2012;78(24):8540–6.

138. Chen L, Sadek M, Stone BA, Brownlee RTC, Fincher GB, Høj PB. Stereochemical course of glucan hydrolysis by barley (1 → 3)- and (1 → 3,1 → 4)-β-glucanases. Biochim Biophys Acta. 1995;1253(1):112–6.

139. Meng X, Slominski BA, Nyachoti CM, Campbell LD, Guenter W. Degradation of cell wall polysaccharides by combinations of carbohydrase enzymes and their effect on nutrient utilization and broiler chicken performance. Poult Sci. 2005;84(1):37–47.

140. Pustjens AM, De Vries S, Schols HA, Gruppen H, Gerrits WJJ, Kabel MA. Understanding carbohydrate structures fermented or resistant to fermentation in broilers fed rapeseed (*Brassica napus*) meal to evaluate the effect of acid treatment and enzyme addition. Poult Sci. 2014;93(4):926–34.

141. Meng X, Slominski BA. Nutritive values of corn, soybean meal, canola meal, and peas for broiler chickens as affected by a multicarbohydrase preparation of cell wall degrading enzymes. Poult Sci. 2005;84(8):1242–51.

142. O'Neill HVM, Smith JA, Bedford MR. Multicarbohydrase enzymes for non-ruminants. Asian-Australasian J Anim Sci. 2014;27(2):290–301.

143. Kornegay ET. Digestion of phosphorus and other nutrients: The role of phytases and factors influencing their activity. In: Bedford MR, Partrdige GG, editors. Enzymes in farm animal nutrition. New York, NY: CABI Publishing; 2001. p. 237–72.

144. Aftab U, Bedford MR. The use of NSP enzymes in poultry nutrition: Myths and realities. Worlds Poult Sci J. 2018;74(2):277–86.

145. Olukosi OA, Beeson LA, Englyst K, Romero LF. Effects of exogenous proteases without or with carbohydrases on nutrient digestibility and disappearance of non-starch polysaccharides in broiler chickens. 2014;2662–9.

146. Munyaka PM, Nandha NK, Kiarie E, Nyachoti CM, Khafipour E. Impact of combined β-glucanase and xylanase enzymes on growth performance, nutrients utilization and gut microbiota in broiler chickens fed corn or wheat-based diets. Poult Sci. 2016;95(3):528–40.

147. Masey-O'Neill H V., Singh M, Cowieson AJ. Effects of exogenous xylanase on performance, nutrient digestibility, volatile fatty acid production and digestive tract thermal profiles of broilers fed on wheat- or maize-based diet. Br Poult Sci. 2014;55(3):351–9.

148. González-Ortiz G, Olukosi O, Bedford MR. Evaluation of the effect of different wheats and xylanase supplementation on performance, nutrient and energy utilisation in broiler chicks. Anim Nutr. 2016;2(3):173–9.

149. Choct M, Kocher A, Waters DLE, Pettersson D, Ross G. A comparison of three xylanases on the nutritive value of two wheats for broiler chickens. Br J Nutr. 2004;92(01):53.

150. Cowieson AJ, Bedford MR, Ravindran V. Interactions between xylanase and glucanase in maize-soy-based diets for broilers. Br Poult Sci. 2010;51(2):246–57.

151. Engberg RM, Hedemann MS, Steenfeldt S, Jensen BB. Influence of whole wheat and xylanase on broiler performance and microbial composition and activity in the digestive tract. Poult Sci. 2004;83(6):925–38.

152. Lee SA, Apajalahti J, Vienola K, González-Ortiz G, Fontes CMGA, Bedford MR. Age and dietary xylanase supplementation affects ileal sugar residues and short chain fatty acid concentration in the ileum and caecum of broiler chickens. Anim Feed Sci Technol. 2017;234:29–42.

153. Józefiak D, Rutkowski A, Jensen BB, Engberg RM. The effect of β-glucanase supplementation of barley- and oat-based diets on growth performance and fermentation in broiler chicken gastrointestinal tract. Br Poult Sci. 2006;47(1):57–64.

154. Khadem A, Lourenço M, Delezie E, Maertens L, Goderis A, Mombaerts R, Höfte M, Eeckhaut V, Van Immerseel F, Janssens GPJ. Does release of encapsulated nutrients have an important role in the efficacy of xylanase in broilers? Poult Sci. 2016;95(5):1066–76.

155. Maisonnier S, Gomez J, Carré B. Nutrient digestibility and intestinal viscosities in broiler chickens fed on wheat diets, as compared to maize diets with added guar gum. Br Poult Sci. 2001;42(1):102–10.

156. Lærke HN, Arent S, Dalsgaard S, Bach Knudsen KE. Effect of xylanases on ileal viscosity, intestinal fiber modification, and apparent ileal fiber and nutrient digestibility of rye and wheat in growing pigs. J Anim Sci. 2015;93(9):4323–35.

157. Ravn JL, Thøgersen JC, Eklöf J, Pettersson D, Ducatelle R, van Immerseel F, Pedersen NR. GH11 xylanase increases prebiotic oligosaccharides from wheat bran favouring butyrate-producing bacteria *in vitro*. Anim Feed Sci Technol. 2017;226:113–23.

158. Ravn JL, Martens HJ, Pettersson D, Pedersen NR. A commercial GH 11 xylanase mediates xylan solubilisation and degradation in wheat, rye and barley as demonstrated by microscopy techniques and wet chemistry methods. Anim Feed Sci Technol. 2016;219:216–25.

159. Le DM, Fojan P, Azem E, Pettersson D, Pedersen NR. Visualization of the anticaging effect of Ronozyme WX xylanase on wheat substrates. Cereal Chem. 2013;90(5):439–44.

160. Lafond M, Bouza B, Eyrichine S, Rouffineau F, Saulnier L, Giardina T, Bonnin E, Preynat A. *In vitro* gastrointestinal digestion study of two wheat cultivars and evaluation of xylanase supplementation. J Anim Sci Biotechnol. 2015;6:5.

161. Sales J, Janssens GPJ. Acid-insoluble ash as a marker in digestibility studies: A review. Vol. 12, Journal of Animal and Feed Sciences. 2003. p. 383–401.

162. De Vries S, Gerrits WJ., Vries D. The use of tracers or markers in digestion studies. In: Moughan PJ, Hendriks WH, editors. Feed evaluation science. Wageningen: Wageningen Academic Publishers; 2018. p. 275–94.

163. Englyst HN, Cummings JH. Simplified method for the measurement of total non-starch polysaccharides by gas-liquid chromatography of constituent sugars as alditol acetates. Analyst. 1984;109(7):937.

164. Thibault JF, Robin JP. Automatisation du dosage des acides uroniques par la méthode de carbazol. Application au cas de matières pectiques. Ann Technol Agric. 1975;24:99–110.

165. Blumenkrantz N, Asboe-Hansen G. New method for quantitative determination of uronic acids. Anal Biochem. 1973;54(2):484–9.

166. McCleary B V., Glennie-Holmes M. Enzymic quantification of (1→3) (1→4)-β-D-glucan in barley and malt. J Inst Brew. 1985 Sep 10;91(5):285–95.

167. Jamroz D, Jakobsen K, Bach Knudsen KE, Wiliczkiewicz A, Orda J. Digestibility and energy value of non-starch polysaccharides in young chickens, ducks and geese, fed diets containing high amounts of barley. Comp Biochem Physiol Part A Mol Integr Physiol. 2002;131(3):657–68.

168. Theander O, Åman P, Westerlund E, Graham H. The Uppsala method for rapid analysis of total dietary fiber. In: Furda I, Brine CJ, editors. New developments in dietary fiber Advances in experimental medicine and biology. Boston, MA: Springer; 1990. p. 273–81.

169. Zhang Z, Smith C, Li W. Extraction and modification technology of arabinoxylans from cereal by-products: A critical review. Food Res Int. 2014;65:423–36.

170. De Ruiter GA, Schols HA, Voragen AGJ, Rombouts FM. Carbohydrate analysis of water-soluble uronic acid-containing polysaccharides with high-performance anion-exchange chromatography using methanolysis combined with TFA hydrolysis is superior to four other methods. Anal Biochem. 1992;207(1):176–85.

171. Bautil A, Verspreet J, Buyse J, Goos P, Bedford MR, Courtin CM. Age-related arabinoxylan hydrolysis and fermentation in the gastrointestinal tract of broilers fed wheat-based diets. Poult Sci. 2019 Oct;98(10):4606–21.

172. Mechelke M, Herlet J, Benz JP, Schwarz WH, Zverlov VV., Liebl W, Kornberger P. HPAEC-PAD for oligosaccharide analysis—novel insights into analyte sensitivity and response stability. Anal Bioanal Chem. 2017;409(30):7169–81.

173. Kabel MA, Schols HA, Voragen AGJ. Mass determination of oligosaccharides by matrix-assisted laser desorption/ionization time-of-flight mass spectrometry following HPLC, assisted by on-line desalting and automated sample handling. Carbohydr Polym. 2001;44(2):161–5.

174. Huisman MMH, Schols HA, Voragen AGJ. Glucuronoarabinoxylans from maize kernel cell walls are more complex than those from sorghum kernel cell walls. Carbohydr Polym. 2000;43(3):269–79.

175. Sanz ML, Martínez-Castro I. Recent developments in sample preparation for chromatographic analysis of carbohydrates. J Chromatogr A. 2007;1153(1–2):74–89.

176. Jonathan MC, DeMartini J, Van Stigt Thans S, Hommes R, Kabel MA. Characterisation of non-degraded oligosaccharides in enzymatically hydrolysed and fermented, dilute ammonia-pretreated corn stover for ethanol production. Biotechnol Biofuels. 2017;10(1):112.

177. Bell RG, Newman KL. Carbohydrate analysis of fermentation broth by high-performance liquid chromatography utilizing solid-phase extraction. J Chromatogr A. 1993;632(1–2):87–90.

178. Robinson RC, Colet E, Tian T, Poulsen NA, Barile D. An improved method for the purification of milk oligosaccharides by graphitised carbon-solid phase extraction. Int Dairy J. 2018;80:62–8.

179. Megherbi M, Herbreteau B, Faure R, Dessalces G, Grenier-Loustalot MF. Solid phase extraction of oligo- and polysaccharides; application to maltodextrins and honey qualitative analysis. J Liq Chromatogr Relat Technol. 2008;31(7):1033–46.

180. Nagy G, Peng T, Pohl NLB. Recent liquid chromatographic approaches and developments for the separation and purification of carbohydrates. Anal Methods. 2017;9(24):3579–93.

181. Bauer S. Mass spectrometry for characterizing plant cell wall polysaccharides. Front Plant Sci. 2012;3:45.

182. Kailemia MJ, Ruhaak LR, Lebrilla CB, Amster IJ. Oligosaccharide analysis by mass spectrometry: A review of recent developments. Anal Chem. 2014;86(1):196–212.

183. Mantovani V, Galeotti F, Maccari F, Volpi N. Recent advances in capillary electrophoresis separation of monosaccharides, oligosaccharides, and polysaccharides. Electrophoresis. 2018;39(1):179–89.

184. Hofmann J, Pagel K. Glycan analysis by ion mobility-mass spectrometry. Angew Chemie Int Ed. 2017 Jul 10;56(29):8342–9.

185. Wang CC, Lai YH, Ou YM, Chang HT, Wang YS. Critical factors determining the quantification capability of matrix-assisted laser desorption/ionization-time-of-flight mass spectrometry. Philos Trans R Soc A Math Phys Eng Sci. 2016;374(2079).

186. Kiely LJ, Hickey RM. Characterization and analysis of food-sourced carbohydrates. In: Davey GP, editor. Glycosylation Methods in Molecular Biology, vol 2370. New York, NY: Humana; 2022. p. 67–95.

187. Kabel MA, Heijnis WH, Bakx EJ, Kuijpers R, Voragen AGJ, Schols HA. Capillary electrophoresis fingerprinting, quantification and mass-identification of various 9-aminopyrene-1,4,6-trisulfonate-derivatized oligomers derived from plant polysaccharides. J Chromatogr A. 2006;1137(1):119–26.

188. Hoffmann RA, Leeflang BR, de Barse MMJ, Kamerling JP, Vliegenthart JFG. Characterisation by [1]H-n.m.r. spectroscopy of oligosaccharides, derived from arabinoxylans of white endosperm of wheat, that contain the elements →4)[α-l-Araf-(1-ar3)]-β-d-Xylp-(1→ or →4)[α-l-Araf-(1→2)][α-lAraf-(1→3)]-β-d-Xylp-(1→. Carbohydr Res. 1991;221(1):63–81.

189. Gruppen H, Hoffmaann RA, Kormelink FJM, Voragen AGJ, Kamerling JP, Vliegenthart JFG. Characterisation by ^{1}H NMR spectroscopy of enzymically derived oligosaccharides from alkali-extractable wheat-flour arabinoxylan. Carbohydr Res. 1992;233:45–64.

190. West C, Elfakir C, Lafosse M. Porous graphitic carbon: A versatile stationary phase for liquid chromatography. J Chromatogr A. 2010;1217(19):3201–16.

191. Maslen SL, Goubet F, Adam A, Dupree P, Stephens E. Structure elucidation of arabinoxylan isomers by normal phase HPLC-MALDI-TOF/TOF-MS/MS. Carbohydr Res. 2007;342(5):724–35.

192. Quéméner B, Ordaz-Ortiz JJ, Saulnier L. Structural characterization of underivatized arabino-xylo-oligosaccharides by negative-ion electrospray mass spectrometry. Carbohydr Res. 2006;341(11):1834–47.

193. Bowman M, Dien B, O'Bryan P, Sarath G, Cotta M. Comparative analysis of end point enzymatic digests of arabino-xylan isolated from switchgrass (*Panicum virgatum* L) of varying maturities using LC-MS[n]. Metabolites. 2012; 19;2(4):959–82.

194. Jonathan MC, Bosch G, Schols HA, Gruppen H. Separation and identification of individual alginate oligosaccharides in the feces of alginate-fed pigs. J Agric Food Chem. 2013;61(3):553–60.

Chapter

2

Impact of xylanase and glucanase on oligosaccharide formation, carbohydrate fermentation patterns, and nutrient utilization in the gastrointestinal tract of broilers

Abstract

This study aimed at determining how the degradation of cereal non-starch polysaccharides (NSP) by dietary enzymes during feed digestion can influence nutrient digestibility and NSP fermentability in broilers. Ninety-six one-day-old male broilers were assigned to 4 different treatments: control and enzyme-supplemented wheat-based (WC, WE) or maize-based (MC, ME) treatments. Enzyme supplementation with endo-xylanase and endo-glucanase occurred from day 20 onwards. On day 28, digesta samples were collected. Nutrient digestibility, NSP recovery, oligosaccharide profile, and short-chain fatty acids (SCFA) content were determined. Enzyme supplementation in WE resulted in a higher starch (3%; $p = 0.004$) and protein (5%; $p = 0.002$) digestion in the ileum compared to WC. Xylanase activity in WE led to *in situ* formations of arabinoxylan-oligosaccharides consisting of 5 to 26 pentose units in the ileum. This coincided with decreased arabinose ($p = 0.059$) and xylose ($p = 0.036$) amounts in the ceca and higher acetate ($p = 0.014$) and butyrate ($p = 0.044$) formation in WE compared to WC. Conversely, complete total tract recovery of arabinoxylan in MC and ME suggested poor maize NSP fermentability. Overall, enzyme action improved nutrient digestibility and arabinoxylan fermentability in the wheat-based diet. The lower response of the maize-based diet to enzyme treatment may be related to the recalcitrance of maize arabinoxylan as well as to the high nutritive value of maize.

1   Introduction

Poultry nutrition is aiming at improving meat production in a cost-effective way while adhering to global strategies, such as animal welfare and reduction in feed antibiotics (1,2). To that end, the development of appropriate interventions is performed in a collaborative way by producers, industry, and academia. Feed supplementation with enzymes has attracted attention since enzymes active on non-starch polysaccharides (NSP) are claimed to offset the anti-nutritive effect of dietary NSP from cereals and legumes (3–5).

NSP are an indispensable part of poultry diets. Once ingested, NSP can be partially soluble or insoluble, depending on their botanical source, chemical structure, chain length, and association degree with the other cell wall components (5–7). Although not digestible by endogenous enzymes, NSP can influence feed use throughout the gastrointestinal tract (GIT) (8,9). The anti-nutritive effect of soluble NSP (arabinoxylan: AX, β-glucan) has been attributed to their ability to increase digesta viscosity, thereby limiting the diffusion of digestive enzymes and nutrients (10–12). Furthermore, increased digesta viscosity may promote pathogen growth in the GIT (10,13). In addition, insoluble NSP (AX, cellulose) can limit the accessibility of the host's enzymes to nutrients enveloped by the cell wall and hinder digestion. NSP can potentially exert prebiotic properties, as they can be fermented by microbiota in the ceca into short-chain fatty acids (SCFA). SCFA can promote gut health and provide additional energy to the host, among others (14,15).

Several animal studies have demonstrated that exogenous NSP-degrading enzymes (NSPases) improved broiler performance (12,16–21). For instance, xylanases (EC 3.2.1.8) are hydrolytic enzymes that split the β-(1→4) bonds between unsubstituted xylosyl residues of the xylan backbone (22). The enzymatic conversion of AX to oligosaccharides (AXOS) with prebiotic potential finds various applications in the feed and food industry (15,22,23). Xylanases belonging to the glycosyl hydrolase (GH) families 10 and 11 are widely used to improve animal performance, alongside other NSPases, such as β-glucanases, mannanases, and galactosidases (23–25). Beta-glucanases target β-glucans and cellulose present in cereal, and their application in animal feed historically preceded that of xylanases (4). The enzymatic depolymerization of soluble AX and β-glucan has been linked with reduced intestinal viscosity and, consequently, improved animal performance (12,26). Nevertheless, viscosity reduction is not the only mechanism involved.

NSPases have been reported to degrade NSP present within the intact cell wall. Such rupture of the cell wall may improve the digestibility of physically entrapped nutrients (18,27). Additionally, the solubilization of polymeric AX and the release of arabinoxylan-oligosaccharides (AXOS) by NSPases has been linked with increased SCFA production in the broiler's ceca and could contribute to the NSP's prebiotic potential (13,15,28,29). Yet, direct evidence of the *in situ* formation of potentially prebiotic AXOS remains elusive. To date, the potential of xylanase and glucanase to release entrapped nutrients and to form prebiotic oligosaccharides is

still under investigation (4). Hence, further research is warranted to understand how the postulated prebiotic formation and encapsulated nutrients release may promote gut health and animal growth.

Therefore, it was hypothesized that dietary supplementation of broilers with carbohydrate-active enzymes would enhance carbohydrate fermentation and nutrient digestion. This research aims at determining the potential of dietary xylanase to form oligosaccharides in the upper gastrointestinal tract of broilers fed wheat- or maize-based finisher diets. We further aim to investigate how the enzymatic degradation of NSP may influence carbohydrate fermentation in the hindgut and nutrient digestion in the small intestine.

2 Materials and methods

2.1 Diets

All experimental basal diets were manufactured by Research Diet Services B.V. (Wijk bij Duurstede, The Netherlands), as summarized in Table 1. Acid-insoluble ash (Diamol; Franz Bertram GmbH, Hamburg, Germany) was added as a digestibility marker to the finisher diets.

Table 1. Ingredient composition (w/w % as-fed) of wheat-based and maize-based diets for the starter (day 0 to 10), grower (day 10 to 20), and finisher (day 20 to 28) phases.

Ingredient (%)	Wheat-Based			Maize-Based		
	Starter	Grower	Finisher	Starter	Grower	Finisher
Wheat	49.4	58.8	65.9	-	-	-
Maize	10.0	5.0	-	57.3	59.6	59.1
Soybean Meal 48CP [1]	24.4	19.5	17.0	27.2	24.3	24.3
Toasted Soybeans	10.0	10.0	8.0	10.0	10.0	8.0
Soybean Oil	1.4	2.4	4.3	0.6	1.7	3.9
Monocalcium phosphate	1.4	1.3	1.0	1.5	1.4	1.2
Limestone	1.4	1.3	1.1	1.4	1.2	1.1
DL-Methionine	0.4	0.3	0.2	0.4	0.3	0.3
L-Lysine HCl	0.3	0.3	0.3	0.3	0.3	0.2
Salt	0.2	0.2	0.3	0.2	0.2	0.3
Na-Bicarbonate	0.3	0.3	0.2	0.3	0.3	0.2
L-Threonine	0.2	0.1	0.1	0.2	0.1	0.1
L-Valine	0.1	0.1	0.1	0.2	0.1	0.0
Coccidiostat	Sacox [2]	Sacox	-	Sacox	Sacox	-
Premix Article [3]	0.5	0.5	0.5	0.5	0.5	0.5
Diamol [4]	-	-	1.0	-	-	1.0
Total	100.0	100.0	100.0	100.0	100.0	100.0

[1]CP: Crude protein. [2]Provided by Huvepharma NV, Berchem, Belgium. [3]Providing per kg of diet: vitamin A (retinyl acetate), 10,000 IU; vitamin D_3 (cholecalciferol), 2500 IU; vitamin E (dl-α-tocopherol acetate), 50 mg; vitamin K_3 (menadione), 1.5 mg; vitamin B_1 (thiamine), 2.0 mg; vitamin B_2 (riboflavin), 7.5 mg; niacin, 35 mg; D-pantothenic acid, 12 mg; vitamin B_6 (pyridoxine-HCl), 3.5 mg; vitamin B_{12} (cyanocobalamine), 20 µg; folic acid, 1.0 mg; biotin, 0.2 mg; choline chloride, 460 mg; Fe ($FeSO_4.H_2O$), 80 mg; Cu ($CuSO_4.5H_2O$), 12 mg; Zn (ZnO), 60 mg; Mn (MnO), 85; I ($Ca(IO_3)_2$), 0.8 mg; Co ($Co_2CO_3(OH)_2$), 0.77 mg; Se (Na_2O_3Se), 0.15 mg. [4]Used as acid-insoluble ash (AIA) digestibility marker.

The finisher diets consisted of two different basal diets (wheat or maize) and were provided in mash form as such (control treatment) or were supplemented with commercially available non-starch polysaccharide-degrading enzymes from *Trichoderma* spp. (Huvepharma NV, Berchem, Belgium) (enzyme treatment). The enzymes present were a GH11 endo-1,4-β-xylanase (EC 3.2.1.8), added at 1500 EPU/kg feed (xylanase

activity), and an endo-1,4-β-glucananase, added at 100 CU/kg feed (glucanase activity). EPU is defined as the amount of enzyme, which releases 0.0083 µmol of reducing sugars (xylose equivalent) per minute from oat spelt xylan at pH 4.7 and 50 °C. CU is defined as the amount of enzyme, which releases 0.128 µmol of reducing sugars (glucose equivalents) per minute from barley β-glucan at pH 4.5 and 30 °C. The above combinations resulted in four dietary treatments (DT); wheat control (WC), wheat enzyme (WE), maize control (MC), and maize enzyme (ME). The analyzed xylanase and glucanase activities of the enzyme-containing DT ranged between 1550 and 1740 EPU/kg feed and 190–240 CU/kg feed, respectively. The measured chemical composition of wheat-based and maize-based DT is shown in Table 2. All reagents used were of analytical grade. The water used throughout laboratory experiments was purified with a Milli-Q Integral 5 (Millipore Corp., Billerica, MN, USA) purification system.

Table 2. Chemical composition (w/w % dry matter basis) and total sugar content of wheat-based and maize-based finisher diets.

Composition (%)	Wheat-Based	Maize-Based
Dry matter (% as-is)	90.3	89.5
Crude protein (N × 6.25)	20.5	20.7
Ash	5.9	6.5
Acid-insoluble ash (AIA)	0.96	0.94
Fat	ca 12.3[1]	ca 16.8[1]
Total carbohydrates	61.3	56.0
Starch	40.4	37.4
NSP[2]	21.0	18.6
Glc[3]	51.6	47.3
Non-glucosyl NSP (NGP)[4]	9.8	8.7
Ara	2.1	1.8
Xyl	2.9	1.6
Gal	2.2	2.8
Uronic acid	1.9	1.7
A/X[5]	0.7	1.1

[1]Not determined, value calculated by difference (fat = dry matter − (crude protein + ash + total carbohydrates)). [2]Non-starch polysaccharides (NSP): residual amount between total carbohydrates and starch. [3]Glc: total glucose content. [4]Non-glucosyl NSP (NGP): sum of all monosaccharides (incl. Man, Rha, Fuc), except Glc. [5]A/X: arabinose/xylose molar ratio.

2.2   Birds management and sample collection

The study was performed at the facilities of the Laboratory for Animal Nutrition and Animal Product Quality (LANUPRO), Department of Animal Sciences and Aquatic Ecology, Ghent University (Belgium), and was conducted in accordance with the ethical standards and recommendations for accommodation and care of laboratory animals covered by the European Directive 2010/63/EU on the protection of animals used for scientific purposes and the Belgian royal decree KB29.05.13 on the use of animals for experimental studies.

Birds were housed in one room throughout the study with 23L:1D and 18L:6D (18L from 4:00 am to 10:00 pm) light schedule during day 0–7 and beyond, respectively. Room temperature was set at 34 °C and linearly decreased to 22 °C by day 28. During the first 5 days, additional infra-red lamp heating (one per pen) was used. Ninety-six (96) one-day-old male broilers (Ross 308) (Vervaeke-Belavi; Tielt, Belgium) were wing-tagged and randomly assigned in two floor pens (48

birds/pen): one receiving wheat-based and one receiving maize-based diets, until day 20 of the experiment. The broilers were vaccinated on the first day of age against Newcastle disease and infectious bronchitis at the hatcheries facilities. At 18 days of age, the vaccination against Newcastle disease was repeated with Nobilis ND Clone 30 by spraying. After arrival, birds were fed the starter diets (day 0–10) and grower diets (day 10–20) *ad libitum* (Table 1). On day 20, the birds were weighed and allocated according to body weight to pens with a wire floor so that the average body weight of birds in each pen was similar. The treatments (WC, WE, MC, and ME) were assigned to pens following a randomized block design. The blocking factor referred to the spatial organization in the facility. Each treatment consisted of 6 replicate pens, with each pen containing 4 birds. During the adaptation period (day 20–24), the birds received the finisher diets ad libitum. The birds were weighed in the morning of day 24 and then continued to be fed finisher diets until day 28. Feed intake was measured per pen and daily (morning of day 25, 26, 27, and 28). During this period, excreta were collected twice daily, homogenized, and an aliquot of a minimum of 250 g fresh material per pen was immediately stored at −20 °C. On day 28, all birds were weighed and euthanized by cervical dislocation followed by bleeding. The gizzard, ileum, and ceca contents were collected, pooled per pen, and frozen at −20 °C. Thawed aliquots were used for the determination of dry matter, ash, and acid-insoluble ash content. Frozen digesta were dried by lyophilization and homogenized with a MM 400 Mixer Mill (Retsch GmbH, Haan, Germany) prior to other chemical analyses. Feed samples were ground to pass a 0.7 mm sieve using a ZM200 mill (Retsch GmbH) prior to analysis.

2.3   Proximate composition analysis

Dry matter, ash, and acid-insoluble ash content

Feed samples and thawed aliquots from the gizzard, ileum, and excreta were dried in an air oven at 80 °C, overnight. Subsequently, the dry matter content was determined by drying at 103 °C, according to the AOAC 935.29 method (30). For that purpose, approximately 5 g feed samples and 1–2 g digesta were weighed in ceramic crucibles. Next, ash and acid-insoluble ash (AIA) contents were determined sequentially, according to the method described by Van Keulen and Young (1977) (31) with certain modifications introduced by Montaño-Vargas et al. (2002) (32), allowing the reduction in sample size. In brief, dried samples were incinerated at 575 °C, and the resulting ash was weighed and boiled with 10 mL 4 N HCl and filtered through ashless filter paper. The retentate was incinerated again at 575 °C, and the remaining AIA was weighed. The organic matter (OM) was calculated by subtracting ash from dry matter.

Cecal dry matter

Due to sample limitations, the dry matter and ash content of cecal digesta were determined gravimetrically using an XP6 Excellence Plus Micro Balance (5 decimals) Mettler-Toledo International Inc., Columbus, OH, USA). Approximately

2 mg of fresh cecal matter was weighed in Eco-Cup LF pyrolysis cups (Frontier Laboratories Ltd., Fukushima, Japan) and were incubated at 80 °C, overnight. Next, the samples were incubated at 103 °C for 4 h and weighed. The ash content was determined by incinerating the dried samples at 575 °C and weighing the remaining material.

Crude protein content

The nitrogen content of feed samples and digesta was determined according to the AOAC 990.03 method (30) using a FlashEA® 1112 NC Analyzer (Thermo Fisher Scien-tific Inc., Waltham, MA, USA). The nitrogen conversion factor used to estimate the crude protein was 6.25.

2.4   Carbohydrate analysis

Sugar composition

The total sugar composition of feed and digesta samples was determined according to Englyst and Cummings (1984) (33). Samples were pre-hydrolyzed in 72% (w/w) H_2SO_4 (30 °C, 1 h) and subsequently hydrolyzed in 1 M H_2SO_4 (100 °C, 3 h). Neutral monosaccharides released were derivatized to alditol acetates and analyzed by gas chromatography on a Trace 1300 GC system (Thermo Fisher Scientific Inc.) equipped with a DB-225 column (Agilent Technologies Inc., Santa Clara, CA, USA) and a flame/ionization detector (FID), using inositol as internal standard. Uronic acid content was determined by the colorimetric m-hydroxyphenyl assay with an automated analyzer (Skalar Analytical B.V., Breda, The Netherlands), according to Blumenkrantz and Asboe-Hansen (1973) and Thibault and Robin (1975) (34,35).

Total starch content

The total starch content of feed and digesta samples was determined according to the AOAC Method 996.11 (KOH format) (36) using the Total Starch Assay Kit (Megazyme, Bray, Ireland) as modified by Martens et al. (2018) (37). In brief, 25 µL supernatant of enzymatically treated samples was transferred in the wells of a 96 well plate followed by the addition of 225 µL glucose oxidase peroxidase (GOPOD) reagent (Megazyme). The reaction was performed in a shaking incubator at 50 °C for 20 min, and the absorbance at 520 nm was read against reagent blank using a Tecan Infinite® F500 (Tecan Group Ltd., Männedorf, Switzerland) spectrophotometer. The glucose (Glc) content was determined using a Glc calibration curve (0.1–0.6 mg/mL).

Oligosaccharide characterization by matrix-assisted laser desorption/ionization time-of-flight mass spectrometry (MALDI-TOF-MS)

The structural characterization of oligosaccharides present in the ileum was performed according to Broxterman et al. (2017) (38) on an ultrafleXtreme™ MALDI-TOF/TOF mass spectrometer (Bruker Daltonics Inc., Billerica, MA, USA). The equipment was controlled with FlexControl 3.3 software and operated in positive mode. The mass spectrometer was calibrated with maltodextrins (Avebe, Veendam, The Netherlands) in a mass range of 500–3000 (m/z). Approximately 100 mg of dried ileal digesta was suspended in 1 mL water and incubated at 99 °C for 30 min. The supernatant was then separated by centrifugation at 20,000 x *g* for 10 min, diluted ten times with water, and desalted with Dowex 50W-X8 resin (Sigma-Aldrich, St. Louis, MO, USA). Next, an aliquot (100 µL) was removed, and NaCl was added at 1 µM to allow the formation of sodium adducts during ionization. Afterward, sample (1 µL) was co-crystallized with matrix solution (1 µL); 25 mg/mL dihydroxy-benzoic acid (Sigma-Aldrich) in 50% (v/v) acetonitrile (VWR International B.V., Amsterdam, The Netherlands) on a target plate under a stream of dry air.

2.5   Microbial metabolites analysis

Short chain fatty acids (SCFA)

The SCFA content of ileal and cecal digesta was determined by gas chromatography (GC-FID), as described by Logtenberg et al. (2020) (39). An aqueous solution of acetic, butyric, propionic, isobutyric, and isovaleric acids (Sigma-Aldrich) was prepared for quantification. The standard solution was diluted to obtain final concentrations in the range of 0.01–1.0 mg/mL and was treated similarly to the samples.

Lactic and succinic acid

The concentrations of lactic and succinic acids in ileal and cecal samples were determined by high-performance liquid chromatography (HPLC), according to Jonathan et al. (2012) (40). The samples were analyzed with an Ultimate 3000 HPLC System (Dionex Corp., Sunnyvale, CA, USA) equipped with an Aminex HPX-87 H column (Bio-Rad, Richmond, VA, USA) and a guard column. The HPLC system was coupled to a Shodex RI-101 refractive index detector (Showa Denko KK, Kawasaki, Japan). The samples (injection volume 10 µL) were run isocratically using 5 mM H_2SO_4 as eluent at 0.6 mL/min flow rate, with column temperature at 40 °C. A standard solution containing lactic and succinic acid (Sigma-Aldrich) was prepared for quantification and was diluted to obtain final concentrations in the range of 0.1–10.0 mg/mL.

2.6 Calculations

The apparent ileal digestibility (AID) and apparent total tract digestibility (ATTD) of organic matter, starch, and protein were estimated with Equation (1), using AIA as an indigestible marker (20):

$$AID \; or \; ATTD \; (\%) = \frac{\left(\left(\frac{NT_d}{AIA_d}\right) - \left(\frac{NT_{i,e}}{AIA_{i,e}}\right)\right)}{\left(\frac{NT_d}{AIA_d}\right)} * 100 \quad (1)$$

Where NT_d, NT_i, NT_e is the measured nutrient content (% DM) in the diet, ileum, and excreta, respectively, and AIA_d, AIA_i, AIA_e is the measured marker content (% DM) in the diet, ileum, and excreta. NT_i and AIA_i, and NT_e and AIA_e were used to determine AID and ATTD, respectively.

The recovery of NSP in the ileum and excreta was determined through the constituting monosaccharides. For that reason, the recovery of xylose, arabinose, galactose, uronic acid, and non-glucosyl NSP (NGP) was estimated using Equation (2):

$$Recovery \; (\%) = 100 - \frac{\left(\left(\frac{M_d}{AIA_d}\right) - \left(\frac{M_{i,e}}{AIA_{i,e}}\right)\right)}{\left(\frac{M_d}{AIA_d}\right)} * 100 \quad (2)$$

Where M_d, M_i, M_e is the measured monosaccharide content (% DM) in the diet, ileum, and excreta, respectively, and AIA_d, AIA_i, AIA_e is the measured marker content (% DM) in the diet, ileum, and excreta. M_i and AIA_i, and M_e and AIA_e were used to determine recovery in the ileum and excreta, respectively.

2.7 Statistical analysis

The obtained data were subjected to analysis of variance (ANOVA) using the R statistical software (R Core Team), with the pen being the experimental unit. The observations from wheat-based and maize-based DT were modeled separately. The effect of enzyme treatment (E; control vs. enzyme) on carbohydrate content and microbial metabolites was determined. Nutrient digestibility and NSP recovery were modeled using E and Sampling Site (S: ileum for AID and excreta for ATTD) as main effects, including their two-way interaction term. The blocking factor was considered as the main effect in the model. To test the significance of the differences between different treatments, Tukey's post-hoc test was performed, with a significance threshold set at $p < 0.05$.

The data obtained for NSP content and recovery along the GIT, SCFA content in the ceca, nutrient digestibility, and animal growth were subjected to principal component analysis (PCA) using R. Next, the Pearson correlation coefficients of the aforementioned variables were calculated, and the corresponding correlation matrix was constructed to visualize the relations. Correlations with $p < 0.05$ were considered significant.

3   Results

3.1   Growth parameters

The growth of broilers was recorded during the finisher period (day 24–28) in order to evaluate the possible effect of enzyme addition on the broiler's nutritional responses (Table S1). It should be noted that the first aim of this experiment was not to evaluate the effect of the enzyme on animal performance. Therefore, the measured growth parameters are approached with caution and only considered in the context of this study. The obtained values for body weight (BW), average daily gain (ADG), and average daily feed intake (ADFI) were lower, and the feed conversion ratio (FCR) was higher than breed performance objectives for 28-day-old male Ross 308 broilers (41), mainly because broilers were fed mash diets. Overall, WE presented increased BW (6% higher; $p = 0.021$), ADG (14% higher; $p = 0.059$) and ADFI (6% higher; $p=0.281$) values compared to WC, while FCR decreased by 7% ($p = 0.018$). ME presented numerically positive responses compared to MC, but not to the extent observed in the wheat-based DT. For example, ME presented increased BW (3% higher; $p = 0.136$), ADG (6% higher; $p = 0.320$) and ADFI (4% higher; $p = 0.285$) values compared to MC, while FCR was decreased by 2% ($p = 0.498$).

3.2   Oligosaccharide profiles in ileal digesta

The addition of dietary xylanase is hypothesized to degrade polymeric arabinoxylan (AX) to oligosaccharides (AXOS) during feed digestion, and these products are expected to be released in solution. The ability of dietary xylanase to form oligosaccharides was determined by MALDI-TOF-MS analysis of the water-soluble fraction of ileal digesta from the four DT (Fig. 1, S1 and S2).

At first glance, m/z values corresponding to homologous series of hexose oligomers were abundantly detected in all samples (sequential increments of m/z 162). The hexose oligomers in both wheat-based DT had a polymerization degree (DP) of 3 to 21 (Fig. 1A,B). Hexose oligomers of DP 3 to 10 were detected in both maize-based DT (Fig. 1C,D). Another series of three oligomers with two consecutive m/z 162 increments (m/z 1419, 1581, and 1743) was present in all four DT. Alongside these compounds, a homologous series with increments of m/z 132 was detected in WE, representing pentose oligomers (Fig. 1B). The pentose oligomers were detected in all six replicate pens (Fig. S1) between m/z 701 and m/z 3444 and presented DP 5–26. The pentose oligomers were unique for the WE treatment and were absent in WC, MC, and ME.
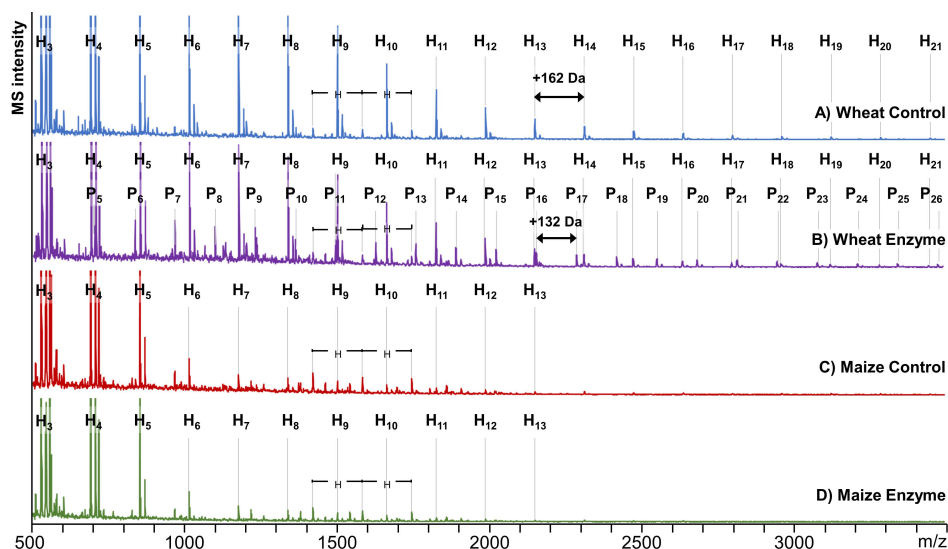
Fig. 1. MALDI-TOF-mass spectra of supernatants of ileal digesta from broilers fed wheat control (**A**), wheat enzyme (**B**), maize control (**C**), and maize enzyme (**E**) dietary treatments (DT). The number of hexose (H_n) or pentose (P_n) monomers constituting each oligomer is presented in the mass spectra.

3.3 Monosaccharide contents in digesta

In order to evaluate the effect of enzyme addition on the carbohydrate content present in digesta, the monosaccharide content after acid hydrolysis of all carbohydrates present in the finisher diets, gizzard, ileum, ceca, and excreta was determined (Table 2, 3, S2). Glucose (Glc) was the most abundant monosaccharide in all diets, followed by xylose (Xyl), arabinose (Ara), galactose (Gal), and uronic acids (UA) (Table 2). Mannose (Man), rhamnose (Rha) and fucose (Fuc) were present in the diets at values lower than 0.6%, 0.1% and 0.2% (w/w), respectively (data not shown). Man, Rha and Fuc were taken into account when estimating the total carbohydrate contents but will not be further discussed due to their low amounts.

Gizzard: Glc was the main carbohydrate present in the gizzard and ranged between 33.7% (w/w) and 38.5% (w/w) (Table 3). In wheat-based DT, Xyl was the second most abundant carbohydrate (7.8–8.9% (w/w)), followed by Ara, Gal and UA. WC presented significantly higher Glc content than WE ($p = 0.014$). At the same time, WC presented lower Ara ($p = 0.043$), Xyl ($p = 0.051$), Gal ($p = 0.001$), UA ($p = 0.010$) and non-glucosyl NSP (NGP) ($p = 0.013$) contents than WE. No differences in total carbohydrates ($p = 0.203$) and A/X ratio ($p = 0.230$) were observed between WC and WE. MC and ME presented similar monosaccharide contents in the gizzard ($p > 0.05$).

Table 3. Effect of the enzyme (E) on the monosaccharide content (% w/w dry matter basis) in the gizzard and ceca of broilers fed wheat-based (WC, WE) (n = 6) and maize-based (MC, ME) (n = 6) DT.

	Gizzard							
% w/w	WC	WE	SEM[1]	*p* value[2]	MC	ME	SEM	*p* value
Ara	5.29	5.80	0.16	0.043	2.68	2.70	0.08	0.861
Xyl	7.80	8.90	0.35	0.051	3.00	2.65	0.13	0.093
Glc	38.49	34.46	0.96	0.014	33.73	34.95	0.55	0.145
Gal	3.52	3.84	0.05	0.001	2.67	2.54	0.06	0.174
UA	2.97	3.28	0.07	0.010	3.48	3.40	0.07	0.417
Total	59.62	58.05	0.82	0.203	46.68	47.27	0.46	0.393
NGP	21.13	23.59	0.58	0.013	12.95	12.31	0.33	0.198
A/X [3]	0.68	0.65	0.01	0.230	0.90	1.03	0.04	0.062
	Ceca							
% w/w	WC	WE	SEM	*p* value	MC	ME	SEM	*p* value
Ara	0.31	0.24	0.02	0.059	0.22	0.19	0.01	0.066
Xyl	0.58	0.23	0.10	0.036	0.10	0.08	0.01	0.217
Glc	6.19	7.72	0.98	0.295	6.18	5.54	0.73	0.553
Gal	1.42	1.44	0.09	0.918	1.12	1.12	0.04	0.997
UA	1.22	1.26	0.04	0.563	1.00	0.88	0.06	0.217
Total	11.41	12.50	1.07	0.488	10.31	9.35	0.74	0.382
NGP	5.22	4.77	0.26	0.248	4.14	3.81	0.10	0.036
A/X	0.64	1.11	0.09	0.005	2.40	2.51	0.19	0.689

[1]Standard error of the mean. [2]Estimated by ANOVA with enzyme addition (E) as a factor. [3]A/X: arabinose/xylose molar ratio.

Ceca: The Xyl content in the ceca significantly decreased upon enzyme addition (p = 0.036), from 0.6% (w/w) in WC to 0.2% (w/w) in WE. The Ara content showed a trend to decrease upon enzyme addition (p = 0.059) from 0.3% (w/w) in WC to 0.2% (w/w) in WE. The decrease in Ara and Xyl contents coincided with a significantly higher A/X ratio in WE (1.11) compared to WC (0.64) (p = 0.005). The Xyl content in the ceca for the maize-based DT was found to be lower than 0.1% (w/w), while higher A/X values (MC: 2.41, ME: 2.52) than in the wheat-based DT were obtained. ME presented significantly lower NGP content than MC (p = 0.036). It should be mentioned that the cecal samples contained 1.1–1.3% (w/w) rhamnose (data not shown). Since this monosaccharide was only present in trace amounts in the diets, it is suspected to originate from the bacterial cell wall.

Ileum and excreta: Carbohydrates accounted for approximately 44.9–48.8% (w/w) of the solids present in the ileum (Table S2). Glc was the most abundant carbohydrate, followed by Xyl, Gal, Ara, and UA. The carbohydrate content in the excreta was somewhat lower than in the ileum (35.0–37.1% (w/w)) (Table S2). Glc was the most abundant carbohydrate, followed by Xyl, Ara, Gal, and UA. To further investigate the transit and fermentability of NSP and individual polymers in the GIT, the recovery values of individual carbohydrates in the ileum and excreta (Equation (2)) were determined and are shown next.

3.4   Recovery of NSP in the ileum and the total tract

The transit and fermentability of NSP and individual polymers in the GIT were studied by estimating the recovery values of Ara, Xyl, Gal, UA, and NGP in the ileum and excreta (total tract) (Table 4). The absence of significant interactions between enzyme (E) and sampling site (S: ileum, total tract) suggested that the

effect of the enzyme was independent of the sampling site for both wheat-based and maize-based DT.

Table 4. Effect of the enzyme (E) and sampling site (S) on Ara, Xyl, Gal, uronic acid (UA), and Non-glucosyl NSP (NGP) recovery (%) in the ileum and total tract of broilers fed wheat-based (WC, WE) (n = 5–6) and maize-based (MC, ME) (n = 5–6) DT.

Dietary Treatment (DT)	NSP Recovery %									
	Ara		Xyl		Gal		UA		NGP	
	Ileum	Total	Ileum	Total	Ileum	Total	Ileum	Total	Ileum	Total
WC	107.97[a]	83.85[b]	94.82[a]	74.74[b]	104.47[a]	57.31[b]	73.55[a]	59.96[b,*]	94.81[a]	68.82[b]
WE	101.02[a]	80.22[b]	88.50[a]	70.29[b]	102.7[a,*]	58.77[b]	74.36[a]	62.49[b]	90.14[a]	68.00[b]
SEM[1]	2.12		2.20		1.42 (* 1.57)		1.25 (* 1.39)		1.70	
	Model established *p* values									
E	0.022		0.025		0.996		0.193		0.125	
S	<0.001		<0.001		<0.001		<0.001		<0.001	
E x S	0.442		0.675		0.325		0.548		0.274	
MC	99.3	104.13	96.73	102.17	99.04[a]	67.63[b]	101.43	96.56	99.02	85.96
ME	105.85	109.47*	102.16	107.88*	107.54[a,*]	66.91[b,*]	96.02	101.66	99.83	92.98
SEM	3.92 (* 4.34)		3.10 (* 3.42)		2.82 (3.12)		3.43		3.53	
	Model established *p* values									
E	0.214		0.112		0.194		0.965		0.281	
S	0.743		0.111		<0.001		0.912		0.011	
E x S	0.665		0.977		0.143		0.143		0.390	

[1]Standard error of the mean, for n = 6. *In case of missingness (n = 5), the adjusted SEM value is presented between brackets. [a,b]Recovery values of the same NSP measured in the ileum and excreta within cereal type not sharing common notation differ significantly (p < 0.05).

In the wheat-based DT, the sampling site significantly influenced the recovery values of all measured monosaccharides (p < 0.05). Significantly lower values were obtained in the total tract compared to the ileum in all cases (p < 0.05). Enzyme addition significantly affected the recovery of Ara (p = 0.022) and Xyl (p = 0.025). Ara recoveries in the ileum were close to 100% for both WC and WE. Furthermore, 94.8% and 88.5% of the Xyl present in the diet was recovered in the ileum for WC and WE, respectively. The differences observed between WC and WE regarding the Ara and Xyl recovery in the ileum were not significant (Ara: p = 0.130*,* Xyl: p = 0.214). Nevertheless, the Ara and Xyl values in WE tended to be lower than in WC by 6.3% and 6.7%, respectively. Similarly, the total tract recoveries of Ara and Xyl obtained in WE tended to be lower than the ones obtained in WC (4.3% and 5.9% lower, respectively) but not significantly different (p = 0.459 and p = 0.628, respectively).

In maize-based DT, the sampling site significantly influenced the Gal (p < 0.001) and NGP (p = 0.011) recovery values, with lower values being obtained in the total

tract compared to the ileum. On the contrary, there was no significant effect of sampling site on Ara ($p = 0.743$), Xyl ($p = 0.111$) and UA ($p = 0.912$) recovery. The ileal and total tract recoveries of Xyl, Ara, and UA were similar, fluctuating around 100% of the constituent monosaccharides present in the diet. No significant effect of enzyme addition was observed in all cases ($p > 0.05$).

3.5 Lactate, succinate, and short-chain fatty acids (SCFA) contents in the ileum and the ceca

The formation of lactate, succinate, and SCFA in the broiler's ileum and ceca was determined to monitor the effect of enzyme supplementation on the fermentation processes along the GIT (Table 5). Lactate was the most abundant metabolite in the ileum (129.4–250.2 µmol/g dry matter basis), while acetate and succinate contents ranged between 2.5 and 9.9 µmol/g. Acetate (172.7–354.5 µmol/g) and butyrate (53.1–78.5 µmol/g) were the two most abundant SCFA in the ceca, followed by propionate (11.0–31.4 µmol/g). Isobutyrate and isovalerate were detected in the ceca in considerably lower amounts (1.3–4.3 µmol/g) for all DT.

Table 5. Effect of the enzyme (E) on acetate (Ace), lactate (Lac) and succinate (Suc) content in the ileum, and acetate (Ace), butyrate (But), propionate (Pro), isobutyrate (Ibu), isovalerate (Iva), and total short-chain fatty acids (SCFA) content (µmol/g dry matter basis) in the ceca of broilers fed wheat-based (WC, WE) ($n = 6$) and maize-based (MC, ME) ($n = 5–6$) DT.

Dietary Treatment (DT)	Ileum (µmol/g)			Ceca (µmol/g)					
	Ace	Lac	Suc	Ace	But	Pro	Ibu	Iva	Total SCFA[2]
WC	2.52	129.42	3.30	172.66	53.12	11.02	1.38	1.51	239.69
WE	9.47	250.20	7.59	250.94	73.08	11.15	1.32	1.54	338.03
SEM[1]	1.34	56.74	1.01	18.70	6.13	0.75	0.13	0.14	24.91
	Model established p values								
E	0.004	0.163	0.013	0.014	0.044	0.906	0.728	0.881	0.019
MC	9.95	239.87	9.47	354.47	78.46	31.43	3.38	4.26	472.42
ME	7.88	145.51	7.83	287.77	59.29	23.60	2.70	3.85	378.16
SEM	1.05	30.95	1.39	19.57	4.31	2.32	0.33	0.28	24.34
	Model established p values								
E	0.195	0.057	0.425	0.037	0.010	0.039	0.185	0.333	0.021

[1]Standard error of the mean, for n = 6, except for isobutyrate and isovalerate in MC and ME, where $n = 5$. [2]Sum of individual SCFA in the ceca.

In the wheat-based DT, enzyme addition significantly increased acetate ($p = 0.004$) and succinate ($p = 0.013$) contents in the ileum. However, it did not significantly affect lactate contents ($p = 0.163$), even though the value obtained in WE was 1.9 times higher than in WC. The reason behind the lack of significance could be the high variation in individual values. Furthermore, enzyme addition significantly increased the contents of acetate ($p = 0.014$), butyrate ($p = 0.044$) and total SCFA ($p = 0.019$) in the ceca. No significant influence of enzyme addition was observed in the contents of propionate ($p = 0.906$), isobutyrate ($p = 0.728$) and isovalerate ($p = 0.881$).

In the maize-based DT, enzyme addition showed a trend to decrease lactate formation in the ileum ($p = 0.057$), but did not impact acetate ($p = 0.195$) and succinate ($p = 0.425$) contents. In the ceca, enzyme addition was found to significantly decrease the contents of acetate ($p = 0.037$), butyrate ($p = 0.010$), propionate ($p = 0.039$) and total SCFA ($p = 0.021$), while it did not impact the contents of isobutyrate ($p = 0.185$) and isovalerate ($p = 0.333$).

Overall, enzyme addition was found to impact the bacterial metabolite formation differently in wheat-based and maize-based DT, highlighting the importance of the cereal type present for hindgut fermentation.

3.6   Nutrient digestibility

The impact of enzyme action on nutrient (organic matter: OM, starch, and crude protein: CP) digestion in the small intestine and OM and starch fermentation in the hindgut is presented in Table 6. The apparent ileal digestibility (AID) values obtained were between 72.2 and 75.3% for OM, 94.8–97.5% for starch, and 77.0–81.2% for CP. The apparent total tract digestibility (ATTD) values obtained ranged between 73.3 and 75.4% for OM and 96.0–98.2% for starch.

Table 6. Effect of the enzyme (E) and sampling site (S) on the apparent ileal digestibility (AID%) and apparent total tract digesti-bility (ATTD%) of organic matter, starch and crude protein of broilers fed wheat-based (WC, WE) ($n = 6$) and maize-based (MC, ME) ($n = 5$–6) DT.

Dietary Treatment (DT)	Organic Matter (OM)		Starch		Crude Protein (CP)	
	AID %	ATTD %	AID %	ATTD %	AID %	ATTD %
WC	72.17[b]	74.02[a]	94.76[b]	95.99[ab]	76.99	-
WE	75.31[a]	75.44[a]	97.35[a]	97.23[a]	81.17	-
SEM[1]	0.38		0.45		0.64	
	Model established p values					
E	<0.001		<0.001		0.002	
S	0.019		0.232		-	
E x S	0.036		0.152		-	
MC	74.60	73.27	97.11[b]	98.15[a]	80.98	-
ME	74.75	73.48	97.48[a,b,*]	98.23[a]	78.21*	-
SEM	0.57		0.23 *(0.26)		0.99 *(1.11)	
	Model established p values					
E	0.757		0.384		0.102	
S	0.033		0.001		-	
E x S	0.955		0.603		-	

[1]Standard error of the mean, for $n = 6$. * In case of missingness, the adjusted SEM value ($n = 5$) is presented between brackets. [a,b] Values corresponding to the same measured parameter (OM, starch, CP) within cereal type not sharing common notation differ significantly ($p < 0.05$).

A significant enzyme (E) and sampling site (S) interaction ($p = 0.036$) was observed only for OM in the wheat-based DT. Firstly, the pair-wise comparison between the OM-AID and ATTD values of WC and WE revealed that WC-ATTD was significantly higher than WC-AID ($p = 0.014$). However, similar values between

WE-AID and WE-ATTD were obtained (p = 0.995). Secondly, WE-AID was significantly higher than WC-AID (p < 0.001). Lastly, WE-ATTD showed a trend to be higher than WC-ATTD (p = 0.074).

Enzyme (E) significantly impacted starch digestibility (p = 0.001). In particular, starch WE-AID was significantly higher than WC-AID (p = 0.004). No significant differences were found between WE-AID and WE-ATTD (p = 0.998). Similarly, no significant differences were found between WC-AID and WC-ATTD (p = 0.255). Lastly, WC-ATTD was similar to WE-AID (p = 0.185) and WE-ATTD (p = 0.248) as well. The similarity of WE-AID and WE-ATTD with WC-ATTD, but not with WC-AID, suggests that the non-significant increase of 1.3% as observed in starch digestibility for WC between the ileum and the total tract could have biological relevance. Finally, enzyme addition significantly increased CP-AID (p = 0.002). The nitrogen content in excreta was not corrected for endogenous secretions, and the CP ATTD values were not estimated.

No significant E x S interactions were observed in the maize-based DT (p > 0.05). Moreover, enzyme addition did not affect significantly OM (p = 0.757), starch (p = 0.384) or CP (p = 0.102) digestibility. Although the sampling site had a significant effect on OM (p = 0.033) digestibility, the individual AID and ATTD values of MC and ME were similar (p > 0.05). Next, starch digestibility was significantly affected by the sampling site (p = 0.001), with higher values being obtained in the total tract compared to the ileum. In particular, MC-ATTD was significantly higher than MC-AID (p = 0.032). ME-AID was not significantly different from MC-AID (p = 0.766), but at the same time was similar to both MC-ATTD (p = 0.242) and ME-ATTD (p = 0.148) values. Hence, a subtle improvement in starch AID due to enzyme addition in maize-based DT could still be of biological importance.

3.7 Interrelationships between nutrient digestibility, NSP fermentation in the hindgut and growth parameters

Principal component analysis was performed to obtain an overview of the response of the different dietary treatments to the investigated parameters (Fig. 2).

The first principal component (PC1) explained 39.65%, and the second principal component (PC2) explained 19.7% of the total variance. Overall, PC1 appeared to separate the wheat-based from the maize-based DT while WC and WE were further separated by PC2. WC presented high Ara and Xyl contents in the cecum (Ara-Cec, Xyl-Cec) and high FCR values. WE formed a separate cluster from WC mainly due to the higher Xyl-Giz, Ara-Giz, OM-AID, OM-ATTD, and CP-AID loadings. The maize-based DT were clustered together and presented differences compared to both WC and WE. Both MC and ME were characterized by high Ara, Xyl, and NGP recovery in the ileum (Ril) and excreta (Rex).
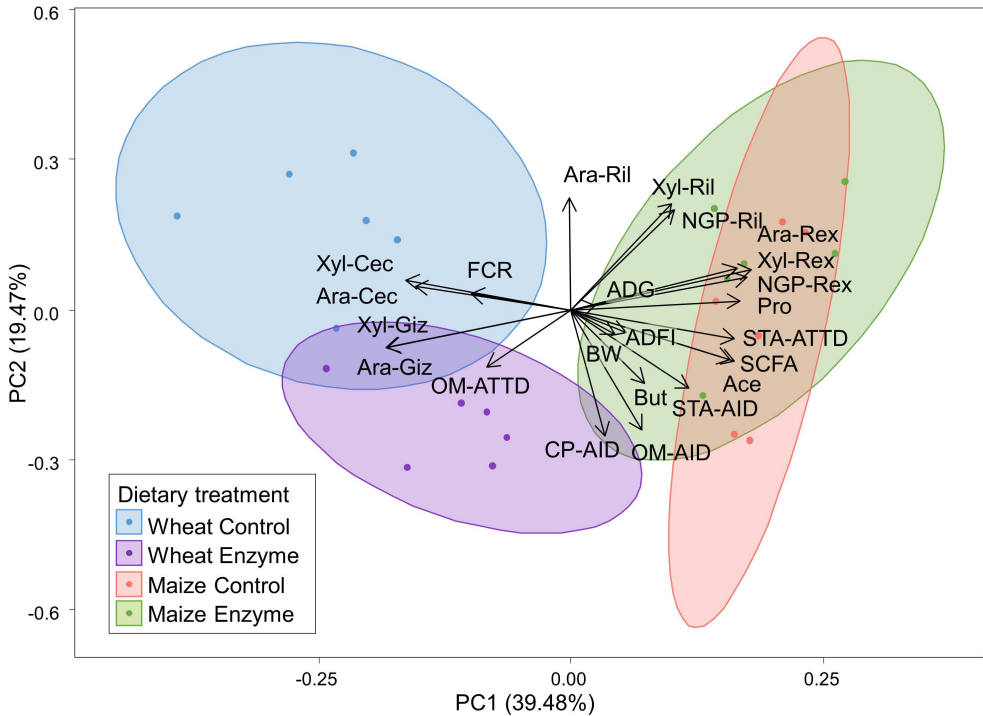
Fig. 2. Principal component analysis (PCA) biplot of wheat control (blue), wheat enzyme (purple), maize control (red), and maize enzyme (green) dietary treatments (DT). The scores were plotted for PC1 and PC2. The amount of variance explained by each PC is shown in parentheses. The variables used were: (i) NSP-related parameters; ileal (Ril) and total tract (Rex) recovery of Ara, Xyl and non-glucosyl NSP (NGP), and Ara and Xyl contents (% w/w) in the gizzard (Giz) and the ceca (Cec), (ii) acetate (Ace), butyrate (But), propionate (Pro) and total short-chain fatty acids (SCFA) contents in the ceca, (iii) nutrient digestibility parameters: apparent ileal digestibility (AID) and apparent total tract digestibility (ATTD) of organic matter (OM) starch (STA), and crude protein (CP), and (iv) animal growth parameters: body weight (BW), feed conversion ratio (FCR), average daily feed intake (ADFI), and average daily gain (ADG).

The potential interrelationships between the investigated parameters were then examined (Fig. 2 and Fig. S3). Organic matter (OM) AID was negatively correlated with Ara-Cec and Xyl-Cec and with Ara-Ril. On the contrary, OM-ATTD presented positive correlations with Ara and Xyl contents in the gizzard (Giz) and the ceca, while it was negatively correlated with their ileal and total tract recoveries. Starch AID and ATTD were negatively correlated with Ara and Xyl contents in the gizzard and the ceca and were positively correlated with Ara and Xyl recovery in the excreta. The SCFA were negatively correlated with Ara and Xyl contents in the gizzard and the ceca but were positively correlated with Ara, Xyl recovery in the excreta (Rex), and starch ATTD. While unexpected, the positive correlation between Ara and Xyl total tract recovery and SCFA content was due to the maize-based DT, as those treatments presented high values for both sets of parameters.

High SCFA loadings were positively correlated with improved animal growth. Improved animal growth was illustrated by high loadings of BW, ADFI, ADG, and low FCR loadings. Finally, the Ara and Xyl contents in the ceca were negatively correlated with animal growth.

4 Discussion

4.1 The effect of NSPase on carbohydrate recovery and oligosaccharide profiles in the upper GIT

NSP content in the gizzard

The activity of dietary NSPases in the gizzard has been reported to be limited, mainly due to the acidic environment (42). Nevertheless, cell wall degradation during the early stages of digestion (43) could set the scene for improved feed assimilation in the small intestine and the hindgut. Hence, the potential influence of dietary NSPases on carbohydrate content in the gizzard was investigated. The combination of xylanase and glucanase used in this study (NSPase) increased the arabinoxylan (AX) concentration in the gizzard but did not impact the A/X ratio (Table 3). This indicates the presence of higher levels of AX with similar structural characteristics in WE compared to WC. In addition, Gal and UA-containing NSP presented higher contents in the gizzard for WE. At the same time, WE presented a lower Glc content in the gizzard than WC. The differences in Glc content between WC and WE probably reflect differentiated starch retention in the gizzard, as affected by the enzyme, since non-starch Glc, such as cellulose, would be expected to behave similarly to other NSP. NSPase has been previously shown to influence the gizzard's contents and empty weight, especially in whole wheat diets (17,42,44,45). In addition, NSPase appeared to influence the type and level of feed components being retained in the gizzard. For example, the enzymatic degradation of the cell wall could have released entrapped nutrients, such as starch, thus facilitating their absorption in the small intestine. On the contrary, cell wall material has also been shown to accumulate in the gizzard, as previously reported (9,46). The above observations were not present in the maize-based DT, as NSPase addition in ME did not impact the carbohydrate content. Still, further research is warranted to investigate the extent of the potential activity of NSPase in the gizzard.

Xylanase releases soluble oligosaccharides in the small intestine

Xylanase activity in the proximal GIT (gizzard, small intestine) is expected to have released arabinoxylan-oligosaccharides (AXOS). Non-digestible oligosaccharides, such as AXOS, are expected to accumulate in the ileum. Hence, the presence of soluble oligosaccharides in the ileum of the broilers was determined (Fig. 1) to provide direct evidence of xylanolytic activity during feed digestion.

Hexose oligosaccharides (HexOS) detection in the ileum could be partly attributed to incomplete starch hydrolysis. For example, the presence of unabsorbed maltodextrins, mainly maltose and maltotriose, has previously been detected in the ileum of pigs (47). The HexOS detected in WC, and WE presented longer chain lengths than the ones detected in MC and ME. Isolated wheat starch has been shown to be more rapidly digestible than maize starch (37). Hence, none or only small differences between wheat and maize regarding the maltodextrins present at the end of the small intestine were expected. Therefore, maltodextrins alone are considered unlikely to account for the observed differences in HexOS profiles. It is suspected that HexOS represent (partly) a series of compounds with similar masses to maltodextrins. Wheat grains are known to contain fructans and fructo-oligosaccharides (FOS) (48), whose presence could further explain differences in HexOS profile between wheat-based and maize-based DT. Preliminary findings (data not shown) demonstrated the disappearance of most HexOS peaks after incubation with a combination of amyloglucosidase and endo- and exo-inulinase. The potential detection of FOS in the ileum presents great interest because these compounds are known for their prebiotic activity and can play an important role during hindgut fermentation (48,49).

Pentose oligosaccharides were detected in WE ileal digesta next to HexOS, and their release upon xylanase addition demonstrates the enzymatic degradation of (hetero)xylan to (A)XOS. Considering that both xylose and arabinose are pentoses, it was not possible to determine their relative ratio in each oligomer. Approximately 60–65% of the Xyl residues of wheat AX is unsubstituted, and these unsubstituted Xyl residues are distributed among Ara-substituted Xyl moieties as clusters of 2 to 5 consecutive residues (7,23,50,51). Longer, unsubstituted xylan fragments would have either been further degraded by the xylanase or would have been adsorbed to cellulose and remained insoluble (52). Consequently, the detected oligosaccharides consisting of 5 to 26 pentose units will contain both Xyl and Ara moieties in their structure, and they correspond to enzymatically released arabinoxylan-oligosaccharides (AXOS). Hence, it is demonstrated that dietary supplementation of xylanase led to the *in situ* release of AXOS in the ileum of broilers fed wheat-based diet. Pentose oligosaccharides below DP 6, ascribed as XOS, were recently detected in the jejunum of broilers fed wheat diets in the presence of xylanase as well as in the control treatment (53). The presence of small, unsubstituted XOS (DP 2–6) could not be confirmed in the present study. AXOS DP > 5 were found to be the dominant oligomeric products of the enzymatic depolymerization of AX in the broiler's small intestine by the supplemented xylanase. AXOS direct supplementation in broiler diets is reported to promote the growth of bifidobacteria in the ceca (15,29). Hence, the current findings strengthen the hypothesis that xylanase action in the upper GIT can generate oligosaccharides exhibiting prebiotic properties.

Enzyme addition in ME did not result in AXOS release. The recalcitrance of maize AX to xylanolytic activity can be attributed to its complex structure and low water-

solubility (5,24,53,54). For instance, substituents such as arabinose and glucuronic acid are known to hinder the activity of certain xylanases, especially the ones belonging to the GH11 family (55). Indeed, the hindrance of GH11 xylanases toward maize AX has been reported in a previous *in vitro* study (56). The potential oligosaccharide release by glucanase could not be confirmed in this study. This could be partly attributed to the low amount of β-glucan present in both wheat and maize (5). Additionally, the high abundance of maltodextrins and FOS observed in the ileum could have potentially masked the presence of cello-oligosaccharides with the same mass. Hydrolysis of cell wall NSP, such as AX and cellulose, by xylanase and/or glucanase, is believed to have occurred in both wheat and maize but not necessarily resulting in oligosaccharide release. Therefore, partial cell wall degradation by NSPases may play an important role in reducing nutrient encapsulation by insoluble NSP (18,27).

Implications of oligosaccharide release on NSP ileal recovery

NSP cannot be digested in the small intestine due to the lack of the necessary enzymes. Thus, they are expected to be fully recovered in the ileum. The high Ara, Xyl, Gal, and non-glucosyl NSP (NSG) ileal recoveries observed for all DT (Table 4) confirmed this assumption. In particular, more than 88% of the Xyl and approximately 100% of the Ara present in the diet were recovered in the ileum, regardless of DT. High AX accumulation in the broiler's ileum (57,58) and complete AX recovery in the pig's ileum (59) have been previously reported. However, insoluble digestibility markers, such as the one used in this study, may poorly estimate the transit of soluble feed components (60). Furthermore, soluble and small feed particles exiting the ileum can enter the ceca, while insoluble, undigested feed components will be excreted (46,60). Hence, the decreased Ara (6.9% lower) and Xyl (6.7% lower) ileal recoveries obtained in WE may imply a higher amount of soluble AX entering the ceca compared to WC. AXOS release by xylanase documented in WE (Figure 1) may have increased the proportion of soluble AX entering the ceca. The use of soluble digestibility marker is further needed to investigate this relationship (60).

Limited NSP fermentation and complete NSP recovery were expected for the small intestine due to short retention time, pH conditions, and small populations of lactobacilli and Clostridia present (49). Although WE presented higher acetate and succinate amounts than WC, the low absolute amounts of these metabolites further suggested limited fermentation in the ileum. Lactobacilli prefer the fermentation of maltodextrins formed during starch digestion compared to other oligosaccharides (61). The marginal effect of NSPase on lactate formation observed in both wheat-based and maize-based DT may, consequently, not be directly related to NSP fermentation in the small intestine. This further strengthens the notion that the majority of NSP reaches the end of the small intestine undegraded by the microbiota, irrespective of enzyme treatment. It should be mentioned that direct AXOS provision to the diet increased lactate formation in the broiler's ileum to a greater extent than xylanase treatment (62).

4.2 Enzyme action improves nutrient ileal digestibility and alters their use in the hindgut

The possible impact of AX degradation in the upper GIT by NSPase on the ileal (AID) and the total tract digestibility (ATTD) of organic matter, starch, and protein was also investigated (Table 6).

Approximately 72.2% of the dietary organic matter (OM) was digested in the small intestine (AID), and an additional 1.8% of OM was fermented in the broiler's hindgut in WC. Enzyme treatment (WE) increased OM-AID. Yet, the OM-ATTD did not increase further. This suggested that enzyme supplementation caused feed components that would have otherwise been fermented in the hindgut to be digested already in the ileum. Such observations were not applicable for the maize-based DT.

The bulk of starch (94.8–97.5%) was digested in the small intestine (AID) in all DT. Still, an additional 1.2% and 1.0% starch was fermented in the hindgut in WC and MC, respectively. It can be argued that part of the starch fraction escaping digestion disappeared through microbial fermentation in chicken's hindgut, as previously mentioned for both pigs and poultry (63–65). Resistant starch fermentation will occur in the ceca, where only soluble compounds and small particles can enter (46,60). Starch fermentation in the hindgut provides less energy to the animal than starch digestion in the ileum (66). Enzyme supplementation in WE and ME increased starch AID by 2.6% and 0.4% compared to WC and MC, respectively, whereas the total tract digestibility did not exceed that of the control DT (WC, MC). These observations indicate that NSPase enabled an increased starch absorption in the ileum. This might be nutritionally beneficial as pronounced ileal starch digestion has been associated with improved broiler performance (67,68).

Crude protein (CP) AID was positively influenced by NSPase in the wheat-based but not in the maize-based diet (Table 6). This remark demonstrates the importance of NSPase inclusion in wheat-based diets. Conversely, the higher protein digestibility of maize-based diets compared to wheat-based diets previously reported (16,68) may have limited the impact of enzyme supplementation. In addition, the higher soybean meal inclusion in the maize-based diet compared to the wheat-based diet (Table 1) meant that maize protein contributed less than wheat protein to the total protein of the diet and could potentially mask any effect of NSPase.

The difference in starch AID between WC and WE was six-fold higher than the difference in starch AID between MC and ME. The marked effect of NSPase on starch and protein digestibility highlighted the importance of enzyme inclusion in wheat-based diets. NSPase promotes nutrient digestion in wheat-based DT partly by reducing the digesta viscosity (12,13,68,69). However, NSPase also subtly improved starch AID in maize-based DT, where digesta viscosity is not a limiting factor. This indicates that viscosity reduction is not the only mechanism involved

(69). Nutrient encapsulation in the cereal cell wall matrix is expected to limit their digestion (47,70). The degradation of the cell wall matrix by xylanase and glucanase followed by the release of encapsulated nutrients could have further improved the nutritional values of both wheat and maize (16,27,59).

4.3 Carbohydrate fermentation patterns in the hindgut of broilers

In the wheat-based diets, AX hindgut fermentation was attested by the decreased Ara and Xyl recoveries for the total tract compared to the ileum (Table 4). Still, more than 80% Ara and 70% Xyl were excreted unutilized. NSPase addition in WE tended to lower the recovery values for both Ara and Xyl compared to control treatment WC and, in addition, decreased Ara and Xyl levels and increased SCFA formation in the ceca. In particular, NSPase increased the formation of acetate and butyrate in the ceca, in line with previous research (17,20,71). These SCFAs can be used by the host as an additional energy source and promote gut health (15). From our results, it is demonstrated that the hydrolysis of wheat AX and the formation of AXOS by xylanase in the ileum in WE promoted AX fermentability by the microbiota in the ceca. Furthermore, the higher A/X ratio in the ceca in WE suggests that especially highly substituted AX fragments remain unfermented.

In contrast to the wheat-based DT, limited Xyl and Ara fermentation was observed in both MC and ME (Table 4). The recovery of both monosaccharides in excreta was approximately 100%, suggesting that maize AX is excreted virtually untouched. The insolubility of maize AX (5) was expected to result in a low proportion of AX entering the ceca. This was demonstrated in our study by the combination of low Xyl amount (<0.1% w/w) present in the ceca and high Xyl total tract recovery in MC and ME (Table 4). Similar to Ara and Xyl, also UA was excreted undegraded. This may reflect the structural complexity of maize glucuronoarabinoxylan, hindering xylanase activity and resulting in poor fermentability (50,54). It should be noted that the higher soybean meal inclusion in maize-based DT compared to wheat-based DT could have impacted the estimation of mainly Ara and UA, as these monosaccharides are known to be abundant in soy NSP (54).

Gal was fermented to a greater extent (18%) in the wheat-based than in the maize-based DT. Additionally, UA fermentation was only observed in the wheat-based DT. These NSP components can derive from cereals (5), but most of Gal, Man, and UA present in the diet are expected to originate from pectins and hemicelluloses from soy (54). It is not clear why the fermentability of these NSP sugars was more pronounced in the wheat-based DT. Possibly, microbiota stimulation due to AX fermentation in the wheat-based DT could have indirectly affected the use of other NSP.

Altogether, AX degradation by NSPase markedly improved AX fermentability and increased SCFA formation in WE. In contrast, NSPase treatment coincided with reduced SCFA contents in ME compared to MC. The subtle improvement in starch

ileal digestibility observed in ME could have resulted in less (resistant) starch being available for fermentation. Hence, less available starch alongside poorly fermentable AX could explain the decrease in SCFA formation upon NSPase inclusion in the maize-based DT. Improved starch AID did not negatively influence SCFA formation in WE, probably due to a more pronounced NSP fermentation.

4.4   Interrelationships between carbohydrate fermentation, nutrient digestibility and growth parameters

Overall, the wheat-based DT was found more responsive to NSPase treatment than the maize-based DT regarding nutrient digestibility and NSP fermentability. The potential interrelationships between the investigated parameters could reveal how NSPases may affect the various biochemical and physiological responses in broilers. A schematic summary of how NSPases may have influenced the use of wheat-based and maize-based DT was based on PCA analysis (Fig. 2).

Organic matter (OM) ATTD presented positive correlations with Ara and Xyl contents in the gizzard (Giz) and the ceca (Cec) and indicated the important role of AX in hindgut fermentation. The importance of AX fermentation in the ceca to produce SCFA was further attested by the negative correlations between SCFA and Ara and Xyl contents in the gizzard and the ceca. Moreover, total SCFA, acetate, butyrate, and propionate correlated positively with BW, ADFI, and ADG and negatively with FCR. It seems that the activity of xylanase and the consequent AXOS formation in the proximal GIT (Fig. 1) boosted the bacterial metabolism in the ceca, which in turn coincided with improved animal growth. This is in accordance with studies reporting the improved performance of wheat-fed broilers upon NSPase addition (12,16,17,20).

The above responses were seen for the wheat-based DT but not for the maize-based DT. The latter exhibited poor AX fermentability and low Ara, Xyl contents in the ceca. Despite that, both maize-based DT exhibited high SCFA contents and pronounced starch digestibility and growth parameters. Hence, the reverse correlations between starch AID and Ara and Xyl contents and the positive correlations of starch ATTD with SCFA and Ara and Xyl total tract recoveries could be explained. Limited maize AX fermentability meant that NSPase supplementation in maize-based diets could not have improved animal growth by a prebiotic mechanism. Moreover, the lower contribution of maize AX to digesta viscosity compared to wheat AX (5,69) could explain the more subtle impact of the enzymes on nutrient digestibility in maize-based DT. Conversely, the NSPase ability to depolymerize AX in wheat diets, thus promoting its fermentability while simultaneously facilitating nutrient digestion, emphasizes the importance of NSPase supplementation in wheat-based diets.

5   Conclusions

This study exhibited the enzymatic activity of dietary NSPase in the broiler's upper gastrointestinal tract by the recognition of arabinoxylan degradation products as oligomers (AXOS) present in the ileum. The beneficial effect of dietary NSPase addition for broilers was dependent on the cereal type and level in the diet. This was affirmed by the more pronounced impact of the NSPase on the wheat-based diet and highlighted the different mechanisms at play for wheat and maize. NSPase promoted nutrient digestibility, especially that of starch and protein in the small intestine, and improved NSP fermentability in the hindgut in the wheat-based diet. The pronounced NSP fermentability might partly be attributed to the *in situ* formation of AXOS in the broiler's upper GIT. The direct detection of oligosaccharides with prebiotic potential further established the link between dietary xylanase and pronounced microbial fermentation.

References

1. World Health Organization. Anti-Infective Drug Resistance Surveillance and Containment Team. WHO global strategy for containment of antimicrobial resistance. 2001 [cited 2021 Feb 3]. p. 99. Available from: https://apps.who.int/iris/handle/10665/66860.

2. Mehdi Y, Létourneau-Montminy MP, Gaucher M Lou, Chorfi Y, Suresh G, Rouissi T, Brar SK, Côté C, Ramirez AA, Godbout S. Use of antibiotics in broiler production: Global impacts and alternatives. Anim Nutr. 2018;4(2):170–8.

3. Slominski BA. Recent advances in research on enzymes for poultry diets. Poult Sci. 2011;90(9):2013–23.

4. Bedford MR. The evolution and application of enzymes in the animal feed industry: the role of data interpretation. Br Poult Sci. 2018;59(5):486–93.

5. Bach Knudsen KE. Fiber and nonstarch polysaccharide content and variation in common crops used in broiler diets. Poult Sci. 2014;93(9):2380–93.

6. Fadel A, Mahmoud AM, Ashworth JJ, Li W, Ng YL, Plunkett A. Health-related effects and improving extractability of cereal arabinoxylans. Int J Biol Macromol. 2018 Apr 1;109:819–31.

7. Saulnier L, Sado P-E, Branlard G, Charmet G, Guillon F. Wheat arabinoxylans: Exploiting variation in amount and composition to develop enhanced varieties. J Cereal Sci. 2007;46(3):261–81.

8. Choct M, Annison G. The inhibition of nutrient digestion by wheat pentosans. Br J Nutr. 1992;67(1):123–32.

9. Hetland H, Choct M, Svihus B. Role of insoluble non-starch polysaccharides in poultry nutrition. Worlds Poult Sci J. 2004;60(04):415–22.

10. Choct M, Annison G. Anti-nutritive effect of wheat pentosans in broiler chickens: Roles of viscosity and gut microflora. Br Poult Sci. 1992;33(4):821–34.

11. Abdollahi MR, Ravindran V, Svihus B. Pelleting of broiler diets: An overview with emphasis on pellet quality and nutritional value. Anim Feed Sci Technol. 2013;179(1–4):1–23.

12. Bedford MR, Classen HL. Reduction of intestinal viscosity through manipulation of dietary rye and pentosanase concentration is effected through changes in the carbohydrate composition of the intestinal aqueous phase and results in improved growth rate and food conversion efficiency of broiler chicks. J Nutr. 1992;122(3):560–9.

13. Choct M, Hughes RJ, Wang J, Bedford MR, Morgan AJ, Annison G. Increased small intestinal fermentation is partly responsible for the anti-nutritive activity of non-starch polysaccharides in chickens. Br Poult Sci. 1996;37(3):609–21.

14. Flint HJ, Scott KP, Duncan SH, Louis P, Forano E. Microbial degradation of complex carbohydrates in the gut. Gut Microbes. 2012 Jul 14;3(4):289–306.

15. Broekaert WF, Courtin CM, Verbeke K, van de Wiele T, Verstraete W, Delcour JA. Prebiotic and other health-related effects of cereal-derived arabinoxylans, arabinoxylan-oligosaccharides, and xylooligosaccharides. Crit Rev Food Sci Nutr. 2011;51(2):178–94.

16. Munyaka PM, Nandha NK, Kiarie E, Nyachoti CM, Khafipour E. Impact of combined β-glucanase and xylanase enzymes on growth performance, nutrients utilization and gut microbiota in broiler chickens fed corn or wheat-based diets. Poult Sci. 2016;95(3):528–40.

17. Masey-O'Neill H V., Singh M, Cowieson AJ. Effects of exogenous xylanase on performance, nutrient digestibility, volatile fatty acid production and digestive tract thermal profiles of broilers fed on wheat- or maize-based diet. Br Poult Sci. 2014;55(3):351–9.

18. Meng X, Slominski BA. Nutritive values of corn, soybean meal, canola meal, and peas for broiler chickens as affected by a multicarbohydrase preparation of cell wall degrading enzymes. Poult Sci. 2005;84(8):1242–51.

19. Choct M, Kocher A, Waters DLE, Pettersson D, Ross G. A comparison of three xylanases on the nutritive value of two wheats for broiler chickens. Br J Nutr. 2004;92(1):53.

20. Kiarie E, Romero LF, Ravindran V. Growth performance, nutrient utilization, and digesta characteristics in broiler chickens fed corn or wheat diets without or with supplemental xylanase. Poult Sci. 2014;93(5):1186–96.

21. Singh A, O'Neill HVM, Ghosh TK, Bedford MR, Haldar S. Effects of xylanase supplementation on performance, total volatile fatty acids and selected bacterial population in caeca, metabolic indices and peptide YY concentrations in serum of broiler chickens fed energy restricted maize-soybean based diets. Anim Feed Sci Technol. 2012;177(3–4):194–203.

22. Polizeli MLTM, Rizzatti ACS, Monti R, Terenzi HF, Jorge JA, Amorim DS. Xylanases from fungi: Properties and industrial applications. Appl Microbiol Biotechnol. 2005;67(5):577–91.

23. Beaugrand J, Chambat G, Wong VWKK, Goubet F, Rémond C, Paës G, Benamrouche S, Debeire P, O'Donohue M, Chabbert B. Impact and efficiency of GH10 and GH11 thermostable endoxylanases on wheat bran and alkali-extractable arabinoxylans. Carbohydr Res. 2004;339(15):2529–40.

24. Paës G, Berrin JG, Beaugrand J. GH11 xylanases: Structure/function/properties relationships and applications. Biotechnol Adv. 2012;30(3):564–92.

25. Cowieson AJ, Hruby M, Pierson EEM. Evolving enzyme technology: impact on commercial poultry nutrition. Nutr Res Rev. 2006;19(1):90–103.

26. Karunaratne ND, Classen HL, Ames NP, Bedford MR, Newkirk RW. Effects of hulless barley and exogenous beta-glucanase levels on ileal digesta soluble beta-glucan molecular weight, digestive tract characteristics, and performance of broiler chickens. Poult Sci. 2021;100(3):100967.

27. Dornez E, Gebruers K, Delcour JA, Courtin CM. Grain-associated xylanases: occurrence, variability, and implications for cereal processing. Trends Food Sci Technol. 2009;20(11–12):495–510.

28. Bedford MR, Cowieson AJ. Exogenous enzymes and their effects on intestinal microbiology. Anim Feed Sci Technol. 2012;173(1–2):76–85.

29. Courtin CM, Swennen K, Broekaert WF, Swennen Q, Buyse J, Decuypere E, Michiels CW, De Ketelaere B, Delcour JA. Effects of dietary inclusion of xylooligo- saccharides, arabinoxylooligosaccha- rides and soluble arabinoxylan on the microbial composition of caecal contents of chickens. J Sci Food Agric. 2008;88(14):2517–22.

30. AOAC International. Official Methods of Analysis. 21st ed. Rockville, MD; 2019.

31. Van Keulen J, Young BA. Evaluation of acid-insoluble ash as a natural marker in ruminant digestibility studies. J Anim Sci. 1977;44(2):282–7.

32. Montaño-Vargas J, Shimada A, Vásquez C, Viana M. Methods of measuring feed digestibility in the green abalone (*Haliotis fulgens*). Aquaculture. 2002;213(1–4):339–46.

33. Englyst HN, Cummings JH. Simplified method for the measurement of total non-starch polysaccharides by gas-liquid chromatography of constituent sugars as alditol acetates. Analyst. 1984;109(7):937.

34. Blumenkrantz N, Asboe-Hansen G. New method for quantitative determination of uronic acids. Anal Biochem. 1973;54(2):484–9.

35. Thibault JF, Robin JP. Automatisation du dosage des acides uroniques par la méthode de carbazol. Application au cas de matières pectiques. Ann Technol Agric. 1975;24:99–110.

36. McCleary B V., Gibson TS, Mugford DC. Measurement of total starch in cereal products by amyloglucosidase-α-amylase method: Collaborative study. J AOAC Int. 1997;80(3):571–9.

37. Martens BMJ, Gerrits WJJ, Bruininx EMAM, Schols HA. Amylopectin structure and crystallinity explains variation in digestion kinetics of starches across botanic sources in an *in vitro* pig model. J Anim Sci Biotechnol. 2018;9:91.

38. Broxterman SE, Picouet P, Schols HA. Acetylated pectins in raw and heat processed carrots. Carbohydr Polym. 2017;177:58–66.

39. Logtenberg MJ, Akkerman R, An R, Hermes GDA, de Haan BJ, Faas MM, Zoetendal EG, Schols HA, de Vos P. Fermentation of chicory fructo-oligosaccharides and native inulin by infant fecal microbiota attenuates pro-inflammatory responses in immature dendritic cells in an infant-age-dependent and fructan-specific way. Mol Nutr Food Res. 2020;2000068.

40. Jonathan MC, Van Den Borne JJGC, Van Wiechen P, Souza Da Silva C, Schols HA, Gruppen H. *In vitro* fermentation of 12 dietary fibres by faecal inoculum from pigs and humans. Food Chem. 2012;133(3):889–97.

41. Aviagen. Ross 308/Ross 308 FF broiler: Performance objectives. 2019 [cited 2021 Mar 25]. p. 16. Available from: https://en.aviagen.com/brands/ross/products/ross-308

42. Gonzalez-Ortiz G, Sola-Oriol D, Martinez-Mora M, Perez JF, Bedford MR. Response of broiler chickens fed wheat-based diets to xylanase supplementation. Poult Sci. 2017;96(8):2776–85.

43. Matthiesen CF, Pettersson D, Smith A, Pedersen NR, Storm AC. Exogenous xylanase improves broiler production efficiency by increasing proximal small intestine digestion of crude protein and starch in wheat-based diets of various viscosities. Anim Feed Sci Technol. 2021;272:114739.

44. Engberg RM, Hedemann MS, Steenfeldt S, Jensen BB. Influence of whole wheat and xylanase on broiler performance and microbial composition and activity in the digestive tract. Poult Sci. 2004;83(6):925–38.

45. Amerah AM, Ravindran V, Lentle RG. Influence of wheat hardness and xylanase supplementation on the performance, energy utilisation, digestive tract development and digesta parameters of broiler starters. Anim Prod Sci. 2009;49(1):71–8.

46. Vergara P, Ferrando C, Jiménez M, Fernández E, Goñalons E. Factors determining gastrointestinal transit time of several markers in the domestic fowl. Q J Exp Physiol. 1989;74(6):867–74.

47. Martens BMJ, Flécher T, De Vries S, Schols HA, Bruininx EMAM, Gerrits WJJ. Starch digestion kinetics and mechanisms of hydrolysing enzymes in growing pigs fed processed and native cereal-based diets. Br J Nutr. 2019;121(10):1124–36.

48. Fincher GB. Cereals: Chemistry and physicochemistry of non-starchy polysaccharides. In: Wrigley CW, Corke H, Seetharaman K, Faubion J, editors. Encyclopedia of food grains. 2nd ed. Amsterdam: Elsevier Inc.; 2016. p. 208–23.

49. Pan D, Yu Z. Intestinal microbiome of poultry and its interaction with host and diet. Gut Microbes. 2013;5(1):108–19.

50. Izydorczyk MS, Biliaderis CG. Cereal arabinoxylans: Advances in structure and physicochemical properties. Carbohydr Polym. 1995;28(1):33–48.

51. Gruppen H, Kormelink FJM, Voragen AGJ. Water-unextractable cell wall material from wheat flour. 3. A structural model for arabinoxylans. J Cereal Sci. 1993;18(2):111–28.

52. Kabel MA, van den Borne H, Vincken JP, Voragen AGJ, Schols HA. Structural differences of xylans affect their interaction with cellulose. Carbohydr Polym. 2007;69(1):94–105.

53. Lin Y, Olukosi OA. Qualitative and quantitative profiles of jejunal oligosaccharides and cecal short-chain fatty acids in broiler chickens receiving different dietary levels of fiber, protein and exogenous enzymes. J Sci Food Agric. 2021;101:5190–5201.

54. Huisman MMH. Elucidation of the chemical fine structure of polysaccharides from soybean and maize kernel cell walls (Doctoral Thesis). Wageningen University; 2000.

55. Biely P, Vršanská M, Tenkanen M, Kluepfel D. Endo-β-1,4-xylanase families: differences in catalytic properties. J Biotechnol. 1997;57(1):151–66.

56. Pedersen MB, Dalsgaard S, Arent S, Lorentsen R, Bach Knudsen KE, Yu S, Lærke HN. Xylanase and protease increase solubilization of non-starch polysaccharides and nutrient release of corn- and wheat distillers dried grains with solubles. Biochem Eng J. 2015;98:99–106.

57. Bautil A, Verspreet J, Buyse J, Goos P, Bedford MR, Courtin CM. Age-related arabinoxylan hydrolysis and fermentation in the gastrointestinal tract of broilers fed wheat-based diets. Poult Sci. 2019;98(10):4606–21.

58. Craig AD, Khattak F, Hastie P, Bedford MR, Olukosi OA. Xylanase and xylo- oligosaccharide prebiotic improve the growth performance and concentration of potentially prebiotic oligosaccharides in the ileum of broiler chickens. Br Poult Sci. 2020;61(1):70–8.

59. Bach Knudsen KE, Jensen BB, Hansen I. Digestion of polysaccharides and other major components in the small and large intestine of pigs fed on diets consisting of oat fractions rich in β-D-glucan. Br J Nutr. 1993;70(2):537–56.

60. De Vries S, Kwakkel RP, Pustjens AM, Kabel MA, Hendriks WH, Gerrits WJJ. Separation of digesta fractions complicates estimation of ileal digestibility using marker methods with Cr_2O_3 and cobalt-ethylenediamine tetraacetic acid in broiler chickens. Poult Sci. 2014;93(8):2010–7.

61. Gänzle MG, Follador R. Metabolism of oligosaccharides and starch in lactobacilli: A review. Front Microbiol. 2012;3:340.

62. Morgan NK, Keerqin C, Wallace A, Wu SB, Choct M. Effect of arabinoxylo-oligosaccharides and arabinoxylans on net energy and nutrient utilization in broilers. Anim Nutr. 2019;5(1):56–62.

63. De Vries S, Gerrits WJJ, Kabel MA, Vasanthan T, Zijlstra RT. β-Glucans and resistant starch alter the fermentation of recalcitrant fibers in growing pigs. PLoS One. 2016;11(12).

64. Zhang Y, Liu Y, Li J, Xing T, Jiang Y, Zhang L, Gao F. Dietary resistant starch modifies the composition and function of caecal microbiota of broilers. J Sci Food Agric. 2020;100(3):1274–84.

65. Giuberti G, Gallo A, Moschini M, Masoero F. New insight into the role of resistant starch in pig nutrition. Anim Feed Sci Technol. 2015;201:1–13.

66. Gerrits WJJ, Bosch MW, van den Borne JJGC. Quantifying resistant starch using novel, *in vivo* methodology and the energetic utilization of fermented starch in pigs. J Nutr. 2012;142(2):238–44.

67. Liu SY, Selle PH. A consideration of starch and protein digestive dynamics in chicken-meat production. Worlds Poult Sci J. 2015;71(2):297–310.

68. Romero LF, Sands JS, Indrakumar SE, Plumstead PW, Dalsgaard S, Ravindran V. Contribution of protein, starch, and fat to the apparent ileal digestible energy of corn- and wheat-based broiler diets in response to exogenous xylanase and amylase without or with protease. Poult Sci. 2014;93(10):2501–13.

69. Maisonnier S, Gomez J, Carré B. Nutrient digestibility and intestinal viscosities in broiler chickens fed on wheat diets, as compared to maize diets with added guar gum. Br Poult Sci. 2001;42(1):102–10.

70. Svihus B. Limitations to wheat starch digestion in growing broiler chickens: a brief review. Anim Prod Sci. 2011;51(7):583.

71. Kubiś M, Kołodziejski P, Pruszyńska-Oszmałek E, Sassek M, Konieczka P, Górka P, Flaga J, Katarzyńska-Banasik D, Hejdysz M, Wiśniewska Z, Kaczmarek SA. Emulsifier and xylanase can modulate the gut microbiota activity of broiler chickens. Animals. 2020;10(12):2197.

2

Supplementary information

Table S1. Effect of the enzyme (E) on the body weight (BW at day (d) 28), feed conversion ratio (FCR), average daily feed intake (ADFI), and average daily gain (ADG) of broilers fed wheat-based (WC, WE) ($n = 5$–6) and maize-based (ME, MC) ($n = 6$) DT during the finisher period (days 24–28).
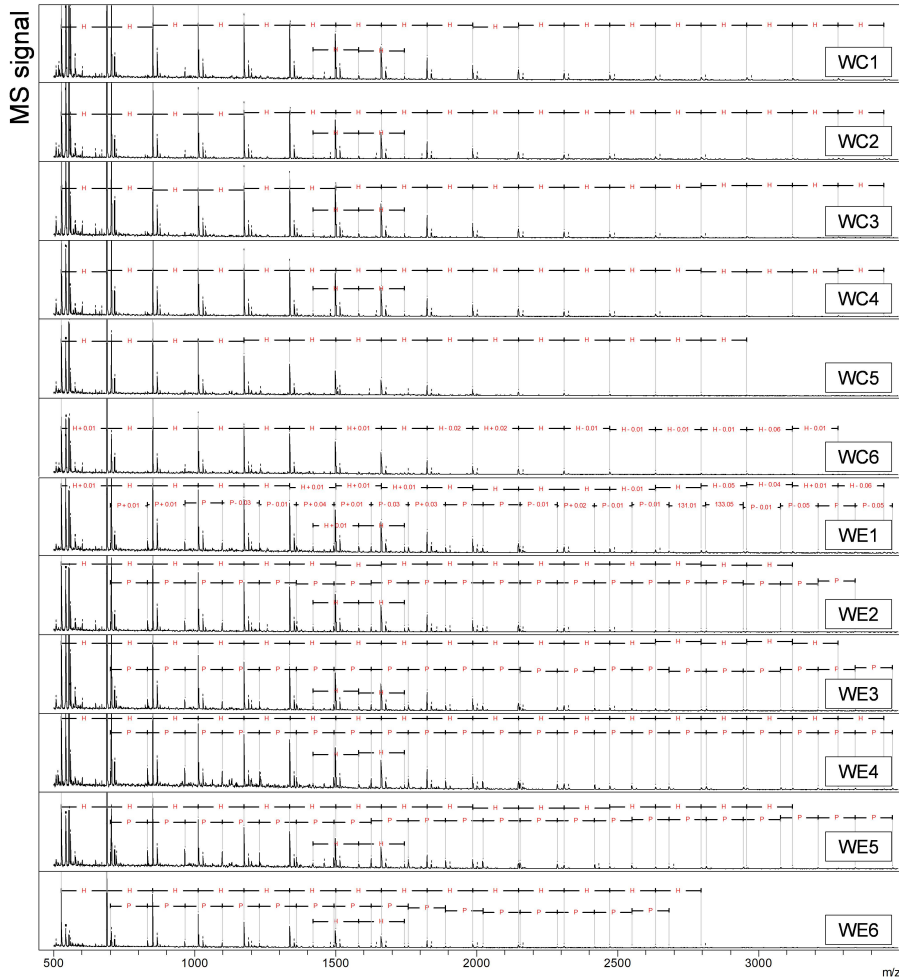
Dietary Treatment (DT)	BW (d28) (g)	FCR (g/g)	ADFI (g/d)	ADG (g/d)
WC	1290.00*	1.62*	123.31*	76.38*
WE	1370.00	1.50	130.17	87.10
SEM[1]	18.80 *(20.60)	0.03 *(0.03)	4.00 *(4.39)	3.30 *(3.60)
	Model established *p* values			
E	0.021	0.018	0.281	0.059
MC	1311.67	1.53	124.55	81.82
ME	1353.92	1.50	129.45	86.73
SEM	18.22	0.03	3.04	3.29
	Model established *p* values			
E	0.136	0.498	0.285	0.320

[1]Standard error of the mean, for $n = 6$. *In case of missingness, the adjusted SEM value ($n = 5$) is presented between brackets.

Table S2. Effect of the enzyme (E) on the monosaccharide content (% w/w dry matter basis) in the ileum and excreta of broilers fed the wheat-based (WC, WE) and maize-based DT (MC, ME) ($n = 6$).

				Ileum				
% (w/w)	WC	WE	SEM [1]	*p* value [2]	MC	ME	SEM	*p*-Value
Ara	6.82	7.02	0.10	0.181	6.17	6.18	0.10	0.899
Xyl	9.24	9.49	0.19	0.367	5.68	5.76	0.08	0.495
Glc	18.25	15.27	0.66	0.009	14.38	14.49	0.44	0.857
Gal	7.59	7.91	0.23	0.349	10.12	9.80	0.51	0.660
UA	4.43	4.98	0.11	0.005	6.22	5.78	0.14	0.047
Total	48.75	47.21	0.54	0.073	45.51	44.88	0.48	0.383
NGP	30.50	31.94	0.52	0.080	31.13	30.39	0.61	0.411
A/X	0.74	0.74	0.01	0.914	1.09	1.07	0.02	0.559
				Excreta				
% (w/w)	WC	WE	SEM	*p* value	MC	ME	SEM	*p*-Value
Ara	5.44	5.42	0.11	0.889	5.56	6.00	0.27	0.265
Xyl	7.64	7.34	0.27	0.439	5.47	5.73	0.20	0.375
Glc	13.87	12.62	0.59	0.162	10.35	10.35	0.34	0.991
Gal	4.36	4.57	0.08	0.090	6.26	6.22	0.20	0.889
UA	3.83	4.07	0.04	0.002	5.47	5.55	0.12	0.630
Total	37.12	36.06	0.44	0.122	34.96	35.95	1.03	0.513
NGP	22.90	23.45	0.33	0.276	24.61	25.60	0.77	0.386
A/X	0.73	0.74	0.01	0.582	1.02	1.04	0.02	0.286

[1]Standard error of the mean. [2]Estimated by ANOVA with enzyme addition (E) as a factor.

Fig. S1. MALDI-TOF-mass spectra of the individual replicates (1–6) of ileal digesta from broilers fed the wheat control (WC) and wheat enzyme (WE) DT. Oligosaccharides consisting of hexose (H; *m/z* 162) or pentose (P; *m/z* 132) units are shown.
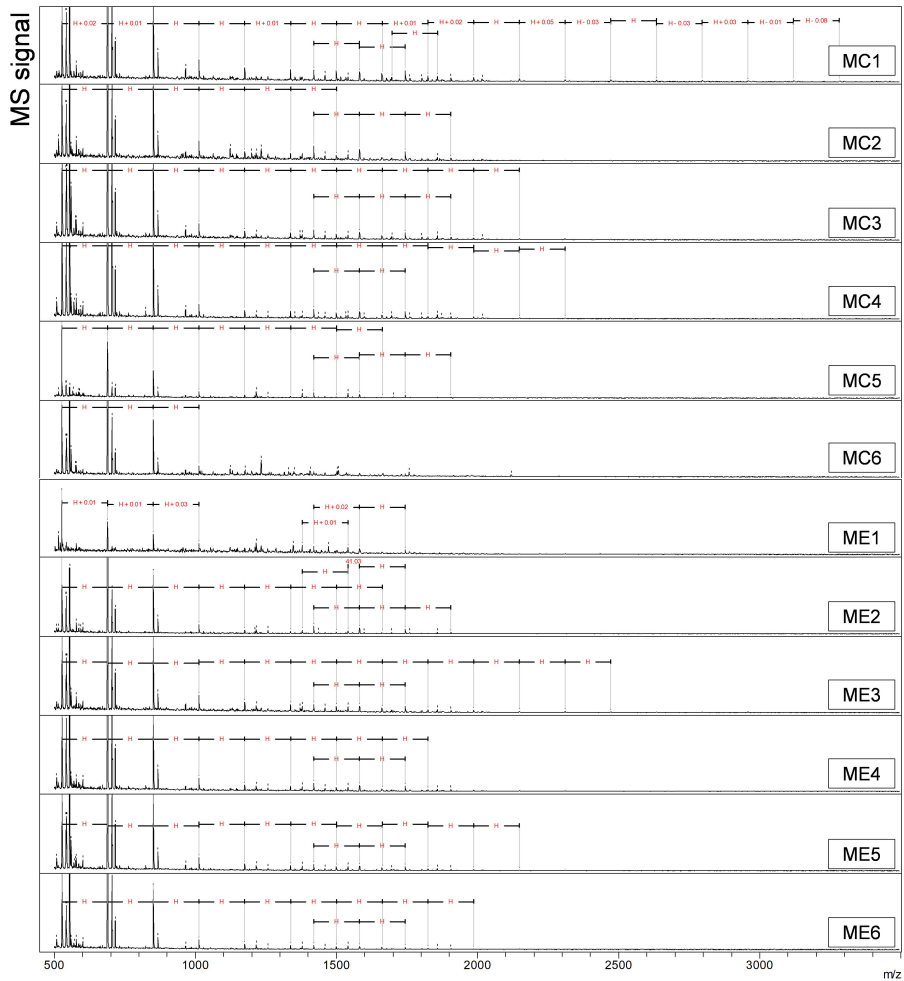
Fig. S2. MALDI-TOF-mass spectra of the individual replicates (1–6) of ileal digesta from broilers fed the maize control (MC) and maize enzyme (ME) DT. Oligosaccharides consisting of hexose (H; *m/z* 162) units are shown.
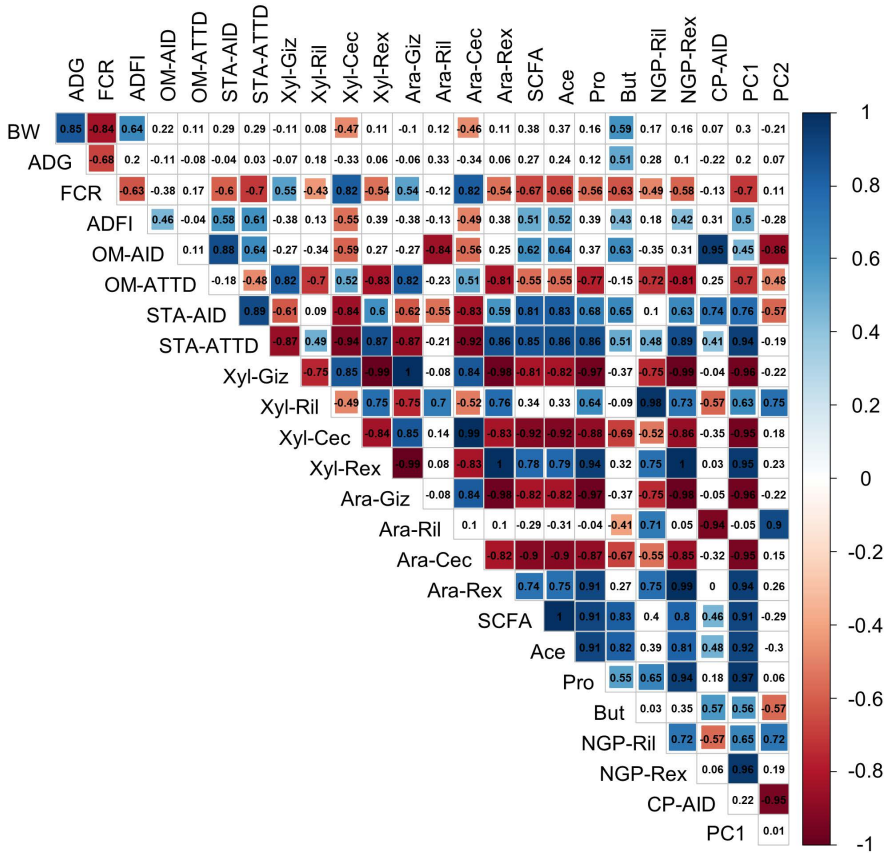
Fig. S3. Pearson coefficients between: (i) NSP-related parameters; ileal (Ril) and total tract (Rex) recovery of Ara, Xyl, and non-glucosyl NSP (NGP), and Ara and Xyl contents (% w/w) in the gizzard (Giz) and the ceca (Cec), (ii) acetate (Ace), butyrate (But), propionate (Pro) and total short-chain fatty acids (SCFA) contents in the ceca, (iii) nutrient digestibility parameters: apparent ileal digestibility (AID) and apparent total tract digestibility (ATTD) of organic matter (OM) starch (STA), and crude protein (CP), and (iv) animal growth parameters; body weight (BW), feed conversion ratio (FCR), average daily feed intake (ADFI) and average daily gain (ADG). Significance was set at $p < 0.05$.

Chapter

3

Cereal type and combined xylanase/glucanase supplementation influence the cecal microbiota composition in broilers

Kouzounis D., Kers J. G., Soares N., Smidt H., Kabel. M. A., Schols H. A.

Abstract

Dietary fiber-degrading enzyme supplementation in broilers aims at off-setting the anti-nutritive effect of non-starch polysaccharides and at promoting broiler health. Recently, we demonstrated that xylanase/glucanase addition in wheat-based diet improved nutrient digestibility, arabinoxylan fermentability and broiler growth. Conversely, maize arabinoxylan was found to be recalcitrant to xylanase action. These findings suggested that enzyme-mediated improvement of nutrient digestion and carbohydrate fermentation depended on the cereal type present in the diet, and may have contributed to broiler growth. Hence, we aimed at further investigating the link between dietary enzymes and carbohydrate fermentation in broilers, by studying the impact of enzyme supplementation in cereal-based diets, to the microbial communities in the ileum and ceca of broilers. For that purpose, 96 one-day-old male broilers were randomly reared in two pens and received either wheat-based or maize-based starter and grower diets. At d 20, the broilers were randomly assigned to one out of four dietary treatments. The broilers received for 8 d the wheat-based or maize-based finisher diet as such (Control treatments; WC, MC) or supplemented with a xylanase/glucanase combination (Enzyme treatments; WE, ME). At d 28, samples from the digestive tract were collected, and the ileal and cecal microbiota composition was determined by 16S ribosomal RNA gene amplicon sequencing. A similar phylogenetic (alpha) diversity was observed among the four treatments, both in the ileal and the cecal samples. Furthermore, a similar microbial composition in the ileum (beta diversity) was observed, with lactobacilli being the predominant community for all treatments. In contrast, both cereal type and enzyme supplementation were found to influence cecal communities. The type of cereal (i.e., wheat or maize) explained 47% of the total variation in microbial composition in the ceca. Further stratifying the analysis per cereal type revealed differences in microbiota composition between WC and WE, but not between MC and ME. Furthermore, the prevalence of beneficial genera, such as *Faecalibacterium* and *Blautia*, in the ceca of broilers fed wheat-based diets coincided with arabinoxylan accumulation. These findings indicated that fermentable arabinoxylan and arabinoxylo-oligosaccharides released by dietary xylanase may play an important role in bacterial metabolism.

1   Introduction

The importance of a balanced microbial gut ecology for healthy broilers is widely acknowledged (1–3). In addition, the interplay between gut microbiota and non-digestible feed components has been described to be crucial for poultry health (2). Therefore, the controlled steering of gut microbiota through dietary interventions may contribute to improved broiler health and growth (4,5). For example, the dietary provision of oligosaccharides exhibiting prebiotic and immunomodulatory properties has been suggested to beneficially impact nutrient digestibility and broiler performance (2,6). In addition, oligosaccharide supplementation was accompanied by the proliferation of beneficial microbiota, such as bifidobacteria and lactobacilli, the decrease of pathogenic bacteria, and the pronounced short chain fatty acids (SCFAs) formation in the hindgut (5,7,8).

In cereal-based poultry diets, non-starch polysaccharides (NSP) are the major carbon source for fermentation. Arabinoxylan (AX) is the main NSP in cereals, such as wheat and maize (9). As such, AX is an important substrate for bacterial fermentation and SCFAs production in the broiler hindgut. AX fermentability was shown to depend on the cereal type, with wheat AX being considered more easily fermentable than maize AX (10–12). At the same time, soluble AX can limit nutrient digestibility and promote pathogen growth in the broiler small intestine (13,14). In addition, insoluble AX may contribute to nutrient encapsulation by the cereal cell wall matrix, and consequently, to decreased digestibility (13). Feed supplementation with NSP-active enzymes (NSPases), such as xylanase and glucanase, has been shown to offset detrimental effects of AX on broiler health (3,13). For instance, xylanase supplementation in wheat-based diets decreased digesta viscosity, and coincided with increased nutrient digestibility and animal performance (10,14,15). Moreover, xylanase improved SCFAs formation similarly to the direct arabinoxylo- and xylo-oligosaccharides (AXOS, XOS) supplementation (7,16). It has been previously shown that both AXOS and XOS exert prebiotic properties *in vitro* when using human fecal samples as inoculum (12,17–19). Recently, we demonstrated that xylanase released AXOS and XOS *in vivo*, in the broiler gut (11). It is, therefore, hypothesized that NSPases can modulate gut microbiota by the provision of fermentable oligosaccharides in the ceca.

Understanding the interaction between dietary components and intestinal microbiota is necessary to optimize NSP utilization, in order to promote broiler growth. Therefore, we investigated for wheat-based and maize-based diets the influence of combined xylanase and glucanase supplementation, on the ileal and cecal microbial communities in broilers, by employing 16S rRNA gene amplicon sequencing.

2   Materials and methods

2.1   Experimental design and dietary treatments

The work discussed here is part of a larger study on NSP utilization in broilers described in detail elsewhere (11; Chapter 2). The study was conducted at the facilities of the Laboratory for Animal Nutrition and Animal Product Quality (LANUPRO), Department of Animal Sciences and Aquatic Ecology, Ghent University (Belgium), in accordance with the ethical standards and recommendations for accommodation and care of laboratory animals covered by the European Directive 2010/63/EU on the protection of animals used for scientific purposes and the Belgian Royal Decree KB29.05.13 on the use of animals for experimental studies. In brief, 96 one-day old male broilers (Ross 308) (Vervaeke-Belavi, Tielt, Belgium) were randomly assigned to two separate pens and were fed *ad libitum* either with wheat-soy or maize-soy starter feed (d 0-10) and grower feed (d 10-20) diets, provided in mash form (Table 1). At d 20 the birds were allocated according to body weight to pens with a wire floor. Four dietary treatments; Wheat Control (WC), Wheat Enzyme (WE), Maize Control (MC) and Maize Enzyme (ME) were assigned to each pen following a randomized block design, with the blocking factor referring to the spatial organization in the facility. Each dietary treatment consisted of six replicate pens, with four birds per pen. The broilers had *ad libitum* access to the finisher feed diet, being fed as such (Control diets) or supplemented with (Enzyme diets) commercial endo-xylanase and endo-glucanase preparation (powder form) from *Trichoderma* spp. (Huvepharma NV, Berchem, Belgium) (Table 1), as prepared by Research Diet Services B.V. (Wijk bij Duurstede, The Netherlands). The birds were weighed after an adaptation period (d 20 - 24), and then continued to be fed finisher diets until d 28. Feed intake was measured daily per pen (d 25 - 28). During this period, excreta were collected twice daily, homogenized, and an aliquot of a minimum of 250 g fresh material per pen was immediately stored at −20 °C. At d 28, all birds were weighed, euthanized by cervical dislocation, and the ileum and ceca contents were collected, pooled per pen, and frozen at −20 °C.

Table 1. Diet composition of wheat-based and maize-based diets. The data were previously determined and are reported elsewhere (11).

Ingredient, %	Wheat-based			Maize-based		
	Starter	**Grower**	**Finisher**	**Starter**	**Grower**	**Finisher**
Wheat	49.4	58.8	65.9	–	–	–
Maize	10.0	5.0	–	57.3	59.6	59.1
Soybean Meal 48CP[1]	24.4	19.5	17.0	27.2	24.3	24.3
Toasted Soybeans	10.0	10.0	8.0	10.0	10.0	8.0
Soybean Oil	1.4	2.4	4.3	0.6	1.7	3.9
Monocalcium phosphate	1.4	1.3	1.0	1.5	1.4	1.2
Limestone	1.4	1.3	1.1	1.4	1.2	1.1
DL-Methionine	0.4	0.3	0.2	0.4	0.3	0.3
L-Lysine HCl	0.3	0.3	0.3	0.3	0.3	0.2
Salt	0.2	0.2	0.3	0.2	0.2	0.3
Na-Bicarbonate	0.3	0.3	0.2	0.3	0.3	0.2
L-Threonine	0.2	0.1	0.1	0.2	0.1	0.1
L-Valine	0.1	0.1	0.1	0.2	0.1	0.0
Coccidiostat	Sacox[2]	Sacox	–	Sacox	Sacox	–
Premix Article[3]	0.5	0.5	0.5	0.5	0.5	0.5
Diamol[4]	–	–	1.0	–	–	1.0
Total	100.0	100.0	100.0	100.0	100.0	100.0
Calculated chemical composition, % as is						
ME[5], MJ/kg	11.8	12.1	12.5	12.0	12.4	12.8
Crude protein	21.8	20.1	18.5	21.2	19.9	19.2
NDF	10.0	10.1	10.0	9.7	9.7	9.4
Crude fat	4.9	5.7	7.1	5.1	6.3	8.0
Arg	1.46	1.31	1.18	1.47	1.37	1.31
Met + Cys	0.69	0.64	0.60	0.67	0.64	0.62
Ile	0.92	0.84	0.76	0.92	0.86	0.83
Leu	1.65	1.49	1.35	1.83	1.74	1.68
Lys	1.14	1.01	0.90	1.18	1.09	1.05
Thr	0.79	0.72	0.65	0.82	0.77	0.74
Val	1.02	0.93	0.85	1.02	0.96	0.92
Ca	0.87	0.81	0.67	0.88	0.78	0.71
Cl	0.16	0.16	0.22	0.16	0.16	0.21
K	0.92	0.83	0.75	0.95	0.90	0.86
Na	0.17	0.17	0.18	0.16	0.16	0.17
Total P	0.68	0.65	0.56	0.70	0.66	0.61
Available P	0.34	0.32	0.27	0.34	0.32	0.29
Analyzed chemical composition, % dry matter						
Dry matter, % as is	–	–	90.3	–	–	89.5
Starch	–	–	40.4	–	–	37.4
Crude protein (N x 6.25)	–	–	20.5	–	–	20.7
Ash	–	–	5.9	–	–	6.5
NSP[6]	–	–	21.0	–	–	18.6
NGP[7]	–	–	9.8	–	–	8.7
AX[8]	–	–	5.0	–	–	3.4
Analyzed enzyme activity (of enzyme-supplemented diets)						
Xylanase, EPU[9]/kg feed	–	–	1550	–	–	1740
Cellulase, CU[10]/kg feed	–	–	240	–	–	190

[1]CP: Crude protein. [2]Provided by Huvepharma NV, Berchem, Belgium. [3]Providing per kg of diet: vitamin A (retinyl acetate), 10000 IU; vitamin D_3 (cholecalciferol), 2500 IU; vitamin E (dl-α-tocopherol acetate), 50 mg; vitamin K_3 (menadione), 1.5 mg; vitamin B_1 (thiamine), 2.0 mg; vitamin B_2 (riboflavin), 7.5 mg; niacin, 35 mg; D-pantothenic acid, 12 mg; vitamin B_6 (pyridoxine-HCl), 3.5 mg; vitamin B_{12} (cyanocobalamine), 20 µg; folic acid, 1.0 mg; biotin, 0.2 mg; choline chloride, 460 mg; Fe ($FeSO_4.H_2O$), 80 mg; Cu ($CuSO_4.5H_2O$), 12 mg; Zn (ZnO), 60 mg; Mn (MnO), 85; I ($Ca(IO_3)_2$), 0.8 mg; Co ($Co_2CO_3(OH)_2$), 0.77 mg; Se (Na_2O_3Se), 0.15 mg. [4]Used as acid insoluble ash (AIA) digestibility marker (Franz Bertram GmbH, Hamburg, Germany). [5]Metabolizable energy. [6]Non-starch polysaccharides; calculated as the difference between total carbohydrates and starch. [7]Non-glucosyl NSP; calculated as the sum of sum of arabinosyl, xylosyl, galactosyl, uronyl, mannosyl, rhamnosyl and fucosyl units. [8]Arabinoxylan; calculated as the sum of arabinosyl and xylosyl units. [9]Amount of enzyme which releases 0.0083 µmol of reducing sugars (xylose equivalents) per minute from oat spelt xylan at pH 4.7 and 50 ºC. [10]Amount of enzyme which releases 0.128 µmol of reducing sugars (glucose equivalents) per minute from barley β-glucan at pH 4.5 and 30 ºC.

2.2   DNA extraction

DNA was extracted from 0.25 g pooled ileal or cecal content, using 700 µL Stool Transport and Recovery (STAR) buffer (Roche Diagnostics Nederland BV, Almere, the Netherlands) and described in detail before (20). DNA concentration was measured with a NanoDrop ND-1000 spectrophotometer (NanoDrop® Technologies, Wilmington, DE, USA), and DNA was stored at −20 °C until further use. Extracted DNA was diluted to 20 ng/µL in nuclease free H_2O. All PCR plastics were UV irradiated for 15 min before use.

2.3   Microbiota analysis

For 16S rRNA gene amplicon sequencing, barcoded amplicons covering the variable regions V4 of the 16S rRNA gene were generated by PCR using the 515F and 806Rd primers. The samples were amplified in duplicate using Phusion hot start II high fidelity polymerase (Finnzymes, Espoo, Finland) and checked for correct size and concentration. The PCR reactions contained 36.5 µL nucleotide free water (Promega, Madison, WI, USA), 0.5 µL of 2 U/µL polymerase, 10 µL of 5 × HF buffer, 1 µL of 10 µmole/L stock solutions of each of the forward and reverse primers, 1 µL 10 mmole/L dNTPs (Promega) and 1 µL template DNA. Reactions were held at 98 °C for 30 s and amplification proceeded for 25 cycles at 98 °C for 10 s, 42 °C for 10 s, 72 °C for 10 s and a final extension of 7 min at 72 °C. Two out of the 24 ileal samples contained a low amount of DNA (< 1 ng/µL) and did not pass our quality control. Synthetic mock communities of known composition were added as positive controls (21), and samples with nuclease free water were added as no-template negative controls to ensure high quality sequencing data. The samples were sent to Eurofins Genomics Germany GmbH (Ebersberg, Germany) for sequencing on an Illumina Hiseq2500 instrument. Data was analyzed using NG-Tax 2.0 (22). *De novo* amplicon sequence variants (ASVs) were generated, using an abundance threshold of 0.1% on a per-sample basis. Taxonomy was assigned using SILVA 132 16S rRNA gene reference database (23). The ASVs associated the family Mitochondria (n = 2) and the order Chloroplasts (n = 2) were removed from the data for all sequenced samples.

2.4   Chemical analyses

The experiments described in this section were previously performed, and are thoroughly described in our recent publication (11). Therefore, they are only briefly mentioned here. The dry matter and crude protein contents of diets, ileal digesta and excreta was determined according to the AOAC 935.29 and 990.03 method, respectively, while the dry matter content of cecal samples was determined separately (11). Ash, and acid insoluble ash (AIA) contents were determined in diets, ileal digesta and excreta (11). Starch content of the diets was determined according to AOAC Method 996.11. Sugar composition and content of finisher diets and digesta was determined by gas chromatography (neutral sugars) and by the colorimetric *m*-hydroxyphenyl assay (uronic acids) with an automated analyzer (Skalar Analytical B.V., Breda, The Netherlands) (24–26). SCFAs (acetate,

butyrate, propionate, isobutyrate and isovalerate) content in the ceca was determined by gas chromatography (27).

2.5   Calculations

Non-starch polysaccharides content was calculated as the difference between total carbohydrates and starch content. The apparent ileal digestibility (AID) of organic matter (OM = DM – Ash), as well as the apparent total tract recovery (Rec) of arabinoxylan (AX: sum of arabinosyl and xylosyl constituents) and non-glucosyl NSP (NGP: sum of arabinosyl, xylosyl, galactosyl, uronyl, mannosyl, rhamnosyl and fucosyl constituents) were determined using acid insoluble ash (AIA) as digestibility marker (11).

2.6   Statistical analysis

The analysis of the 16S rRNA gene sequence data was carried out using R version 4.0.2. Alpha diversity was determined using phylogenetic diversity and tested with a Kruskal-Wallis test. Pairwise comparisons were tested using a Wilcoxon rank-sum test. Beta diversity was determined using Jaccard-, Bray-Curtis-, unweighted UniFrac (UF)- and weighted UniFrac (WUF)- metrics. Non-parametric permutational analysis of variance (PERMANOVA) tests were used to analyze group differences within multivariate community data. Multivariate microbiota data were visualized using principal coordinates analysis (PCoA). To test for differences in relative abundance of individual genera between two groups a Wilcoxon rank-sum test was used, and corrected for multiple testing with the Benjamini-Hochberg (BH) procedure. Weighted UniFrac distance-based redundancy analysis (WUF-db-RDA), a multivariate canonical ordination analysis method that takes the phylogenetic makeup of microbial communities into consideration, was performed using ASV level data and other measured parameters (28). The parameters included as variables were the broiler body weight (BW, d 28), AX total tract recovery (AX_Trec), NGP (NGP_Cec) and AX (AX_Cec) content (% w/w, dry matter basis) in the ceca, SCFAs (acetate, butyrate and propionate content (µmol/g, dry matter basis) in the ceca (Table S1). Values for these parameters have been reported earlier (11).

3   Results and discussion

In our previous work, we investigated the impact of enzyme supplementation in wheat-based and maize-based diets on nutrient digestibility, NSP fermentability and broiler growth (11; Chapter 2), and results have been summarized in Table 2. Addition of a commercial preparation containing xylanase and glucanase in the wheat-based diet (WE) was found to improve the apparent ileal digestibility of organic matter compared to the control diet (WC). In addition, dietary xylanase in WE was shown to release AXOS *in vivo,* in the upper gastrointestinal tract (GIT) (11). Simultaneously, enzyme action in WE improved AX fermentability to SCFAs in the ceca, while it decreased the total tract recovery of AX compared to WC. Conversely, no direct effect of glucanase on carbohydrate fermentation in the ceca

could be discerned. The observed improvement in nutrient digestibility and NSP fermentability by enzyme supplementation coincided with higher body weight values in WE compared to WC (Table2). In contrast, enzyme addition in the maize-based diet (ME) was not found to impact NSP fermentability or nutrient digestibility (11). These findings were in line with previous research (10,15), and suggested that AX fermentation proceeded differently in the ceca of broilers fed wheat-based and maize-based diets. Consequently, the cereal type in the diet was expected to affect the impact of xylanase on AX fermentability. Therefore, continuing our efforts to further substantiate the link between dietary NSPases and NSP fermentation in broilers we now employed next-generation 16S rRNA gene amplicon sequencing to examine the potential impact of cereal type and xylanase/glucanase supplementation, on the ileal and cecal microbiota composition of broilers.

Table 2. Effect of diet and enzyme supplementation on broiler growth, nutrient digestibility and NSP fermentability (11).

Dietary treatment	BW[1], g	FCR[2], g/g	OM-AID, %	AX Rec, %	NGP Rec, %	SCFAs[3], µmol/g
WC	1290.00[#b]	1.62[#]	72.17[b]	84.78[b]	68.82[b]	239.69[c]
WE	1370.00[a]	1.50	75.31[a]	76.96[b]	68.00[b]	338.03[b]
MC	1311.67[ab]	1.53	74.60[a]	129.29[a]	85.96[a]	472.42[a]
ME	1353.92[ab]	1.50	74.74[a]	116.95[a]	92.98[a]	378.16[ab]
SEM[4]	18.4 [#]20.4	0.03 [#]0.03	0.55	4.25	2.58	24.00
p values[5]	0.029	0.053	0.004	<0.001	<0.001	<0.001
Effect of cereal type (Wheat *vs* Maize)						
Wheat	1333.64[#]	1.55[#]	73.7	80.9	68.4	288.9
Maize	1332.79	1.51	74.7	123.1	89.5	425.3
SEM	16.0 [#]16.7	0.02 [#]0.02	0.51	3.28	1.91	22.2
p values	0.990	0.275	0.210	<0.001	<0.001	<0.001
Effect of enzyme supplementation (stratified per cereal type)						
Wheat (WC *vs* WE)						
SEM	18.80 [#]20.60	0.03 [#]0.03	0.34	2.58	1.63	1.67
p values	0.021	0.018	<0.001	0.064	0.731	0.021
Maize (MC *vs* ME)						
SEM	18.22	0.03	0.71	5.47	3.23	1.59
p values	0.136	0.498	0.889	0.149	0.163	0.024

[1]Body weight measured at d 28. [2]Feed conversion ratio measured during the finisher period (d 24-28). [3]Sum of acetate, butyrate, propionate, isobutyrate and isovalerate in the ceca, expressed on dry matter basis. [4]Standard error of the mean (*n* = 6). [#]In case of missingness, the adjusted SEM value (*n* = 5) is presented. [5]Estimated by one-way ANOVA. The significance threshold was $P < 0.05$.

3.1 The type of cereal and enzyme supplementation influences microbial communities

First, phylogenetic diversity, representing biodiversity, was compared across diets and was found to be similar for all diets either in the ileum or in the ceca (Fig. 1A).

Other alpha diversity metrics were in agreement and showed similarities among the diets (data not shown). Second, the ileal samples presented similarities in beta diversity across all diets (Fig. 1B). Our findings were in agreement with previous studies showing no effect of cereal type and enzyme supplementation on total anaerobic bacteria and lactobacilli counts (29–31) and on alpha and beta diversity indices in the ileum (10).
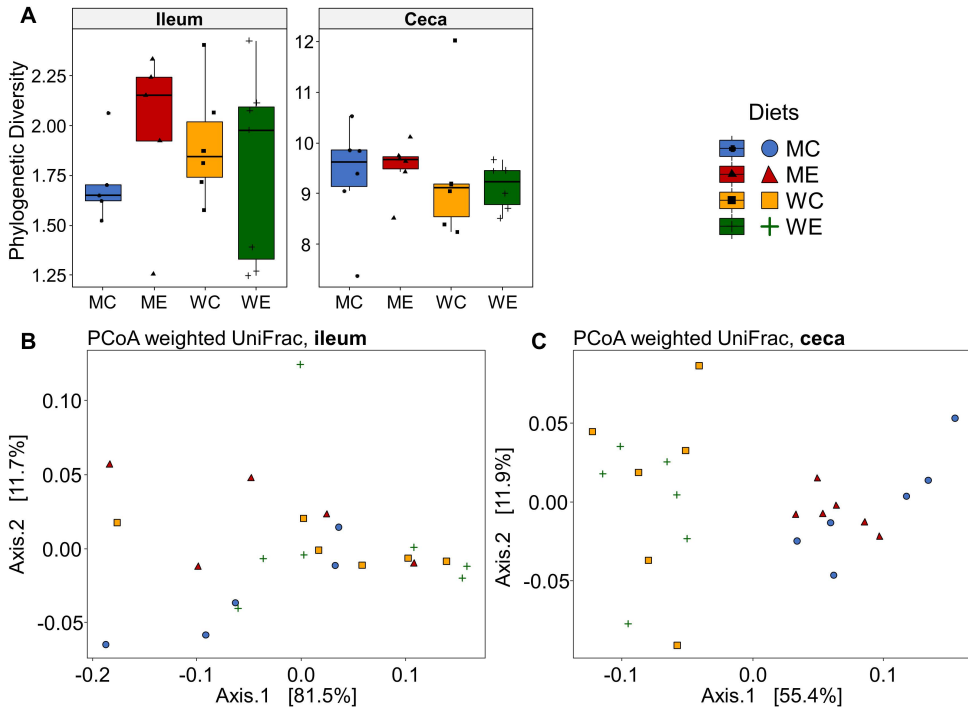

Fig. 1. Alpha and beta diversity in the ileum and the ceca across dietary treatments; maize control (MC), maize enzyme (ME), wheat control (WC) and wheat enzyme (WE), Phylogenetic diversity (ASV level) (**A**) across dietary treatments. Whiskers show 95% interval, box 50% interval. Pairwise Wilcoxon rank sum tests (separately for ileum and ceca), corrected for multiple comparisons using the Benjamini-Hochberg procedure showed no difference between groups, Principal coordinate plots (PCoA) (**B**) based on weighted UniFrac distances of ileum samples. Principal coordinate plots (PCoA) (**C**) based on weighted UniFrac distances of ceca samples.

The microbial composition was compared at family level in the ileum and ceca across the four diets (Fig. 2). Lactobacillaceae (approximately 90%) and Streptococcaceae (< 10%) were predominant in the ileum. No difference in relative abundance between the diets was observed either at family or genus level. The predominance of Lactobacillaceae in the ileum was in accordance with previous studies (1,10,32). The current findings concur with those stating that lactobacilli in the ileum were not affected by cereal type and xylanase supplementation, with or without addition of glucanase (10,16,31). The ceca are known to harbor a more

diverse microbiota composition than the ileum (32,33). Indeed, various families were observed in the cecal samples of the wheat-based diets, with members of the family Lachnospiraceae being the main species, followed by members of the families Ruminococaceae and Lactobacillaceae (Fig. 2). The high relative abundance of these families was in line with previous reports (10,20,32,33). The maize-based diets also presented a diverse microbial ecology in the ceca, though different in composition from the wheat-based diets. For example, members of the families Streptococcaceae, Christensenellaceae, Erysipelotrichaceae and Peptostreptococcaceae presented higher relative abundance, and Bacteroidaceae presented lower relative abundance in the maize-based diets compared to the wheat-based diets (Fig. 2).
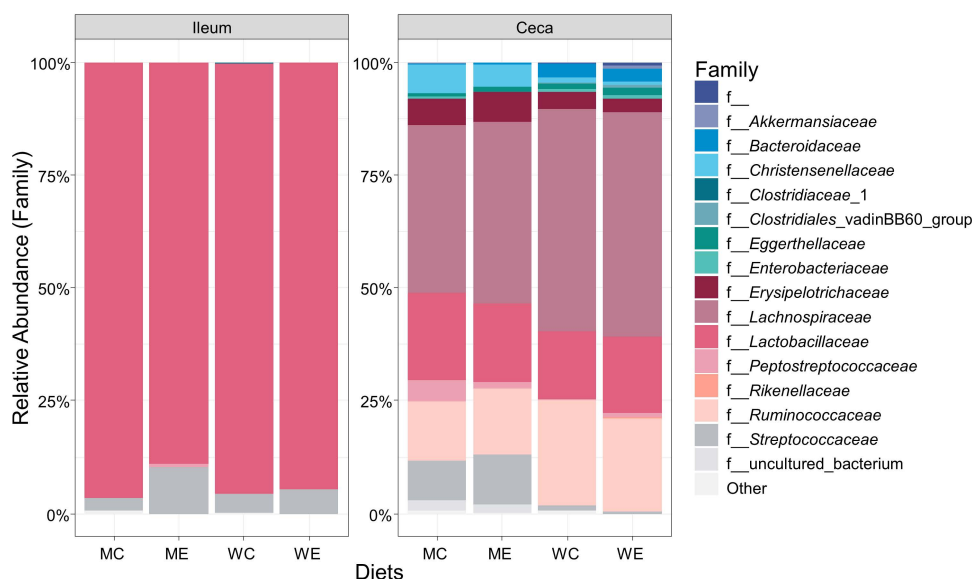
Fig. 2. Cumulative relative abundance (%) of microbial taxa at family level. The abundance threshold is 0.01% and each bar represents six samples.

The observed effect of the diet on beta diversity corroborated its modulatory influence on cecal microbiota composition (Table 3). Weighted Unifrac metrics demonstrated that dietary treatment explained 51.6% (R^2), and cereal type explained 47.6% of the observed variation between treatments (Table 3). Other beta diversity metrics were in line, but explained a lower proportion of the variation (Table 3). Hence, it was demonstrated that cereal type (wheat versus maize) in the diet markedly affected the microbial composition in the ceca, regardless of enzyme supplementation. The diet, and the type of cereal in particular, have previously been proposed to influence the broiler intestinal microbiota (34), but experimental evidence is scarce (30,31,35). Nevertheless, a recent study reported increased bifidobacteria counts in the ceca of 35-d old broilers fed with a wheat-based diet compared to a maize-based diet (31). Additionally, cereal NSP like AX, are known to be utilized as substrates during microbial fermentation to produce

SCFAs (2,36). Differences in NSP physicochemical properties and inclusion level, as a consequence of their botanical source, may dictate the extent of NSP utilization, and hence, SCFAs formation by microbiota (12,18). For instance, the less complex structure and higher water-solubility of wheat AX compared to maize AX (9), are believed to be associated with pronounced cecal fermentation in broilers (10,11).

Table 3. Beta diversity analysis with different distance measures determining microbiota interindividual diversity in the broiler ceca.

	n	Bray-Curtis		Jaccard		Unweighted Unifrac		Weighted Unifrac	
		$R^{2,1}$	p^2	R^2	p	R^2	p	R^2	p
Dietary treatment	24	0.348	<0.001	0.281	<0.001	0.413	<0.001	0.516	<0.001
Wheat *vs* Maize	**Effect of cereal type (Wheat *vs* Maize)**								
	24	0.205	<0.001	0.162	<0.001	0.350	<0.001	0.476	<0.001
	Effect of enzyme supplementation (Control *vs* Enzyme; stratified per cereal type)								
Wheat (WC *vs* WE)	12	0.276	0.012	0.204	0.014	0.083	0.585	0.064	0.729
Maize (MC *vs* ME)	12	0.054	0.765	0.067	0.741	0.115	0.163	0.095	0.351

[1]Percentage of the variation between broilers explained. [2]p value permutational analysis of variance (PERMANOVA).

It should be noted that enzyme supplementation occurred only during the finisher phase lasting eight days. Therefore, the influence of enzyme supplementation on beta diversity was determined by stratifying the analysis per cereal type (Table 3). No effect of enzyme supplementation during the finisher phase was observed in the maize-based treatments. Conversely, enzyme supplementation for the same period appeared to influence beta diversity in the wheat-based treatments. In particular, the Bray-Curtis and Jaccard distance metrics showed that enzyme supplementation explained 27.6% and 20.4% of the total variation between WC and WE, respectively. However, the corresponding weighted and unweighted UniFrac distance metrics that take phylogenetic relatedness of observed microorganisms into account, did not show significant differences between WC and WE. This suggested that microorganisms of close phylogenetic proximity were predominantly influenced by enzyme supplementation. Overall, NSPase supplementation in the finisher phase exerts a modulatory effect on cecal microbiota, probably related to improved AX fermentability (10,11,37).

3.2 Distinct cecal microbial communities coincide with arabinoxylan fermentation

The heatmap in Fig. 3 shows all ASV that significantly differed in relative abundance between wheat-based and maize-based treatments. The two hierarchical clusters

visualized in Fig. 3 corresponded to either wheat-based or maize-based treatments, further emphasizing the impact of cereal on cecal microbial ecology.
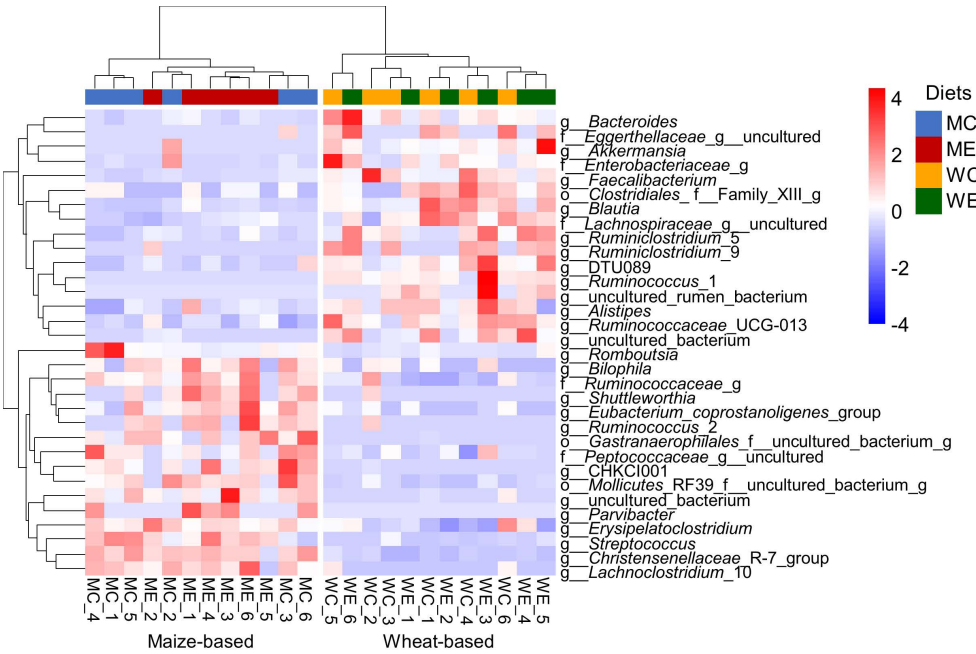

Fig. 3. Heatmap of the genera that were significantly different in relative abundance between dietary treatments (Wilcoxon rank-sum test, adjusted P-values are corrected for multiple testing using the Benjamini-Hochberg procedure, $p < 0.05$). Each red, white, blue square represents the relative abundance.

In specific, 31 genera were identified as being significantly different, and appeared to distinguish the wheat-based from the maize-based treatments (Fig. 3). Next, body weight, AX, non-glucosyl NSP (NGP) and SCFAs contents in the ceca and AX total tract recovery were added in the WUR-db-RDA model to further disentangle the influence of the diet on cecal microbiota composition (Fig. 4). The top six visualized ASVs separating the diets were classified as one member of an uncultured genus of the family Lachnospiraceae, two ASVs within the genus *Faecalibacterium*, and single ASVs within the genera *Lactobacillus*, *Blautia* and *Streptococcus*.
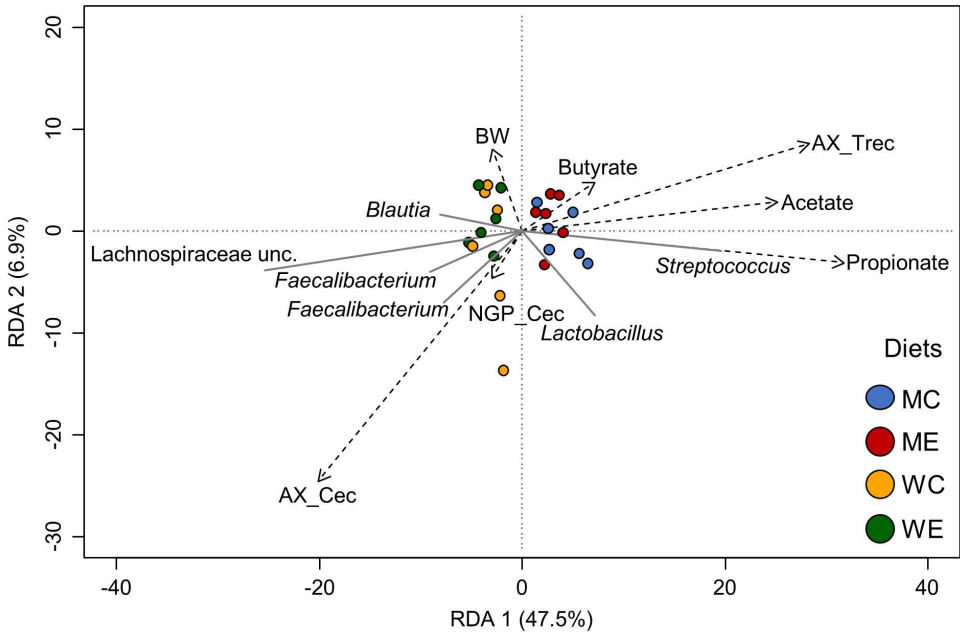
Fig. 4. WUF-db-RDA showing the associations between chemical parameters and microbial ASVs. The six best fitting ASV are displayed and samples are colour based on the dietary treatment. The dashed arrows depict broiler body weight (BW, d 28), AX total tract recovery (AX_Trec), NGP (NGP_Cec) and AX (AX_Cec) content (% w/w, dry matter basis) in the ceca and acetate, butyrate and propionate content (μmol/g dry matter basis) in the ceca, and the solid arrows depict the abundance of bacterial groups.

Members of bacterial taxa such as Lachnospiraceae*, Subdoligranulum*, *Coprococcus, Faecalibacterium* and *Blautia*, all being members of the class Clostridia, are reported to possess an enzymatic arsenal to degrade AX and AXOS (38). Such genera can be involved in carbohydrate metabolism to produce SCFAs, and may contribute to a healthy gut (2,39,40). Therefore, we hypothesized that an increase in fermentable AX/AXOS in the ceca as a result of xylanase action, present in the NSPase preparation, promoted the proliferation of such microbial communities. To this end, we further explored the potential interrelationships between cecal microbial communities and carbohydrate fermentation patterns using redundancy analysis (Fig. 4). The first dimension (RDA1) explained 47.5% of the total variation and separated the wheat-based from the maize-based diets. RDA2 explained an additional 6.9% of the total variation. MC and ME presented higher total SCFAs (Table 2) and higher individual acetate, butyrate and propionate amounts (μmol/g dry matter) compared to WC and WE (Fig. 4., Table S1). This observation can partly be explained by different dry matter contents in WC/WE and MC/ME (Table S1). However, it would have been expected that wheat-based diets would present higher SCFAs values compared to maize-based diets, as a consequence of pronounced NSP fermentability and higher AX content (15,31).

Both WC and WE presented higher scores for NGP, e.g. AX contents in the ceca than MC and ME, as reported in our recent publication (11). Therefore, the higher solubility of wheat AX compared to maize AX (9) indicated that more AX entered the ceca and was fermented by the gut microbiota, in the wheat-based diets. The pronounced AX fermentation in wheat-based diets was further documented by the lower AX total tract recovery compared to the maize-based diets (Fig. 4: AX_Trec) (11).

ASVs within *Faecalibactirium*, *Blautia* and Lachnospiraceae were positively associated with AX content in the ceca (Fig. 4). It, therefore, appeared that the proliferation of such genera in the wheat-based treatments coincided with pronounced AX fermentation. It has been previously suggested that fructooligosaccharides (FOS) and long-chain fructans were present in the soluble fraction of ileal digesta of wheat-based diets (11). FOS and inulin supplementation has been mentioned to also lead to the proliferation of microbiota such as *Bifidobacterium, Lactobacillus, Faecalibacterium* and *Blautia* in both animal and human studies (5,40,41). Consequently, it is expected that both FOS and AX/AXOS present in the wheat-based diets may exhibit bacteria-modulating properties. Still, more research is warranted to determine the relative contribution of different dietary NSP to a healthy gut.

The subtle shift in microbiota composition observed in this study in WE compared to WC (Table 3), could be related to AXOS formation in the proximal GIT by xylanase (11). The prebiotic potential of AXOS and XOS has been mainly demonstrated by their ability to selectively promote the growth of *Bifidobacterium* and *Lactobacillus* species during *in vitro* incubations with human fecal inocula (17,19). Likewise, supplementation of wheat-based diets with AXOS, XOS and xylanase has been previously shown to exert bifidogenic effect in broilers (7,42). Nevertheless, differences in the microbial composition of the human and avian gut (43) may impede the direct extrapolation of AXOS prebiotic potential in poultry. The present findings indicate that AX/AXOS fermentation could be important for the proliferation and function of other beneficial microbiota. So far, *Faecalibacterium* and *Blautia* have been reported to exhibit probiotic properties, while several Clostridiales have been previously associated with improved broiler performance (44,45). Therefore, their abundant presence may be highly important for a healthy gut. Although, no direct associations between beneficial microbiota and body weight could be currently established (Fig. 4), it is considered likely that their increased presence may benefit the host. Yet, further research is warranted to unravel potential interactions between dietary enzymes and microbial communities along the GIT, and their impact on animal growth.

4   Conclusion

The present study explores for a wheat-based and a maize-based diet the impact of NSPases on the broiler gut microbiota. Findings indicated that the microbial composition in the ceca strongly depended on the cereal type present in the diet. The proliferation of beneficial microbiota such as Lachnospiraceae, *Faecalibacterium* and *Blautia* in the wheat-based treatments compared to the maize-based treatments may be related to the pronounced fermentability of wheat-NSP. In particular, positive associations between fermentable AX content in the ceca and bacterial genera involved in carbohydrate metabolism to SCFAs were observed. These findings further support the importance of AX fermentation for a healthy broiler gut. The present outcomes provide further insight on how the xylanase-mediated AXOS release *in vivo* improve cecal fermentation and ecology. Notwithstanding, co-fermentation of other dietary NSP next to AX may have proceeded differently in wheat-based and maize-based diets. Consequently, AX fermentability is not expected to be the sole factor explaining the observed differences in microbial composition. The present findings provide important insight on the ability of dietary NSPases to modulate microbial ecology and metabolism in the broiler ceca.

3

5   References

1.   Stanley D, Hughes RJ, Moore RJ. Microbiota of the chicken gastrointestinal tract: Influence on health, productivity and disease. Appl Microbiol Biotechnol. 2014;98(10):4301–10.

2.   Pan D, Yu Z. Intestinal microbiome of poultry and its interaction with host and diet. Gut Microbes. 2013;5(1):108–19.

3.   Oviedo-Rondón EO. Holistic view of intestinal health in poultry. Anim Feed Sci Technol. 2019;250:1–8.

4.   Yadav S, Jha R. Strategies to modulate the intestinal microbiota and their effects on nutrient utilization, performance, and health of poultry. J Anim Sci Biotechnol. 2019;10:2.

5.   Azad MAK, Gao J, Ma J, Li T, Tan B, Huang X, Yin J. Opportunities of prebiotics for the intestinal health of monogastric animals. Anim Nutr. 2020;6(4):379–88.

6.   Iji PA, Tivey DR. Natural and synthetic oligosaccharides in broiler chicken diets. Worlds Poult Sci J. 1998;54(2):139–41.

7.   Ribeiro T, Cardoso V, Ferreira LMA, Lordelo MMS, Coelho E, Moreira ASP, Coimbra MA, Bedford MR, Fontes CMGA. Xylo-oligosaccharides display a prebiotic activity when used to supplement wheat or corn-based diets for broilers. Poult Sci. 2018;97(12):4330–41.

8.   Baurhoo B, Ferket PR, Zhao X. Effects of diets containing different concentrations of mannanoligosaccharide or antibiotics on growth performance, intestinal development, cecal and litter microbial populations, and carcass parameters of broilers. Poult Sci. 2009;88(11):2262–72.

9.   Bach Knudsen KE. Fiber and nonstarch polysaccharide content and variation in common crops used in broiler diets. Poult Sci. 2014;93(9):2380–93.

10.   Munyaka PM, Nandha NK, Kiarie E, Nyachoti CM, Khafipour E. Impact of combined β-glucanase and xylanase enzymes on growth performance, nutrients utilization and gut microbiota in broiler chickens fed corn or wheat-based diets. Poult Sci. 2016;95(3):528–40.

11.   Kouzounis D, Hageman JA, Soares N, Michiels J, Schols HA. Impact of xylanase and glucanase on oligosaccharide formation, carbohydrate fermentation patterns, and nutrient utilization in the gastrointestinal tract of broilers. Animals. 2021;11(5):1285.

12.   Rose DJ, Patterson JA, Hamaker BR. Structural differences among alkali-soluble arabinoxylans from maize (*Zea mays*), rice (*Oryza sativa*), and wheat (*Triticum aestivum*) brans influence human fecal fermentation profiles. J Agric Food Chem. 2010;58(1):493–9.

13.   Bedford MR. The evolution and application of enzymes in the animal feed industry: the role of data interpretation. Br Poult Sci. 2018;59(5):486–93.

14.   Choct M, Annison G. Anti-nutritive effect of wheat pentosans in broiler chickens: Roles of viscosity and gut microflora. Br Poult Sci. 1992;33(4):821–34.

15.   Kiarie E, Romero LF, Ravindran V. Growth performance, nutrient utilization, and digesta characteristics in broiler chickens fed corn or wheat diets without or with supplemental xylanase. Poult Sci. 2014;93(5):1186–96.

16.   Morgan NK, Keerqin C, Wallace A, Wu SB, Choct M. Effect of arabinoxylo-oligosaccharides and arabinoxylans on net energy and nutrient utilization in broilers. Anim Nutr. 2019;5(1):56–62.

17.   Kabel MA, Kortenoeven L, Schols HA, Voragen AGJ. *In vitro* fermentability of differently substituted xylo-oligosaccharides. J Agric Food Chem. 2002;50(21):6205–10.

18.   Rumpagaporn P, Reuhs BL, Kaur A, Patterson JA, Keshavarzian A, Hamaker BR. Structural features of soluble cereal arabinoxylan fibers associated with a slow rate of *in vitro* fermentation by human fecal microbiota. Carbohydr Polym. 2015;130:191–7.

19. Broekaert WF, Courtin CM, Verbeke K, van de Wiele T, Verstraete W, Delcour JA. Prebiotic and other health-related effects of cereal-derived arabinoxylans, arabinoxylan-oligosaccharides, and xylooligosaccharides. Crit Rev Food Sci Nutr. 2011;51(2):178–94.

20. Kers JG, Fischer EAJ, Stegeman JA, Smidt H, Velkers FC. Comparison of different invasive and non-invasive methods to characterize intestinal microbiota throughout a production cycle of broiler chickens. Microorganisms. 2019;7(10):431.

21. Ramiro-Garcia J, Hermes GDA, Giatsis C, Sipkema D, Zoetendal EG, Schaap PJ, et al. NG-Tax, a highly accurate and validated pipeline for analysis of 16S rRNA amplicons from complex biomes. F1000Research. 2016;5:1791.

22. Poncheewin W, Hermes GDA, van Dam JCJ, Koehorst JJ, Smidt H, Schaap PJ. NG-Tax 2.0: A semantic framework for high-throughput amplicon analysis. Front Genet. 2020;10:1366.

23. Quast C, Pruesse E, Yilmaz P, Gerken J, Schweer T, Yarza P, et al. The SILVA ribosomal RNA gene database project: Improved data processing and web-based tools. Nucleic Acids Res. 2013;41(D):590–6.

24. Englyst HN, Cummings JH. Simplified method for the measurement of total non-starch polysaccharides by gas-liquid chromatography of constituent sugars as alditol acetates. Analyst. 1984;109(7):937-42.

25. Blumenkrantz N, Asboe-Hansen G. New method for quantitative determination of uronic acids. Anal Biochem. 1973;54(2):484–9.

26. Thibault JF, Robin JP. Automatisation du dosage des acides uroniques par la méthode de carbazol. Application au cas de matières pectiques. Ann Technol Agric. 1975;24:99–110.

27. Logtenberg MJ, Akkerman R, An R, Hermes GDA, de Haan BJ, Faas MM, et al. Fermentation of chicory fructo-oligosaccharides and native inulin by infant fecal microbiota attenuates pro-inflammatory responses in immature dendritic cells in an infant-age-dependent and fructan-specific way. Mol Nutr Food Res. 2020;2000068.

28. Shankar V, Agans R, Paliy O. Advantages of phylogenetic distance based constrained ordination analyses for the examination of microbial communities. Sci Rep. 2017;7:6481.

29. Shakouri MD, Iji PA, Mikkelsen LL, Cowieson AJ. Intestinal function and gut microflora of broiler chickens as influenced by cereal grains and microbial enzyme supplementation. J Anim Physiol Anim Nutr. 2009;93(5):647–58.

30. Hübener K, Vahjen W, Simon O. Bacterial responses to different dietary cereal types and xylanase supplementation in the intestine of broiler chicken. Arch Anim Nutr fur Tierernahrung. 2002;56(3):167–87.

31. Nguyen HT, Bedford MR, Wu S-B, Morgan NK. Soluble non-starch polysaccharide modulates broiler gastrointestinal tract environment. Poult Sci. 2021;100(8):101183.

32. Rychlik I. Composition and fnction of chicken gut microbiota. Animals. 2020;10(1):103.

33. Oakley BB, Lillehoj HS, Kogut MH, Kim WK, Maurer JJ, Pedroso A, Lee MD, Collett SR, Johnson TJ, Cox NA. The chicken gastrointestinal microbiome. FEMS Microbiol Lett. 2014;360(2):100–12.

34. Yegani M, Korver DR. Factors affecting intestinal health in poultry. Poult Sci. 2008;87(10):2052–63.

35. Wang J, Cao H, Bao C, Liu Y, Dong B, Wang C, et al. Effects of xylanase in corn- or wheat-based diets on cecal microbiota of broilers. Front Microbiol. 2021;12:757066.

36. Józefiak D, Rutkowski A, Martin SA. Carbohydrate fermentation in the avian ceca: A review. Anim Feed Sci Technol. 2004;113(1–4):1–15.

37. Singh AK, Mandal RK, Bedford MR, Jha R. Xylanase improves growth performance, enhances cecal short-chain fatty acids production, and increases the relative abundance of fiber fermenting cecal microbiota in broilers. Anim Feed Sci Technol. 2021;277:114956.

38. Sergeant MJ, Constantinidou C, Cogan TA, Bedford MR, Penn CW, Pallen MJ. Extensive microbial and functional diversity within the chicken cecal microbiome. PLoS One. 2014;9(3):e91941.

39. Polansky O, Sekelova Z, Faldynova M, Sebkova A, Sisak F, Rychlik I. Important Metabolic Pathways and Biological Processes Expressed by Chicken Cecal Microbiota. Appl Environ Microbiol. 2016;82(5):1569–76.

40. Flint HJ, Scott KP, Duncan SH, Louis P, Forano E. Microbial degradation of complex carbohydrates in the gut. Gut Microbes. 2012;3(4):289–306.

41. Kumar S, Shang Y, Kim WK. Insight into dynamics of gut microbial community of broilers fed with fructooligosaccharides supplemented low calcium and phosphorus diets. Front Vet Sci; 2019;6:95.

42. Lee SA, Apajalahti J, Vienola K, González-Ortiz G, Fontes CMGA, Bedford MR. Age and dietary xylanase supplementation affects ileal sugar residues and short chain fatty acid concentration in the ileum and caecum of broiler chickens. Anim Feed Sci Technol. 2017;234:29–42.

43. Waite DW, Taylor MW. Exploring the avian gut microbiota: Current trends and future directions. Front Microbiol. 2015;6:673.

44. Torok VA, Hughes RJ, Mikkelsen LL, Perez-Maldonado R, Balding K, MacAlpine R, Percy NJ, Ophel-Keller K. Identification and characterization of potential performance-related gut microbiotas in broiler chickens across various feeding trials. Appl Environ Microbiol. 2011;77(17):5868–78.

45. Liu X, Mao B, Gu J, Wu J, Cui S, Wang G, Zhao J, Zhang H, Chen W. *Blautia*—a new functional genus with potential probiotic properties? Gut Microbes. 2021;13(1):e1875796.

Supplementary information

Table S1. Dry matter content (% w/w) (standard deviation), total carbohydrate, constituent arabinosyl (Ara) xylosyl (Xyl) content (% dry matter basis), and acetate, butyrate and propionate content (mg/g dry matter basis) in the ceca of broilers fed the various dietary treatments. The data were previously determined and are reported elsewhere (1).

Analyzed parameter (in ceca)	Diets			
	Wheat Control (WC)	**Wheat Enzyme (WE)**	**Maize Control (MC)**	**Maize Enzyme (ME)**
Dry matter, % w/w	26.57 (1.71)	23.12 (1.24)	18.19 (1.59)	19.02 (0.54)
Carbohydrate content, % dry matter basis				
NGP[1]	5.22	3.88	4.14	3.81
AX[2]	0.89	0.52	0.32	0.27
Short chain fatty acid content, μmol/g dry matter basis[3]				
Acetate	172.66	250.94	354.47	287.77
Butyrate	53.12	73.08	78.46	59.29
Propionate	11.02	11.15	31.43	23.60

[1]Non-glucosyl NSP; calculated as the sum of sum of arabinosyl, xylosyl, galactosyl, uronyl, mannosyl, rhamnosyl and fucosyl units. [2]Arabinoxylan; calculated as the sum of arabinosyl and xylosyl units. [3]ANOVA results for 1) WC vs WE: Acetate, $P = 0.014$, Butyrate, $P = 0.044$, Propionate, $P = 0.906$, 2) MC vs ME: Acetate, $P = 0.037$, Butyrate, $P = 0.010$, Propionate, $P = 0.039$. Significance was set at $p < 0.05$.

Supplementary information references

1. Kouzounis D, Hageman JA, Soares N, Michiels J, Schols HA. Impact of xylanase and glucanase on oligosaccharide formation, carbohydrate fermentation patterns, and nutrient utilization in the gastrointestinal tract of broilers. Animals. 2021;11(5):1285.

Chapter

4

Strategy to identify reduced arabinoxylo-oligosaccharides by HILIC-MS^n

Kouzounis D., Sun P., Bakx E. J., Schols H. A., Kabel. M. A.

Abstract

Identification of arabinoxylo-oligosaccharides (AXOS) within complex mixtures is an ongoing analytical challenge. Here, we established a strategy based on hydrophilic interaction chromatography coupled to collision induced dissociation-mass spectrometry (HILIC-MS^n) to identify a variety of enzyme-derived AXOS structures. Oligosaccharide reduction with sodium borohydride remarkably improved chromatographic separation of isomers, and improved the recognition of oligosaccharide ends in MS-fragmentation patterns. Localization of arabinosyl substituents was facilitated by decreased intensity of Z ions relative to corresponding Y ions, when fragmentation occurred in the vicinity of substituents. Interestingly, the same B fragment ions (MS^2) from HILIC-separated AXOS isomers showed distinct MS^3 spectral fingerprints, being diagnostic for the linkage type of arabinosyl substituents. HILIC-MS^n identification of AXOS was strengthened by using specific and well-characterized arabinofuranosidases. The detailed characterization of AXOS isomers currently achieved can be applied for studying AXOS functionality in complex (biological) matrices. Overall, the present strategy contributes to the comprehensive carbohydrate sequencing.

1   Introduction

Arabinoxylan (AX) is an abundant cereal fiber in both human and animal diets. Investigating the prebiotic and immunomodulatory properties of AX and (enzymatically) derived arabinoxylo-oligosaccharides (AXOS) is of great nutritional, scientific and commercial interest (1,2). Previous studies have shown that the prebiotic potential of AXOS depended on degree of polymerization (DP) and substitution pattern (2–4). Therefore, detailed characterization of AXOS in complex matrices may greatly improve our understanding about their bio-functionality.

In general, cereal grain AX (i.e., from wheat, maize, rye, rice) is composed of a backbone of β-(1→4)-linked D-xylosyl (Xyl) residues, substituted mainly by L-arabinofuranosyl (Ara) units at the *O*-2- and/or *O*-3-positions of Xyl units. To a lesser extent, 4-*O*-D-methyl-glucuronoyl and acetyl substituents occur, and a part of the Ara units might be further *O*-5-substituted by feruloyl units (5,6). Cereal grains present diverse AX populations, primarily due to variation in the type and distribution of Ara substituents over the AX backbone (7–10). Consequently, the corresponding (enzyme-derived) AXOS mixtures contain a range of differently substituted structures.

Although oligosaccharide identification has considerably improved in the last decades (11–13), detailed identification of AXOS in mixtures remains an ongoing analytical challenge due to the aforementioned complexity. High Performance Anion Exchange Chromatography (HPAEC) has been shown to provide valuable information regarding the oligosaccharide composition of enzymatic (A)XOS digests (14–17). However, scarcely available standards and low compatibility with mass spectrometric techniques, due to the high salt concentration of eluents, hamper the identification of unknown oligosaccharides by HPAEC (13,16). AXOS purified from enzymatic digests were subjected to nuclear magnetic resonance (^{1}H NMR) spectroscopy to accurately determine the position and linkage type of Ara substituents (17–20). Still, ^{1}H NMR analysis requires high purity and amount of analytes (21), which complicates the analysis of (minorly present) AXOS from complex biological matrices. Next to ^{1}H NMR, direct infusion mass spectrometry (MS[n]), has been widely used for AXOS structural analysis (11,22–24). In specific, hyphenation of MS[n] to normal phase and reverse phase liquid chromatography (LC-MS[n]) further progressed AXOS characterization (25,26). Still, chromatographic resolution was not sufficient to address AXOS identification in complex biological mixtures. Hydrophilic interaction liquid chromatography (HILIC) was recently reviewed to exhibit increased selectivity for glycan analysis compared to reverse phase chromatography, and higher compatibility with MS compared to normal phase chromatography (13). HILIC coupled to MS has been assessed to separate and characterize *in vitro*-generated AXOS, human milk oligosaccharides, as well as cello-, galacto-, manno-, arabino- and pectic oligosaccharides mixtures (27–32). Furthermore, the characterization of alginate-oligosaccharides in fecal samples by

HILIC-MS (33) demonstrated the potential of HILIC-based approaches to separate and identify oligosaccharides present in complex biological matrices. Still, further research is warranted to improve HILIC separation and MS-based identification of AXOS isomers present in mixtures.

The chromatographic resolution of α- and β-anomers of oligosaccharides in LC, including HILIC, has been shown to result in signal loss and peak broadening (34,35). The latter can be overcome by reducing oligosaccharides, for example with sodium borohydride ($NaBH_4$) (36,37). Such reduction has been shown to result in better HILIC separation for cello-oligosaccharide mixtures with increased signal intensities, and allows the discrimination in MS of fragment ions originating from either the non-reducing or reduced end (27,38,39). So far, to the best of our knowledge, chromatographic resolution and MS fragmentation patterns of $NaBH_4$-reduced (A)XOS subjected to HILIC-MS[n] have not been studied.

Hence, the present study aimed at developing a strategy to characterize individual (A)XOS present in complex mixtures formed during arabinoxylan depolymerization by endo-xylanases. For that, AXOS mixtures were further treated with arabinofuranosidases and were reduced by $NaBH_4$, prior to their HILIC-MS[n] analysis. Hereto, it was hypothesized that structurally different $NaBH_4$-reduced (A)XOS show chromatographic resolution in HILIC and exhibit distinct MS fragmentation patterns. The principles on which this strategy is based are considered compatible with analytical needs for the structural elucidation of other types of polysaccharides.

2   Materials and methods

2.1   Materials

Wheat flour arabinoxylan (medium viscosity; WAX), linear XOS (DP 2–6; X_2-X_6), branched AXOS standards (XA^3XX, XA^2XX & XA^3XX mixture, $A^{2+3}XX$), GH10 endo-1,4-β-xylanase from *Thermotoga maritima* (Xyn_10), GH43 α-arabinofuranosidase from *Bifidobacterium adolescentis* (Abf_43) and GH51 α-arabinofuranosidase from *Aspergillus niger* (Abf_51) were obtained from Megazyme (Bray, Ireland). A commercial enzyme preparation (HX) enriched in GH11 endo-1,4-β-xylanase from *Trichoderma citrinoviride* was provided by Huvepharma NV (Berchem, Belgium). In AXOS abbreviations, unsubstituted xylosyl residues are annotated as X, while xylosyl residues substituted at *O*-2, *O*-3 or at both *O*-2 and *O*-3 positions by arabinosyl units are annotated as A^2, A^3 and A^{2+3}, respectively, according to Fauré et al. (2009) (5).

2.2   *In vitro* production of arabinoxylo-oligosaccharides (AXOS)

WAX (5.5 mg/mL) was dissolved in 50 mM sodium acetate (NaOAc) buffer (pH 5.0). Next, 4.55 mL WAX solution was transferred in a 15 mL tube, and 455 µL of HX or Xyn_10 solution pre-diluted in the same NaOAc buffer was added to start

the incubations. The enzyme doses used were chosen to result in total or 'end-point' degradation of WAX. Incubations were carried out at 40 °C overnight followed by enzyme inactivation at 99 °C for 15 min. Supernatants (e.g., AXOS mixtures) were analyzed with HPAEC-PAD (10 times diluted), and after reduction (see 2.4) with HILIC-ESI-CID-MS^n.

2.3 Enzymatic fingerprinting of arabinosyl substituents in AXOS

Two AXOS mixtures obtained (see 2.2) by using the two distinct endo-xylanases were subsequently treated with Abf_43, Abf_51 and a combination thereof (Abf_43/Abf_51). GH51 Abfs release single O-2- or O-3-linked arabinosyl substitutions (reviewed by Lagaert et al. (2014) (40)), while Abf_43 only releases the O-3 arabinosyl from a disubstituted Xyl moiety (41,42). Although the Abf_51 currently used was previously shown to be also active toward disubstituted AXOS, especially A^{2+3}XX (43), in our research, only a very minor amount of A^{2+3}XX was degraded after 8 h and current experimental conditions, as shown by HPAEC (see Fig. S1). Aliquots (500 µL) of the AXOS mixtures were transferred in clean reaction tubes and were mixed with 480 µL or 460 µL 50 mM sodium acetate buffer (pH 5.0) for single or combined Abf incubations, respectively. Next, 20 µL of Abf_43 and/or Abf_51 solution was added to achieve a final dosing of 0.1 U/mL. The samples, alongside controls with no Abf added, were incubated at 40 °C for 8 h, followed by enzyme inactivation at 99 °C for 15 min. Oligosaccharide and Abf digests were analyzed with HPAEC-PAD (10 times diluted), and after reduction with HILIC-ESI-CID-MS^n.

2.4 Reduction of oligosaccharides

Aliquots (200 µL) of DP 2-6 XOS mixture (1 mg/mL each), A^{2+3}XX (1 mg/mL), A^{2}XX (1 mg/mL; see supplementary information), XA^{3}XX (1 mg/mL), XA^{2}XX/XA^{3}XX (2 mg/mL), AXOS mixtures (1 mg/mL; see 2.2) and AXOS mixtures digested with Abfs (1 mg/mL; see 2.3) were reduced with 200 µL 0.5 M NaBH$_4$ solution in 1M NH$_4$OH at room temperature for 4 h. The reaction was stopped by addition of 50 µL acetic acid and was followed by sample clean up on Supelclean™ ENVI-Carb™ solid phase extraction (SPE) cartridges (250 mg, Sigma Aldrich, St. Louis, MO, USA). The cartridges were activated with 80% (v/v) acetonitrile (ACN; Biosolve, Valkenswaard, The Netherlands) containing 0.1% (v/v) trifluoroacetic acid (Sigma Aldrich) and conditioned with water. Samples were loaded on the cartridges and washed with water. Analytes eluting with 40% (v/v) ACN containing 0.1% (v/v) TFA were collected and dried by evaporation. The dried analytes were redissolved in 400 µL 50% ACN prior to their HILIC-ESI-CID-MS^n analysis.

2.5 Separation and identification of reduced AXOS with HILIC-ESI-CID-MS^n

Separation and identification of individual AXOS in mixtures was performed by hydrophilic interaction chromatography - electrospray ionization - collision induced

dissociation - tandem mass spectrometry (HILIC-ESI-CID-MS[n]) using a previously described method (27), with modifications. The analysis was performed on a Vanquish UHPLC system (Thermo Fisher Scientific, Waltham, MA, USA) equipped with an Acquity UPLC BEH Amide column (Waters, Millford, MA, USA; 1.7 µm, 2.1 mm ID × 150 mm) and a VanGuard pre-column (Waters; 1.7 µm, 2.1 mm ID × 5mm). The column temperature was set at 35 °C and the flow rate was 0.45 mL/min; injection volume was 1 µL. Water (A) and ACN (B), both containing 0.1 % (v/v) formic acid (FA) (all solvents were UHPLC-grade; Biosolve), were used as mobile phases. The separation was performed by using the following elution profile: 0−2 min at 82 % B (isocratic), 2−32 min from 82 % to 71 % B (linear gradient), 32–32.5 min from 71 % to 42 % B (linear), 32.5−39 min at 42 % B (isocratic), 39−40 min from 42 % to 82 % B (linear) and 40−50 min at 82 % B (isocratic). Oligosaccharide mass (m/z) was on-line detected with an LTQ Velos Pro mass spectrometer (Thermo Fisher Scientific) operated in a negative ion mode. The mass spectrometer was equipped with a heated ESI probe, and was run at three modes: Full MS, MS[2] on selected MS ions, and MS[3] on selected MS[2] ions. Ion selection was different for DP 3, 4, 5, 6 and 7 oligosaccharides (Table S1), and each DP series was analyzed in separate runs. The settings used were: source heater temperature 425 °C, capillary temperature 263 °C, sheath gas flow 50 units and source voltage 2.5 kV. MS[2] scanning was performed at m/z range 150-1200: CID with normalized collision energy set at 40%, activation Q of 0.25 and activation time of 10 ms. The m/z range of MS[3] scan events depended on the m/z value of the daughter ion. The CID was set at 35%, while all other parameters were similar to MS[2] scanning. Mass spectrometric data were processed by using Xcalibur 2.2 software (Thermo Fisher Scientific).

3   Results and discussion

3.1   Separation and identification of reduced, isomeric AXOS standards

The aim of this research was to develop a strategy for AXOS identification in complex mixtures, making use of HILIC-MS[n]. It was hypothesized that reduction of the oligosaccharides would not only improve chromatographic resolution, but would also aid in their MS-based identification, as has been suggested for other types of oligosaccharides (37,38,44). First, the elution and fragmentation patterns of reduced, standard (A)XOS all having a DP of 5 (A[2+3]XX, XA[3]XX, XA[2]XX, X_5) were investigated (Fig. 1; Fig. 2), before delving into complex AXOS mixtures. The overall separation and resolution of reduced DP 5 isomers was enormously improved (Fig.1A) in comparison to that of underivatized (A)XOS (Fig. S2). The reduced (A)XOS isomers eluted in the following order: A[2+3]XX, XA[3]XX, XA[2]XX and X_5 (Fig. 1A). Interestingly, the observed shorter retention times of reduced AXOS compared to the linear (reduced) counterpart (e.g., X_5), provides a first indication of arabinosyl substitution when specific analytical standards are not available.

Fig. 1. HILIC-MS extracted ion chromatograms (**A**) of four NABH4-reduced DP5 (*m/z* 679; [M–H]⁻) isomers: $A^{2+3}XX$ (**1**), XA^3XX(**2**), XA^2XX (**3**) and X_5 (**4**). Negative ion mode CID-MS² spectra (**B**) of eluted isomers **1-4**; average spectra across the chromatographic peaks. The fragments are annotated according to Domon & Costello (1988) and Juvonen et al. (2019) (31,39). Blue: glycosidic linkage fragments; Red: cross-ring fragments; /: double cleavage; x: α or β antennae. Alternative fragments are presented in brackets.

Full-scan MS mode (data not shown) indicated that oligosaccharides were present in a single-charged, deprotonated state ([M–H]⁻) or as deprotonated formate adducts ([M+FA–H]⁻). The [M–H]⁻ products were preferred for further MS analysis, because fragmentation of [M+FA–H]⁻ products was either not obtained or resulted in complex spectra with various formate-adducted fragments, as was also observed by Sun et al. (2020) (27) for cello-oligosaccharides.

The obtained fragmentation spectra were annotated according to the nomenclature proposed by Domon & Costello (1988) (39). MS² analysis (Fig. 1B) revealed that for all separated reduced standard DP 5 AXOS (Fig. 1A), Y (Y_{4-2}: *m/z* 547, 415, 283), Z (Z_{4-2}: *m/z* 529, 397, 265) and B (B_{4-2}: *m/z* 527, 395, 263) ions were the

main fragments, while C ions (C_3: m/z 413, C_2: m/z 281) were only visible at highest zoom levels (not shown). Z ions were predominant for X_5, but less abundant for Ara-substituted isomers (Fig. 1). In particular, the abundance of Z_3 and Z_2 was lower in $A^{2+3}XX$ compared to XA^3XX and XA^2XX. The lower abundance of C ions in negative ion mode MS^2 has not been previously observed for underivatized oligosaccharides, such as AXOS and cello-oligosaccharides (23,27,31). More explicitly, C ions occurring from the reducing end, have been previously described as integral diagnostic fragments for such underivatized AXOS structures (23,31). Most likely, reduction resulted in less stable C ions compared to Y, Z and B ions. This observation is in line with previous studies reporting the decrease in C ion abundance after reduction of mucin-derived oligosaccharides, cello-oligosaccharides, and galacto-oligosaccharides (27,45,46). Cross-ring fragments $^{0,2}A_n$ and $^{2,4}A_n$ were observed at relatively low abundances (Fig. 1B), mainly with further loss of water (e.g., $^{0,2}A_{4(3)}$–H_2O: m/z 467, $^{0,2}A_{3(2)}$–H_2O: m/z 335). Nevertheless, these two cross-ring fragment types have been proven to be important indicators of the β-(1→4) linkages between xylosyl backbone residues (23). Furthermore, double cleavages involving B and Y or Z glycosidic ions, as well as $Y_{3\alpha}/Y_{3\beta}$, $Z_{3\alpha}/Z_{3\beta}$, Y_{3x}/Z_{3x} double cleavages were observed (Fig. 1), in line with MS^2 fragmentation spectra of underivatized oligosaccharides in previous reports (31,39,47). Additional double cleavages involving glycosidic and cross-ring fragments ($^{0,2}A_n/Y$ ($^{0,2}A_n$–H_2O/Z)) currently observed have been also reported for underivatized AXOS (31). For example, m/z 335 was observed in all four isomers (Fig. 1), and represented a cross-ring cleavage ($^{0,2}A_{2(3)}$–H_2O) in XA^3XX and X_5. Yet, the formation of m/z 335 in XA^2XX and $A^{2+3}XX$ could not be explained by $^{0,2}A_x$ cleavage alone, and might have resulted from double cleavage that involved the loss of O-2-linked Ara. The formation of such double cleavage fragment ions is not uncommon (39,47,48), but impedes conclusive identification of the four isomers based on their MS^2 spectra.

Therefore, relevant Y and B fragment ions (MS^2) were further investigated by MS^3. To that end, MS^3 analysis of $Y_{3(4)}$ (m/z 547) (Fig. S3), $B_{3(4)}$ (m/z 527) and $B_{2(3)}$ (m/z 395) (Fig. 2) was carried out. MS^3 analysis of m/z 679→547 ion across all four DP 5 isomers mainly showed B and Y fragments, while the formation of Z_3 (m/z 397) was more restricted in $A^{2+3}XX$ than in XA^3XX and XA^2XX (Fig. S3). The latter confirmed the MS^2 analysis of AXOS structures (Fig. 1), pointing out that Z ions were less favored in the vicinity of Ara substituents. Conversely, the corresponding MS^3 spectra of m/z 679→547 ions for XA^3XX and XA^2XX resembled that of X_5 (Fig. S3). This observation indicated the loss in MS^3 of Ara instead of the terminal xylosyl moiety from both MS^2 ions having the same m/z value.
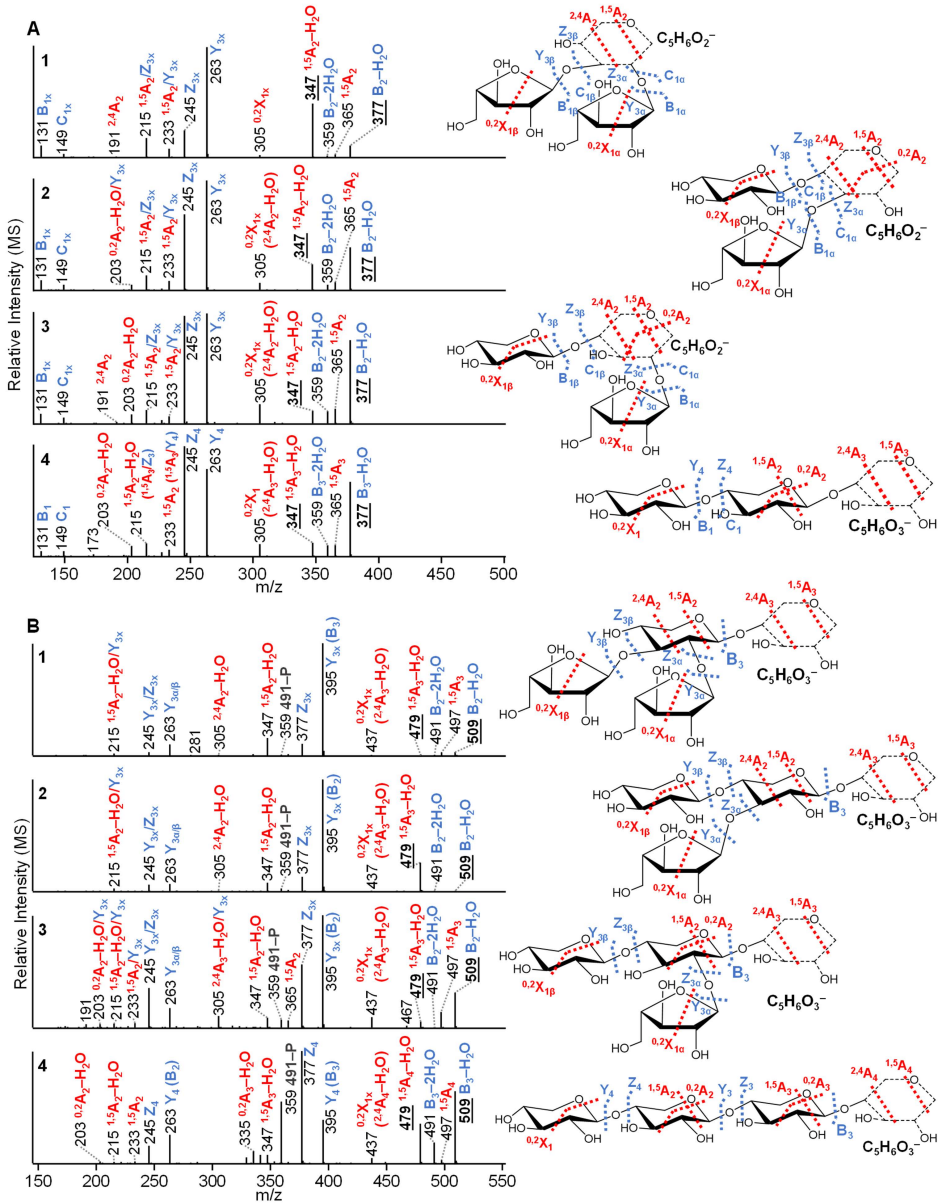
Fig. 2. Negative ion mode CID-MS^3 spectra of m/z 679→395 [M–H]$^-$ (**A**) and *m/z* 679→527 [M–H]$^-$ (**B**) corresponding to A^{2+3}XX (**1**), XA^{3}XX (**2**), XA^{2}XX (**3**) and X$_5$ (**4**) (MS^2; see Fig. 1). The fragments are annotated according to Domon & Costello (1988) and Juvonen et al. (2019) (31,39). Blue: glycosidic fragments; Red: cross-ring fragments; /: double cleavage; x: α or β antennae. Alternative fragments are presented in brackets. The precise structure of the newly formed end of B fragment ions is unknown as it may undergo several rearrangements (dashed ring), hence corresponding MS^3-ring-fragments have been annotated tentatively.

In MS^3, the spectra of all isomers in the case of *m/z* 679→395 and *m/z* 679→527 were dominated by B, Y and Z ions, while ^{1,5}A and ^{2,4}A ions were also present (Fig. 2). In particular, isomers presented distinct MS^3 spectra for *m/z* 679→395, mainly differing in relative intensities of *m/z* 377, 359, 365 and 347 ions (Fig. 2A). The ions *m/z* 377 and *m/z* 359 were most likely formed by the loss of one (B$_{2(3)}$–H$_2$O) or two (B$_{2(3)}$–2H$_2$O) water molecules, respectively, due to the dehydration of the MS^2 fragment ion. The ions *m/z* 365 and *m/z* 347 were assigned to ^{1,5}A cross-ring fragments, without or with additional loss of water, respectively.

Furthermore, the intensity ratio of ^{1,5}A$_{2(3)}$–H$_2$O:B$_{2(3)}$–H$_2$O (*m/z* 347:377) was approximately 5 for A^{2+3}XX, 0.6 for XA^{3}XX and 0.2 for XA^{2}XX and X$_5$. Additionally Z$_3$ presented lower relative intensity for A^{2+3}XX compared to mono-substituted isomers. The *m/z* 305 (^{0,2}X$_1$) ion was mainly observed in XA^{2}XX, while it was not very abundant in A^{2+3}XX. Although X-type fragments have been reported to be scarce in negative ion mode (39), their formation has been observed in recent studies for underivatized oligomers (27,31). Alternatively, the same ion (*m/z* 305) could have resulted from the ^{2,4}A$_2$ or ^{2,4}A$_3$ cleavage in XA^{3}XX and X$_5$ respectively. The *m/z* 679→527 ion (B$_{3(4)}$) corresponding to different isomers was also investigated by MS^3 (Fig. 2B). The observed spectral fingerprint was comparable to that of *m/z* 679→395, with the fragment ions B$_{3(4)}$–H$_2$O, B$_{3(4)}$–2H$_2$O, ^{1,5}A$_{3(4)}$, ^{1,5}A$_{3(4)}$–H$_2$O and Z$_{3x(4)}$ being differently abundant between isomers. In this case, the ^{1,5}A$_{3(4)}$–H$_2$O:B$_{3(4)}$–H$_2$O ratio (*m/z* 509:479) was approximately 0.3 for A^{2+3}XX, 152 for XA^{3}XX, 0.2 for XA^{2}XX and 0.5 for X$_5$. It was observed that while XA^{2}XX and X$_5$ presented low values for fragment ion ratios in MS^3, for both *m/z* 679→395 and *m/z* 679→527, this was not the case in the presence of *O*-3-linked Ara. In specific, A^{2+3}XX and XA^{3}XX demonstrated contrasting MS^3 profiles for *m/z* 679→527 and *m/z* 679→395. Consequently, it could be concluded that both the linkage type and position of Ara substituents influenced the MS^3 fragmentation patterns of reduced AXOS. Overall, MS^3 analysis was instrumental in discriminating between AXOS isomers by distinguishing between different linkage types and positions of Ara substituents on the xylan backbone.

3.2 Chromatographic separation and MS-based annotation of (reduced) AXOS in mixtures obtained by enzymatic hydrolysis of arabinoxylan

The approach discussed in 3.1 for standard AXOS was further applied to two types of AXOS mixtures: wheat arabinoxylan (WAX) digested by a GH11 endo-xylanase (HX) or by a GH10 endo-xylanase (Xyn_10). The obtained AXOS mixtures were subsequently digested by Abf_51 and/or Abf_43. HPAEC-PAD analysis (Fig. S4) confirmed that Abf_51 removed Ara from single substituted Xyl residues, resulting a mixture of XOS and AXOS with intact doubly-substituted xylosyl residues. Abf_43 only cleaved *O*-3-linked Ara from doubly substituted xylosyl residues (41,42), releasing singly substituted AXOS. The combination of both Abfs resulted mainly in (unsubstituted) XOS (Fig. S4).

The (A)XOS mixtures were further subjected to NaBH$_4$ reduction, followed by HILIC-MS[n] analysis (Fig. 3). Distinct peaks were observed corresponding to reduced DP 3-7 pentose oligomers as based on their *m/z* values, and were coded accordingly as explained below (i-vii; Table 1). HX mainly released X$_2$, 4.ii and 5.iii, while Xyn_10 mainly released X$_2$, 3.i and 4.ii as end products from WAX. The different AXOS profiles obtained by HX and Xyn_10 were linked to the previously demonstrated lower tolerance of GH11 endo-xylanases to Ara substituents compared to GH10 endo-xylanases (20,49). Apart from the oligosaccharides shown in Fig. 3, other minorly present DP 6 and 7 (A)XOS were released as well, and are shown at a higher sensitivity in Fig. S5.
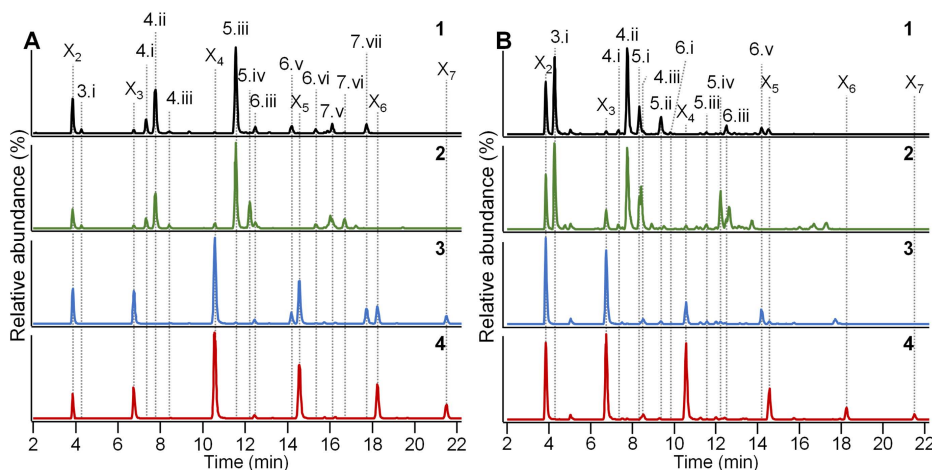
Fig. 3. HILIC-MS extracted ion chromatograms of NaBH$_4$-reduced AXOS and XOS from WAX digested by HX (**A.1**) and Xyn_10 (**B.1**). Subsequent digestions with Abf_43 (**2**), Abf_51 (**3**) or Abf_43/Abf_51 combination (**4**). see Table 1 for explanation of coded peaks.

First, XOS (DP 2-6) mainly formed by the combination of Abf_43/Abf_51 were identified on the basis of elution time and MS^2 spectra of corresponding standards. As has been observed for the DP 5 standards (section 3.1), AXOS eluted before linear XOS with the same DP. Second, 4.iii, 5.ii, 5.iii and 5.iv were annotated as A^{2}XX, A^{2+3}XX, XA^{3}XX and XA^{2}XX, respectively, based on retention time and (identical) MS^2 spectra of available standards (Fig. 2; Fig. S6; Table 1). Next, Abf_43 and Abf_51 treatment of HX and Xyn_10 WAX digests further assisted in tentatively identifying individual AXOS. For example, the peaks 5.ii, 6.v and 7.vii disappeared upon Abf_43 treatment, while the relative abundance of 4.iii and 5.iv increased (Fig. 3). At the same time, peak 6.viii was formed (Fig. S5). Consequently, it was concluded that 5.ii (A^{2+3}XX), 6.v and 7.vii represented disubstituted AXOS, while 4.iii (A^{2}XX), 5.iv (XA^{2}XX) and 6.viii, represented *O*-2 monosubstituted AXOS. The peaks (partly) removed by Abf_51 treatment represented AXOS with single Ara substitutions (40,41). As a consequence, mainly XOS as well as disubstituted 5.ii, 6.v and 7.vii AXOS remained in the Abf_51

digests. Peaks like 4.iii and 6.iii were minorly visible in Abf_51 digests (Fig. 3), suggesting almost complete Abf_51 action under the current experimental conditions.

3.3 Detailed identification of enzymatically derived (reduced) DP 3, 4 and 5 AXOS isomers in mixtures

In addition to the first annotation described in 3.2, the structure of partially annotated AXOS was further investigated by MS^n. Apart from 5.ii-iv, an additional pentasaccharide (5.i) was released by Xyn_10, but not by HX. Digestion by Abfs demonstrated that 5.i was singly-substituted (Fig. 3). Its MS^2 and MS^3 (m/z 679→547, 527, 395) spectra are shown in Fig. 4. In line with the observations made for AXOS standards (section 3.1), the Z_4 ion was less abundant compared to the Y_4 ion in MS^2, suggesting that Ara substitution was present at, or next to, the non-reducing terminal Xyl residue.

MS^3 analysis of m/z 679→547 demonstrated that Z_3 formation was suppressed in 5.i compared to XA^{3}XX, XA^{2}XX and X$_5$ (Fig. 4). This confirmed the presence of an additional arabinosyl attached to the penultimate xylosyl residue from the non-reducing end in 5.i. Next, the MS^3 spectrum of m/z 679→395 fragment ion (B$_4$/Y$_4$) was comparable to those of A^{2+3}XX and XA^{3}XX standards (Fig. 2), and the ^{1,5}A$_3$-H$_2$O:B$_4$/Y$_4$–H$_2$O ratio (m/z 347:377) was estimated to be ~10 (Table 1). The observation that 5.i presented similar features to both A^{2+3}XX and XA^{3}XX, demonstrated the presence of O-3-linked arabinosyl substituents, reflecting the most abundant substitution type in wheat arabinoxylan (18,50). Additionally, the absence of the corresponding diagnostic ions from the MS^3 spectrum of m/z 679→527 for 5.i, indicated that fragmentation was more restricted in comparison to other DP 5 (A)XOS (Fig. 2), and reflected a different substitution pattern. Based on the above, we propose that 5.i is substituted by two single, consecutive O-3-linked Ara units (A^{3}A^{3}X; Table 1). It should be noted that the m/z 395 ion in 5.i was a product of double cleavage (B$_4$/Y$_4$), involving the loss of one of the two Ara substituents (Fig. 4). The release of A^{3}A^{3}X and A^{2+3}XX from WAX by a GH10 endo-xylanase exhibiting similar mode of action as Xyn_10, has been previously demonstrated by ^{1}H NMR (49).
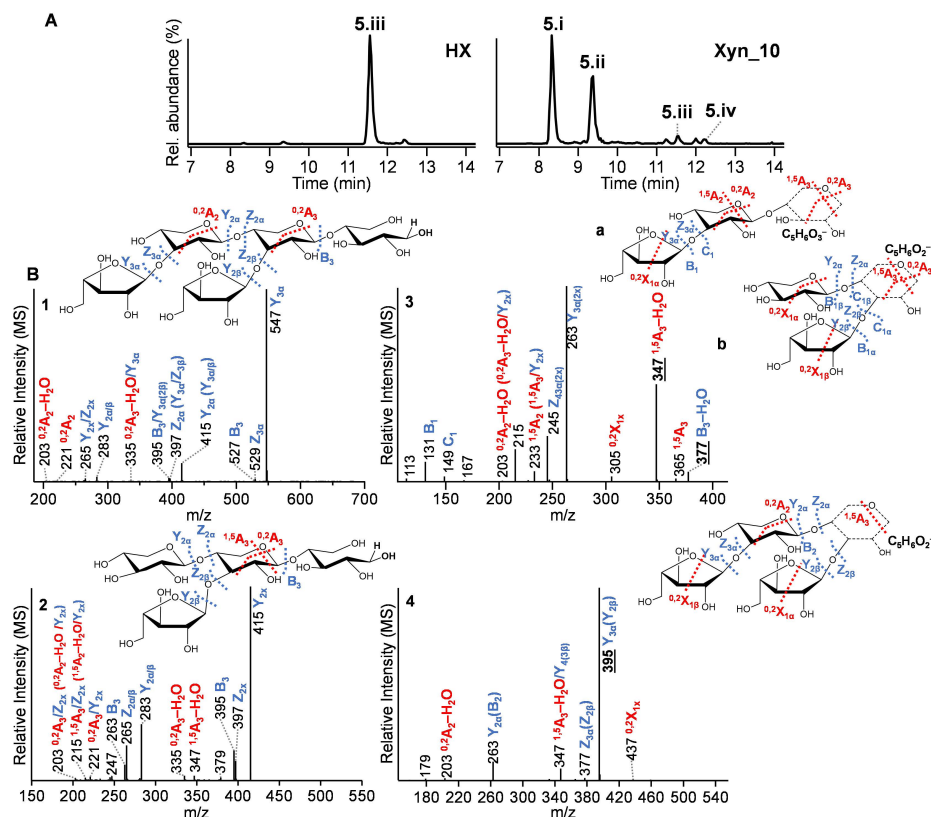
Fig. 4. Negative ion mode CID-MS[2] (**1**) and CID-MS[3] spectra of m/z 679→547 [M–H][−] (**2**), m/z 679→395 [M–H][−] (**3**) and m/z 679→527 [M–H][−] (**4**) for 5.i. Average spectra (**B**) of the chromatographic peak present in Xyn_10 treatment (**A**). The fragments are annotated according to Domon & Costello (1988) and Juvonen et al. (2019) (31,39). Blue: glycosidic fragments; Red: cross-ring fragments; /: double cleavage; x: α or β antennae. Alternative fragments are presented in brackets. Structures **a, b** correspond to **3** due to the loss of either arabinosyl substituent. The precise structure of the newly formed end of B fragment ions is unknown as it may undergo several rearrangements (dashed ring), hence corresponding MS[3]-ring-fragments have been annotated tentatively.

Having obtained an overview of the influence of Ara substitution on the fragmentation of DP 5 AXOS, we proceeded in identifying DP 3 and 4 isomers in a similar manner. Both HX and Xyn_10 treatments resulted in the release of one trisaccharide (3.i), eluting before X_3 and three DP 4 AXOS (4.i, 4.ii, 4.iii: A[2]XX) (Fig. 3). In specific, 3.i and 4.ii were major products released by Xyn_10, while 4.i and 4.ii were main products released by HX. A[2]XX was minorly present in both cases. Abf treatment revealed that all four (reduced) DP 3 and 4 AXOS detected were singly substituted (Fig. 3).
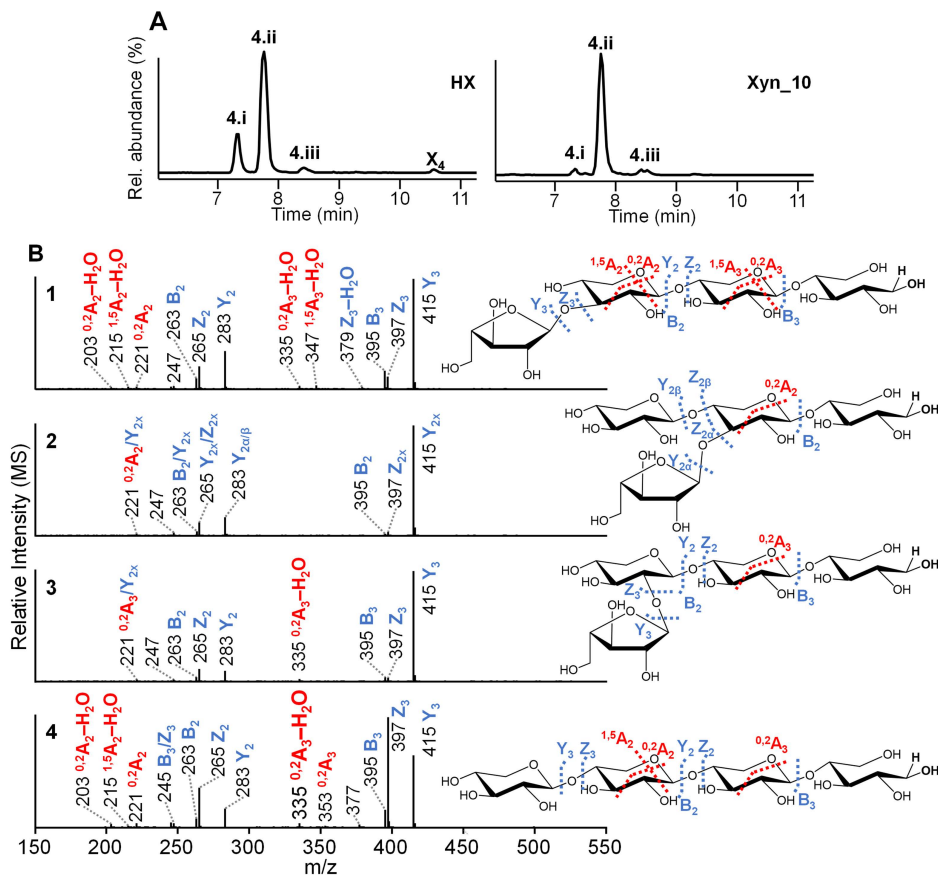
Fig. 5. Negative ion mode CID-MS^2 (**B**) spectra of 4.i (**1**), 4.ii (**2**), 4.iii (**3**) and X$_4$ (**4**) DP4 AXOS/XOS isomers (*m/z* 547; [M–H]$^-$). Average spectra across the most abundant chromatographic peaks between treatments (**A**). The fragments are annotated according to Domon & Costello (1988) and Juvonen et al. (2019) (31,39). Blue: glycosidic fragments; Red: cross-ring fragments; /: double cleavage; x: α or β antennae.

 Starting with DP 4 isomers, the suppression of Z$_3$ ion in MS^2 (Fig. 5) confirmed the substitution site for both 4.i and 4.ii. Next, MS^3 analysis of the daughter ion (*m/z* 547→395) in 4.i and 4.ii was performed (Fig. 6). In this case, 4.i presented similar MS^3 spectrum for *m/z* 547→395 as A^{2+3}XX (Fig. 2) and A^{3}A^{3}X (Fig. 4). Moreover, 4.i presented ^{1,5}A$_2$-H$_2$O:B$_3$-H$_2$O (*m/z* 347:377) ratio ~10, which was comparable to the value obtained for A^{3}A^{3}X (Table 1). Hence, it is proposed that a high ^{1,5}A$_x$-H$_2$O:B$_x$-H$_2$O ratio, accompanied by the observed spectral fingerprint during fragmentation of MS^2 ion *m/z* 395, was characteristic for *O*-3-linked arabinosyl at the non-reducing terminus, albeit not diagnostic for the entire oligomeric structure. The spectral fingerprint and ^{1,5}A$_2$-H$_2$O:B$_2$-H$_2$O ratio (*m/z* 347:377 ~0.6) observed for 4.ii during fragmentation of *m/z* 395 MS^2 ion were comparable to XA^{3}XX (Fig. 2B.2, Table 1). Hence, it is postulated that such findings

were indicative of internal *O*-3-linked arabinosyl. Consequently, 4.i was annotated as A[3]XX and 4.ii as XA[3]X. Although this assignment is approached with caution, the elution of 4.ii between A[3]XX and A[2]XX further supports its validity.

Fig. 6. Negative ion mode CID-MS[3] spectra of the daughter ion *m/z* 547→395 [M−H]⁻ corresponding to 4.i (**1**), 4.ii (**2**), 4.iii (**3**) and X_4 (**4**) (MS[2]; see Fig. 5). The fragments are annotated according to Domon & Costello (1988) and Juvonen et al. (2019) (31,39). Blue: glycosidic fragments. Red: cross-ring fragments; /: double cleavage; x: α or β antennae. Alternative fragments are presented in brackets. The precise structure of the newly formed end of B fragment ions is unknown as it may undergo several rearrangements (dashed ring), hence corresponding MS[3]-ring-fragments have been annotated tentatively.

MS[2] analysis of 3.i and X_3 (Fig. 7A) confirmed that arabinosyl substitution suppressed the intensity of Z_2 ion (*m/z* 265) in 3.i. MS[3] analysis of *m/z* 415→263 (Fig. 7B) showed that the $^{1,5}A_2$−H_2O:B_2−H_2O (*m/z* 215 and 245, respectively) ratio was approximately 40 for 3.i and 0.4 for X_3. Therefore, the presence of a terminal *O*-3-linked arabinosyl was deduced, based on the fragmentation fingerprints of *m/z* 395 MS[2] ions corresponding to DP 4 and 5 AXOS. Hence, 3.i was labelled A[3]X. This was substantiated by the presence of $^{2,4}A_2$ cross-ring cleavage (Fig. 7).
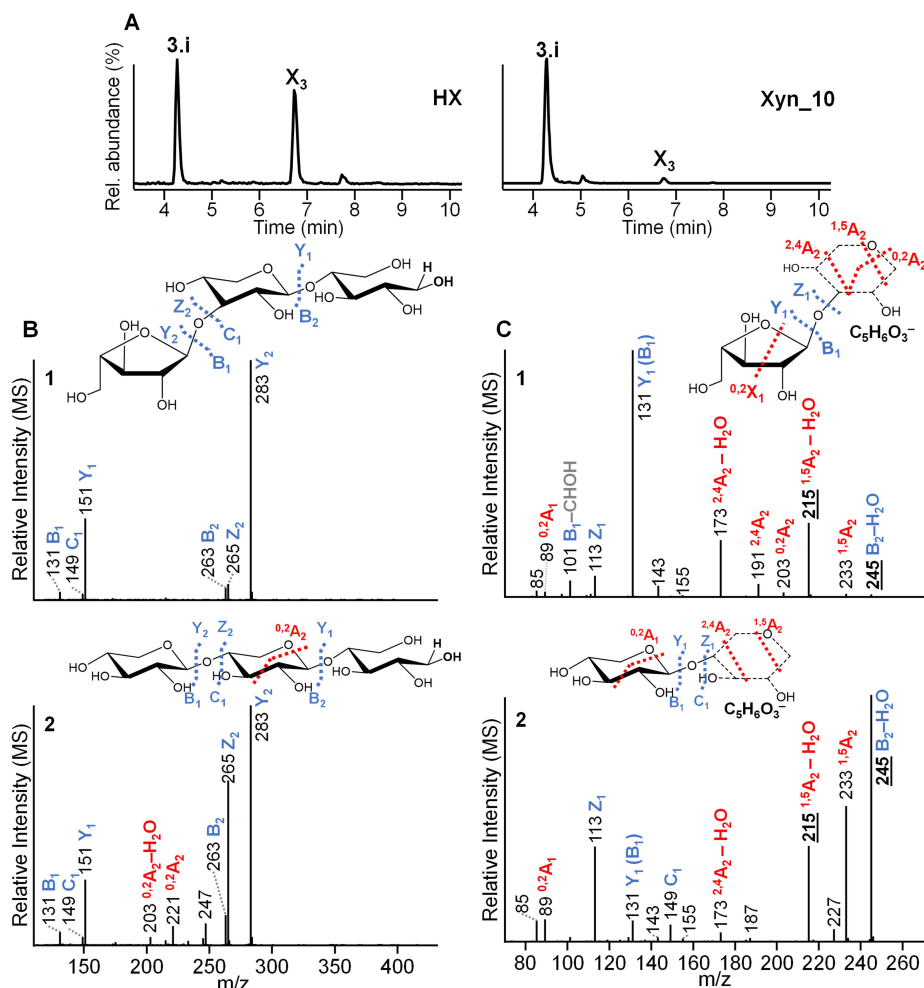
Fig. 7. Negative ion mode CID-MS^2 (**B**) spectra of 3.i (**1**) and X$_3$ (**2**) DP3 AXOS/XOS isomers (*m/z* 415; [M–H]$^-$) and CID-MS^3 (**C**) spectra of the daughter ion *m/z* 415→263 [M–H]$^-$. Average spectra across the most abundant chromatographic peaks between treatments (**A**). The fragments are annotated according to Domon & Costello (1988) and Juvonen et al. (2019) (31,39). Blue: glycosidic fragments; Red: cross-ring fragments; /: double cleavage; x: α or β antennae. Alternative fragments are presented in brackets. The precise structure of the newly formed end of B fragment ions is unknown as it may undergo several rearrangements (dashed ring), hence corresponding MS^3-ring-fragments have been annotated tentatively.

We further aimed at identifying several of the multiple DP 6-7 AXOS released in minor quantities during WAX endo-xylanase treatment (Fig. 3 and Fig. S5) on the basis of observations made so far for DP 3-5 isomers. To begin with, Abf profiling enabled the assignment of 6.v to XA^{2+3}XX (see 3.2, Fig. 3). Based on the

observations so far, 6.i-iv and 7.i-vi were substituted at multiple Xyl residues. Conversely, 6.vi, 6.vii and 6.viii were classified as singly substituted, and 7.vii as doubly substituted AXOS.

MS^2 analysis of singly substituted DP 6 (Fig. S7) isomers demonstrated that differences in the Y/Z ratios between branched and linear isomers were less pronounced than those observed for pentasaccharides (Fig. 1). Consequently, deduction of the branching point in AXOS > DP 5 may not be solely achieved by the relative intensity between Y and Z ions in MS^2. Subsequent MS^3 experiments revealed that the m/z 811→679 fragment ion corresponding to 6.vi presented similar spectral fingerprint to X_6 (Fig. S8), indicating arabinosyl attachment to the penultimate xylosyl residue for 6.vi. In contrast, the m/z 811→679 MS^3 spectrum for 6.vii demonstrated Ara substitution at the third Xyl residue from the non-reducing end.

MS^3 fragmentation of the 6.vi and 6.vii m/z 811→527 fragment ion (B_3) (Fig. S9) resulted in similar spectral fingerprints to O-3-linked AXOS such as XA^3XX (Fig. 2B) and XA^3X (Fig. 6). Additionally, the higher $^{1,5}A_3$–H_2O:B_3–H_2O ratios (m/z 479:509; 6.vi~1.7, 6.vii~7.2) compared to X_6 (Table 1) confirmed the presence of O-3-linked Ara in both 6.vi and 6.vii, which were then annotated as XA^3XXX and XXA^3XX, respectively. Following the same procedure, 6.viii was identified as XA^2XXX. Furthermore, MS^2 and MS^3 (m/z 811→679, m/z 811→547) analysis of 6.iii revealed the presence of a xylotetraose backbone, that was substituted by two Ara, most likely attached to two contiguous, internal Xyl residues (Fig. S10). Furthermore, 6.iii presented a similar MS^3 spectrum for m/z 811→527 ($B_3/Y_{3\alpha''(2\beta)}$) compared to XA^3XX and A^3A^3X (Fig. 2B, Fig. 4), revealing the presence of O-3-linked Ara, likely attached to the penultimate Xyl from the non-reducing end. Therefore, 6.iii was putatively annotated as XA^3A^3X, although the linkage type of the second Ara could not be confirmed. Similarly, 6.i, and 7.v were tentatively annotated as $A^{2+3}X^3X$ and XA^3A^3XX (Fig. S11, Fig. S12), respectively. Finally, the conversion of 7.vii to 6.viii (XA^2XXX) upon Abf_43 treatment suggested that the former was $XA^{2+3}XXX$ (see 3.2, Fig. S5).

Overall, our annotation of DP 3-7 AXOS based on MS^n spectra and Abf action was substantiated by previous studies reporting the release of similar structures from wheat AX by GH10 and GH11 endo-xylanases. In those studies, AXOS were firstly purified, and then identified by ^1H NMR (14,17,18,49).

3.4 Developing a rationale for identifying AXOS isomers by HILIC-MS[n]

In this study, structurally different $NaBH_4$-reduced (A)XOS were separated and identified by HILIC-MS^2 and MS^3 analysis. It should be emphasized that AXOS debranching by Abfs exhibiting distinct mode of action was integral in distinguishing between doubly and singly substituted oligomers. An overview of the current findings is presented in Table 1.

Table 1. Overview of (A)XOS isomers DP 2-7 detected by HILIC-ESI-CID-MS^n. The m/z [M−H]$^-$, number of isomers (n), code, retention time (RT), relative abundance, characteristic MS^2 and MS^3 ions, diagnostic MS^3 ion ratio and the resolved structures of (A)XOS are included.

m/z [M-H]$^-$ (DP)	Isomers (n)	Code	RT (min) (ΔRT, min)^a	Relative abundance (%) HX	Xyn_10	Characteristic fragment ions (m/z)^c	MS^2 fragment ion (m/z) 263^d	395^d	527^d	Structure
							Diagnostic MS^3 ion ratio^e			
283 (2)	1	X$_2$	3.9	12.0	14.8	–	–	–	–	XX^g
415 (3)	2	3.i	4.3 (2.5)	1.3	24.4	MS^2: 283, 265, 263, 221 MS^3: **263** (245, 215, 173, 131, 113)	40.9	–	–	A^{3}X
		X$_3$	6.8	1.2	1.0		0.4	–	–	XXX^g
547 (4)	4	4.i	7.3 (3.3)	5.6	1.3	MS^2: 415, 397 MS^3: **395** (377, 347, 305, 263, 245)	–	9.6	–	A^{3}XX
		4.ii	7.8 (2.8)	20.5	31.1		–	0.6	–	XA^{3}X
		4.iii	8.4 (2.2)	1.0	1.0		–	0.1	–	A^{2}XX^g
		X$_4$	10.6	0.4	–		–	0.2	–	XXXX^g
679 (5)	5	5.i	8.3 (6.3)	–	8.3	MS^2: 547, 529 MS^3: **547** (415, 397), 527 (509, 479, 437, 395, 377) **395** (same as DP 4)	–	9.7	–	A^{3}A^{3}X^f
		5.ii	9.3 (5.3)	0.7	6.6		–	4.7	0.3	A^{2+3}XX^g
		5.iii	11.5 (3.1)	37.8	0.6		–	0.6	152	XA^{3}XX^g
		5.iv	12.2 (2.4)	–	0.4		–	0.2	0.2	XA^{2}XX^g
		X$_5$	14.6	–	–		–	0.2	0.5	XXXXX^g
811 (6)	9	6.i	9.8 (8.4)	–	0.4	MS^2: 679, 661 MS^3: **679** (547, 529), **547** (415, 397), **527** (same as DP 5)	–	–	–	A^{2+3}A^{3}X^f
		6.ii	12.0 (6.2)	–	0.3		–	–	1.2	Mlt$_{sin}^h$
		6.iii	12.5 (5.7)	3.3	3.2		–	–	20.8	XA^{3}A^{3}X^f
		6.iv	13.1 (5.1)	0.5	0.3		–	–	2.4	–
		6.v	14.2 (4.0)	3.8	2.5		–	–	1.4	XA^{2+3}XX
		6.vi	15.3 (2.9)	1.9	–		–	–	1.7	XA^{3}XXX
		6.vii	15.7 (2.5)	0.2	0.1		–	–	7.2	XXA^{3}XX
		6.viii	16.0 (2.2)	–	0.1		–	–	0.7	XA^{2}XXX
		X$_6$	18.2	–	–		–	–	0.6	XXXXXX^g
943 (7)	7	7.i	12.9 (8.6)	–	0.5	MS^2: 811, 793 MS^3: **811** (679, 661), **679** (same as DP 6), **527** (same as DP 5)	–	–	–	Mlt$_{sin}^h$
		7.ii	13.9 (7.6)	–	0.5		–	–	2.0	Mlt$_{mix}^h$
		7.iii	14.5 (7.0)	–	2.2		–	–	0.9	Mlt$_{mix}^h$
		7.iv	15.9 (5.6)	0.8	–		–	–	2.9	Mlt$_{sin}^h$
		7.v	16.1 (5.4)	4.1	–		–	–	3.7	XA^{3}A^{3}XX^f
		7.vi	16.6 (4.9)	0.3	0.2		–	–	–	–
		7.vii	17.7 (3.7)	4.3	0.1		–	–	0.9	XA^{2+3}XXX
		X$_7$	21.5	–	–		–	–	0.6	XXXXXXX

^{a}Relative retention time (ΔRT) of AXOS compared to linear XOS of the same DP. ^{b}Determined by integration of (A)XOS peaks in HILIC-MS, with the sum of all peaks present in each digest set at 100%. ^{c}m/z values of MS^3 ions are indicated within brackets, next to their parent MS^2 ion, in bold. ^{d}m/z values of MS^2 fragment ions (B$_x$) investigated by MS^3 per DP, to generate the diagnostic ion ratios ^{1,5}A$_x$–H$_2$O:B$_x$–H$_2$O (see below). ^{e}Values represent ratios between m/z 215:245 (DP 3), m/z 347:377 (DP 4, 5) and m/z 479:509 (DP 5, 6, 7). ^{f}Tentative structures. ^{g}Identified based on

standards. ^{h}Structure was not unambiguously determined by MS^n, but substitution pattern was confirmed by Abf treatment (Fig. S5); Mlt$_{sin}$: containing multiple (≥ 2) single arabinosyl substituents, Mlt$_{mix}$: containing both single and double arabinosyl substituents.

Reduced (A)XOS elution in HILIC depended on DP, with smaller molecules eluting earlier. This elution behavior has previously been described for reduced cello-oligosaccharides and human milk oligosaccharides (27,29). Similar behavior has been observed for underivatized DP 3-7 XOS and AXOS as well (28,31). Moreover, the elution of (reduced) isomeric structures of the same DP strongly depended on the number, linkage type and position of Ara substituents. In specific, di- and multiple-substituted AXOS eluted before monosubstituted ones, while linear (reduced) XOS eluted at the end of each DP series. Within disubstituted species, AXOS with two single arabinosyl substitutions eluted before doubly substituted AXOS. Within monosubstituted species, O-3-linked AXOS eluted earlier than O-2-linked ones. Finally, (reduced) AXOS substituted at, or closer to, the non-reducing terminus, eluted before AXOS with similar number and linkage type of internal arabinosyl branches.

Structural elucidation of HILIC-separated AXOS by MS^n typically involved a two-step approach: localization of the branching unit(s) by MS^2 and MS^3, followed by assigning MS^3 spectral fingerprints to specific structures (Scheme 1). The relative intensities of Y and Z ions deriving from the first glycosidic linkage from the non-reducing end in MS^2, and by subsequent glycosidic fragments in MS^3, were revealing of the substitution site(s). In specific, Z ion formation was found to be suppressed when glycosidic cleavage occurred in the vicinity of Ara substituents. On the contrary, Y and Z ions from the cleavage of the first glycosidic linkage from the non-reducing end presented similar intensities when two or more contiguous unsubstituted xylosyl residues were present. MS^3 analysis of selected MS^2 ions revealed the formation of rather similar fragments, but at different relative intensities for (A)XOS isomers. In particular, MS^3 fragmentation of B$_x$ MS^2 ions generated the ^{1,5}A$_x$-H$_2$O and B$_x$-H$_2$O ions, whose relative ratio was indicative of the arabinosyl substituent linkage type. Selection of B fragment ions for MS^3 analysis depended on AXOS DP, with larger B fragment ions being selected for higher DP oligosaccharides. It was observed that disubstituted AXOS resulted in higher ratios than monosubstituted ones. MS^3 analysis of B ions m/z 263 and m/z 395 for DP 3-5, demonstrated that terminal O-3-linked Ara resulted in higher ^{1,5}A$_x$-H$_2$O:B$_x$-H$_2$O ion ratios than internal O-3-linked Ara. However, this was not the case for MS^3 fragmentation of B ions m/z 527 for DP 5-7. Still, all AXOS containing O-3-linked Ara presented higher ^{1,5}A$_x$-H$_2$O:B$_x$-H$_2$O ion ratios than AXOS with internal O-2-linked Ara and XOS. Thus, distinct spectral fingerprints can now be attributed to particular structures, and can be used as discriminants of the branching pattern of unknown AXOS.

In this study, reduced AXOS structures were discerned by combining the information obtained for oligomer HILIC (relative) retention time, degradation by Abfs and MS^2 and MS^3 fragmentation patterns and diagnostic ion ratios (Scheme 1). As an example, XA^{3}XXX, XXA^{3}XX and XA^{2}XXX (Table 1) were identified as singly

substituted due to their degradation by Abf_51. Next, the position of the substituent along the backbone was determined by MS^2 analysis, followed by MS^3 analysis of Y fragment ions. Finally, MS^3 analysis of B fragment ions demonstrated that both XA^3XXX and XXA^3XX presented higher values for diagnostic ion ratio $B–H_2O$:$^{1,5}A–H_2O$ compared to XA^2XXX. This annotation was further supported by the earlier elution in HILIC of the peak identified as XA^3XXX compared to the peaks corresponding to XXA^3XX and XA^2XXX. Moreover, all three AXOS eluted earlier than their linear counterpart (X_6), with the latter being identified with the use of an analytical standard.

AXOS identification workflow

1. HILIC-MS
- DP assignment based on *m/z* value
- Separation of isomers based on RT
- Distinction of singly and doubly substituted structures after **Abf_43**, **Abf_51** treatments

2. MS^2
- Localization of substituted Xyl based on **Y *vs* Z** ion* intensity.

  *both ions result from the same glycosidic linkage

3. MS^3
- <u>**Y type**</u> fragment ions → Localization of substituted Xyl based on **Y *vs* Z** ion* intensity
- <u>**B type**</u> fragment ions → Identification of Ara-substituent linkage type based on $^{1,5}A_X–H_2O^{\#}$: $B_X–H_2O$ ion ratio

  *both ions result from the same glycosidic linkage
  $^{\#}$cross-ring fragment from Xyl adjacent to the (B) glycosidic cleavage

Scheme 1. AXOS identification workflow by the currently developed HILIC-MS^n strategy.

Currently, AXOS reduction resulted in differentiated fragmentation patterns compared to those of underivatized AXOS (23,31), confirming previous MS^n studies of reduced oligosaccharides (27,46). More importantly, AXOS reduction allowed a clear distinction between Y/Z and B/C fragmentation pathways. Hence, reduced AXOS were identified by comparing well-defined ions, and not by the presence or absence of double cleavage fragment ions, as in previous research for underivatized AXOS (23,31). Our approach was established for DP 5 AXOS standards and validated for unknown DP 3-7 AXOS. Finally, the present findings suggest that despite being tedious, pre-column derivatization might still be necessary to fairly elucidate oligosaccharide structure by ESI-CID-MS^n. As a note of critical reflection, the proposed strategy for (A)XOS identification can be complemented with optimization of the chromatographic separation for higher DPs as well as expansion of the spectral library, by purifying and analyzing additional AXOS standards. Moreover, reduction has been previously shown to enable the chromatographic separation and MS-based annotation of fucoidan, human milk and

galacto-oligosaccharides (29,45,51). Similar to our current observations, DP 3 galacto-oligosaccharides isomers also presented different relative intensities for Y and Z fragment ions in MS^2 (45). Therefore, apart from AXOS, the strategy currently developed is expected to be relevant for other (hetero)xylan-derived oligosaccharides as well as other oligosaccharide species, and can thus contribute to the more comprehensive characterization of carbohydrates.

4   Conclusion

We currently present a strategy for the identification of AXOS isomers in enzyme digests, assisted by $NaBH_4$ reduction of the oligomer followed by HILIC-MS[n]. Z ion formation was suppressed in the vicinity of Ara substituents. Therefore, the relative intensity between corresponding Y and Z ions revealed the position of arabinosyl substituents. Further structural elucidation was achieved by assigning diagnostic spectral fingerprints to structural motifs containing *O*-3-, *O*-2-, and *O*-2,3-linked arabinosyl substituents. Moreover, arabinosyl-debranching enzymes were crucial tools for revealing oligosaccharide structures, establishing MS fragmentation rules and setting up an oligosaccharide library. The identification strategy currently described will be highly relevant for studying the functionality of individual AXOS structures in complex matrices such as digesta and waste streams. Moreover, it is expected to further contribute to the characterization of novel xylanolytic enzymes. Finally, a similar approach may be relevant for identification of other oligosaccharide species as well as polysaccharide sequencing.

References

1. Mendis M, Leclerc E, Simsek S. Arabinoxylans, gut microbiota and immunity. Carbohydr Polym. 2016;139:159–66.

2. Broekaert WF, Courtin CM, Verbeke K, van de Wiele T, Verstraete W, Delcour JA. Prebiotic and other health-related effects of cereal-derived arabinoxylans, arabinoxylan-oligosaccharides, and xylooligosaccharides. Crit Rev Food Sci Nutr. 2011;51(2):178–94.

3. Rumpagaporn P, Reuhs BL, Kaur A, Patterson JA, Keshavarzian A, Hamaker BR. Structural features of soluble cereal arabinoxylan fibers associated with a slow rate of *in vitro* fermentation by human fecal microbiota. Carbohydr Polym. 2015;130:191–7.

4. Mendis M, Martens EC, Simsek S. How fine structural differences of xylooligosaccharides and arabinoxylooligosaccharides regulate differential growth of *Bacteroides* species. J Agric Food Chem. 2018;66(31):8398–405.

5. Fauré R, Courtin CM, Delcour JA, Dumon C, Faulds CB, Fincher GB, Sébastien F, Fry SC, Halila S, Kabel MA, Pouvreau L, Quemener B, Rivet A, Saulnier L, Schols HA, Driguez H, O'Donohue MJ. A brief and informationally rich naming system for oligosaccharide motifs of heteroxylans found in plant cell walls. Aust J Chem. 2009;62(6):533–7.

6. Izydorczyk MS, Biliaderis CG. Cereal arabinoxylans: Advances in structure and physicochemical properties. Carbohydr Polym. 1995;28(1):33–48.

7. Vinkx CJA, Delcour JA. Rye (*Secale cereale* L.) arabinoxylans: A critical review. J Cereal Sci. 1996;24(1):1–14.

8. Wang J, Bai J, Fan M, Li T, Li Y, Qian H, Wang L, Zhang H, Qi X, Rao Z. Cereal-derived arabinoxylans: Structural features and structure–activity correlations. Trends Food Sci Technol. 2020;96:157–65.

9. Gruppen H, Kormelink FJM, Voragen AGJ. Water-unextractable cell wall material from wheat flour. 3. A structural model for arabinoxylans. J Cereal Sci. 1993;18(2):111–28.

10. Saulnier L, Sado P-E, Branlard G, Charmet G, Guillon F. Wheat arabinoxylans: Exploiting variation in amount and composition to develop enhanced varieties. J Cereal Sci. 2007;46(3):261–81..

11. Wang J, Zhao J, Nie S, Xie M, Li S. Mass spectrometry for structural elucidation and sequencing of carbohydrates. TrAC - Trends Anal Chem. 2021;144:116436.

12. Kamerling JP, Gerwig GJ. Strategies for the structural analysis of carbohydrates. In: Kamerling JP, editor. Comprehensive glycoscience. Amsterdam: Elsevier Inc.; 2007. p. 1–68.

13. Nagy G, Peng T, Pohl NLB. Recent liquid chromatographic approaches and developments for the separation and purification of carbohydrates. Anal Methods. 2017;9(24):3579–93.

14. McCleary B V., McKie VA, Draga A, Rooney E, Mangan D, Larkin J. Hydrolysis of wheat flour arabinoxylan, acid-debranched wheat flour arabinoxylan and arabino-xylo-oligosaccharides by β-xylanase, α-l-arabinofuranosidase and β-xylosidase. Carbohydr Res. 2015;407:79–96.

15. Gruppen H, Kormelink FJM, Voragen AGJ. Enzymic degradation of water-unextractable cell wall material and arabinoxylans from wheat flour. J Cereal Sci. 1993;18(2):129–43.

16. Mechelke M, Herlet J, Benz JP, Schwarz WH, Zverlov VV., Liebl W, Kornberger P. HPAEC-PAD for oligosaccharide analysis—novel insights into analyte sensitivity and response stability. Anal Bioanal Chem. 2017;409(30):7169–81.

17. Pastell H, Tuomainen P, Virkki L, Tenkanen M. Step-wise enzymatic preparation and structural characterization of singly and doubly substituted arabinoxylo-oligosaccharides with non-reducing end terminal branches. Carbohydr Res. 2008;343(18):3049–57.

18. Hoffmann RA, Leeflang BR, de Barse MMJ, Kamerling JP, Vliegenthart JFG. Characterisation by [1]H-n.m.r. spectroscopy of oligosaccharides, derived from arabinoxylans of white endosperm of wheat, that contain the elements →4)[α-L-Araf-(1-ar3)]-β-D-Xylp-(1→ or →4)[α-L-Araf-(1→2)][α-LAraf-(1→3)]-β-D-Xylp-(1→. Carbohydr Res. 1991;221(1):63–81.

19. Gruppen H, Hoffmaann RA, Kormelink FJM, Voragen AGJ, Kamerling JP, Vliegenthart JFG. Characterisation by ^{1}H NMR spectroscopy of enzymically derived oligosaccharides from alkali-extractable wheat-flour arabinoxylan. Carbohydr Res. 1992;233:45–64.

20. Biely P, Vršanská M, Tenkanen M, Kluepfel D. Endo-β-1,4-xylanase families: differences in catalytic properties. J Biotechnol. 1997;57(1):151–66.

21. Kiely LJ, Hickey RM. Characterization and analysis of food-sourced carbohydrates. In: Davey GP, editor. Glycosylation Methods in Molecular Biology, vol 2370. New York, NY: Humana; 2022. p. 67–95.

22. Mazumder K, York WS. Structural analysis of arabinoxylans isolated from ball-milled switchgrass biomass. Carbohydr Res. 2010;345(15):2183–93.

23. Quéméner B, Ordaz-Ortiz JJ, Saulnier L. Structural characterization of underivatized arabino-xylo-oligosaccharides by negative-ion electrospray mass spectrometry. Carbohydr Res. 2006;341(11):1834–47.

24. Matamoros Fernández LE, Obel N, Scheller HV, Roepstorff P. Differentiation of isomeric oligosaccharide structures by ESI tandem MS and GC-MS. Carbohydr Res. 2004;339(3):655–64.

25. Bowman M, Dien B, O'Bryan P, Sarath G, Cotta M. Comparative analysis of end point enzymatic digests of arabino-xylan isolated from switchgrass (*Panicum virgatum* L) of varying maturities using LC-MS[n]. Metabolites. 2012; 19;2(4):959–82.

26. Maslen SL, Goubet F, Adam A, Dupree P, Stephens E. Structure elucidation of arabinoxylan isomers by normal phase HPLC-MALDI-TOF/TOF-MS/MS. Carbohydr Res. 2007;342(5):724–35.

27. Sun P, Frommhagen M, Kleine Haar M, van Erven G, Bakx EJ, van Berkel WJH, Kabel MA. Mass spectrometric fragmentation patterns discriminate C1- and C4-oxidised cello-oligosaccharides from their non-oxidised and reduced forms. Carbohydr Polym. 2020;234:115917.

28. Demuth T, Boulos S, Nyström L. Structural investigation of oxidized arabinoxylan oligosaccharides by negative ionization HILIC-qToF-MS. Analyst. 2020;145(20):6691–704.

29. Remoroza CA, Mak TD, De Leoz MLA, Mirokhin YA, Stein SE. Creating a mass spectral reference library for oligosaccharides in human milk. Anal Chem. 2018;90(15):8977–88.

30. Hernández-Hernández O, Calvillo I, Lebrón-Aguilar R, Moreno FJ, Sanz ML. Hydrophilic interaction liquid chromatography coupled to mass spectrometry for the characterization of prebiotic galactooligosaccharides. J Chromatogr A. 2012;1220:57–67.

31. Juvonen M, Kotiranta M, Jokela J, Tuomainen P, Tenkanen M. Identification and structural analysis of cereal arabinoxylan-derived oligosaccharides by negative ionization HILIC-MS/MS. Food Chem. 2019;275:176–85.

32. Leijdekkers AGM, Sanders MG, Schols HA, Gruppen H. Characterizing plant cell wall derived oligosaccharides using hydrophilic interaction chromatography with mass spectrometry detection. J Chromatogr A. 2011;1218(51):9227–35.

33. Jonathan MC, Bosch G, Schols HA, Gruppen H. Separation and identification of individual alginate oligosaccharides in the feces of alginate-fed pigs. J Agric Food Chem. 2013;61(3):553–60.

4

34. Churms SC. High performance hydrophilic interaction chromatography of carbohydrates with polar sorbents. In: Rassi Z El, editor. Carbohydrate analysis by modern chromatography and electrophoresis. Amsterdam: Elsevier Inc.; 2002. p. 121–163.

35. Schumacher D, Kroh LW. A rapid method for separation of anomeric saccharides using a cyclodextrin bonded phase and for investigation of mutarotation. Food Chem. 1995;54(4):353–6.

36. Abdel-Akher M, Hamilton JK, Smith F. The reduction of sugars with sodium borohydride. J Am Chem Soc. 1951;73(10):4691–2.

37. York WS, Kolli VSK, Orlando R, Albersheim P, Darvill AG. The structures of arabinoxyloglucans produced by solanaceous plants. Carbohydr Res. 1996;285:99–128.

38. Vierhuis E, York WS, Kolli VSK, Vincken JP, Schols HA, Van Alebeek GJWM, Voragen AGJ. Structural analyses of two arabinose containing oligosaccharides derived from olive fruit xyloglucan: XXSG and XLSG. Carbohydr Res. 2001;332(3):285–97.

39. Domon B, Costello CE. A systematic nomenclature for carbohydrate fragmentations in FAB-MS/MS spectra of glycoconjugates. Glycoconj J. 1988;5(4):397–409.

40. Lagaert S, Pollet A, Courtin CM, Volckaert G. β-Xylosidases and α-L-arabinofuranosidases: Accessory enzymes for arabinoxylan degradation. Biotechnol Adv. 2014;32(2):316–32.

41. Sørensen HR, Jørgensen CT, Hansen CH, Jørgensen CI, Pedersen S, Meyer AS. A novel GH43 α-L-arabinofuranosidase from *Humicola insolens*: Mode of action and synergy with GH51 α-L-arabinofuranosidases on wheat arabinoxylan. Appl Microbiol Biotechnol. 2006;73(4):850–61.

42. Van den Broek LAM, Lloyd RM, Beldman G, Verdoes JC, McCleary B V., Voragen AGJ. Cloning and characterization of arabinoxylan arabinofuranohydrolase-D3 (AXHd3) from *Bifidobacterium adolescentis* DSM20083. Appl Microbiol Biotechnol. 2005;67(5):641–7.

43. Koutaniemi S, Tenkanen M. Action of three GH51 and one GH54 α-arabinofuranosidases on internally and terminally located arabinofuranosyl branches. J Biotechnol. 2016;229:22–30.

44. Bennett R, Olesik S V. Gradient separation of oligosaccharides and suppressing anomeric mutarotation with enhanced-fluidity liquid hydrophilic interaction chromatography. Anal Chim Acta. 2017;960:151–9.

45. Logtenberg MJ, Donners KMH, Vink JCM, Van Leeuwen SS, De Waard P, De Vos P, Schols HA. Touching the high complexity of prebiotic Vivinal galacto-oligosaccharides using porous graphitic carbon ultra-high-performance liquid chromatography coupled to mass spectrometry. J Agric Food Chem. 2020;68(29):7800–8.

46. Doohan RA, Hayes CA, Harhen B, Karlsson NG. Negative Ion CID Fragmentation of *O*-linked oligosaccharide aldoses—charge induced and charge remote fragmentation. J Am Soc Mass Spectrom. 2011;22(6):s13361-011-0102–3.

47. Bauer S. Mass spectrometry for characterizing plant cell wall polysaccharides. Front Plant Sci. 2012;3:45.

48. Rodrigues JA, Taylor AM, Sumpton DP, Reynolds JC, Pickford R, Thomas-Oates J. Mass spectrometry of carbohydrates: Newer aspects. In: Advances in carbohydrate chemistry and biochemistry. Amsterdam: Elsevier Inc.; 2007. p. 59–141.

49. Kormelink FJM, Gruppen H, Viëtor RJ, Voragen AGJ. Mode of action of the xylan-degrading enzymes from *Aspergillus awamori* on alkali-extractable cereal arabinoxylans. Carbohydr Res. 1993;249(2):355–67.

50. Pandeirada CO, Merkx DWH, Janssen HG, Westphal Y, Schols HA. TEMPO/NaClO$_2$/NaOCl oxidation of arabinoxylans. Carbohydr Polym. 2021;259:117781.

51.   An Z, Zhang Z, Zhang X, Yang H, Lu H, Liu M, et al. Oligosaccharide mapping analysis by HILIC-ESI-HCD-MS/MS for structural elucidation of fucoidan from sea cucumber *Holothuria floridana*. Carbohydr Polym. 2022;275:118694.

4

Supplementary information

Supplementary materials and methods

Enzymatic fingerprinting of arabinosyl substituents in standard AXOS

The standard $A^{2+3}XX$ (1.25 mg/mL) was incubated with Abf_43 (0.1 AU/mL) at 40 °C and pH 5.0 for 8 h to produce the oligosaccharide A^2XX. The reaction was stopped by heating at 99 °C for 15 min. A^2XX was used as an analytical standard for HPAEC-PAD and after $NaBH_4$ reduction, for HILIC-ESI-CID-MS^n.

The standards XA^2XX/XA^3XX and $A^{2+3}XX$ (0.25 mg/mL) were incubated with Abf_51 (0.1 AU/mL) at 40 °C and pH 5.0 for 8 h and 16 h. The reactions were stopped by heating at 99 °C for 15 min. The samples were diluted 10 times and analyzed by HPAEC-PAD.

Profiling of oligosaccharides with HPAEC-PAD

The elution pattern of underivatized AXOS mixtures, as is (see 2.2) and as Abf digests (see 2.3) was analyzed by High Performance Anion Exchange Chromatography with Pulsed Amperometric Detection (HPAEC-PAD). Hereto, an ICS5000 HPLC system (Dionex, Sunnyvale, CA, USA) was used, equipped with a CarboPac PA-1 column (2mm ID x 250 mm; Dionex) in combination with a CarboPac PA guard column (2 mm ID×50 mm; Dionex), and coupled to pulsed amperometric detection (Dionex). The column temperature was set at 20 °C, the flow rate was 0.3 mL/min, and the injection volume was 10 µL. The mobile phase was comprised of 0.1 M sodium hydroxide (NaOH) (A) and 1 M sodium acetate in 0.1 M NaOH (B). The separation was performed using the following elution profile: 0−32 min from 0% to 38% B (linear gradient), 32-37 min from 32 % to 100% B (linear), 37-42 min at 100% B (isocratic), and 42-55 min 100% A (isocratic).

Supplementary data

Table S1. List of MS and MS^2 ions selected for MS^2 and MS^3 analysis, respectively, for each (A)XOS series of different Degree of Polymerization (DP).

DP	MS ion selected for MS^2 (m/z [M−H]⁻)	MS^2 ions selected for MS^3 (m/z [M−H]⁻)
3	415	263
4	547	395
5	679	395, 527, 547
6	811	527, 547, 679
7	943	527, 679, 811
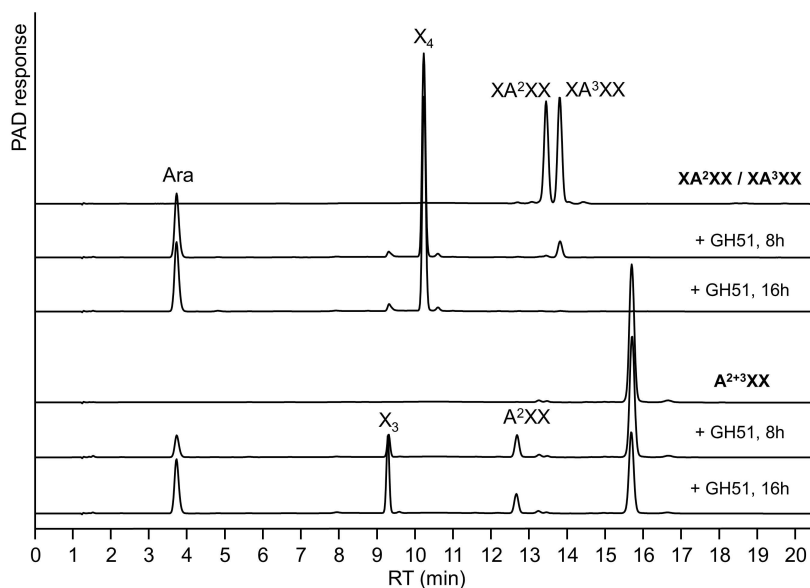
Fig. S1. HPAEC-PAD chromatograms of XA^{2}XX/XA^{3}XX and A^{2+3}XX standards (0.25 mg/mL) before and after treatment with Abf_51 (0.1 AU/mL) for 8 h and 16 h, at 40 ºC and pH 5.0. Samples were diluted 20 times prior to analysis.
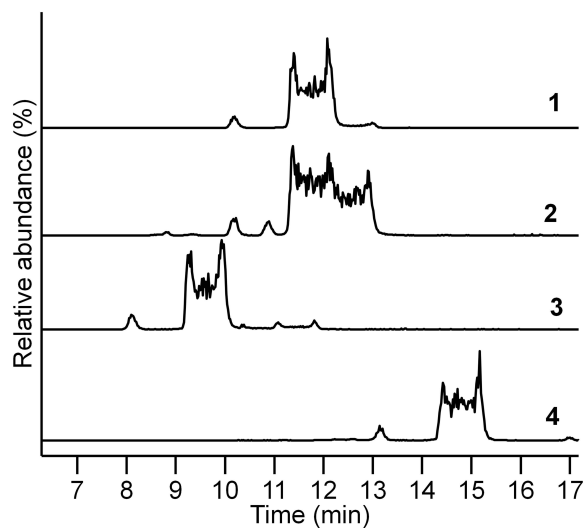
Fig. S2. HILIC-MS ion extracted chromatograms of four underivatized DP 5 AXOS isomers (*m/z* 677; [M–H]$^-$): XA^{3}XX (**1**), XA^{2}XX/XA^{3}XX (**2**), A^{2+3}XX (**3**) and X$_5$ (**4**).

Fig. S3. Negative ion mode CID-MS[3] spectra of m/z 679→547 [M–H][-] corresponding to A[2+3]XX (**1**), XA[3]XX (**2**), XA[2]XX (**3**) and X$_5$ (**4**) (see **Fig. 1**). The fragments are annotated according to Domon & Costello (1988) and Juvonen et al. (2019) (1,2). Blue: glycosidic fragments; Red: cross-ring fragments; /: double cleavage; x: α or β antennae. Alternative fragments are presented in brackets. Structures **a**, **b** correspond to A[2+3]XX due to the loss of either arabinosyl substituent, and structure **c** corresponds to XA[3]XX, XA[2]XX and X$_5$.

Fig. S4. HPAEC-PAD chromatograms of AXOS and XOS from WAX digested by HX (**A.1**) and Xyn_10 (**B.1**). Subsequent digestions with Abf_43 (**2**), Abf_51 (**3**) or Abf_43/Abf_51 combination (**4**). Monosaccharides (Ara: arabinose, Xyl: xylose) and linear XOS (DP 2-6) were identified based on comparison of elution of standards (not shown); AXOS (Mono-sub = monosubstituted, Di-sub = disubstituted, Multi-sub = multiple-substituted) were according to van Gool et al. (2013) (3).
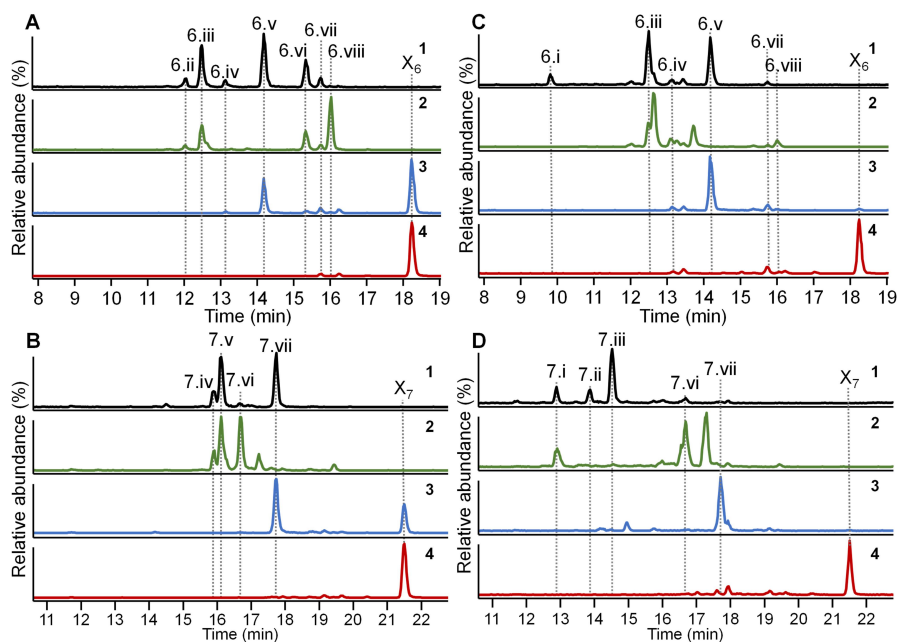
Fig. S5. HILIC-MS ion-extracted chromatograms of NABH$_4$-reduced DP 6 (m/z 811; [M–H]$^-$) (**A**, **C**) and DP7 (m/z 943; [M–H]$^-$) (**B**, **D**) (A)XOS from WAX digested by HX (**A.1**) and Xyn_10 (**B.1**). Subsequent digestions with Abf_43 (**2**), Abf_51 (**3**) or Abf_43/Abf_51 combination (**4**). see Table 1 for explanation of coded peaks. Zoomed-in chromatograms for better resolution of minor DP 6,7 AXOS shown in **Fig. 3**.
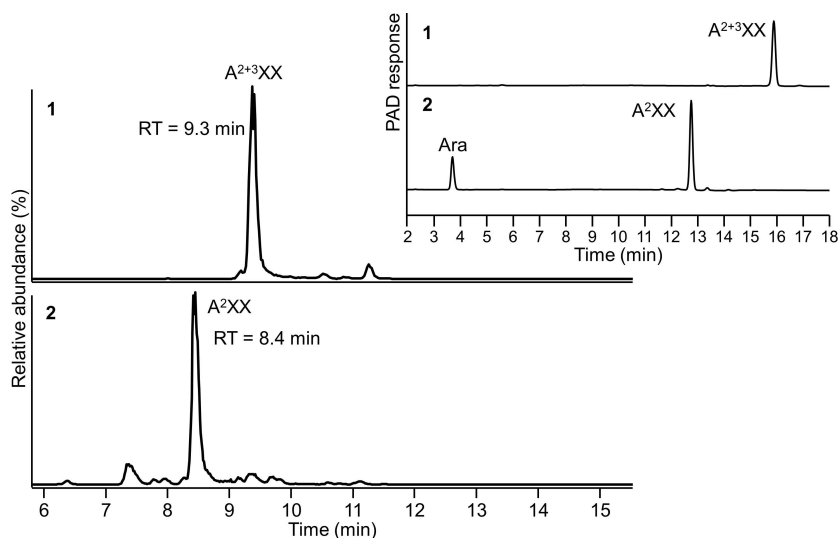
Fig. S6. HILIC-MS ion extracted chromatograms of A^{2+3}XX (m/z 679 [M–H]$^-$, retention time (RT) 9.3 min) (**1**) and A^{2+3}XX treated with Abf_43 (m/z 547 [M–H]$^-$, RT 8.4 min)

(**2**). HPAEC-PAD chromatograms of $A^{2+3}XX$ (**1**) and $A^{2+3}XX$ treated with Abf_43 (**2**) (insert).
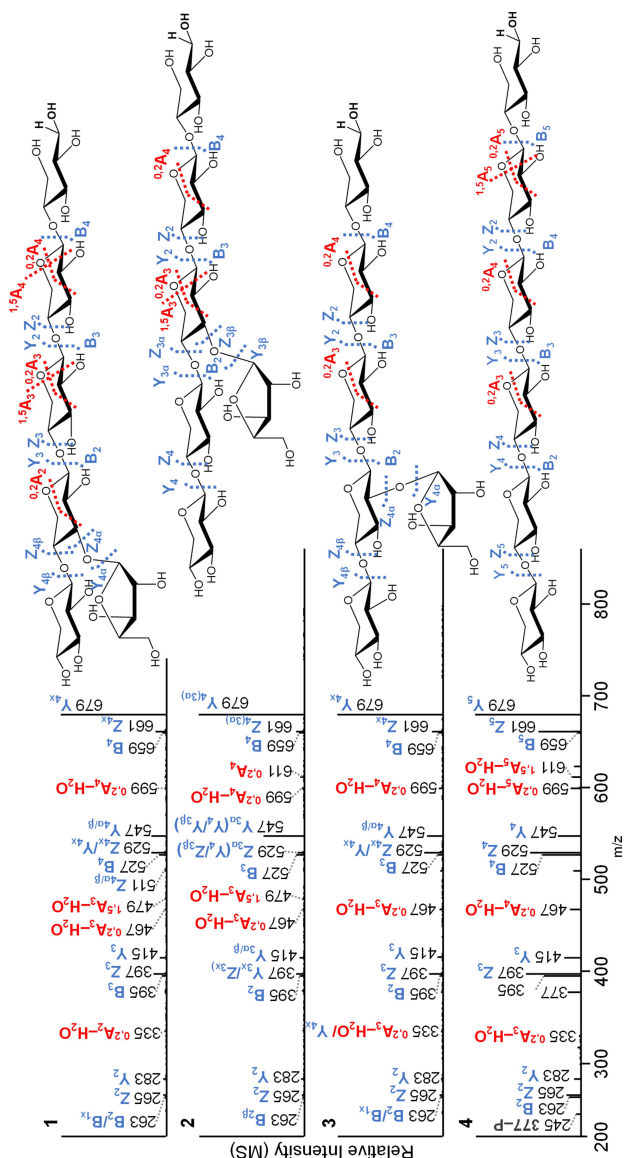
Fig. S7. Negative ion mode CID-MS[2] spectra of DP 6 (A)XOS isomers (*m/z* 811 [M−H]−) 6.vi (**1**), 6.vii (**2**), 6.viii (**3**) and X6 (**4**); average spectra across the most abundant chromatographic peaks between treatments (**Fig. S5**). The fragments are annotated according to Domon & Costello (1988) and Juvonen et al. (2019) (1,2). Blue: glycosidic fragments; Red: cross-ring fragments; /: double cleavage; x: α or β antennae. Alternative fragments are presented in brackets.
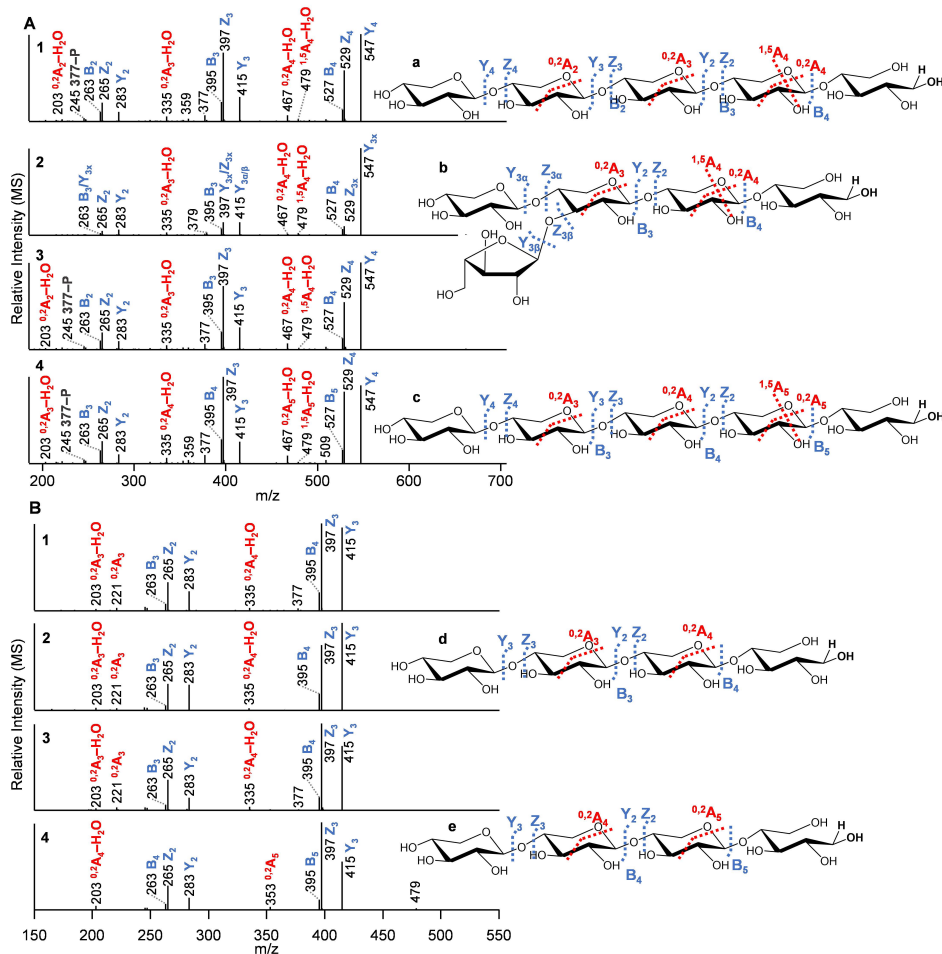
Fig. S8. Negative ion mode CID-MS³ spectra of *m/z* 811→679 [M−H]⁻ (**A**) and *m/z* 811→547 [M−H]⁻ (**B**) corresponding to (A)XOS 6.vi (**1**), 6.vii (**2**), 6.viii (**3**) and X₆ (**4**). (MS²; see **Fig. S7**). The fragments are annotated according to Domon & Costello (1988) and Juvonen et al. (2019) (1,2). Blue: glycosidic fragments; Red: cross-ring fragments; /: double cleavage; x: α or β antennae, P: pentose unit (*m/z* 132). Structure **a** corresponds to 6.vi and 6.viii, **b** to 6.vii, **c** to X6, **d** to 6.vi-viii and **e** to X₆.

4

Fig. S9. Negative ion mode CID-MS[3] spectra of *m/z* 811→527 [M–H][-] corresponding to (A)XOS 6.vi (**1**), 6.vii (**2**), 6.viii (**3**) and X₆ (**4**). (MS[2]; see **Fig. S8**). The fragments are annotated according to Domon & Costello (1988) and Juvonen et al. (2019) (1,2). Blue: glycosidic fragments; Red: cross-ring fragments; /: double cleavage; x: α or β antennae, P: pentose unit (*m/z* 132). The precise structure of the newly formed end of B fragment ions is unknown as it may undergo several rearrangements (dashed ring), hence corresponding MS[3]-ring-fragments have been annotated tentatively.

Fig. S10. Negative ion mode CID-MS^2 (**1**) and CID-MS^3 spectra of m/z 811→679 [M–H]$^-$ (**2**), m/z 811→547 [M–H]$^-$ (**3**) and m/z 811→527 [M–H]$^-$ (**4**) corresponding to 6.iii. Average spectra across the most abundant chromatographic peaks between treatments (**Fig. S5**). The fragments are annotated according to Domon & Costello (1988) and Juvonen et al. (2019) (1,2). Blue: glycosidic fragments; Red: cross-ring fragments; /: double cleavage; x: α or β antennae; Alternative fragments are presented in brackets. Structure **a, b** correspond to m/z 811→679 (**2**), **c** corresponds to m/z 811→547 [M–H]$^-$ (**3**) and **d, e** correspond to m/z 811→527 [M–H]$^-$ due to the loss of either (**a, b, d, e**) or both (**c**) arabinosyl substituents. The precise structure of the newly formed end of B fragment ions is unknown as it may undergo several rearrangements (dashed ring), hence corresponding MS^3-ring-fragments have been annotated tentatively.
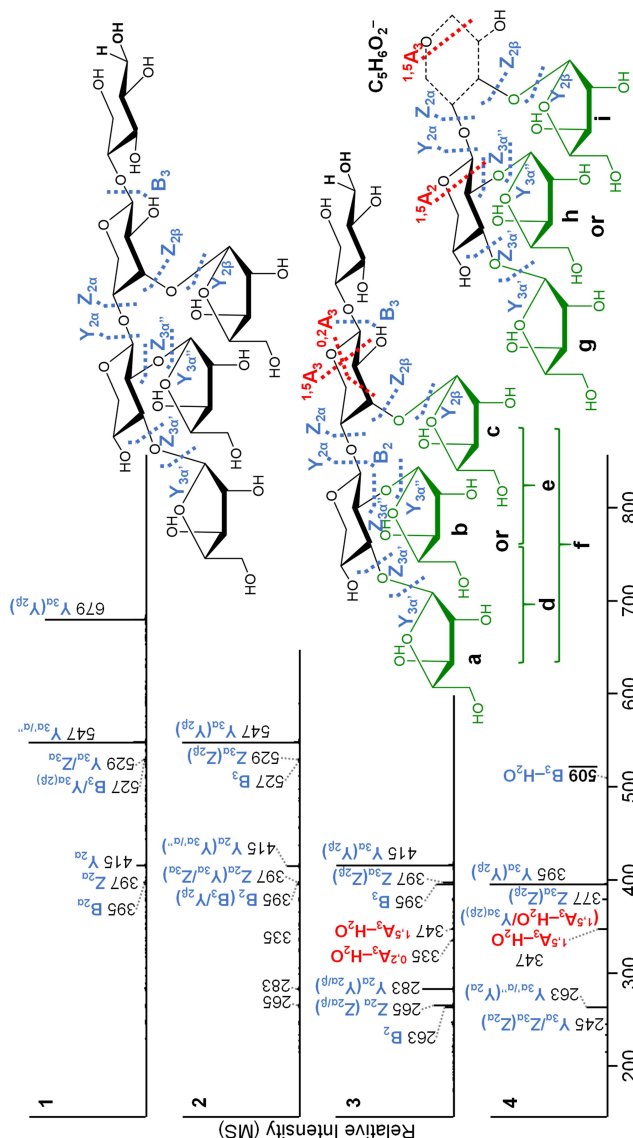
Fig. S11. Negative ion mode CID-MS[2] (**1**) and CID-MS[3] spectra of *m/z* 811→679 [M–H][−] (**2**), *m/z* 811→547 [M–H][−] (**3**) and *m/z* 811→527 [M–H][−] (**4**) corresponding to 6.i. Average spectra across the most abundant chromatographic peaks between treatments (**Fig. S5**). The fragments are annotated according to Domon & Costello (1988) and Juvonen et al. (2019) (1,2). Blue: glycosidic fragments; Red: cross-ring fragments; /: double cleavage; Alternative fragments are presented in brackets. Structures **a, b, c** correspond to *m/z* 811→679 [M–H][−] (**2**), **d, e, f** correspond to *m/z* 811→547 [M–H][−] (**3**) and **g, h, i** correspond to *m/z* 811→527 [M–H][−] due to the loss of one (**a-c, g-i**) or two (**d-f**) arabinosyl substituents. The precise structure of the newly formed end of B fragment ions is unknown as it may undergo several rearrangements (dashed ring), hence corresponding MS[3]-ring-fragments have been annotated tentatively.
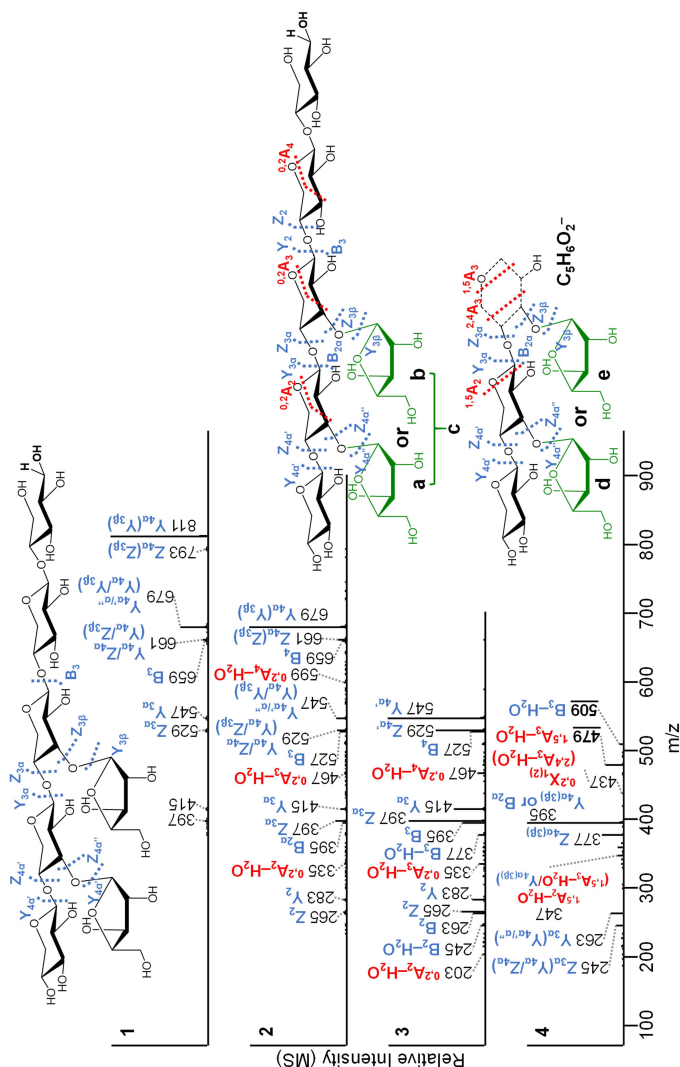
Fig. S12. Negative ion mode CID-MS^2 (**1**) and CID-MS^3 spectra of *m/z* 943→811 [M–H]$^-$ (**2**), *m/z* 943→679 [M–H]$^-$ (**3**) and *m/z* 943→527 [M–H]$^-$ (**4**) corresponding to 7.v. The fragments are annotated according to Domon & Costello (1988) and Juvonen et al. (2019) (1,2). Blue: glycosidic fragments; Red: cross-ring fragments; /: double cleavage. Alternative fragments are presented in brackets. Structure **a, b** correspond to *m/z* 943→811 [M–H]$^-$ (**2**), **c** corresponds to *m/z* 943→679 [M–H]$^-$ (**3**) and **d, e** correspond to *m/z* 943→527 [M–H]$^-$ due to the loss of either (**a, b, d, e**) or both (**c**) arabinosyl substituents. The precise structure of the newly formed end of B fragment ions is unknown as it may undergo several rearrangements (dashed ring), hence corresponding MS^3-ring-fragments have been annotated tentatively.

Supplementary information references

1.   Domon B, Costello CE. A systematic nomenclature for carbohydrate fragmentations in FAB-MS/MS spectra of glycoconjugates. Glycoconj J. 1988;5(4):397–409.

2.   Juvonen M, Kotiranta M, Jokela J, Tuomainen P, Tenkanen M. Identification and structural analysis of cereal arabinoxylan-derived oligosaccharides by negative ionization HILIC-MS/MS. Food Chem. 2019;275:176–85.

3.   van Gool MP, van Muiswinkel GCJ, Hinz SWA, Schols HA, Sinitsyn AP, Gruppen H. Two novel GH11 endo-xylanases from Myceliophthora thermophila C1 act differently toward soluble and insoluble xylans. Enzyme Microb Technol. 2013;53(1):25–32.

4

Chapter

5

In vivo formation of arabinoxylo-oligosaccharides by dietary endo-xylanase alters arabinoxylan utilization in broilers
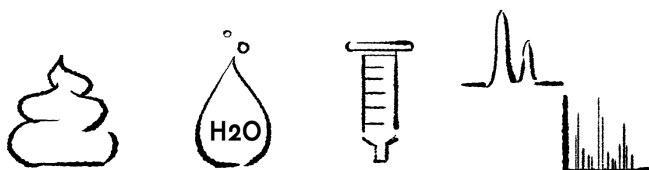
Kouzounis D., Jonathan M. C., Soares N., Kabel. M. A., Schols H. A.

Abstract

Previously, arabinoxylan (AX) depolymerization by dietary endo-xylanase was observed in the broiler ileum, but released arabinoxylo-oligosaccharides (AXOS) were not characterized in detail. This study aimed at extracting and identifying AXOS released *in vivo* in broilers, in order to delineate the influence of endo-xylanase on AX utilization. Hereto, digesta from the gizzard, ileum, ceca and excreta of broilers fed a wheat-soybean diet without (Con) or with endo-xylanase supplementation (Enz) were assessed. Soluble AX content in the ileum was higher for Enz diet (26.9%) than for Con diet (18.8%), indicating a different type and amount of AX entering the ceca. Removal of maltodextrins and fructans enabled monitoring of AX depolymerization to AXOS (Enz diet) using HPSEC-RI and HPAEC-PAD. A recently developed HILIC-MS^n methodology allowed AXOS (DP 4-10) identification in ileal digesta and excreta. Xylanase-induced AXOS formation coincided with decreased total tract AX recovery, which indicated improved AX hindgut utilization.

1   Introduction

Wheat grains are a major starch source in poultry nutrition. Next to starch, wheat grains contain about 9% non-starch polysaccharides (NSP) present in the cell walls (1,2). Arabinoxylan (AX) is the most abundant NSP, accounting for 5-7% of the grain dry matter (3). AX is a well characterized polymer composed of a β-(1→4) linked D-xylosyl (Xyl) backbone, mainly substituted with L-arabinosyl (Ara) units. For endosperm AX, approximately 66% of all Xyl residues are unsubstituted, 21% are monosubstituted mainly by *O*-3-linked Ara, while doubly substituted Xyl by Ara at both *O*-2 and *O*-3 account for 13% of backbone Xyl residues. *O*-2-linked Ara may also be present in minor amounts (3–5). AX from wheat aleurone and pericarp tissues may present different Ara-substitution pattern compared to endosperm AX, and can be further substituted with 4-*O*-methyl-D-glucuronyl, acetyl and/or feruloyl moieties (3,4).

Polymeric AX is reported to increase intestinal viscosity and hinder nutrient digestibility, thus negatively influencing broiler growth (6,7). Nonetheless, certain soluble AX fractions can be readily fermented to short chain fatty acids (SCFAs) by gut microbiota in the ceca, thus benefiting the host (8–10). Endo-xylanase supplementation has been a successful strategy to offset the aforementioned anti-nutritive effects of AX, predominantly in wheat-based diets. Xylanase-mediated improvements in nutrient digestibility and broiler performance have been associated with reduced digesta viscosity, decreased nutrient encapsulation by the cereal cell wall matrix and increased AX fermentation to SCFAs (6,11,12).

Endo-xylanases hydrolyze the β-(1→4) linkage between two Xyl residues of the AX backbone, depolymerizing AX and releasing (arabino)xylo-oligosaccharides ((A)XOS) (13,14). The (A)XOS formed are known for their prebiotic properties for humans (15). In particular, it has been demonstrated that the beneficial impact of (A)XOS on hindgut fermentation depends on their chemical structure (i.e. degree of polymerization (DP), degree/type of substitution) (15,16). Similar to human studies, (A)XOS supplementation resulted in bifidobacterial growth as well as pronounced SCFAs formation in the broiler ceca (17,18). Likewise, endo-xylanase supplementation has been shown to influence microbiota ecology and to promote cecal SCFAs formation (12,18,19). Such observations outline that improvement of hindgut fermentation can be expected as a result of the xylanase-driven degradation of AX to (A)XOS *in vivo*. Indeed, several studies have reported AX solubilization and size reduction upon endo-xylanase supplementation in broilers (20–22). However, a detailed characterization of *in vivo* released AXOS has yet to be performed, mainly due to the challenge of analyzing such structures in complex digesta matrices.

Recently, we demonstrated that endo-xylanase supplementation in a wheat-based diet led to *in vivo* formation of pentose oligomers with degree of polymerization (DP) of 5-26 in the proximal GIT of broilers (23). The current research aims at defining the detailed structure of AXOS released by dietary endo-xylanase in the

broiler GIT. It is hypothesized that the detailed characterization of AXOS formed *in vivo* by dietary endo-xylanase will improve our understanding on how such dietary enzymes may promote AX fermentation in broilers. This work is considered to contribute to the more comprehensive study of carbohydrate fermentation in animals, and is of interest for academia, policy makers and the industry.

2 Materials and methods

Wheat flour arabinoxylan (medium viscosity) (WAX), linear XOS standards (DP 2–6; X_2-X_6), amyloglucosidase from *Aspergillus niger* (AMG) and fructanase preparation (FRM) were obtained from Megazyme (Bray, Ireland). Hostazym X (HX) containing a GH11 endo-1,4-β-xylanase (EC 3.2.1.8) from *Trichoderma* sp. was from Huvepharma NV (Berchem, Belgium). All reagents used were of analytical grade and were obtained by either Sigma Aldrich (St. Louis, MO, USA) or Merck (Darmstadt, Germany), unless stated otherwise. The water used throughout laboratory experiments was purified with a Milli-Q Integral 5 (Millipore Corp., Billerica, MN, USA) purification system.

2.1 Samples from broiler GIT

Broiler digesta and excreta samples were obtained from our recent work (23). The animal study was conducted at the facilities of the Laboratory for Animal Nutrition and Animal Product Quality (LANUPRO), Department of Animal Sciences and Aquatic Ecology, Ghent University (Belgium), in accordance with the ethical standards and recommendations for accommodation and care of laboratory animals covered by the European Directive 2010/63/EU on the protection of animals used for scientific purposes and the Belgian royal decree KB29.05.13 on the use of animals for experimental studies. In brief, 48 one-day old male broilers were reared in a floor pen and were fed wheat-soybean starter (day 0-10) and grower (day 10-20) diets. On day 20, the birds were allocated to pens and were assigned to control (Con) or enzyme (Enz) diets following a randomized block design. Each diet consisted of 6 replicate pens, with 4 birds per pen. The wheat-soybean finisher diet (Table S1) was provided as such (Con) or supplemented with a commercially available enzyme preparation (Enz) of GH11 endo-1,4-β-xylanase (EC 3.2.1.8) and endo-1,4-β-glucanase (EC 3.2.1.4) from *Trichoderma* spp. (Huvepharma NV, Berchem, Belgium) (Table S2). The excreta were collected per pen, daily (twice) between day 24 and 28 and immediately stored at -20°C. On day 28, birds were euthanized, and the gizzard, ileum and ceca contents were collected, pooled per pen, and frozen at -20°C. Frozen material was dried by lyophilization and homogenized with a MM 400 Mixer Mill (Retsch GmbH, Haan, Germany) prior to analysis. Three out of six replicate pens were randomly selected, and digesta samples originating from these three pens were used for the current study.

2.2 Aqueous extraction of broiler digesta

Approximately 1,000 mg digesta was mixed with 35 mL water heated at 99 °C and was incubated at 99 °C for 20 min, with continuous mixing. Next, the mixture was

centrifuged at 30,000 x g, 20 min and the supernatant was filtered over 595 Whatman® filter paper. The residue was added to 30 mL water, mixed thoroughly and centrifuged at 30,000 x g, 20 min. The washing step was repeated once and the resulting supernatants were combined with the filtrate. The extracts and residue were freeze-dried, and the weight of the water extractable solids (WES) and water unextractable solids (WUS) was recorded. All fractions were homogenized with a MM 400 Mixer Mill.

2.3   Amyloglucosidase and fructanase treatment of WES from digesta

A combination of AMG/FRM was applied to remove maltodextrins and inulin from WES from all digesta samples (i.e. gizzard, ileum, ceca and excreta). The individual activity of AMG and FRM was predetermined on WES from the ileum (see supplement; p. 150). Potential side-activity of AMG and FRM on raffinose series oligosaccharides from soybean was also evaluated (see supplement; p. 150). Hereto, WES was dissolved in MilliQ water (10 mg/mL), helped by heating at 80 °C for 30 min. The resulting solutions were cooled at ambient temperature, centrifuged at 20,000 x g for 10 min, and 0.25 mL supernatant was diluted with 4.5 mL 50 mM NaOAc buffer solution (pH 5.0). Subsequently, pre-diluted AMG and FRM solutions were added (0.125 mL each). AMG and FRM were added in excess to ensure total or 'end-point' degradation. The mixture was incubated at 50 °C, overnight under continuous mixing. In parallel, 0.05 mL WES-in-buffer-solution was mixed with 0.95 mL NaOAc and incubated under otherwise similar conditions, but without AMG/FRM addition. The enzymatic reactions were stopped by heating at 99 °C for 15 min, and the samples were cooled at ambient temperature. The resulting solutions were then subjected to solid phase extraction (SPE).

2.4   Reversed-phase (C18) SPE of AMG/FRM-treated WES

SPE with C18 stationary phase was used to remove enzymatically released hexoses (see 2.3) from AMG/FRM-treated WES from the gizzard (G_{WES}), ileum (I_{WES}), ceca (C_{WES}) and excreta (E_{WES}), while retaining oligomers and polymers, and was performed as described elsewhere (24). Sep-Pak® C18 cartridges (6 cc, 1g, Waters Corp., Milford, MA, USA) were activated with 80% (v/v) methanol (MeOH) and subsequently washed with water (5 mL; 3 times, respectively). The samples were quantitatively loaded onto the cartridges and washed with water (5 mL; 3 times). The effluents during the loading and washing steps were pooled. Next, C18-bound analytes were eluted with 30% (v/v) MeOH (5 mL; 2 times). Per sample combined water fractions (coded: G_{WES}-W, I_{WES}-W, C_{WES}-W and E_{WES}-W) were freeze dried. Per sample combined 30% MeOH fractions (coded: G_{WES}-M, I_{WES}-M, C_{WES}-M and E_{WES}-M) were dried under a constant air stream with a sample concentrator. The dried W and M fractions were dissolved in 1 mL water, centrifuged at 20,000 x g for 10 min, and were analyzed for molecular weight distribution by HPSEC (as is), for their oligosaccharide profile by HPAEC (5 times dilution) and for sugar composition after methanolysis by HPAEC (see 2.6).

2.5 Preparative C18-SPE of AMG/FRM-treated pooled ileum and excreta WES

In a separate experiment, 150 mg ileum or excreta WES from the three biological replicates were pooled together (coded: IP_{WES}, EP_{WES}, respectively) and dissolved in 450 mL 50 mM NaOAc (pH 5.0) by heating at 80 °C for 30 min. Upon cooling at ambient temperature, AMG and FRM were added in excess and the solution was incubated overnight at 50 °C. The enzymatic reactions were stopped by heating at 99 °C for 15 min, and the samples were cooled at ambient temperature. Next, the samples were subjected to SPE, as follows; The Sep-Pak® C18 cartridges (35 cc, 10g, Waters Corp.) were activated with 100 mL 80% (v/v) MeOH and subsequently washed with 100 mL water. The samples were quantitatively loaded onto the cartridges and washed with 100 mL water. The effluents during the loading and washing steps were pooled. Next, C18-bound analytes were eluted with 30% (v/v) MeOH (35 mL; 2 times). Eluates were dried under a constant air stream overnight followed by lyophilization, and the obtained solids were labelled as IP_{WES}-M and EP_{WES}-M. IP_{WES}-M and EP_{WES}-M were dissolved in water at 10 mg/mL, and the derived solutions were subjected to sodium borohydride ($NaBH_4$) reduction (see 2.10), followed by HILIC-MS^n analysis.

2.6 Neutral carbohydrate content and composition analysis

The neutral sugar composition of whole digesta and WUS fractions thereof, was determined after pre-hydrolysis with 72% (w/w) H_2SO_4 (1 h, 30 ºC) and hydrolysis with 1 M H_2SO_4 (3 h, 100 ºC), followed by derivatization of the released sugars to alditol acetates and subsequent analysis by gas-chromatography (25,26).

The neutral sugar composition of WES, and the SPE fractions thereof, was determined by methanolysis followed by TFA hydrolysis (25). Due to fructose (Fru) instability during methanolysis and TFA hydrolysis, the Fru content in WES was determined enzymatically according to Stöber, Bénet, & Hischenhuber (2004) (27), with certain modifications. 100 µL aliquots of 10 mg/mL WES solutions were mixed with 892 µL of 55 mM NaOAc buffer (pH 4.5), followed by the addition of 8 µL FRM. The mixtures were incubated at 60 °C for 1h, and the reaction was stopped by heating at 99 °C for 15 min. The free monosaccharide content of untreated samples, and the monosaccharide composition of methanolized and FRM-treated WES, as well as that of methanolized SPE fractions was determined by HPAEC-PAD. Samples were dissolved/diluted in water prior to injection to achieve individual monosaccharide concentrations of 1-50 µg/mL. For quantification, a standard solution containing arabinose, xylose, glucose, fructose, galactose, mannose, fucose and rhamnose was prepared, treated similarly to unknown samples and diluted in the range of 1-50 µg/mL.

2.7 Monosaccharide analysis and oligosaccharide profiling by HPAEC-PAD

Monosaccharide composition and oligosaccharide profiles were determined by High-Performance Anion Exchange Chromatography with Pulsed Amperometric Detection (HPAEC-PAD) using a ICS7000 HPLC system (Dionex, Sunnyvale, CA) with and ICS7000 ED PAD detector (Dionex), and equipped with a CarboPac™ PA1 IC column (250 mm x 2 mm i.d.) and a CarboPac™ PA guard column (50 mm x 2 mm i.d.). The column temperature was set at 20 °C and the injection volume was 10 µL.

For monosaccharide analysis, three mobile phases were used: A) 0.1 M NaOH, B) 1 M NaOAc in 0.1 M NaOH and C) Water. Neutral monosaccharides were eluted at 0.4 mL/min with 100% C (isocratic) for 0–35 min, with post column addition of 0.5 M NaOH (0.1 mL/min) to enable PAD detection. The subsequent elution profile was: 35.1-50 min linear gradient 0-40% B (100-60% A); 50.1-55 min isocratic 100% B, 55.1-63 min isocratic 100% A; 63.1-78 min isocratic 100% C with post column addition.

For oligosaccharide characterization, 0.1 M sodium hydroxide (NaOH) (A) and 1 M sodium acetate in 0.1 M NaOH (B) were used as mobile phases. The flow rate was 0.3 mL/min. The separation was performed by using the following elution profile: 0−32 min from 0 % to 38 % B (linear gradient), 32-37 min from 32 % to 100 % B, 37-42 min at 100 % B (isocratic), 42-42.1 min to 100 % A (linear gradient) and 42.1-55 min 100 % A (isocratic). Linear XOS were identified based on elution of analytical standards (Megazyme).

2.8 Molecular weight distribution analysis by HPSEC-RI

The molecular weight distribution was determined by high performance size-exclusion chromatography with refractive index detection (HPSEC-RI) as described elsewhere (28), with an Ultimate 3000 HPLC System (Dionex Corp., Sunnyvale, CA, USA) equipped with a set of three TSK-Gel Super columns 4000AW, 3000AW, and 2500AW (6 mm ID ×150 mm per column, 6 µm), and a TSK Super AW-L guard column (4.6 mm ID ×35 mm, 7 µm) (Tosoh Bioscience Tokyo, Japan). The HPLC system was coupled to a Shodex RI-101 refractive index detector (Showa Denko KK, Kawasaki, Japan). The system was calibrated using a pullulan series of known Mw.

2.9 Oligosaccharide profiling by MALDI-TOF-MS

Oligomeric characterization by matrix-assisted laser desorption/ionization time-of-flight mass spectrometry (MALDI-TOF-MS) was carried out as described elsewhere (23), with an ultrafleXtreme™ MALDI-TOF/TOF mass spectrometer (Bruker Daltonics Inc., Billerica, MA, USA) operated at mass range *m/z* 900-2700. Mass calibration was performed with maltodextrins (Avebe B.V., the Netherlands).

2.10   Identification of (reduced) (A)XOS by HILIC-ESI-CID-MS^n

Structural analysis of AXOS and XOS isomers present in IP$_{WES}$-M and EP$_{WES}$-M solutions (10 mg/mL) (section 2.5) was conducted by hydrophilic interaction chromatography - electrospray ionization - collision induced dissociation - tandem mass spectrometry (HILIC-ESI-CID-MS^n), according to Kouzounis et al. (2022) (29). In brief, oligosaccharide reduction was performed by mixing 500 µL aliquots with 500 µL 0.5 M NaBH$_4$ in 1 M NH$_4$OH (4 h, ambient temperature), and was followed by acidification and sample clean-up (Supelclean™ ENVI-Carb™ SPE). Recovered analytes were dissolved in 100 µL 50% ACN and reduced oligosaccharides were analyzed with a Vanquish UHPLC system (Thermo Scientific, Waltham, MA, USA), equipped with an Acquity UPLC BEH Amide column (Waters, Millford, MA, USA; 1.7 µm, 2.1 mm ID × 150 mm) and a VanGuard pre-column (Waters; 1.7 µm, 2.1 mm ID × 50 mm), coupled with an LTQ Velos Pro mass spectrometer (Thermo Scientific). The mass spectrometer was equipped with a heated ESI probe, was operated in negative ion mode, and was run at three modes: Full MS (*m/z* 150-2000), MS^2 on selected MS ions, and MS^3 on selected MS^2 ions (29). Mass spectrometric data were processed by using Xcalibur 2.2 software (Thermo Scientific).

2.11   AX distribution in WES and WUS and marker-based AX recovery

The proportion of AX (sum of Ara and Xyl) in whole digesta from the gizzard, ileum, ceca and excreta that was recovered in WES (WE-AX) was determined according to Eq. (1):

$$WE\text{-}AX \ (\%) = \frac{AX_{WE} * WES \ \%}{(AX_{WE} * WES \ \%) \ + \ AX_{WU} * WUS \ \%} * 100 \ (1)$$

Where AX$_{WE,WU}$ is the measured AX content (% dry matter) in WES or WUS of digesta from the gizzard, ileum, ceca and excreta. WES % and WUS % represent the fraction of WES and WUS, out of whole digesta (% dry matter). AX recovery in WUS (WU-AX) was determined in a similar manner.

The proportion of AX (sum of Ara and Xyl) ingested by broilers, that was recovered in WES (WE-AX) in the ileum and excreta, was determined, according to Eq. (2):

$$marker \ based \ WE\text{-}AX \ (\%) = AX_{Rec} * \frac{WE\text{-}AX}{100} \ (2)$$

Where AX$_{Rec}$ (%) is the recovery of total AX in the ileum or excreta previously determined using acid insoluble ash (AIA) as a digestibility marker, as described in our recent publication (23). Mean values of AX$_{Rec}$ for Con and Enz are given in Table S3. WE-AX (%) was determined by Eq. (1). Marker-based AX recovery in WUS (WU-AX) was determined in a similar manner.

2.12 Statistical analysis

The obtained data was subjected to analysis of variance (ANOVA) using R version 4.0.2 (R Core Team), with pen being the experimental unit. Statistical analysis was carried out for each sampling site (gizzard, ileum, ceca, excreta) separately. Arabinoxylan solubilization and arabinose-to-xylose (Ara/Xyl) ratio were modelled using diet (D; Con or Enz) and fraction (F_{aq}; WES, WUS) as main effects including their two-way interaction term. Monosaccharide recovery during SPE of WES samples was modelled using D and SPE fraction (F_{SPE}; water (W), 30% (v/v) methanol (M)) as main effects including their two-way interaction term. Normality of data residuals and homogeneity of variance were additionally checked. The significance of differences between treatments was determined by Fisher's least significant difference procedure, with a significance threshold set at $p < 0.05$.

3 Results and discussion

3.1 Soluble carbohydrate level and composition varied along the GIT

The first step to characterize AX and xylanase-released AXOS was to subject digesta samples from the gizzard, ileum, ceca and excreta from broilers fed with Con and Enz diets, to aqueous extraction and subsequent analysis (Table S4). Water-extractable solids (WES) represented 32.3-39.0% of total solids in gizzard, ileum or excreta, while more than 59% of total solids was recovered in the corresponding water-unextractable solids (WUS) for both diets. In contrast, in the ceca, the WES and WUS presented similar yields, approximately 50% of the total dry matter. Next, the constituent monosaccharide composition and total carbohydrate content of WES was determined (Table 1). The monosaccharide composition of the corresponding WUS is provided in Table S5, in order to facilitate an overview of NSP distribution between WES and WUS.

WES fractions of the gizzard, ileum, ceca and excreta from both diets were composed of ~53%, ~44%, ~11% and ~17% carbohydrates (% w/w), respectively (Table 1). Soluble carbohydrates originated predominantly from wheat whole grains and soybean meal, that composed 66% and 17% of the diets (% as fed), respectively (Table S1). Glc, mainly representing starch, was the main water-extractable carbohydrate in the gizzard (79-81 mol % of neutral sugars), while non-starch carbohydrates Gal, Xyl, Ara and Fru were considerably less abundant (4.0-5.4 mol %). Starch digestion in the small intestine decreased the relative amount of Glc and revealed the building blocks of soluble NSP more clearly. Part of the Glc (17-18 mol %) was present in the ileum as unabsorbed monomer, while the majority of Glc was still present as building block of undigested carbohydrates. Soybean-derived NSP accounted for the high Gal presence in the ileum (~19 mol %) and may have had a limited contribution to Ara content as well (30). Next, Ara and Xyl mainly represented arabinoxylan (AX), which is the most abundant NSP in wheat (3), and together accounted for ~20% and ~30% (mol %) of the water-

extractable carbohydrates present in the ileum in Con and Enz. This observation was already suggestive of the influence of enzyme addition on AX solubilization. Ceca WES presented high free monosaccharide content, while Rha abundance might be attributed to bacterial polysaccharides (31). Finally, soluble NSP escaping fermentation were still present in the excreta, and were mainly composed of Glc (~37 mol %), Ara+Xyl (~32 mol %) and Gal (~14 mol %).

Table 1. Constituent neutral monosaccharide composition and total carbohydrate content (% w/w) of water-extractable solids (WES) in the gizzard, ileum, ceca and excreta, after acid or enzymatic (FRM) hydrolysis. Standard deviations (n = 3) are shown in Table S6. The values in parentheses represent the proportion (%) of each constituent monosaccharide present as free sugar.

	Constituent neutral monosaccharide composition (mol%)								Carb. content (% w/w)
	Ara	Xyl	Glc	Fru	Gal	Man	Fuc	Rha	
Gizzard									
Con[1]	4.0 (6%)	4.5 n.d.[2]	81.1 (1%)	4.4 (23%)	5.0 (2%)	1.0 n.d.	0.1 n.d.	0.0 n.d.	52.9
Enz[1]	5.4 (3%)	6.0 n.d.	78.7 (1%)	3.6 (21%)	5.2 (3%)	0.9 n.d.	0.1 n.d.	0.0 n.d.	52.5
Ileum									
Con	9.3 (1%)	10.5 n.d.	41.9 (17%)	16.2 (10%)	18.7 (14%)	2.5 n.d.	0.9 n.d.	0.0 n.d.	43.7
Enz	12.9 (1%)	16.4 n.d.	27.7 (18%)	19.6 (18%)	19.6 (23%)	2.7 n.d.	1.1 n.d.	0.0 n.d.	44.2
Ceca									
Con	2.8 (95%)	6.7 (13%)	60.9 (48%)	8.8 (116%)	9.9 (14%)	3.5 (112%)	1.7 (1%)	5.6 n.d.	10.1
Enz	2.7 (95%)	5.5 (13%)	64.7 (48%)	8.3 (116%)	8.4 (14%)	4.4 (112%)	1.3 (1%)	4.7 n.d.	13.0
Excreta									
Con	14.0 (7%)	17.8 n.d.	37.5 (5%)	10.2 (28%)	14.1 (11%)	4.5 n.d.	2.0 n.d.	0.0 n.d.	17.4
Enz	13.9 (7%)	18.2 n.d.	37.4 (9%)	9.3 (51%)	14.3 (16%)	4.7 n.d.	2.2 n.d.	0.0 n.d.	17.1

[1]Con: control diet; Enz: xylanase supplemented diet. [2]Not detected.

3.2 Xylanase-driven solubilization of AX species along the GIT

Next, we studied the impact of dietary endo-xylanase on the marker-based recovery of AX (Eq. (2)) in WES (WE-AX) and WUS (WU-AX) for ileum and excreta (Fig. 1). Insoluble digestibility markers are differently retained in the gizzard than soluble feed components, and cannot follow soluble feed components in the ceca (32,33). Consequently, the relative WE-AX and WU-AX proportion in the gizzard, ceca and finisher diets was determined instead (Eq. (1), Table 2, Table S7). HPSEC-RI and MALDI-TOF-MS analysis of WES from both Con and Enz finisher diets only showed the presence polymeric material, while AX-deriving oligomers were not detected (data not shown). The Ara/Xyl ratio at the different GIT locations was determined as well (Table 3).

p values (ANOVA)	Ileum	Excreta
Diet (D: Con vs Enz)	0.099	0.130
Fraction (F_{aq}: WES vs WUS)	<0.001	<0.001
D x F_{aq}	<0.001	0.110
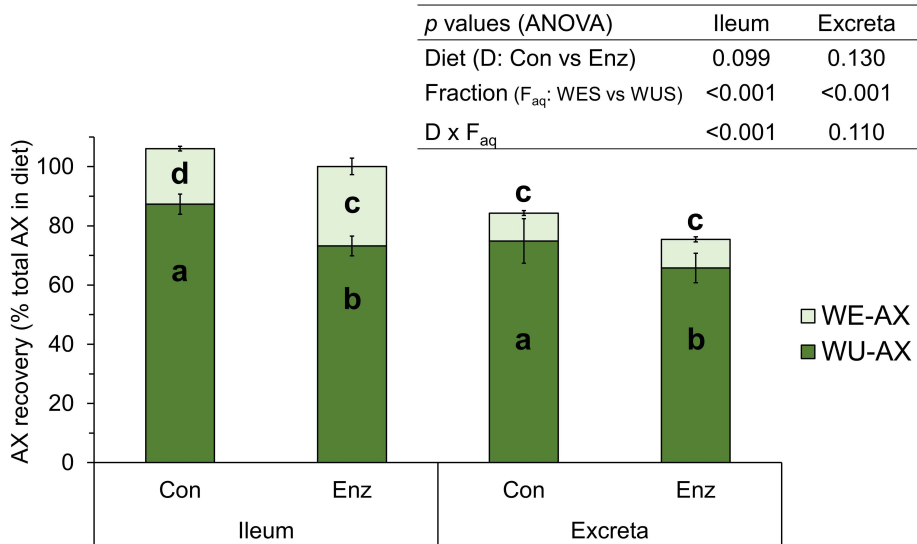
Fig. 1. Marker-based recovery of water-extractable (WE-AX) and water-unextractable (WU-AX) arabinoxylan in the ileum and excreta, expressed as percentage (%) of the total AX present in the control diet (Con) and endo-xylanase supplemented diet (Enz). Bars corresponding to ileum or excreta not sharing common notation differ significantly (*p* < 0.05). The error bars indicate standard deviation (*n* = 3); ANOVA results are presented in the table inserted.

WE-AX in the ileum represented 18.9% and 26.8% of AX consumed by broilers in Con and Enz, respectively (Fig. 1). The observed increase of soluble AX by endo-xylanase in the ileum (*p < 0.05*) was accompanied by a concomitant decrease in WU-AX from 82.3% to 73.2% (*p < 0.05*). The Ara/Xyl values above 0.8 obtained for WES (Table 3) were higher than the ones reported for soluble wheat AX (Ara/Xyl 0.5-0.7), suggesting co-extraction of Ara-containing soybean polysaccharides (1,30). Still, comparing the Ara/Xyl values between Con and Enz may reveal structural aspects of enzymatically-released AX species. For example, WE-AX in the ileum was found to be less substituted for Enz than for Con (Ara/Xyl: 0.78 *vs* 0.88; *p < 0.05*). Our findings are in agreement with previous studies reporting the increased AX solubilization in the ileum of broilers and pigs upon GH11 endo-xylanase supplementation (21,22,34). In addition, endo-xylanase action resulted in significantly lower WU-AX recovery in excreta, compared to Con (Fig. 1; 65.8% vs 74.9%; *p* < 0.05). At the same time, Enz and Con presented similar WE-AX recovery in excreta, with similar Ara/Xyl ratio (*p* > 0.05). Overall, the decreased AX recovery from ileum to excreta (Fig. 1) indicated that xylanase-mediated WU-AX solubilization coincided with increased WE-AX fermentation. The later has been confirmed by a more pronounced acetate and butyrate formation for Enz compared to Con, as was previously found for the same ceca samples (23).

Table 2. Total arabinoxylan (AX: sum of Ara and Xyl) recovery during aqueous extraction (% AX in digesta), and WE-AX and WU-AX recovery, expressed as percentage (%) of AX present in the gizzard and ceca. Values within GIT location not sharing common notation differ significantly ($p < 0.05$). The ANOVA results ($n = 3$) are presented in Table S8.

	Arabinoxylan (AX) recovery (% AX in GIT location)		
	Total	WE-AX	WU-AX
Gizzard			
Con	91.1	11.7[b]	88.3[a]
Enz	88.2	13.2[b]	86.8[a]
Ceca			
Con	86.6	38.0[b]	62.0[a]
Enz	117.1	70.2[a]	29.8[b]

Finally, a similar WE-AX recovery in Con and Enz in the gizzard (*p > 0.05*) suggested limited enzymatic activity under gastric conditions (35). Overall, the present findings indicated that endo-xylanase increased the proportion of AX becoming available for fermentation in the ceca (Fig. 1, Table 2), which could be beneficial for SCFAs formation, and ultimately, for broiler health (15,17).

Table 3. Arabinosyl to xylosyl ratio (Ara/Xyl) at the different GIT locations (gizzard, ileum, ceca, excreta). The ratio is corrected for free Ara and Xyl present. Values within GIT location not sharing common notation differ significantly ($p < 0.05$). The ANOVA results ($n = 2$-3) are presented in Table S9.

	Ara/Xyl ratio							
	Gizzard		Ileum		Ceca		Excreta	
	Con	**Enz**	**Con**	**Enz**	**Con**	**Enz**	**Con**	**Enz**
WE-AX	0.85[a]	0.88[a]	0.88[a]	0.78[bc]	0.13[c]	0.29[bc]	0.73[b]	0.72[b]
WU-AX	0.65[b]	0.57[b]	0.72[c]	0.81[ab]	0.35[b]	0.87[a]	0.76[ab]	0.81[a]

3.3 Maltodextrins and fructans were dominant oligosaccharide species in the ileum

To further delineate the influence of endo-xylanase on AX fermentability, we investigated by MALDI-TOF-MS the types of oligosaccharides released in the ileum, and recovered in WES. Representative mass spectra of *m/z* 900-2700 are shown in Fig. 2. AX hydrolysis by endo-xylanase was substantiated in Enz by the detection of soluble pentose oligosaccharides of DP 7-20 (Fig. 2; *m/z* series with 132 Da difference), as previously published (23). In addition, hexose oligosaccharides (HexOS) of DP 6-15 were dominant in ileal WES for both Con and Enz (Fig. 2; *m/z* series with 162 Da difference). MS analysis at *m/z* 500-900 showed smaller pentose oligosaccharides (DP 4-6) and HexOS (DP 3-5) as well, but the resulting spectra were rather noisy (data not shown). HexOS enzymatic fingerprinting and removal was conducted to resolve AXOS, and was achieved by treatment with

amyloglucosidase (AMG), fructanase (FRM), and their combination (AMG/FRM) (Fig. 2; Fig. S1). AMG/FRM combination resulted in complete Fru release, followed by the release of 65.5-67.5% of Glc and 26.8-28.5% of Gal present in ileal WES, regardless of diet. At the same time, HexOS disappeared, while (A)XOS present only in Enz gained in relevance. Consequently, the abundance of Glc and Fru in ileal WES (Table 1) was now explained as being part of HexOS maltodextrins and fructan oligosaccharides. In addition, Gal and part of Glc and Fru formed by AMG/FRM could be attributed to a series of raffinose oligosaccharides (Fig. S2), whose degradation may account for the apparent release of more than 100% Fru (Fig. 2). The present findings are in agreement with the detection of maltodextrins in the small intestine of pigs, as well as with the occurrence of fructans in wheat grains at approximately 1.5% of the dry matter (36–38). Overall, the enzymatic degradation of HexOS mixtures present in digesta now enables the further characterization of enzymatically released (A)XOS.
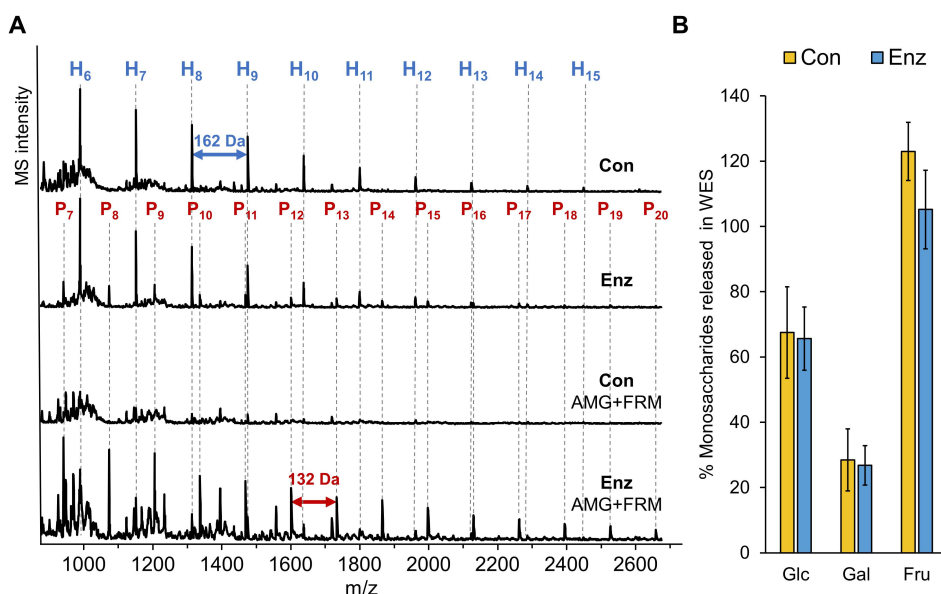
Fig. 2. MALDI-TOF-mass spectra (*m/z* 900-2700) (**A**) of ileal WES, from Con and Enz diets before (top two spectra) and after (bottom two spectra) incubation with AMG/FRM; Glc, Gal and Fru released by AMG/FRM (**B**), expressed as proportion of the corresponding total constituent monosaccharides present in WES from ileal digesta. The number of hexose (H_n) or pentose (P_n) residues per oligomer is indicated.

3.4   AX/AXOS-enriched fractions were obtained from digesta by solid phase extraction

AMG/FRM-treated G_{WES}, I_{WES}, C_{WES} and E_{WES} were subjected to reversed phase (C18) SPE, in order to separate monosaccharides (hexoses) from AX/AXOS (Fig. 3 and Fig. S4). The SPE procedure was evaluated beforehand for reference polymeric

WAX and WAX digested with GH11 endo-xylanase (HX). It was found that WAX could only be partially recovered during SPE as polymer (~52%; Fig. S3), while it was fully recovered after endo-xylanase treatment. In particular, xylose and DP 2-4 linear XOS were eluted with water, while retained AXOS were eluted with MeOH up to 30% (v/v). Previously published C18-SPE behavior of soluble carbohydrates from corn stover demonstrated that Xyl-rich DP 3-4 pentose oligomers eluted with water and Ara-substituted DP 4-7 pentose oligomers eluted with 30% MeOH (24).
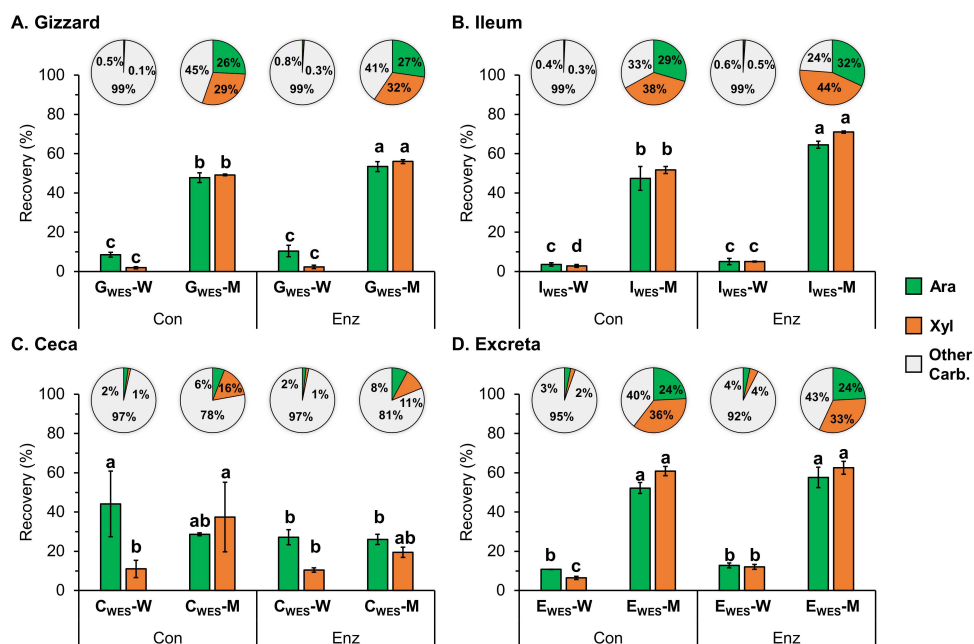
Fig. 3. Constituent arabinosyl (Ara:▢) and xylosyl (Xyl: ▢) recovery (%) in the water (W) and 30% (v/v) MeOH (M) fractions, after SPE of AMG/FRM-treated WES from the gizzard (**A**: G$_{WES}$), ileum (**B**: I$_{WES}$), ceca (**C**: C$_{WES}$) and excreta (**D**: E$_{WES}$); Pie charts (inserts) show the carbohydrate composition (mol %) of Ara, Xyl and other carbohydrates (Other Carb.: ▢). Bars representing either Ara or Xyl not sharing common notation differ significantly ($p < 0.05$). The error bars indicate standard deviation ($n = 3$). The ANOVA results are given in Table S10.

Approximately 47.5-64.5% of total Ara and 49.2-71.0% of total Xyl was recovered in G$_{WES}$-M, I$_{WES}$-M and E$_{WES}$-M fractions, while less than 12.8% of total Ara and 12.1% of total Xyl was recovered in the corresponding G$_{WES}$-W, I$_{WES}$-W and E$_{WES}$-W fractions. Most of the Fru, Glc and Gal was recovered in the W fractions, according to expectations (Fig. S4). Consequently, the resulting M fractions were enriched in AX/AXOS, as indicated by their carbohydrate composition (Fig. 3; inserts). Interestingly, significantly higher Ara and Xyl recovery in both G$_{WES}$-M and I$_{WES}$-M was observed for Enz compared to Con ($p < 0.05$) (Fig. 3). Apparently, *in vivo* depolymerization of both WE-AX and WU-AX to AXOS resulted in higher AX

recovery after SPE for Enz compared to Con, as already described in Fig. S3. Therefore, a correspondingly higher amount of polymeric AX is expected to be retained on the SPE column for Con than for Enz. The higher Xyl recovery observed in I_{WES}-W for Enz compared to Con ($p < 0.05$) was more likely due to low DP XOS removal by water. The ceca presented a distinct case, as low Ara and Xyl recovery and amounts were recorded in C_{WES}-M. Instead, C_{WES}-W presented elevated Ara and Xyl recovery compared to other GIT locations for both Con and Enz. C_{WES}-M also exhibited elevated Gal recovery compared to other GIT locations for both Con and Enz (Fig. S4). These observations highlight a rather complete utilization of (A)XOS entering the ceca. No differences in Ara and Xyl recovery in E_{WES}-M between Con and Enz were observed ($p > 0.05$). On the contrary, Enz presented significantly higher Xyl recovery in E_{WES}-W compared to Con ($p < 0.05$).

3.5 Characterization of AX and AXOS in SPE digesta fractions

Xylanase-mediated AX degradation began in the gizzard

To further detail the isolated (A)XOS structures in the M fractions (see 3.4), these M fractions were subjected to molecular weight distribution analysis by HPSEC-RI and the oligomers present were profiled by HPAEC-PAD (Fig. 4). G_{WES}-M presented different HPSEC profile for Enz compared to Con (Fig. 4A). Additionally, compounds eluting at similar retention times as AXOS were detected by HPAEC in G_{WES}-M for Enz only, although the signal was rather low (Fig. 4B). Still, only a marginal increase in WE-AX was observed in the gizzard for Enz compared to Con (Table 2). It can, therefore, be concluded that endo-xylanase mainly degraded soluble, polymeric AX in the gizzard to smaller fragments (Mw between 10-100 kDa). Soluble, polymeric WE-AX for wheat can exhibit molecular weight (Mw) up to 300 kDa, although showing broad polydispersity (70-655 kDa; (3)). Currently, high Mw AX populations (i.e., > 100 kDa) potentially present in digesta, appeared to be retained on the C18-SPE column (Fig. S3). Therefore, such polymers may be underrepresented in the HPSEC profiles of M fractions, especially for Con (Fig. 4A). Furthermore, AX depolymerization by endo-xylanase may further explain the increased Ara and Xyl recoveries observed in G_{WES}-M for Enz, compared to Con (Fig. 3A). These findings demonstrate that AX hydrolysis by endo-xylanase began in the gizzard, in line with recent reports of AX degradation in the crop and gizzard (39,40). Nevertheless, the acidic pH (1.0-4.5) and short feed retention time (30-60 min) in the gizzard were expected to result in limited activity of supplemented fungal xylanases (35,41,42).

Enzymatic fingerprint and chemical structure of in vivo formed AXOS

I_{WES}-M for Con mainly presented Mw populations between 10-100 kDa, while 10-1 kDa material was more abundant for Enz (Fig. 4A). This shift in size distribution was accompanied by AXOS presence in I_{WES}-M for Enz, as clearly demonstrated by HPAEC (Fig. 4B). In particular, the *in vivo* AXOS profile matched the one obtained

during *in vitro* hydrolysis (see supplement; p. 150) of soluble WAX by the same enzyme preparation (Fig 4B; WAX-HX), and by a different GH11 endo-xylanase (not shown;(43)).
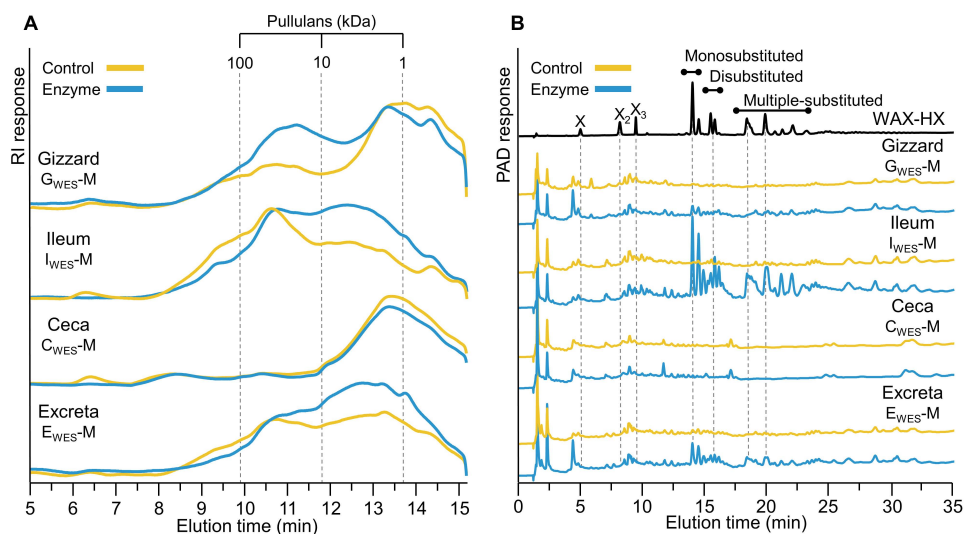
Fig. 4. HPSEC-RI (**A**) and HPAEC-PAD (**B**) elution patterns of SPE-M fractions of the WES from the gizzard, ileum, ceca and excreta of broilers fed with control and enzyme diets. Pullulans were used as calibrants for HPSEC. X: xylose, X_2: xylobiose, X_3: xylotriose were labelled according to analytical standards; AXOS were eluted in groups of monosubstituted, disubstituted and multiple-substituted oligosaccharides (43).

This corroborated that AXOS detected in I_{WES}-M for Enz were formed by the supplemented GH11 endo-xylanase. AXOS were also detected in excreta (E_{WES}-M) for Enz, which presented similar profiles as the ileum (Fig. 4). AXOS *in vivo* formation currently coincided with WE-AX depolymerization as well as AX solubilization from the water-unextractable cell wall matrix (Fig. 1, Fig. 4). These findings confirm previous studies reporting the ability of GH11 endo-xylanases to hydrolyze both soluble and insoluble AX *in vitro,* under optimal conditions (44–46). So far, our findings demonstrate that dietary GH11 endo-xylanase depolymerized both soluble and insoluble AX from wheat grains, and released AXOS *in vivo*. Depolymerization of WE-AX is consistent with the previously reported xylanase-mediated decrease in digesta viscosity (7,11,40). Besides, the enzymatic WU-AX degradation *in vivo* is postulated to offset nutrient encapsulation by the cell wall matrix, thus promoting nutrient digestion (6,40).

The chemical structure of *in vivo* formed AXOS was further investigated for pooled ileal (IP_{WES}) and excreta (IP_{WES}) samples from Enz diet after SPE (section 2.5). Specifically, the obtained M fractions (IP_{WES}-M, EP_{WES}-M) were analyzed by HILIC-MS^n (Fig. 5), and the individual AXOS present were identified based on a database built up with retention times and MS^2 and MS^3 mass spectra of known (A)XOS, as

described by Kouzouis et al. (2022) (29). Ileum and excreta samples presented similar HILIC-MS profiles, with various DP 4-10 (A)XOS isomers being resolved (Fig. 5; Figs. S5-7). Based on the present identification by HILIC-MS^n, the main identified AXOS contained no more than two Ara substituents, mainly present as single *O*-3-linked and double *O*-2,3-linked Ara, and were further composed of two or more contiguous unsubstituted xylosyl residues at the reducing end. The presence of at least one unsubstituted xylosyl adjacent to the cleavage site was in accordance with the mode of action of GH11 endo-xylanases targeting low-substituted AX populations (13,14,47). GH11 endo-xylanases were previously found to release low-substituted DP 5-7 AXOS from wheat bran and wheat flour WUS (45,48,49). The low substitution degree of AXOS currently observed is in agreement with the lower Ara/Xyl ratio observed in ileal digesta for WE-AX for Enz diet compared to Con diet (Table 3). Moreover, the DP 8-10 AXOS currently detected were expected to be more complex, possibly containing multiple single and/or double Ara substitutions.
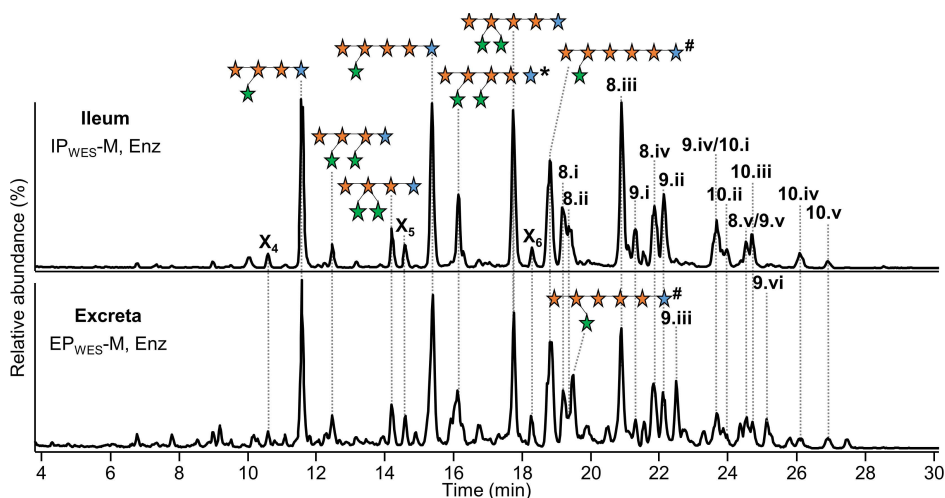
Fig. 5. HILIC-MS ion-extracted base peak chromatograms of NaBH$_4$-reduced DP 4-10 (A)XOS present in M fractions obtained by SPE of pooled ileum (IP$_{WES}$-M) and excreta (EP$_{WES}$-M) samples for Enz diet. Peak annotation was performed according to (29). *putative structure; #identification by MS^n is presented in Figs. S5-7; Unidentified DP 8-10 (A)XOS are labelled (i-v) according to their elution order; Arabinosyl (Ara: ★), xylosyl (Xyl: ★, xylitol: ★).

The fate of in vivo formed AXOS in the broiler hindgut

AXOS formation by dietary GH11 endo-xylanase in the upper GIT currently coincided with pronounced hindgut fermentation of AX for Enz compared to Con (Fig. 1, Table 2). Studies on AX and (A)XOS fermentation demonstrated that low Mw XOS and low-substituted AXOS are preferentially fermented by *Bifidobacterium* and *Bacteroides* spp. in human fecal inocula compared to more complex AX oligo- and polymers (15,16,50). On this basis, the release of relatively simple (A)XOS

structures may further explain the pronounced cecal fermentation previously documented upon endo-xylanase supplementation (12,18,19,23). Soluble compounds with Mw < 10 kDa were present in the ceca (C$_{WES}$-M), for both Con and Enz (Fig. 4A). However, AXOS were not detected by HPAEC (Fig. 4B), confirming the low Ara, Xyl recoveries in C$_{WES}$-M (Fig. 3C) for both Con and Enz. In this view, it is demonstrated that extensive fermentation of both polymeric and oligomeric AX species had occurred in the ceca. Still, low Mw AX species (< DP 5) may still be present in the broiler ceca, as recently reported (21). Finally, soluble unfermented structures mainly between 1-10 kDa were observed in excreta (Fig. 4A), partly corresponding to a similar WE-AX recovery for both Con and Enz (Fig. 1). Soluble feed components may first reach the cloaca and then enter the ceca via antiperistalsis, while insoluble and indigestible feed fractions will be excreted directly (9,51). It, therefore, appeared that a WE-AX fraction, including AXOS, passed from the ileum to the hindgut and was excreted unutilized, alongside WU-AX, instead of entering the ceca. This observation became more evident by the similar HILIC profile of (A)XOS in excreta and ileum (Fig. 5).

4   Conclusions

In this study, endo-xylanase supplementation in broilers resulted in AXOS formation *in vivo*. The detection and characterization of released oligosaccharides further delineated the xylanase-mediated improvement of AX fermentation in the broiler ceca. In particular, it is proposed that low-substituted AXOS and XOS, released *in vivo* by the dietary GH11 endo-xylanase, were more extensively fermented than polymeric AX by cecal microbiota. Still, further research in terms of AXOS quantification is warranted to better understand and optimize AX fermentation in livestock. Our work highlights the contribution of dietary endo-xylanase to broiler health and provides valuable insight on the utilization of AX and AXOS along the GIT. Overall, the detailed oligosaccharide analysis in complex digesta currently performed is expected to further progress the study of carbohydrate fermentation *in vivo*, in the GIT of animals. Such approach is of interest for academia, policy makers and the industry regarding the efficacy of feed additives.

5   References

1. Bach Knudsen KE. Fiber and nonstarch polysaccharide content and variation in common crops used in broiler diets. Poult Sci. 2014;93(9):2380–93.

2. Black JL. Cereal grains as animal feed. In: Wrigley CW, Corke H, Seetharaman K, Faubion J, editors. Encyclopedia of Food Grains. 2nd ed. Amsterdam: Elsevier Inc.; 2016. p. 215–22.

3. Saulnier L, Sado P-E, Branlard G, Charmet G, Guillon F. Wheat arabinoxylans: Exploiting variation in amount and composition to develop enhanced varieties. J Cereal Sci. 2007;46(3):261–81.

4. Izydorczyk MS, Biliaderis CG. Cereal arabinoxylans: Advances in structure and physicochemical properties. Carbohydr Polym. 1995;28(1):33–48.

5. Gruppen H, Hamer RJ, Voragen AGJ. Water-unextractable cell wall material from wheat flour. 2. Fractionation of alkali-extracted polymers and comparison with water-extractable arabinoxylans. J Cereal Sci. 1992;16(1):53–67.

6. Bedford MR. The evolution and application of enzymes in the animal feed industry: The role of data interpretation. Br Poult Sci. 2018;59(5):486–93.

7. Choct M, Annison G. The inhibition of nutrient digestion by wheat pentosans. Br J Nutr. 1992;67(1):123–32.

8. Pan D, Yu Z. Intestinal microbiome of poultry and its interaction with host and diet. Gut Microbes. 2013;5(1):108–19.

9. Svihus B, Choct M, Classen HL. Function and nutritional roles of the avian caeca: A review. Worlds Poult Sci J. 2013;69(2):249–64.

10. Sergeant MJ, Constantinidou C, Cogan TA, Bedford MR, Penn CW, Pallen MJ. Extensive microbial and functional diversity within the chicken cecal microbiome. PLoS One. 2014;9(3):e91941.

11. Bedford MR, Classen HL. Reduction of intestinal viscosity through manipulation of dietary rye and pentosanase concentration is effected through changes in the carbohydrate composition of the intestinal aqueous phase and results in improved growth rate and food conversion efficiency of broiler chicks. J Nutr. 1992;122(3):560–9.

12. Masey-O'Neill H V., Singh M, Cowieson AJ. Effects of exogenous xylanase on performance, nutrient digestibility, volatile fatty acid production and digestive tract thermal profiles of broilers fed on wheat- or maize-based diet. Br Poult Sci. 2014;55(3):351–9.

13. Biely P, Vršanská M, Tenkanen M, Kluepfel D. Endo-β-1,4-xylanase families: differences in catalytic properties. J Biotechnol. 1997;57(1):151–66.

14. Kormelink FJM, Gruppen H, Viëtor RJ, Voragen AGJ. Mode of action of the xylan-degrading enzymes from *Aspergillus awamori* on alkali-extractable cereal arabinoxylans. Carbohydr Res. 1993;249(2):355–67.

15. Broekaert WF, Courtin CM, Verbeke K, van de Wiele T, Verstraete W, Delcour JA. Prebiotic and other health-related effects of cereal-derived arabinoxylans, arabinoxylan-oligosaccharides, and xylooligosaccharides. Crit Rev Food Sci Nutr. 2011;51(2):178–94.

16. Mendis M, Martens EC, Simsek S. How fine structural differences of xylooligosaccharides and arabinoxylooligosaccharides regulate differential growth of *Bacteroides* species. J Agric Food Chem. 2018;66(31):8398–405.

17. Courtin CM, Swennen K, Broekaert WF, Swennen Q, Buyse J, Decuypere E, Michiels CW, De Ketelaere B, Delcour JA. Effects of dietary inclusion of xylooligo- saccharides, arabinoxylooligosaccha- rides and soluble arabinoxylan on the microbial composition of caecal contents of chickens. J Sci Food Agric. 2008;88(14):2517–22.

18. Morgan NK, Keerqin C, Wallace A, Wu SB, Choct M. Effect of arabinoxylo-oligosaccharides and arabinoxylans on net energy and nutrient utilization in broilers. Anim Nutr. 2019;5(1):56–62.

19. Singh AK, Mandal RK, Bedford MR, Jha R. Xylanase improves growth performance, enhances cecal short-chain fatty acids production, and increases the relative abundance of fiber fermenting cecal microbiota in broilers. Anim Feed Sci Technol. 2021;277:114956.

20. Choct M, Kocher A, Waters DLE, Pettersson D, Ross G. A comparison of three xylanases on the nutritive value of two wheats for broiler chickens. Br J Nutr. 2004;92(1):53.

21. Bautil A, Buyse J, Goos P, Bedford MR, Courtin CM. Feed endoxylanase type and dose affect arabinoxylan hydrolysis and fermentation in ageing broilers. Anim Nutr. 2021;7(3):787–800.

22. Lee SA, Apajalahti J, Vienola K, González-Ortiz G, Fontes CMGA, Bedford MR. Age and dietary xylanase supplementation affects ileal sugar residues and short chain fatty acid concentration in the ileum and caecum of broiler chickens. Anim Feed Sci Technol. 2017;234:29–42.

23. Kouzounis D, Hageman JA, Soares N, Michiels J, Schols HA. Impact of xylanase and glucanase on oligosaccharide formation, carbohydrate fermentation patterns, and nutrient utilization in the gastrointestinal tract of broilers. Animals. 2021;11(5):1285.

24. Jonathan MC, DeMartini J, Van Stigt Thans S, Hommes R, Kabel MA. Characterisation of non-degraded oligosaccharides in enzymatically hydrolysed and fermented, dilute ammonia-pretreated corn stover for ethanol production. Biotechnol Biofuels. 2017;10(1):112.

25. Broxterman SE, Schols HA. Characterisation of pectin-xylan complexes in tomato primary plant cell walls. Carbohydr Polym. 2018;197:269–76.

26. Englyst HN, Cummings JH. Simplified method for the measurement of total non-starch polysaccharides by gas-liquid chromatography of constituent sugars as alditol acetates. Analyst. 1984;109(7):937.

27. Stöber P, Bénet S, Hischenhuber C. Simplified enzymatic high-performance anion exchange chromatographic determination of total fructans in food and pet food - limitations and measurement uncertainty. J Agric Food Chem. 2004;52(8):2137–46.

28. van Gool MP, Toth K, Schols HA, Szakacs G, Gruppen H. Performance of hemicellulolytic enzymes in culture supernatants from a wide range of fungi on insoluble wheat straw and corn fiber fractions. Bioresour Technol. 2012;114:523–8.

29. Kouzounis D, Sun P, Bakx EJ, Schols HA, Kabel MA. Strategy to identify reduced arabinoxylo-oligosaccharides by HILIC-MS^n. Carbohydr Polym. 2022;289:119415.

30. Huisman MMH, Schols HA, Voragen AGJ. Cell wall polysaccharides from soybean (*Glycine max.*) meal. Isolation and characterisation. Carbohydr Polym. 1998;37(1):87–95.

31. Mäki M, Renkonen R. Biosynthesis of 6-deoxyhexose glycans in bacteria. Glycobiology. 2004;14(3).

32. De Vries S, Kwakkel RP, Pustjens AM, Kabel MA, Hendriks WH, Gerrits WJJ. Separation of digesta fractions complicates estimation of ileal digestibility using marker methods with Cr_2O_3 and cobalt-ethylenediamine tetraacetic acid in broiler chickens. Poult Sci. 2014;93(8):2010–7.

33. Vergara P, Ferrando C, Jiménez M, Fernández E, Goñalons E. Factors determining gastrointestinal transit time of several markers in the domestic fowl. Q J Exp Physiol. 1989;74(6):867–74.

34. Lærke HN, Arent S, Dalsgaard S, Bach Knudsen KE. Effect of xylanases on ileal viscosity, intestinal fiber modification, and apparent ileal fiber and nutrient digestibility of rye and wheat in growing pigs. J Anim Sci. 2015;93(9):4323–35.

35. Gonzalez-Ortiz G, Sola-Oriol D, Martinez-Mora M, Perez JF, Bedford MR. Response of broiler chickens fed wheat-based diets to xylanase supplementation. Poult Sci. 2017;96(8):2776–85.

36. Bach Knudsen KE. Carbohydrate and lignin contents of plant materials used in animal feeding. Anim Feed Sci Technol. 1997;67:319–38.

37. Fincher GB. Cereals: Chemistry and physicochemistry of non-starchy polysaccharides. In: Wrigley CW, Corke H, Seetharaman K, Faubion J, editors. Encyclopedia of food grains. 2nd ed. Amsterdam: Elsevier Inc.; 2016. p. 208–23.

38. Martens BMJ, Flécher T, De Vries S, Schols HA, Bruininx EMAM, Gerrits WJJ. Starch digestion kinetics and mechanisms of hydrolysing enzymes in growing pigs fed processed and native cereal-based diets. Br J Nutr. 2019;121(10):1124–36.

39. González-Ortiz G, Lee SA, Vienola K, Raatikainen K, Jurgens G, Apajalahti J, Bedford MR. Interaction between xylanase and a proton pump inhibitor on broiler chicken performance and gut function. Anim Nutr. 2022;8(1):277–88.

40. Matthiesen CF, Pettersson D, Smith A, Pedersen NR, Storm AC. Exogenous xylanase improves broiler production efficiency by increasing proximal small intestine digestion of crude protein and starch in wheat-based diets of various viscosities. Anim Feed Sci Technol. 2021;272:114739.

41. Polizeli MLTM, Rizzatti ACS, Monti R, Terenzi HF, Jorge JA, Amorim DS. Xylanases from fungi: Properties and industrial applications. Appl Microbiol Biotechnol. 2005;67(5):577–91.

42. Svihus B. Function of the digestive system. J Appl Poult Res. 2014;23(2):306–14.

43. van Gool MP, van Muiswinkel GCJ, Hinz SWA, Schols HA, Sinitsyn AP, Gruppen H. Two novel GH11 endo-xylanases from *Myceliophthora thermophila* C1 act differently toward soluble and insoluble xylans. Enzyme Microb Technol. 2013;53(1):25–32.

44. Bonnin E, Daviet S, Sorensen JF, Sibbesen O, Goldson A, Juge N, Saulnier L. Behaviour of family 10 and 11 xylanases towards arabinoxylans with varying structure. J Sci Food Agric. 2006;86(11):1618–22.

45. Courtin CM, Delcour JA. Relative activity of endoxylanases towards water-extractable and water-unextractable arabinoxylan. J Cereal Sci. 2001;33(3):301–12.

46. Moers K, Celus I, Brijs K, Courtin CM, Delcour JA. Endoxylanase substrate selectivity determines degradation of wheat water-extractable and water-unextractable arabinoxylan. Carbohydr Res. 2005;340(7):1319–27.

47. Beaugrand J, Reis D, Guillon F, Debeire P, Chabbert B. Xylanase-mediated hydrolysis of wheat bran: Evidence for subcellular heterogeneity of cell walls. Int J Plant Sci. 2004;165(4):553–63.

48. Beaugrand J, Chambat G, Wong VWKK, Goubet F, Rémond C, Paës G, Benamrouche S, Debeire P, O'Donohue M, Chabbert B. Impact and efficiency of GH10 and GH11 thermostable endoxylanases on wheat bran and alkali-extractable arabinoxylans. Carbohydr Res. 2004;339(15):2529–40.

49. Gruppen H, Kormelink FJM, Voragen AGJ. Enzymic degradation of water-unextractable cell wall material and arabinoxylans from wheat flour. J Cereal Sci. 1993;18(2):129–43.

50. Rumpagaporn P, Reuhs BL, Kaur A, Patterson JA, Keshavarzian A, Hamaker BR. Structural features of soluble cereal arabinoxylan fibers associated with a slow rate of *in vitro* fermentation by human fecal microbiota. Carbohydr Polym. 2015;130:191–7.

51. Duke GE. Relationship of cecal and colonic motility to diet, habitat, and cecal anatomy in several avian species. J Exp Zool. 1989;252:38–47.

5

Supplementary information

Supplementary materials and methods

Amyloglucosidase and fructanase treatment of WES from ileal digesta

Soluble maltodextrins and inulin were degraded by incubating ileal WES with AMG, FRM and a combination of both (AMG/FRM). Hereto, WES from ileal digesta (5 mg/mL water) was diluted to 0.5 mg/mL in 50 mM sodium acetate (NaOAc) buffer (pH 5.0), and subsequently incubated at 50 °C for 16 h with AMG and FRM separately and in combination. AMG and FRM were added in excess to ensure 'end-point' degradation. In parallel, 0.05 mL WES solution was mixed with 0.95 mL NaOAc and incubated under otherwise similar conditions. The enzymatic reactions were stopped by heating at 99 °C for 15 min. Samples were centrifuged at 20,000 x g for 10 min, diluted 20 times, and the corresponding release of monomers (Glc, Fru) was monitored by HPAEC-PAD. Oligosaccharide profiles of (incubated) WES was also monitored by MALDI-TOF-MS after diluting the samples 10 times.

Amyloglucosidase and fructanase activity towards raffinose and stachyose

Potential activity of amyloglucosidase (AMG) and fructanase (FRM) preparations on raffinose series oligosaccharides was assessed using raffinose (Raff) and stachyose (Stach) (Merck Life Science B.V., the Netherlands) as substrates. Raff and Stach solutions (0.5 mg/mL) were prepared in 50 mM NaOAc (pH 5.0) and subsequently incubated at 50 °C for 16 h with AMG and FRM, separately and in combination (AMG/FRM). AMG and FRM were added in excess to ensure total or 'end-point' degradation. In parallel, Raff and Stach solutions (0.5 mg/mL) were incubated without enzyme addition, under otherwise similar conditions. The enzymatic reactions were stopped by heating at 99 °C for 15 min. Samples were centrifuged at 20,000 x g for 10 min, diluted 20 times, and the corresponding release of mono- and di-saccharides was monitored by HPAEC-PAD. For Raff and Stach analysis, 0.1 M sodium hydroxide (NaOH) (A), 1 M sodium acetate in 0.1 M NaOH (B) and water (C) were used as mobile phases. The flow rate was 0.3 mL/min. The separation was performed using the following elution profile: 0−33 min from 16% (84% C) to 100% A (linear gradient), 33.1−45 min from 0% (100% A) to 4% B (96% A), 45.1−50 min at 100 % B (isocratic), 50.1−55 min to 100 % A (isocratic) and 55.1-65 min at 16% A and 84% C (isocratic).

In vitro production of arabinoxylan oligosaccharides (AXOS)

WAX in 50 mM sodium acetate (NaOAc) buffer pH 5.5 (5.0 mg/mL) was incubated overnight with HX (WAX-HX) resulting in total or 'end-point' degradation of WAX. The enzyme was inactivated by heating at 99 °C for 15 min and samples were subsequently stored at −20 °C.

Reversed-phase (C18) SPE of polymeric and xylanase-treated arabinoxylan

Untreated WAX (WAX-C) and enzymatically produced AXOS (WAX-X) were subjected to solid-phase extraction (SPE) with C18 stationary phase. Sep-Pak® C18 cartridges (6 cc, 1g, Waters Corp., Milford, MA, USA) were activated with 80% (v/v) Methanol (MeOH) solution and subsequently washed with water (5 mL; 3 times, respectively). Next, 1 mL of 5 mg/mL WAX-C and WAX-X solution was loaded onto the cartridges and washed with water (5 mL; 3 times). The effluents during the loading and washing steps were pooled. Next, C18-bound analytes were eluted sequentially with 2.5%, 20%, 30% and 80% (v/v) MeOH (5 mL; 1 time). The water fractions were freeze dried while the MeOH eluates (Me) were dried under a constant air stream.

Supplementary data

Table S1. Base diets (% as fed) manufactured by Research Diet Services B.V. (Wijk bij Duurstede, the Netherlands). The data were previously reported elsewhere (1).

Ingredient (%)	Diet		
	Starter	**Grower**	**Finisher**
Wheat	49.4	58.8	65.9
Soybean Meal 48CP[1]	24.4	19.5	17.0
Toasted Soybeans	10.0	10.0	8.0
Soybean Oil	1.4	2.4	4.3
Monocalcium phosphate	1.4	1.3	1.0
Limestone	1.4	1.3	1.1
DL-Methionine	0.4	0.3	0.2
L-Lysine HCl	0.3	0.3	0.3
Salt	0.2	0.2	0.3
Na-Bicarbonate	0.3	0.3	0.2
L-Threonine	0.2	0.1	0.1
L-Valine	0.1	0.1	0.1
Coccidiostat	Sacox[2]	Sacox	-
Premix Article[3]	0.5	0.5	0.5
Diamol[4]	-	-	1.0
Total	100.0	100.0	100.0

[1]CP: Crude protein. [2]Provided by Huvepharma NV, Berchem, Belgium. [3]Providing per kg of diet: vitamin A (retinyl acetate), 10000 IU; vitamin D_3 (cholecalciferol), 2500 IU; vitamin E (dl-α-tocopherol acetate), 50 mg; vitamin K_3 (menadione), 1.5 mg; vitamin B1 (thiamine), 2.0 mg; vitamin B_2 (riboflavin), 7.5 mg; niacin, 35 mg; D-pantothenic acid, 12 mg; vitamin B_6 (pyridoxine-HCl), 3.5 mg; vitamin B_{12} (cyanocobalamine), 20 µg; folic acid, 1.0 mg; biotin, 0.2 mg; choline chloride, 460 mg; Fe ($FeSO_4.H_2O$), 80 mg; Cu ($CuSO_4.5H_2O$), 12 mg; Zn (ZnO), 60 mg; Mn (MnO), 85; I ($Ca(IO_3)_2$), 0.8 mg; Co ($Co_2CO_3(OH)_2$), 0.77 mg; Se (Na_2O_3Se), 0.15 mg. [4]Used as acid insoluble ash (AIA) digestibility marker (Franz Bertram GmbH, Hamburg, Germany).

Table S2. Chemical composition (w/w % dry matter basis) of diets. The data were previously determined and are reported elsewhere (1). Values are mean values of Control and Enzyme diets.

Chemical composition (%)	Finisher diet
Crude protein (N x 6.25)	20.5
Total carbohydrates[1]	61.3
Starch[2]	40.4
NSP[3]	21.0
Glc	51.6
Ara	2.1
Xyl	2.9
Gal	2.2
Man	0.6
UA	1.9
Fru	ND[4]
Fuc	0.1
Man	<0.1
Enzymatic activities (Enzyme diet)	
Xylanase (EPU[5]/kg feed)	1550
Cellulase (CU[6]/kg feed)	240

[1]Determined according to Englyst and Cummings (1984) (2). [2]Determined according to AOAC Method 996.11 (KOH format). [3]NSP: non-starch polysaccharides; calculated as the difference between Total Carbohydrates and Starch. [4]Not determined. [5]Amount of enzyme which releases 0.0083 µmol of reducing sugars (xylose equivalent) per minute from oat spelt xylan at pH 4.7 and 50 °C. [6]Amount of enzyme which releases 0.128 µmol of reducing sugars (glucose equivalents) per minute from barley β-glucan at pH 4.5 and 30 °C.

Table S3. Arabinoxylan (AX) recovery, expressed as percentage (%) of total ingested AX, estimated with acid insoluble ash as digestibility marker. The values have been reported previously (1) and are now recalculated for $n = 3$.

	AX recovery (% ingested AX)	
	Ileum	**Excreta**
Con	106.1	84.3
Enz	100.9	75.4
SEM[1]	2.2	5.4
***p* value**	0.056	0.178

[1]Standard error of the mean for $n = 3$.

Table S4. Dry matter yield (% w/w) of total, water-extractable (WES) and water-unextractable solids (WUS) during aqueous extraction of samples from the broiler gizzard, ileum, ceca and excreta (± SD, n = 3). Aqueous extraction of finisher diets was performed as described in 2.2.

	Dry matter yield (%)		
	Total solids	**WES**	**WUS**
Diet			
Con	90.3	17.5	72.8
	(0.4)	*(0.8)*	*(1.0)*
Enz	88.7	17.4	71.2
	(0.6)	*(0.6)*	*(0.9)*
Gizzard			
Con	96.9	36.4	60.5
	(3.8)	*(4.6)*	*(2.2)*
Enz	97.1	34.9	62.2
	(0.5)	*(0.3)*	*(0.8)*
Ileum			
Con	96.6	37.6	59.0
	(0.8)	*(3.1)*	*(2.4)*
Enz	97.9	39.0	58.9
	(0.9)	*(1.6)*	*(1.1)*
Ceca			
Con	100.8	48.5	52.3
	(4.5)	*(5.6)*	*(6.0)*
Enz	95.2	46.2	49.0
	(0.7)	*(6.2)*	*(6.0)*
Excreta			
Con	94.1	33.5	61.8
	(0.8)	*(2.1)*	*(1.4)*
Enz	95.9	32.3	62.4
	(1.2)	*(1.7)*	*(0.4)*

5

Table S5. Constituent neutral monosaccharide composition and total carbohydrate content (% w/w) of water-unextractable solids (WUS) in the gizzard, ileum, ceca and excreta, after acid hydrolysis. Standard deviations (n = 3) are shown in parentheses.

	Constituent monosaccharide composition (mol%)								Carb. content (% w/w)
	Ara	**Xyl**	**Glc**	**Gal**	**Man**	**Fuc**	**Rha**	**UA**	
Gizzard									
Con	13.8	22.0	48.8	6.0	2.6	0.5	0.8	5.5	55.3
	(2.2)	(6.7)	(10.3)	(0.2)	(0.9)	(0.0)	(0.1)	(0.5)	(3.2)
Enz	15.6	27.4	39.1	6.8	3.0	0.6	0.9	6.6	48.7
	(1.0)	(2.5)	(3.6)	(0.8)	(0.4)	(0.1)	(0.1)	(0.5)	(1.9)
Ileum									
Con	20.4	28.3	28.1	10.7	2.3	1.1	1.1	8.1	50.4
	(0.8)	(0.6)	(2.6)	(1.1)	(0.2)	(0.1)	(0.1)	(0.8)	(1.6)
Enz	21.3	26.4	24.5	12.9	2.7	1.3	1.1	9.8	48.0
	(0.3)	(1.7)	(0.5)	(0.9)	(0.0)	(0.1)	(0.0)	(0.4)	(1.0)
Ceca									
Con	2.9	9.1	47.2	14.6	1.8	1.2	15.6	7.6	12.3
	(0.4)	(3.5)	(6.2)	(1.3)	(0.4)	(0.2)	(0.8)	(0.1)	(0.9)
Enz	1.7	1.8	53.4	15.6	1.9	1.4	17.5	6.7	12.3
	(0.5)	(0.8)	(6.4)	(2.5)	(0.7)	(0.1)	(1.0)	(1.6)	(2.9)
Excreta									
Con	19.0	24.8	32.8	11.1	2.1	1.2	1.2	7.8	51.8
	(0.8)	(0.7)	(3.2)	(1.1)	(0.2)	(0.1)	(0.1)	(1.0)	(3.9)
Enz	19.6	24.5	29.0	12.7	2.4	1.4	1.3	9.2	44.5
	(1.3)	(1.0)	(4.1)	(1.2)	(0.1)	(0.1)	(0.1)	(0.5)	(1.9)

Table S6. Standard deviations (n = 3) for Table 1: Constituent neutral monosaccharide composition and total carbohydrate content (% w/w) of water-extractable solids (WES) in the gizzard, ileum, ceca and excreta, after acid or enzymatic (FRM) hydrolysis.

	Standard deviations (Table 1)								
	Ara	**Xyl**	**Glc**	**Fru**	**Gal**	**Man**	**Fuc**	**Rha**	**Total**
Gizzard									
Con	0.8	0.8	1.3	0.9	0.1	0.2	0.0	0.0	5.8
Enz	0.4	0.4	0.3	0.2	0.6	0.1	0.1	0.0	2.8
Ileum									
Con	0.9	0.9	6.8	3.6	2.1	0.4	0.0	0.0	3.5
Enz	1.1	1.7	3.1	1.3	1.5	0.1	0.2	0.0	3.2
Ceca									
Con	0.8	3.7	9.8	1.7	2.7	0.8	0.5	2.1	2.6
Enz	0.9	2.7	7.5	0.4	2.5	1.2	0.2	1.1	2.2
Excreta									
Con	1.5	1.1	8.7	3.0	2.4	0.6	0.3	0.0	1.5
Enz	1.5	0.7	7.2	2.5	2.2	0.2	0.2	0.0	1.8

Table S7. Total arabinoxylan (AX: sum of Ara and Xyl) and water-extractable (WE-AX) and water-unextractable (WU-AX) recovery during aqueous extraction recovery, expressed as percentage (%) of AX present in the finisher diet. Aqueous extraction was performed as described in 2.2.

	Arabinoxylan (AX) recovery (% AX in Diet)		
	Total	WE-AX[3]	WU-AX[3]
Con	90.5	14.0	86.0
Enz	92.8	15.1	84.9
SEM[1]	-	0.7	0.7
***p* value[2]**	-	0.335	0.335

[1]Standard error of the mean for *n* = 3. [2]Estimated by One-way ANOVA.[3]Estimated using Eq. 1. (see 2.11)

Table S8. Model-adjusted *p*-values, representing the effect of Diet (D; Con, Enz), Fraction (F_{aq}; WES, WUS) and their interaction term (D x F_{aq}) on AX recovery (Table 2), obtained by two-way analysis of variance. The significance threshold was set at *p* < 0.05.

	SEM[1]	Model-adjusted *p*-values (Table 2)		
		Diet	Fraction	D x F_{aq}
Gizzard	0.73	1.0	<0.001	0.08
Ceca	4.47	1.0	0.106	<0.001

[1]Standard error of the mean for *n* = 3.

Table S9. Model-adjusted *p* values, representing the effect of Diet (D; Con, Enz), Fraction (F_{aq}; WES, WUS) and their interaction term (D x F_{aq}) on Ara/Xyl ratio (Table 3), obtained by two-way analysis of variance. The significance threshold was set at *p* < 0.05.

	SEM[1]	Model-adjusted *p*-values (Table 3)		
		Diet	Fraction	D x F_{aq}
Gizzard	0.05	0.649	0.001	0.295
Ileum	0.02	0.898	0.027	0.004
Ceca*	0.04 (0.05)	0.001	0.000	0.010
Excreta	0.02	0.521	0.021	0.180

[1]Standard error of the mean for *n* = 3. *Adjusted SEM value for *n* = 2 (WE-AX; Con, WU-AX; Enz) is shown between brackets.
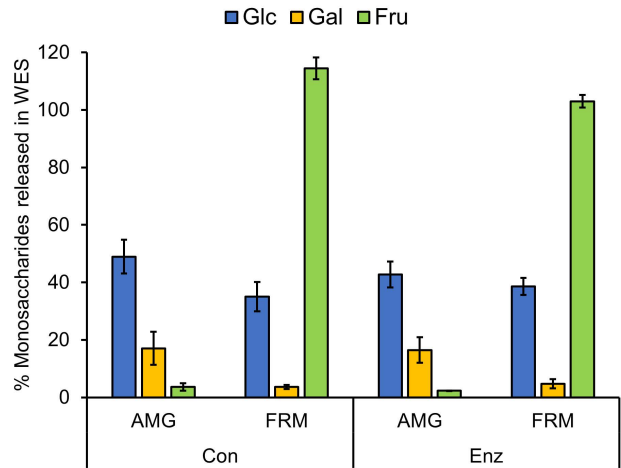
Fig. S1. Glc (■), Gal(■) and Fru (■) released by AMG and FRM individually, expressed as proportion of the corresponding total constituent monosaccharides present in WES from ileal digesta.
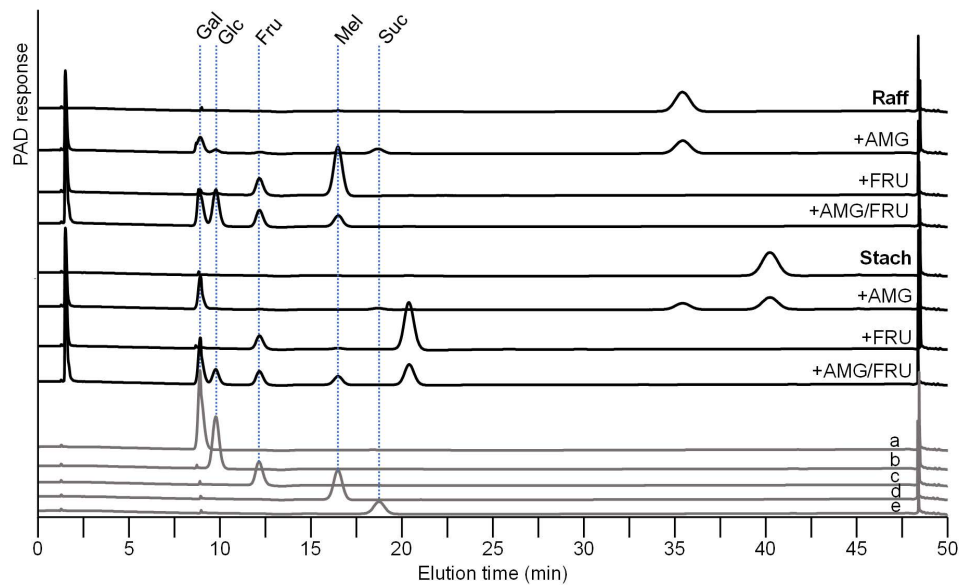
Fig. S2. HPAEC-PAD chromatograms of raffinose (Raff) and stachyose (Stach) without or with treatment by amyloglucosidase (AMG), fructanase (FRU) and AMG/FRU combination (see supplement; p. 150); peak labelling was according to analytical standards: Galactose (Gal; **a**), glucose (Glc; **b**), fructose (Fru; **c**), melibiose (Mel; **d**) and sucrose (Suc; **e**). The peak eluting before 5 min corresponds to salts from the enzyme preparations.

Table S10. Model-adjusted *p* values, representing the effect of Diet (D; Con, Enz), SPE fraction (F_{SPE}; W, M) and their interaction term (D x F_{SPE}) on NSP constituent (Ara, Xyl, Glc, Gal) recovery during SPE (Fig. 3; S4), obtained by two-way analysis of variance. Observations for gizzard, ileum, ceca and excreta were modelled separately. The significance threshold was set at *p* < 0.05.

	Diet (D)	F_{SPE}	D x F_{SPE}
Gizzard			
Ara	0.062	<0.001	0.090
Xyl	<0.001	<0.001	<0.001
Glc	0.233	<0.001	0.593
Gal	0.688	0.039	0.336
Ileum			
Ara	0.001	<0.001	0.003
Xyl	<0.001	<0.001	<0.001
Glc	0.867	<0.001	0.243
Gal	0.559	<0.001	0.974
Ceca			
Ara	0.061	0.192	0.141
Xyl	0.190	0.007	0.319
Glc	0.621	<0.001	0.142
Gal	0.239	<0.001	0.016
Excreta			
Ara	0.068	<0.001	0.351
Xyl	0.018	<0.001	0.149
Glc	0.005	<0.001	0.649
Gal	0.421	0.978	0.152

5
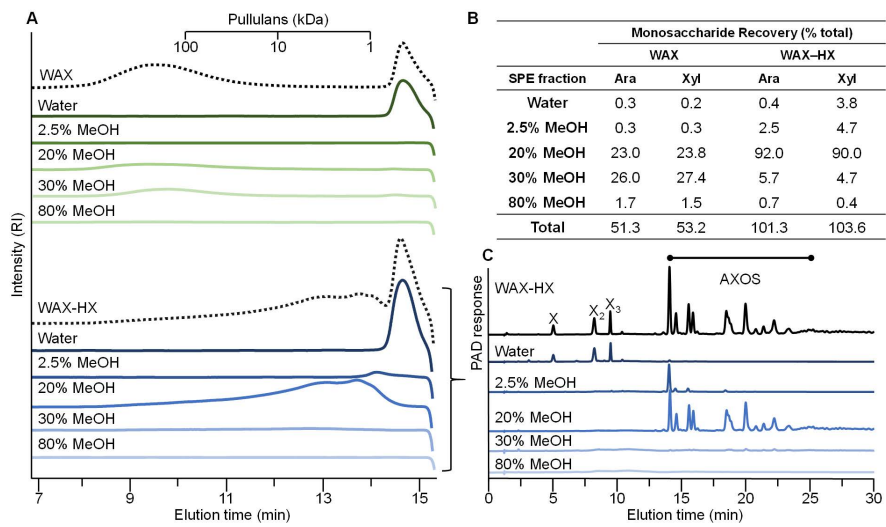
Fig. S3. HPSEC-RI chromatograms (**A**) of reference WAX polymer and xylanase-treated WAX (WAX–HX) (see supplement; p. 150) and the SPE fractions thereof obtained by elution with water, 2.5% MeOH, 20% MeOH, 30% MeOH and 80% MeOH; Pullulans were used as calibrants; Arabinose (Ara) and xylose (Xyl) recovery (% total) during SPE (**B**); HPAEC-PAD chromatograms (**C**) of WAX+HX and SPE fractions thereof eluting with water, 2.5% MeOH, 20% MeOH, 30% MeOH and 80% MeOH; X: xylose, X_2: xylobiose, X_3: xylotriose were identified based on analytical standards. SPE was performed as described in supplement p. 151.
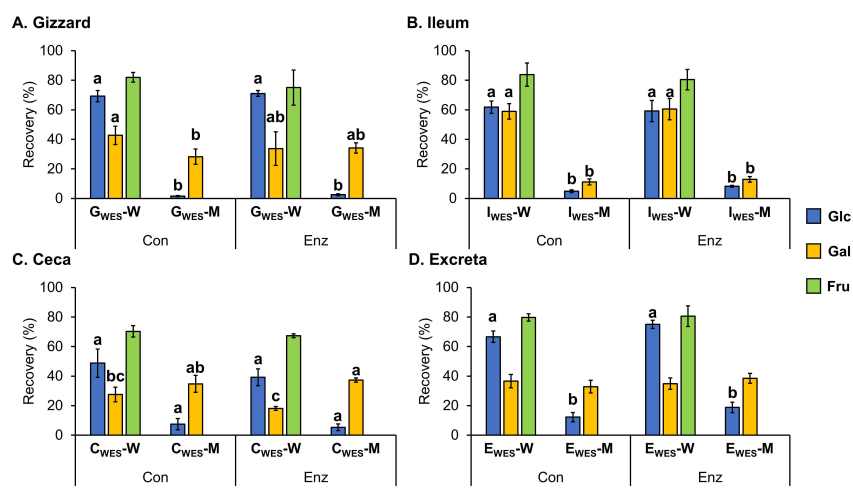
Fig. S4. Constituent glucosyl (Glc: ■), galactosyl (Gal: ■) and fructosyl (Fru: ■) recovery (%) in the water (W) and 30% (v/v) MeOH (M) fractions, after SPE of AMG/FRM-treated WES from the gizzard (A: G_{WES}), ileum (B: I_{WES}), ceca (C: C_{WES}) and excreta (D: E_{WES}); Bars representing either Glc or Gal not sharing common notation differ significantly ($p < 0.05$). The error bars indicate standard deviation. The ANOVA

results are given in Table S10. Fru recovery was determined only in W and not in M fractions, and therefore excluded from statistical analysis.
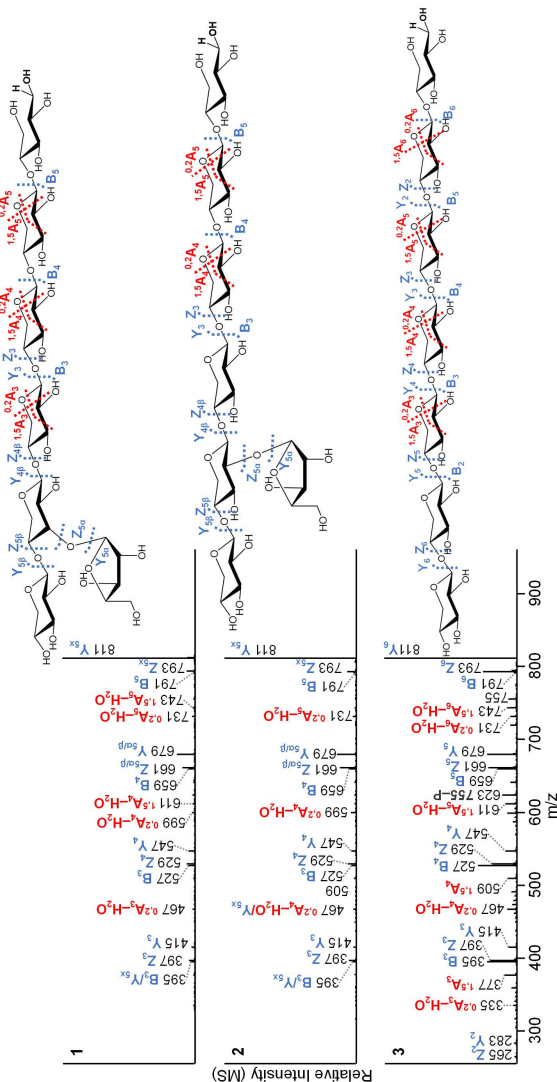
Fig. S5. Negative ion mode CID-MS^2 spectra of *m/z* 943 XA^{3}XXXX (**1**), XA^{2}XXXX (**2**) and xyloheptaose (X$_7$) (**3**); average spectra across the most abundant chromatographic peaks (Fig. 5); The fragments are annotated according to Domon & Costello (1988) and Kouzounis et al. (2022) (3-4); Blue: glycosidic fragments; Red: cross-ring fragments; /: double cleavage; x: α or β antennae. The lower intensity of Z$_{5x}$ relatively to Y$_{5x}$ for 1 and 2, in comparison to X$_7$, suggested the presence of Ara in the vicinity of the non-reducing end for the former structures. Determination of the Ara substituent location and linkage type required subsequent MS^3 experiments of Y$_{5x}$ and Y$_4$ (**Fig. S6**) and B$_3$ (**Fig. S7**) fragment ions. The MS^3 spectra of Y$_6$, Y$_5$ and B$_4$ fragment ions for X$_7$ are shown for comparison.
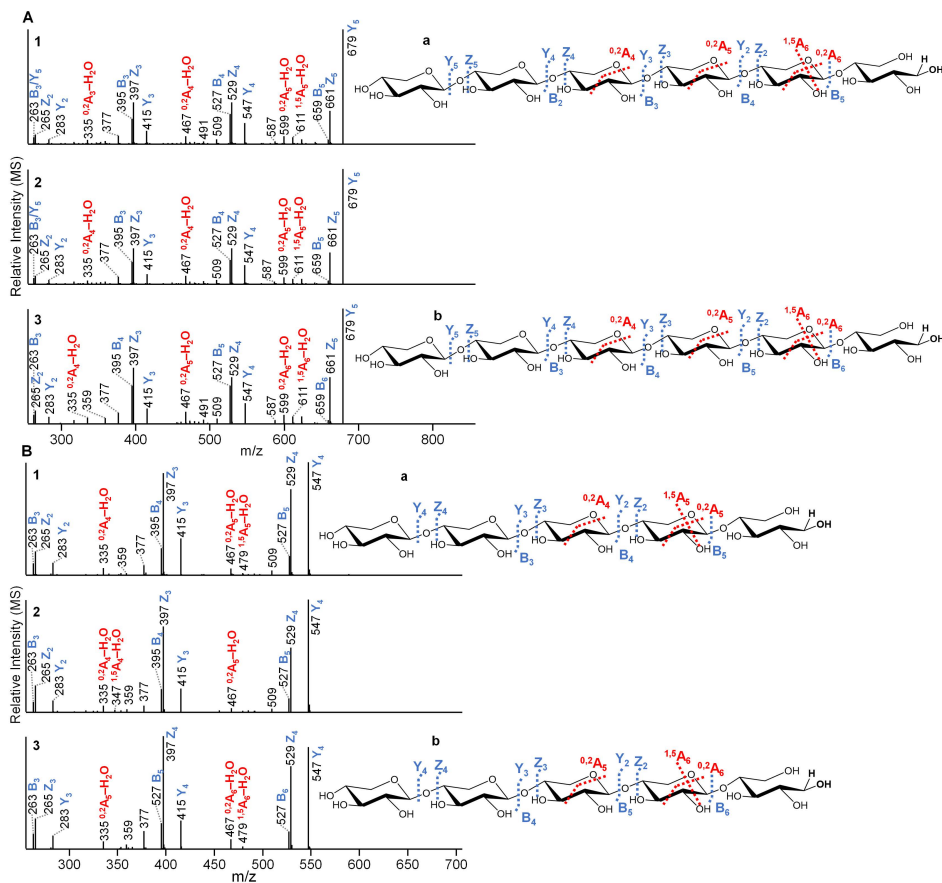
Fig. S6. Negative ion mode CID-MS^3 spectra of *m/z* 943→811 (**A**), *m/z* 943→679 (**B**) corresponding to XA^{3}XXXX (**1**), XA^{2}XXXX (**2**) and X$_7$ (**3**) (MS^2; see **Fig. S5**); The fragments are annotated according to Domon & Costello (1988) and Kouzounis et al. (2022) (3-4); Blue: glycosidic fragments; Red: cross-ring fragments; /: double cleavage; x: α or β antennae; Structure a corresponds to XA^{3}XXXX and XA^{2}XXXX, and b to X$_7$. The overall similar spectra for AXOS and X$_7$ were due to the loss of Ara during MS^3, indicating that it was attached to the penultimate Xyl residue from the non-reducing end.

5
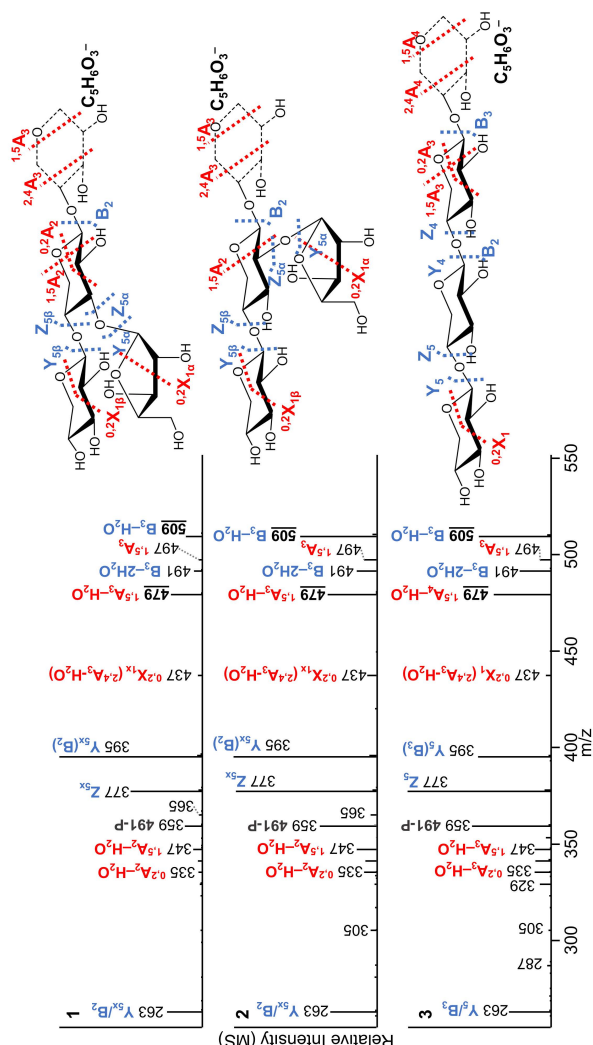
Fig. S7. Negative ion mode CID-MS³ spectra of *m/z* 943→527 corresponding to XA³XXXX (**1**), XA²XXXX (**2**) and X₇ (**3**) (MS²; see **Fig. S5**); The fragments are annotated according to Domon & Costello (1988) and Kouzounis et al. (2022) (3-4); Blue: glycosidic fragments; Red: cross-ring fragments; /: double cleavage; x: α or β antennae, P: pentose unit (m/z 132); Alternative fragmentation pathways are presented in brackets. The higher $^{1,5}A_x–H_2O$: $B_x–H_2O$ ion ratio (*m/z* 479:509) observed for **1**, compared to X₇, was characteristic for *O*-3-linked Ara, while the similar ion ratio to X₇ observed for **2**, was characteristic for *O*-2-linked Ara (4). Hence, **1** was identified as XA³XXXX and **2** as XA²XXXX. The precise structure of the newly formed end of B fragment ions is unknown as it may undergo several rearrangements (dashed ring), hence corresponding MS³-ring-fragments have been annotated tentatively.

Supplementary information references

1. Kouzounis D, Hageman JA, Soares N, Michiels J, Schols HA. Impact of xylanase and glucanase on oligosaccharide formation, carbohydrate fermentation patterns, and nutrient utilization in the gastrointestinal tract of broilers. Animals. 2021;11(5):1285.

2. Englyst HN, Cummings JH. Simplified method for the measurement of total non-starch polysaccharides by gas-liquid chromatography of constituent sugars as alditol acetates. Analyst. 1984;109(7):937.

3. Domon B, Costello CE. A systematic nomenclature for carbohydrate fragmentations in FAB-MS/MS spectra of glycoconjugates. Glycoconj J. 1988;5(4):397–409.

4. Kouzounis D, Sun P, Bakx EJ, Schols HA, Kabel MA. Strategy to identify reduced arabinoxylo-oligosaccharides by HILIC-MS^n. Carbohydr Polym. 2022;119415.

Chapter

6

The fate of insoluble arabinoxylan and lignin in broilers: Influence of cereal type and dietary enzymes
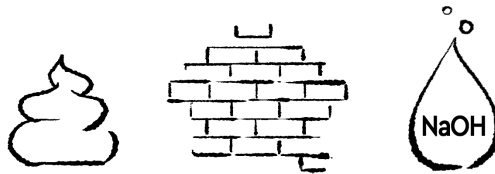
Kouzounis D., van Erven G., Soares N., Kabel. M. A., Schols H. A.

(submitted for publication)

Abstract

Insoluble fiber degradation by supplemented enzymes was previously shown to improve fermentation in broilers. The aim of this study was to further characterize feed fiber components and insoluble polysaccharide structures in broiler digesta from the gizzard, ileum, ceca and excreta of broilers fed wheat-soybean and maize-soybean diets without or with xylanase/glucanase supplementation. Enzyme supplementation in wheat-soybean diet increased the yield of water extractable arabinoxylan (AX) in the ileum. Still, most AX (> 73%) remained insoluble across wheat-soybean and maize-soybean diets. Next, analysis of so far largely ignored lignin demonstrated that a lignin-rich fiber fraction accumulated in the gizzard, while both insoluble AX and lignin reaching the ileum appeared to be excreted unfermented. More than 20% of water insoluble AX was extracted by 1 M NaOH and 11-20% was sequentially extracted by 4 M NaOH, alongside other hemicelluloses, across all diets. The hypothesis that enzyme-mediated release of water soluble AX-oligosaccharides (AXOS) further influenced the interaction of insoluble cell wall polymers was not accompanied by improvements in AX extractability by alkali. Additional research on the interactions between insoluble cell wall components is warranted to further increase NSP degradation by dietary enzymes *in vivo*.

1   Introduction

Cereal grains are integral feedstocks for poultry, as they provide birds with energy in the form of starch (1). Additionally, wheat and maize grains contain 13 and 10% (w/w) fiber, respectively (1). Fiber is a broad term that collectively describes feed-derived, indigestible and chemically distinct biomolecules, such as carbohydrates (polysaccharides and oligo-saccharides) and the alkyl-aromatic polymer lignin, whose influence in livestock health and growth is still under investigation (1,2). Arabinoxylan (AX) is the major non-starch polysaccharide (NSP) in wheat and maize grains (5-7% w/w DM), followed by β-glucan (0.1-1.0% w/w DM) and cellulose (2% w/w DM) (1,3). AX is composed of a β-(1→4)-linked D-xylosyl (Xyl) backbone, mainly substituted by L-arabinofuranosyl (Ara) units at the O-2- and/or O-3-positions of the Xyl units. 4-O-D-methyl-glucuronoyl and acetyl moieties comprise additional substituents, while Ara units might be further O-5-substituted with feruloyl units (4,5). Maize AX is more heavily substituted than wheat AX (1,6–8). AX is the main component of endosperm and aleurone cell walls (CW) in wheat. In contrast, the more rigid pericarp cell walls mainly consist of AX, cellulose, lignin and to a lesser extent protein (9). For example, lignin present in bran from wheat and maize is mainly composed of syringyl (S) and guaiacyl (G) units, and Klason lignin contents, amount to 5-7% and 1-3% (w/w) of bran DM respectively (1,6,10,11).

Based on their chemical and macromolecular structure, AX molecules may associate with each other and with other cell wall polymers. For example, AX can associate by hydrogen bonding with cellulose fibrils, while it can form covalent cross-links with other AX and lignin molecules via ferulate and dehydrodiferulate cross-links (12). Therefore, AX plays an important role in tethering the cell wall matrix, providing the cells with structural integrity (9,12,13). Characterization of water-insoluble polysaccharides typically requires their extraction from the CW matrix. In particular, alkali solutions (e.g., 0.5-6 M NaOH) have been widely applied to extract pectin, heteroxylans and xyloglucan from plant material, while cellulose remains insoluble (5,8,14–19). In the presence of alkali, the hydrogen bonds between hemicellulose and cellulose are known to be disrupted. Additionally, if present, alkali-labile ester cross-links between cell wall polymers are cleaved, thus solubilizing water-unextractable AX (8,20,21).

Both soluble and insoluble NSP can increase digesta viscosity and compromise nutrient digestion in the small intestine (22,23). Soluble polysaccharides can contribute to broiler health by stimulating short chain fatty acids formation and beneficial microbiota growth in the ceca (24,25). On the contrary, insoluble CW structures have been postulated to form a physical barrier, encapsulating nutrients (e.g., starch and proteins) and consequently limiting their digestion (26,27). Moreover, the dominant (insoluble) NSP fraction (>70% w/w) remains associated within the CW and is largely excreted by broilers unutilized (28–30). Dietary inclusion of NSP-degrading enzymes, predominantly xylanases, is widely

performed to improve broiler performance (30–33). Dietary xylanases have been found to degrade both soluble and insoluble AX in the GIT of broilers and pigs (34,35), and to release arabinoxylan oligosaccharides (AXOS) *in vivo* (30,36). AX depolymerization has been associated with decreased intestinal viscosity, improved nutrient digestion and NSP fermentation in the ceca (30,35–38). In addition, xylanase and β-glucanase have been associated with rupturing of the cell wall and nutrient release from cereal *in vitro* (39–41). From this perspective, CW degradation by enzymes has been hypothesized to alleviate the encapsulating effect of insoluble NSP, and to positively contribute to nutrient digestion (27,42). Nevertheless, limited studies have focused on CW degradation *in vivo* by different dietary enzymes, as well as on the fate of insoluble CW components during feed digestion (28,43).

Although alkaline extraction has been widely used to extract polysaccharides from plant material, it has rarely been applied to characterize the fate of insoluble NSP throughout the broiler gastro-intestinal tract (GIT). One exception is the study of Pustjens and coworkers (28), who extracted broiler excreta with 6 M NaOH solution in order to characterize unfermented NSP. That study primarily focused on characterizing pectin from rapeseed meal, and not cereal AX. Therefore, the fate and structure of insoluble cereal cell wall components present in the broiler GIT still remains poorly understood.

The present study aimed to investigate the amount and composition of insoluble cell wall components along the broiler GIT. Furthermore, insoluble NSP structure from wheat-based or maize-based diets, as well as the potential impact of enzyme supplementation on NSP structure and extractability was investigated in detail. We hypothesized that the ratio between arabinoxylan and lignin content would provide further insight on the composition of insoluble fiber through the broiler gut. It was also investigated whether enzyme supplementation could change the interaction of insoluble CW polymers, and consequently alter AX extractability by alkali compared to the control treatment.

2 Materials and methods

All reagents used were of analytical grade and supplied by Sigma Aldrich (St. Louis, MO, USA), Merck KGaA (Darmstadt, Germany) or VWR International B.V. (Amsterdam, The Netherlands), unless stated otherwise. The water used throughout laboratory experiments was purified with a Milli-Q Integral 5 (Millipore Corp., Billerica, MN, USA) purification system.

2.1 Samples from broiler GIT

Broiler digesta were obtained from our recent study, described in Chapter 2 (30). The animal study was conducted in accordance with the ethical standards and recommendations for accommodation and care of laboratory animals covered by the European Directive 2010/63/EU on the protection of animals used for scientific purposes and the Belgian royal decree KB29.05.13 on the use of animals for

experimental studies. In brief, 96 one-day old male broilers were fed either wheat-soybean (W) or maize-soybean (M) starter and grower diets (Table S1). On d 20, the birds were allocated to pens and were assigned to control or enzyme treatments following a randomized block design. Each dietary treatment consisted of 6 replicate pens, with 4 birds per pen. The finisher diets were provided as such (control: WC, MC) or supplemented with a commercially available enzyme preparation (enzyme: WE, ME) of GH11 endo-1,4-β-xylanase (EC 3.2.1.8) and endo-1,4-β-glucanase (EC 3.2.1.4) from *Trichoderma spp.* (Huvepharma NV, Berchem, Belgium) (Table S1). The excreta were collected per pen, daily (twice) between d 24 and 28 and immediately stored at -20°C. On d 28, birds were euthanized, and the gizzard, ileum and ceca contents were collected, pooled per pen, and frozen at -20°C. Frozen material was dried by lyophilization and homogenized with a MM 400 Mixer Mill (Retsch GmbH, Haan, Germany) prior to analysis. Three out of six replicate pens were randomly selected, and digesta samples originating from these three pens were used for the current study, as previously described (Chapter 5 (36)).

2.2 Aqueous extraction of digesta

Aqueous extraction of digesta was performed as described in Chapter 5 (36). In brief 1 g digesta and finisher feed was dispersed in 35 mL water heated at 99 °C and was incubated at 99 °C for 20 min under head-over-tail rotation. Next, the supernatant was separated by centrifugation (30,000 x g, 20 min, 20 °C), followed by filtration over 595 Whatman® filter paper. The residue was further washed with 30 mL water and the obtained supernatant was separated as described above. The washing step was repeated once and all resulting supernatants were combined. Supernatants (water-extractable solids; WES) and residues (water-unextractable solids; WUS) from the feed (Feed), gizzard (Giz), ileum (Ile), ceca (Cec) and excreta (Exc) were freeze-dried, and their dry weight was recorded.

2.3 Sequential alkali extraction of digesta water-unextractable solids

WUS from ileal digesta (WUS_{Ile}) and from excreta (WUS_{Exc}) were sequentially extracted with alkali solution (1 M NaOH and 4 M NaOH), as described by Murciano-Martínez and coworkers (2016) (18), with several modifications. A schematic overview of the extraction is presented in Fig. 1, including all fractions obtained. Approximately 100 mg WUS was extracted with 12 mL 1 M NaOH solution containing 260 mM $NaBH_4$ at ambient temperature for 2 h. The supernatant was separated by centrifugation (4,000 x g, 15 min, 20 °C). The procedure was repeated once. Corresponding extracts were combined, placed in an ice bath and their pH value was adjusted pH 5.0 by the addition of glacial acetic acid. The acidified pooled extract (1 M alkali soluble solids; 1M-ASS) was stored at 4 °C. The remaining residue was further extracted with 12 mL 4 M NaOH solution (+260 mM $NaBH_4$) at room temperature for 16 h. The 4 M NaOH extract was collected after centrifugation (4,000 x g, 15 min, 20 °C). Next, 12 mL water was added to the

residue, the mixture was thoroughly vortexed and the supernatant (water wash) was separated from the residue by centrifugation (4,000 x g, 15 min, 20 ˚C). The 4 M NaOH and water wash fractions were combined (4 M alkali soluble solids; 4M-ASS), acidified at pH 5.0 and stored at 4 °C. The final residue (RES) was suspended in water, acidified to pH 5.0, washed twice with 10 mL water, stored at -20 °C, and freeze-dried.
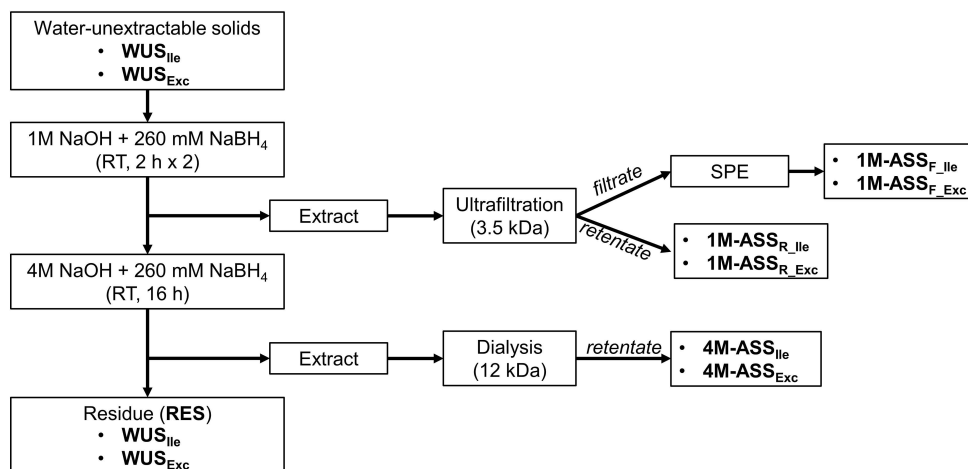
Fig. 1. Schematic overview of sequential alkali extraction of water-unextractable solids from the ileum (WUS_{Ile}) and excreta (WUS_{Exc}). The retentate (> 3.5 kDa) from ultrafiltration of the 1 M NaOH extract was labelled $1M\text{-}ASS_R$ and the filtrate after further desalting by SPE was labelled $1M\text{-}ASS_F$. The retentate obtained from dialysis of the 4 M NaOH extract was labelled 4M-ASS. The alkali-unextractable residue was labelled RES.

The 1M-ASS fractions were extensively desalted with regenerated cellulose centrifugal filter units (molecular weight cut-off (MWCO): 3.5kDa) (Amicon® Ultra-15: MilliporeSigma, Burlington, MA, USA), until the conductivity value of the retentate was at least tenfold lower than that of 50 mM sodium acetate (NaOAc) buffer solution (pH 5.0). The retentates (labelled: $1M\text{-}ASS_R$) were collected in pre-weighed containers and freeze-dried. The filtrates were further subjected to solid-phase extraction (SPE) to separate oligosaccharides below 3.5 kDa from salts. To achieve that, the filtrates were quantitatively loaded on 500 mg Supelclean™ ENVI-Carb™ solid-phase extraction (SPE) cartridges (Supelco Inc., Bellefonte, PA, USA), pre-conditioned with 10 mL 80% (v/v) acetonitrile (ACN) containing 0.1% (v/v) trifluoroacetic acid (TFA) and washed with 10 mL water. Next, the retained analytes were eluted twice with 5 mL 40% (v/v) ACN solution containing 0.1% (v/v) TFA. Analytes eluting with 40% (v/v) ACN (+0.1% (v/v) TFA) solution (labelled: $1M\text{-}ASS_F$) were collected in pre-weighed glass tubes, and were dried with a sample concentrator. The 4M-ASS fractions were desalted by dialysis against distilled water, using Visking dialysis membranes (12 kDa MWCO for proteins; Medicell Membranes Ltd., London, UK). The dialyzed material was transferred in pre-

weighed containers, and was freeze-dried (labelled: 4M-ASS). Freeze dried materials were used for subsequent analyses.

2.4 Dry and organic matter yield determination during sequential alkali extraction

The total solids obtained in 1M-ASS$_R$, 1M-ASS$_F$, 4M-ASS and RES during alkali extraction were determined gravimetrically, after drying. Next, the organic matter (OM) was determined to account for residual salts present. Approximately 1-2 mg sample was weighed using an XP6 Excellence Plus Micro Balance (5 decimals) (Mettler-Toledo International Inc., Columbus, OH, USA) in Eco-Cup LF pyrolysis cups (Frontier Laboratories Ltd., Fukushima, Japan), followed by incineration at 550 °C, overnight. The ash content was determined gravimetrically, and the organic matter (OM) content was estimated as the difference between total solids and ash content. OM determination was not feasible for 1M-ASS$_F$ due to the low sample amounts recovered. In this case, the dry matter content of 1M-ASS$_F$ was assumed to equal OM content, given the complete salt removal by SPE.

2.5 Lignin content analysis

The lignin content and structural composition in WUS was determined by quantitative pyrolysis-GC-MS according to van Erven et al. (2019) (44). ^{13}C-labelled lignin isolated from uniformly ^{13}C-labelled wheat straw (97.7%, IsoLife, Wageningen, the Netherlands) was used as internal standard (^{13}C-IS) (45). In brief, 100-200 µg sample was weighed in Eco-Cup LF pyrolysis cups with an XP6 Excellence Plus Micro Balance in duplicate, followed by the addition of 10 µL 1 µg/µL ^{13}C-IS solution (50/50% v/v chloroform/ethanol). Pyrolysis, GC and MS settings were identical as previously described (44). Processing excluded low-abundance lignin-derived pyrolysis products and *p*-hydroxyphenyl products from the samples (^{12}C only, Table S2), the latter also substantially derived from aromatic amino acids as deduced from the semi-quantification of the protein marker indole. Lignin content calculations also excluded the pyrolysis product 4-vinylguaicol, largely derived from ferulic acid and not necessarily incorporated into the lignin macromolecule (44).

2.6 Monosaccharide composition and content analysis

For WUS and RES samples (Fig. 1), neutral constituent monosaccharide analysis was performed according to Englyst and Cummings (46). Samples were pre-hydrolyzed in 72% (w/w) H_2SO_4 (30 °C, 1 h) and subsequently hydrolyzed in 1 M H_2SO_4 (100 °C, 3 h). The neutral monosaccharides released were derivatized to alditol acetates and analyzed by gas chromatography on a Trace 1300 GC system (Thermo Fisher Scientific Inc.) equipped with a DB-225 column (Agilent Technologies Inc., Santa Clara, CA, USA) and a flame/ionization detector (FID), using inositol as internal standard. Uronic acid content was determined by the colorimetric *m*-hydroxyphenyl assay with an automated analyzer (Skalar Analytical

B.V., Breda, The Netherlands), according to Blumenkrantz and Asboe-Hansen (1973) and Thibault and Robin (1975) (47,48).

For 1M-ASS$_R$ and 4M-ASS samples (Fig. 1), neutral constituent monosaccharide analysis was performed according to Broxterman & Schols (2018) (15). Following similar hydrolysis conditions as described above, samples were diluted 50 times and the neutral monosaccharides were determined by high performance anion exchange chromatography with pulsed amperometric detection (HPAEC-PAD). The analysis was performed using an ICS5000 ED ion chromatography system (Dionex Corp., Sunnyvale, CA, USA), equipped with a CarboPac^{TM} PA1 IC column (250 mm x 2 mm i.d.) and a CarboPac^{TM} PA guard column (50 mm x 2 mm i.d.). Three mobile phases were used: A) 0.1 M NaOH, B) 1 M NaOAc in 0.1 M NaOH and C) Water. The injection volume was 10 µL, and neutral monosaccharides were eluted at 0.4 mL/min with 100% C (isocratic) for 0–27 min, with post column addition of 0.5 M NaOH (0.1 mL/min) to enable PAD detection. The subsequent elution profile (v/v) was: 27.1-38 min linear gradient 10-17.3% B (90-82.7% A); 38.1-43 min isocratic 100% B, 43.1-51 min isocratic 100% A; 51.1-66 min isocratic 100% C with post column addition.

For 1M-ASS$_F$ samples (Fig. 1), the material obtained after SPE was dissolved in water at 5 mg/mL. Aliquots (50 µL) were transferred in glass tubes, and dried with a sample concentrator. Neutral constituent monosaccharide analysis was determined by TFA hydrolysis, according to de Ruiter et al. (1992) (49). In brief, 1 mL 2 M TFA solution was added, and the samples were hydrolyzed at 121 °C for 1 h. Next, TFA was removed by evaporation. The hydrolyzed samples were dissolved in 500 µL water and the neutral monosaccharides were determined by HPAEC-PAD as described above.

2.7   Molecular weight distribution analysis by HPSEC-RI

The molecular weight distribution of 1M-ASS$_F$, 1M-ASS$_R$ and 4M-ASS (see Fig. 1) was determined by high performance Size-Exclusion Chromatography using an Ultimate 3000 system (Dionex, Sunnyvale, CA, USA) coupled to an ERC Refractomax 520 detector (Biotech AB, Onsala, Sweden). A set of TSK-Gel super AW columns 4000, 3000, 2000 (6 mm × 150 mm) equipped with a TSK-Gel super AW guard column (6 mm ID × 40 mm) (Tosoh Bioscience, Tokyo, Japan) was used in series. The column temperature was set to 55 °C. Samples were injected (10 µl) and eluted with 0.2 M NaNO$_3$ at a flow rate of 0.6 mL/min. Prior to analysis, aliquots 1M-ASS$_R$ and 4M-ASS were dispersed at 5 mg/mL in 50 mM NaOAc (pH 5.0), heated at 80 °C for 30 min and centrifuged (15,000 x g, 10 min, 20 °C). The obtained supernatants were analyzed by HPSEC (injection volume 10 µL). For analysis of 1M-ASS$_F$ samples, aliquots of solutions (5 mg/mL) used for sugar composition analysis (see 2.6) were used.

2.8   Oligosaccharide profiling by MALDI-TOF-MS

The presence of oligosaccharides released by alkali was determined in 1M-ASS$_F$ by Matrix-Assisted Laser Desorption/Ionization Time-of-Flight Mass Spectrometry using an ultrafleXtremeTM MALDI-TOF/TOF mass spectrometer (Bruker Daltonics Inc., Billerica, MA, USA). The equipment was controlled with FlexControl 3.3 software and operated in positive mode. The mass spectrometer was calibrated with maltodextrins (Avebe, Veendam, The Netherlands) in a mass range of 700–2500 (*m/z*). 1M-ASS$_F$ solutions (5 mg/mL; see 2.6) were diluted ten times with water. WUS samples were also examined to account for the presence of residual water-soluble oligosaccharides. For that, 5 mg WUS was suspended in 1 mL water for 20 min, and the supernatant was separated by centrifugation (20,000 x g, 10 min, 20 ^{o}C). Aliquots (100 µL) were desalted with Dowex 50W-X8 resin (Sigma-Aldrich, St. Louis, MO, USA). After desalting, 10 µL was removed, followed by the addition of 1 µM NaCl to direct the formation of sodium adducts during ionization. Afterwards, 1 µL sample was co-crystallized with 1 µL matrix solution (25 mg/mL dihydroxy-benzoic acid in 50% (v/v) acetonitrile) on a target plate under a stream of dry air.

2.9   Calculations

The proportion of AX (sum of Ara and Xyl) in whole digesta from the gizzard, ileum, ceca and excreta that was recovered in WUS and WES was determined according to Eq. (1):

$$AX \text{ } in \text{ } WUS \text{ } (\% \text{ } w/w) = \frac{AX_{WU} \text{ } * \text{ } WUS \text{ } \%}{(AX_{WE} \text{ } * \text{ } WES \text{ } \%) \text{ } + \text{ } AX_{WU} \text{ } * \text{ } WUS \text{ } \%} * 100 \text{ } (1)$$

Where AX$_{WE,WU}$ is the measured AX content (% w/w dry matter) in WES or WUS of digesta from the gizzard, ileum, ceca and excreta. WES% and WUS% are the amount (% w/w dry matter) of WES and WUS out of total digesta. AX recovery in WES and glucan (Glc units) recovery in WUS and WES were determined in a similar manner.

2.10   Statistical analysis

The obtained data was subjected to analysis of variance (ANOVA) using R version 4.1.0, with pen being the experimental unit. The observations for WC, WE, MC and ME were used to model the effect of diet on arabinoxylan (AX) and glucan recovery and lignin content is WUS. The effect of diet (D) and GIT location (G: gizzard, ileum, ceca, excreta) as well as their two-way interaction on AX to Lignin weight ratio (AX/L) was also modelled. Finally, AX recovery during alkali extraction was modelled using diet as the sole factor. To test the significance of the differences between treatments, Tukey's post-hoc test was performed, with a significance threshold set at *p* < 0.05.

3   Results and discussion

3.1   Yield, content and composition of water-unextractable cell wall material

Insoluble carbohydrate content and recovery along the GIT

To understand the fate of insoluble fibers throughout the GIT of broilers, digesta from the gizzard, ileum, ceca and excreta were subjected to aqueous extraction (Fig. S1). More than 60% (w/w) of the total solids remained unextractable (WUS), while WES represented approximately 35-39% (w/w) of the total solids in the gizzard, ileum and excreta, demonstrating > 90% dry matter recovery, for both wheat and maize diets. On the contrary, WES and WUS demonstrated a comparable yield in the ceca (∼50% w/w of total dry matter), indicating the presence of equal amounts of soluble and insoluble components.

The monosaccharide composition and content in WUS was determined to further distinct the types of insoluble NSP present (Table S3). Glc was the main carbohydrate constituent in WUS from the gizzard (WUS$_{Giz}$: 39-57 mol %) and the ceca (WUS$_{Cec}$: 54-47 mol %) for all four diets. Insoluble Glc may be of diverse origin, representing undigested starch, particularly in the gizzard, as well as cellulose and β-glucan (1,17). Next to Glc, Ara (19-22 mol %) and Xyl (20-28 mol %) were highly abundant in WUS$_{Ile}$ and WUS$_{Exc}$, highlighting that AX was a major constituent of unfermented insoluble carbohydrates, for both wheat and maize diets. Although AX is the main NSP in both wheat and maize grains (1,3), a proportion of the Ara, Gal and UA analyzed in the WUS might still have derived from soybean meal in the diet (50). Finally, Man (< 3 mol %) and Fuc (traces; data not shown) were present at relatively low levels in all cases. Rha was present at ∼1 mol % in WUS$_{Giz}$, WUS$_{Ile}$ and WUS$_{Exc}$ but was more abundant in WUS$_{Cec}$ (16-19 mol %), across all diets, probably due to the presence of bacterial glycans (51).

The recovery of AX and glucans in WUS during aqueous extraction was determined according to Eq (1), as they were the main NSP present in all WUS fractions (Table S3). Water-unextractable AX recovered in WUS accounted for 90%, 82%, 44% and 90% (w/w) on average of total AX for the gizzard, ileum, ceca and excreta, respectively (Fig. 2). Water-unextractable glucans represented 53%, 60%, 41% and 82% (w/w) on average of total Glc units for the gizzard, ileum, ceca and excreta, respectively. It was observed that enzyme supplementation did not impact AX solubilization in ME and glucan solubilization in both WE and ME. The lower AX recovery in the WUS for WE compared to WC, mainly indicated in WUS$_{Ile}$, was attributed to AXOS release by xylanase, as covered in Chapter 5 (36). In contrast, similar recovery of Glc units in WUS$_{Ile}$ for WC and WE implied that glucanase did not release oligomers from insoluble glucans. The maize diets presented significantly higher AX recovery in WUS$_{Giz}$, WUS$_{Ile}$ and WUS$_{Exc}$ than the wheat diets ($p < 0.05$).
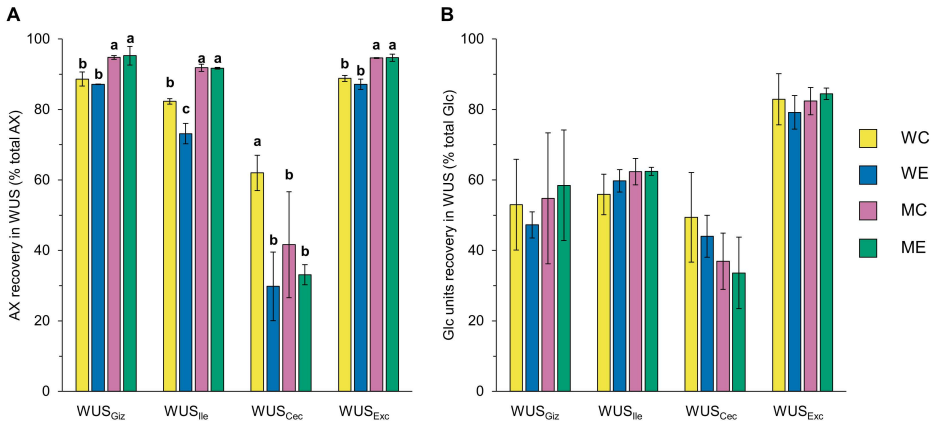
Fig. 2. Recovery of arabinoxylan (AX) (**A**) and Glc units (**B**) in WUS obtained from the gizzard (WUS$_{Giz}$), ileum (WUS$_{Ile}$), ceca (WUS$_{Cec}$) and excreta (WUS$_{Exc}$) corresponding to wheat control (WC), wheat enzyme (WE), maize control (MC) and maize enzyme (ME) diets, expressed as percentage of the total AX and Glc in whole digesta, respectively. Bars within GIT location not sharing common notation differ significantly ($p < 0.05$). The error bars indicate standard deviation ($n = 3$).

Lignin content in WUS along the GIT

Having established the prevalence of insoluble AX throughout the GIT, we further aimed at investigating the occurrence of lignin that is known to associate with AX (52). Therefore, lignin was selectively quantified by using a recently developed pyrolysis-GC-MS technique relying on the use of uniformly ^{13}C labelled lignin as internal standard (45). Pyrolysis products deriving from both lignin and aromatic amino acids or both lignin and ferulic acid were excluded (Table S2) (44). Although this method has been shown to very accurately quantify lignin in other lignified grass tissues, the method should still be further validated for cereal grains and WUS from digesta samples before absolute lignin contents can be considered fully reliable (44). Yet, the method can certainly be used to accurately and specifically compare lignin presence throughout the GIT in the relative sense. The lignin contents for WUS$_{Feed}$, WUS$_{Giz}$, WUS$_{Ile}$, WUS$_{Cec}$ and WUS$_{Exc}$ are presented in Table 1. The values obtained for WUS$_{Feed}$ after exclusion of the aforementioned pyrolysis products ranged between 0.08-0.12% (w/w). For comparison, the values obtained without excluding 4-vinylguaiacol were approximately two to nine times higher across WUS samples (Table S4). Interestingly, the values reported in Table 1 for WUS$_{Feed}$ were tenfold lower than the Klason lignin values reported in broiler diets of similar composition (43), as well as those reported for wheat and maize whole grains and soybean meal (1). Though clearly lower, the values currently obtained should be considered as certainly representative of the lignin content, measured directly, and not by a non-specific, gravimetric procedure.

Table 1. Lignin content (% w/w) in WUS obtained from the diet (WUS$_{Feed}$), gizzard (WUS$_{Giz}$), ileum (WUS$_{Ile}$), ceca (WUS$_{Cec}$) and excreta (WUS$_{Exc}$) (n = 3) corresponding to wheat control (WC), wheat enzyme (WE), maize control (MC) and maize enzyme (ME) diets, and determined based on lignin-specific pyrolysis products (Table S2) by ^{13}C-IS pyrolysis-GC-MS and excluding H-units and 4-vinylguaiacol.

| Diet | Lignin content (% w/w) | | | | |
	WUS$_{Feed}$[1]	WUS$_{Giz}$	WUS$_{Ile}$	WUS$_{Cec}$	WUS$_{Exc}$
WC	0.12	1.87	0.71[a]	0.11[a]	0.62[a]
WE	0.17	1.66	0.71[a]	0.11[a]	0.60[a]
MC	0.09	1.65	0.43[b]	0.06[b]	0.45[ab]
ME	0.08	2.10	0.37[b]	0.06[b]	0.28[b]
SEM[2]	0.03	0.42	0.06	0.01	0.08
p value	0.063	0.683	<0.001	<0.001	0.008

[1]Mean values of analytical triplicates. [2]Standard error of the mean. Values within GIT location not sharing common notation differ significantly (p < 0.05).

Comparison between diets demonstrated that the lignin content in WUS$_{Feed}$ tended to be higher for WC and WE, compared to MC and ME (p < 0.1) (Table 1). Next, the highest lignin content was found in WUS$_{Giz}$, ranging between 1.65% and 2.10% (w/w) (Table 1). The higher lignin content of WUS$_{Giz}$ compared to WUS$_{Feed}$ demonstrated that insoluble, coarse feed particles that are known to accumulate in the gizzard (53), conceivably contained relatively high lignin contents. Next, the lignin contents in WUS$_{Ile}$ were two to six times lower than in WUS$_{Giz}$. In particular, WC and WE presented significantly higher lignin content than both MC and ME in WUS$_{Ile}$ and ME in WUS$_{Exc}$ (p < 0.05). These differences were attributed to the higher lignin content recorded for the wheat diets. WUS$_{ceca}$ presented relatively low lignin content compared to WUS from other GIT locations, specifically indicating the presence of insoluble feed-derived fiber in the ceca, that may have entered alongside soluble feed components (24,53,54).

3.2 Insoluble AX and lignin contents along the GIT revealed fiber transit patterns

To the best of our knowledge, this is the first study selectively determining lignin contents of broiler digesta. The ^{13}C-IS pyrolysis-GC-MS analysis permitted us to use lignin as an indicator of the presence of insoluble cell wall material along the broiler GIT. For that, the weight ratio of AX and lignin (AX/L) in WUS was determined to obtain more insight on the chemical composition of insoluble cell wall components along the GIT (Fig. 3A). In addition, the ratio between syringyl (S) to guaiacyl (G) units (S/G), comprising the main monolignols of grain lignin (55), was evaluated at different GIT locations to investigate the structure of lignin present at various GIT locations (Fig. 3B).
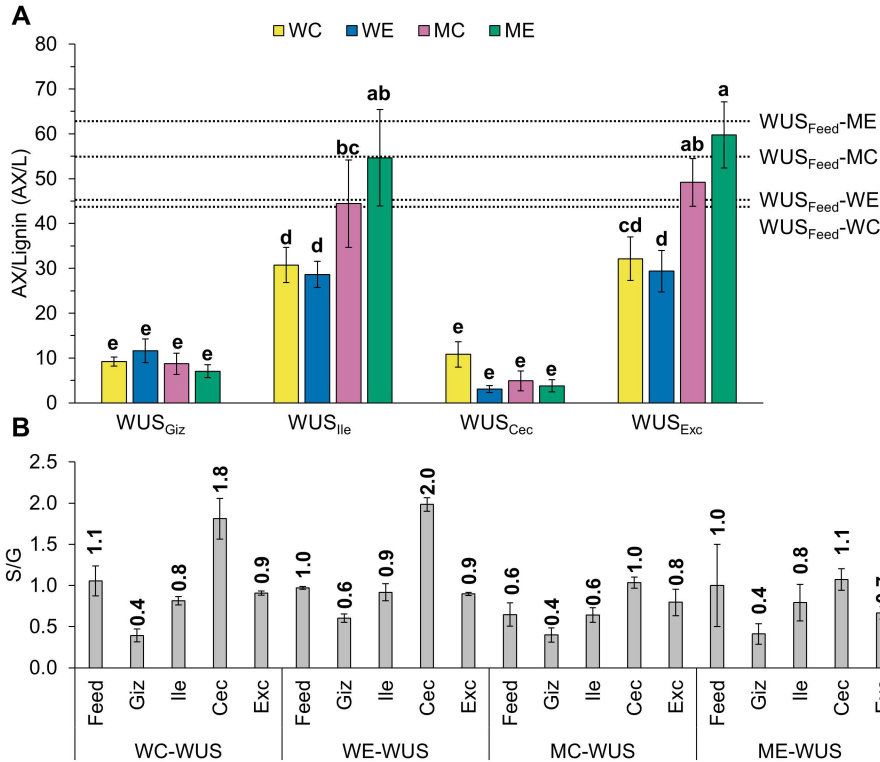
Fig. 3. Arabinoxylan (AX) to lignin (L) weight ratio (AX/L) (**A**) in WUS at different GIT locations. Bars corresponding to wheat control (WC), wheat enzyme (WE), maize control (MC) and maize enzyme (ME) diets across GIT locations (interaction effect Diet x GIT location, $p < 0.001$) not sharing common notation differ significantly ($p < 0.05$). Syringyl to guaiacyl units molar ratio (S/G) (**B**) in WUS obtained from the gizzard (WUS$_{Giz}$), ileum (WUS$_{Ile}$), ceca (WUS$_{Cec}$) and excreta (WUS$_{Exc}$). Error bars indicate standard deviations ($n = 3$). AX/L values in WUS$_{Feed}$ (WC: 44.5 ± 8.1, WE: 44.1 ± 16.1, MC: 55.2 ± 5.7, ME: 63.2 ± 2.9) are shown as dashed lines (**A**), for comparison.

Our analyses showed that AX/L values significantly depended on both diet and GIT location ($p < 0.001$). The low AX/L values obtained for WUS$_{Giz}$ indicated that relatively more lignin than insoluble AX was present in the gizzard compared to WUS$_{Feed}$. WUS$_{Giz}$ also presented lower S/G ratios (0.4-0.6) than WUS$_{Feed}$ (0.6-1.1), pointing at the accumulation of a specific lignin fraction in this GIT segment. Interestingly, both content-wise and structure-wise, lignin in WUS$_{Giz}$ is expected to increase fiber recalcitrance, as high S/G ratios have been associated with higher enzymatic lignocellulose degradation (11,56). Both AX/L and S/G values increased in WUS$_{Ile}$ compared to WUS$_{Giz}$. Still, wheat diets presented lower AX/L values in WUS$_{Ile}$ than in WUS$_{Feed}$, while both maize diets presented similar AX/L values between WUS$_{Ile}$ and WUS$_{Feed}$. This difference between diets was most likely due to the higher proportion of insoluble AX and lower lignin content determined for MC

175

and ME compared to WC and WE (Table 3, Fig. 2). Overall, WUS$_{Ile}$ appeared to contain the main insoluble AX and lignin fractions present in the diet, while WUS$_{Giz}$ seemed to mainly represent a specific fiber fraction originating from the diet. WUS$_{Exc}$ presented similar AX/L and S/G values compared to WUS$_{Ile}$ (Fig. 3), indicating that insoluble fiber complexes reaching the ileum were excreted unfermented. This was in line with previous research reporting more than 98% recovery of dietary lignin in broiler and ostrich excreta, as determined by non-specific gravimetric methods (57,58). Although a lignin fraction presenting high S/G values was present in the ceca, our observations for WUS$_{Ile}$ and WUS$_{Exc}$ further confirmed the low fermentability of insoluble NSP in the broiler hindgut (24,28,53). Finally, AX/L values were not found to be influenced by enzyme supplementation. Overall, analysis of both NSP and lignin provided a more complete overview of fiber transit and fermentation in broilers, and highlighted how the chemical composition of cell wall components may influence their behavior along the GIT.

3.3 Alkali extractability of AX from WUS was influenced by enzyme supplementation

Having established that WUS$_{Ile}$ and WUS$_{Exc}$ were representative for insoluble fiber present in the feed, these two WUS fractions were subjected to alkali extraction to further investigate the impact of enzyme supplementation on insoluble NSP structure. In a previous study, alkali extraction (6 M NaOH) of broiler excreta, followed by dialysis with 14 kDa membranes, resulted in significant loss of alkali-extractable oligosaccharides and polysaccharides (28). To prevent such losses in our study, the 1 M NaOH extract was not subjected to dialysis, but instead was desalted with 3.5 kDa ultrafiltration tubes, resulting in a salt-free retentate (1M-ASS$_R$) and a salt-rich filtrate. The salt from the filtrate was removed via SPE to yield the salt-free fraction 1M-ASS$_F$, potentially containing 'alkali-extractable' oligomers. Overall, 70-78% (w/w) of OM in WUS was recovered during alkali extraction, regardless of diet (Fig. S2). The considerable losses of OM (25-30% w/w) observed were partly attributed to the low amounts of starting material influencing handling accuracy. Most of alkali-extractable OM was extracted with 1 M NaOH, with 17-24% (w/w) of WUS OM being recovered in 1M-ASS$_R$, and 4-7% (w/w) of WUS OM being recovered in 1M-ASS$_F$. Subsequent extraction of WUS with 4 M NaOH further solubilized 12-17% (w/w) of OM. The alkali-unextractable residue (RES) accounted for 29-37% (w/w) of OM.

Continuing our efforts to disentangle the fate of insoluble AX in broilers, we focused on the impact of enzyme addition on AX extractability by alkali (Table 2). The majority of AX in WUS$_{Ile}$ and WUS$_{Exc}$ was extractable by 1 M NaOH and recovered in 1M-ASS$_R$ (19.1-27.9% w/w), while AX below 3.5 kDa in 1M-ASS$_F$ accounted for less than 0.4% (w/w) of AX in WUS, irrespective of diet. Sequential extraction with 4 M NaOH solubilized additionally 17.5%-19.9% and 11.0%-12.3% (w/w) AX from WUS$_{Ile}$ and WUS$_{Exc}$, respectively, while unextractable AX recovered in RES accounted for 30.5-40.8% (w/w) of total AX. Previous research has shown that 90% (w/w) wheat endosperm AX and 40-60% (w/w) wheat bran and maize grain

glucuronoarabinoxylan was alkali-extractable (7,8,17,19,59). Currently, the alkali treatment of digesta containing various cereal fractions was expected to have solubilized structurally different AX populations (5,60).

Table 2. Arabinoxylan (AX) recovery in alkali extracts (1M-ASS$_F$, 1M-ASS$_R$, 4M-ASS) and residue (RES) expressed as percentage (%) of AX in WUS$_{Ile}$ and WUS$_{Exc}$ corresponding to wheat control (WC), wheat enzyme (WE), maize control (MC) and maize enzyme (ME) diets.

Diet	Arabinoxylan (AX) recovery (% AX in WUS)				
WUS$_{Ile}$	**1M-ASS$_{F\_Ile}$**	**1M-ASS$_{R\_Ile}$**	**4M-ASS$_{Ile}$**	**RES$_{Ile}$**	**Losses[1]**
WC	0.3	24.7	17.6	31.8	25.7
WE	0.4	26.0	18.6	38.3	16.7
MC	0.3	25.4	20.0	32.6	21.7
ME	0.3	20.5	19.2	34.0	26.0
SEM[2]	0.0	2.4	0.7	1.5	3.2
p-value	0.325	0.403	0.186	0.059	0.225
WUS$_{Exc}$	**1M-ASS$_{F\_Exc}$**	**1M-ASS$_{R\_Exc}$**	**4M-ASS$_{Exc}$**	**RES$_{Exc}$**	**Losses[1]**
WC	0.3[ab]	24.4	11.0	30.8[b]	33.4
WE	0.4[a]	27.9	12.3	40.5[a]	18.8
MC	0.1[c]	19.1	11.2	34.5[ab]	35.0
ME	0.2[bc]	21.1	11.1	31.3[b]	36.3
SEM	0.0	2.5	1.5	1.5	3.9
p-value	0.001	0.154	0.154	0.008	0.044

[1]Estimated by the difference between total AX in WUS and the sum of AX recovered in the different fractions. [2]Standard error of the mean, *n* = 3.

Overall, WC exhibited lower AX recovery in RES compared to WE for both WUS$_{Ile}$ (RES$_{Ile}$, *p* < 0.1) and WUS$_{Exc}$ (RES$_{Exc}$, *p* < 0.05). Although a relatively larger AX proportion was shown to be extracted for WC, this was not accompanied by significantly different AX recoveries in 1M-ASS$_F$, 1M-ASS$_R$ and 4M-ASS between WC and WE (*p* > 0.05). On the contrary, WE presented elevated values for both 1M-ASS$_{F\_Ile}$ and 1M-ASS$_{R\_Ile}$ compared to WC, as well as for 1M-ASS$_{F\_Exc}$ and 1M-ASS$_{R\_Exc}$. It should be noted that a considerable AX proportion (16.7-36.3 % w/w) was not recovered during extraction (Table 2; Losses), in line with the observed losses in OM (Fig. S2). WE presented a numerically lower proportion of unrecovered AX compared to WC for both WUS$_{Ile}$ and WUS$_{Exc}$, but these differences did not reach statistical significance. Maize diets presented comparable AX recovery values to the wheat diets, while no differences were observed between MC and ME (*p* > 0.05). Still, lower AX recovery was obtained in 1M-ASS$_{R\_Exc}$ and RES$_{Exc}$ for MC and ME compared to WC and WE.

The previously documented AXOS release upon enzyme addition in WE (Chapter 5), was currently found to also decrease the relative amount of alkali extractable AX in WUS, as indicated by higher AX recovery in RES for WE compared to WC (RES$_{Ile}$; 38% *vs* 32%, RES$_{Exc}$; 40% *vs* 31%) (Table 2). These findings were in agreement with previous work reporting that xylanase and cellulase pre-treatment of hardwood pulp decreased the relative amount of alkali extractable xylan (61). Similar to our observations, the decrease in the relative amount of alkali-

6

extractable NSP from broiler excreta was previously observed when pectolytic enzymes were included in maize-rapeseed meal diet (28). Yet, the absence of significant differences across alkali extracts indicated that, overall, enzyme supplementation did not affect the structure of AX populations recovered. However, there seemed to be an influence of enzyme addition on the estimated proportion of unrecovered AX. To explain that, we hypothesized that part of the unrecovered AX could have been adsorbed on to the cellulose filter during ultrafiltration of the 1 M NaOH extract (see 2.3), and that this process would be dependent on AX molecular weight (Mw), degree of substitution and distribution of Ara-substituents (62–64). It is, therefore, conceivable that enzymatic cell wall degradation resulted in the yield of alkali-extractable AX having subtle differences in the Mw and structure after all. However, the incomplete AX recovery did not permit further investigation of those differences at this stage.
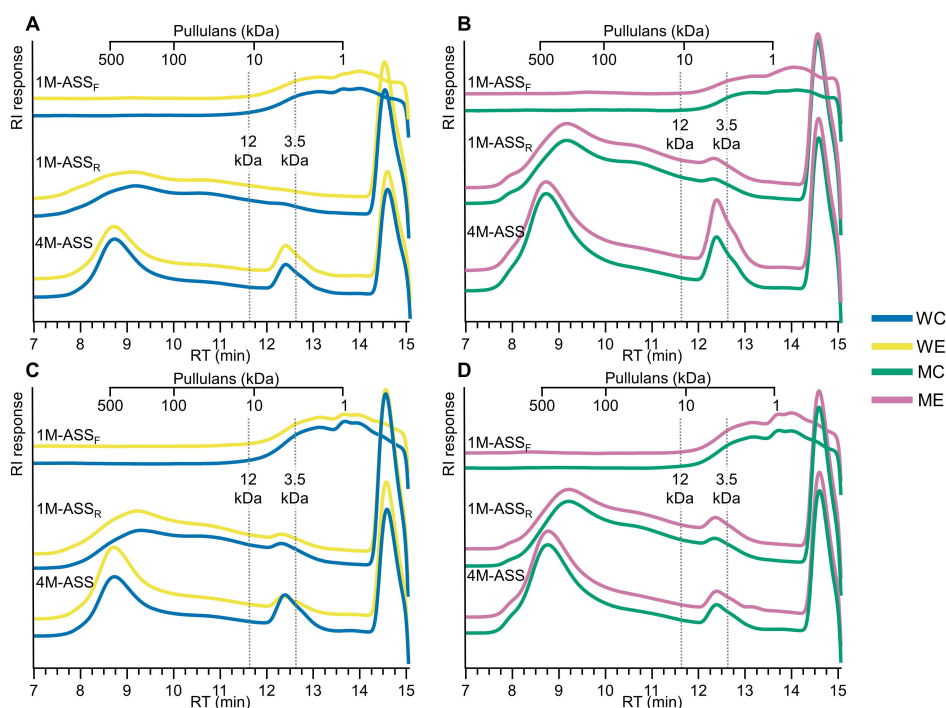
Fig. 4. HPSEC-RI chromatograms of alkali extracts obtained from WUS_{Ile} (**A:** wheat control (WC), wheat enzyme (WE) diets, **B:** maize control (MC), maize enzyme (ME) diets) and WUS_{Exc} (**C:** WC, WE, **D:** MC, ME). $1M-ASS_F$ were dissolved in water at 5 mg/mL whereas $1M-ASS_R$ and 4M-ASS were dissolved in 50 mM NaOAc (pH 5.0) at 5 mg/mL. Pullulan standards were used as calibrants.

3.4 Characterization of alkali-extractable NSP

Mw distribution in alkali extracts

The impact of enzyme addition on the structural characteristics of insoluble NSP recovered during alkali extraction was further investigated by determining the Mw distribution of alkali extractable solids by HPSEC (Fig. 4). According to expectations, only compounds below 3.5 kDa were present in all 1M-ASS$_F$ fractions. In contrast, HPSEC of 1M-ASS$_R$ presented a broad molecular weight distribution with Mw between 10 and 500 kDa. The signal observed between 12 and 3.5 kDa was attributed to borate salts. Overall, both WC and WE presented broad Mw distribution between 100-500 kDa in 1M-ASS$_{R\_Ile}$ and 1M-ASS$_{R\_Exc}$. Finally, polymers with Mw > 500 kDa were abundant in 4M-ASS fractions. MC and ME presented similar chromatograms for all WUS$_{Ile}$ and WUS$_{Exc}$ fractions, while a more intense signal of Mw > 100 kDa compounds was noted for 1M-ASS$_R$ and 4M-ASS compared to WC and WE. In conclusion, no effect of enzyme treatment on the Mw distribution of alkali extractable solids was observed, presumably reflecting the similar AX recovery values obtained in the respective fractions (Table 2).

Oligosaccharide profiles in 1M-ASS$_{F\_Ile}$

The 1M-ASS$_{F\_Ile}$ fractions obtained by SPE were further analyzed for oligosaccharide profiles by MALDI-TOF-MS (Fig. 5). This analysis was performed to assess the presence of enzymatically-formed oligosaccharides that remained embedded or associated in the cell wall matrix and were released from WUS by alkali extraction, as previously suggested (28). 1M-ASS$_{F\_Ile}$ fraction across all diets presented a homologous series of hexose oligosaccharides (HexOS) with degree of polymerization (DP) 5-12. 1M-ASS$_{F\_Ile}$ for WE also contained a series of pentose oligosaccharides (DP 6-14), representing AXOS (30). Pentose oligomers were not detected in MC and ME 1M-ASS$_{F\_Ile}$ fractions, as already indicated in our previous work (Chapters 2,5) (30,36), and presented only weak signal in WC. It therefore appeared that oligomeric AXOS accounted for part of the low Mw AX (< 3.5 kDa) recovered in 1M-ASS$_{F\_Ile}$, which accounted for less than 0.4% of AX in WUS$_{Ile}$ (Table 2). Subsequent comparison of MALDI-TOF mass spectra between 1M-ASS$_{F\_Ile}$ and WUS$_{Ile}$ for WE (Fig. 5B) suggested that the detected oligosaccharides were present only in minor levels in WUS. However, it remained unclear whether these AXOS were embedded in the cell wall matrix and were released by alkali or that their signal became more intense after extraction and purification by SPE.

6
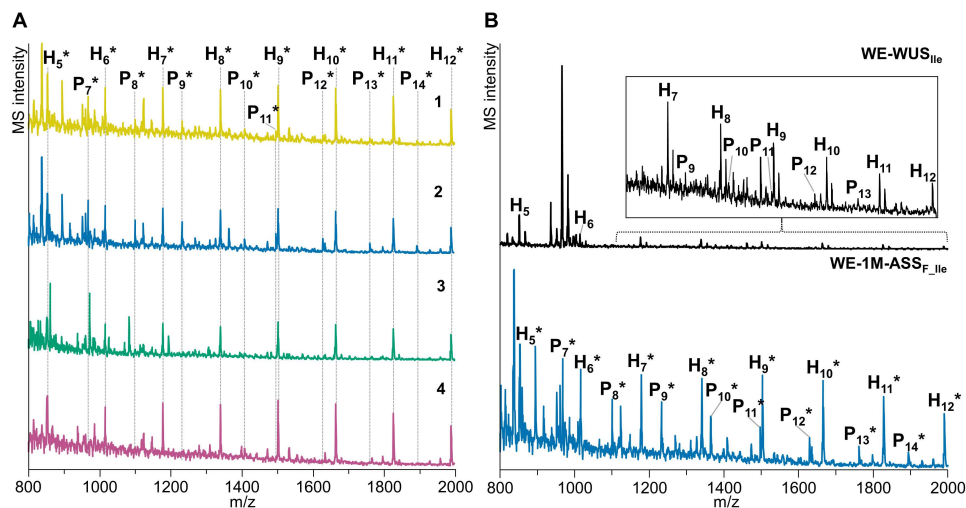
Fig. 5. MALDI-TOF mass spectra of 1M-ASS_{F_Ile} solutions (**A**) corresponding to wheat control (WC: **1**), wheat enzyme (WE: **2**), maize control (MC: **3**) and maize enzyme (ME: **4**) diets. MALDI-TOF mass spectra (**B**) of WUS_{Ile} dispersion (**1**) and 1M-ASS_{F_Ile} extract (**2**) belonging to WE diet. The number of pentose (P_n) or hexose (H_n) units comprising the detected oligosaccharides are shown next to the *m/z* values; **m/z* values of reduced oligosaccharides formed due to the presence of $NaBH_4$ in the extractant present +2 mass increment compared to their neutral counterparts*.

Diverse insoluble NSP populations were present in digesta WUS

Next to AX, we reported the recovery of Glc units during alkali extraction, given the high Glc abundance in WUS (Table S3). As mentioned earlier, Glc in WUS represents a diverse population of glucans, such as insoluble starch, β-glucan and cellulose. Consequently, differences in Glc recovery were most likely indicative for differences in the relative amounts of the aforementioned glucans in WUS (Table S5). For example, the recovery above 90% observed in RES_{Ile} and RES_{Exc} for MC and ME was indicative of cellulose abundance in WUS for maize diets. In contrast, WC and WE presented lower Glc recovery values in RES_{Ile} (WC: 68.2%, WE: 87.8%, $p > 0.05$) and RES_{Exc} (WC: 55.2%, WE: 72.6%, $p < 0.05$) highlighting the more abundant presence of glucans other than cellulose. The higher RES values obtained for WE compared to WC suggested that lower amount of glucans remained insoluble upon enzyme addition in WE. This could be mainly explained by the higher starch digestibility observed for WE (30), as glucanase action did not seem to impact non-starch Glc solubility (Fig. 3). Swelling of RES by alkali could have caused more complete cellulose hydrolysis during sugar composition analysis compared to WUS, thus resulting in more than 100% glucan recovery (65). Further research is warranted to determine the impact of enzyme supplementation on the extractability of specific glucans.

Except for AX and glucan, other carbohydrates were extracted as well (Table S6, S7). Overall, 1M-ASS$_F$ extracts from WUS$_{Ile}$ and WUS$_{Exc}$ presented low total carbohydrate contents (7.7-11.6% w/w), and were composed of Glc (26-41 mol %), Gal (21-28 mol %), Man (18-26 mol %) and to a lower extent of Ara (7-13 mol %) and Xyl (2-10 mol %). Co-extraction of soybean NSP is expected to have confounded the final AX values, as evidenced by the unrealistically high Ara/Xyl values in the 1M-ASS$_F$ fractions (Ara/Xyl = 1.3-4.1), especially for the maize diets. In contrast, higher carbohydrate contents were obtained in 1M-ASS$_R$ corresponding to WUS$_{Ile}$ (63.5-71.3% w/w OM) and WUS$_{Exc}$ (39.3-61.4% w/w OM) across all diets and GIT locations. For both WUS$_{Ile}$ and WUS$_{Exc}$, Ara and Xyl represented 20-28 mol % and 29-41 mol % of extracted carbohydrates, respectively. This indicated the prevalence in 1M-ASS$_R$ of AX with Ara/Xyl value of 0.6 and 0.9 for the wheat and maize diets, respectively. No additional differences in monosaccharide composition were observed between WC and WE and MC and ME. Finally, co-extraction of other NSP such as soybean arabinogalactans and β-glucan from wheat (16,17) from both WUS$_{Ile}$ and WUS$_{Exc}$ was evidenced by the abundant presence of Gal (12-22 mol %) and Glc (17-30 mol %).

The carbohydrates extracted in 4M-ASS from both WUS$_{Ile}$ and WUS$_{Exc}$ presented different amounts for wheat (41.8-54.8% w/w) and for maize (78.3-88.5% w/w) diets, but similar carbohydrate composition. The main constituent monosaccharides were Ara (31-33 mol %), Xyl (27-30 mol %) and Gal (18-24 mol %), while Glc was less abundant (11-16 mol%) and Man and Rha were minorly present (< 4 mol %). Previously, the use of 4 M NaOH as final extractant in sequential extraction procedures solubilized a minor AX fraction (< 10%) from wheat flour, while it resulted in a hemicellulose-rich extract from soybean (16,17). Overall, the similarities between 4M-ASS fractions from wheat and maize diets in terms of monosaccharide composition and Ara/Xyl ratio (1.1-1.2) suggested the low prevalence of AX in this fraction. Finally, Glc prevalence in RES (49-55 mol %) was indicative of cellulose, while Ara (13-19 mol %) and Xyl (15-18 mol %) indicated the presence of unextractable AX (8,16,17).

3.5   Implications of enzyme supplementation for insoluble cell wall polysaccharides in broiler digesta

Associations between cell wall matrix components, such as AX, lignin, cellulose, has been postulated to encapsulate nutrients and hinder their digestion. Moreover, most AX is tethered in this insoluble structure cannot be fermented in the broiler hindgut, as shown by the high AX recovery in WUS, especially for maize diets (Fig. 2,3). AX release by alkali indicated that associations between cell wall components were mainly ester-mediated by ferulate and di-ferulate intramolecular AX and intermolecular AX-lignin cross-links, alongside non-covalent interactions between AX and cellulose. Moreover, the different AX/L and S/G ratios observed along the GIT (Fig. 3) suggested that a relatively recalcitrant fiber subfraction accumulated in the gizzard. Cell wall degradation by xylanase *in vivo* was mainly reflected by AXOS release resulting in pronounced cecal fermentation, as covered in our recent

6

work (Chapters 2,5) (30,36). However, AX depolymerization did not further impact insoluble AX extractability by alkali (Table 2). It is, therefore, suggested that only limited loosening of cell wall-associated AX occurred upon enzyme supplementation in wheat and maize diets. Still, optimization of NSP extraction is necessary to further study the impact of dietary enzymes on cell wall structure.

4   Conclusions

This study provided novel insights into insoluble arabinoxylan and lignin content and structure along the GIT of broilers fed wheat and maize diets. Investigating the chemical composition of cell wall material present in digesta demonstrated that lignin-rich fibers accumulated in the gizzard and that insoluble fibers reaching the ileum were not fermented in the broiler hindgut. Enzyme supplementation in the wheat diet released AXOS, thus altering the content and composition of insoluble AX. Still, enzyme action in the GIT did not improve NSP extraction by alkali. Consequently, associations between cell wall components that render the majority of AX insoluble, and therefore, unavailable for cecal fermentation, appeared unaffected by enzyme supplementation. Our work highlights that despite improvements in AX fermentation by dietary xylanase, further research is needed toward optimization of insoluble NSP degradation by dietary enzymes in broilers.

5   References

1.   Bach Knudsen KE. Fiber and nonstarch polysaccharide content and variation in common crops used in broiler diets. Poult Sci. 2014;93(9):2380–93.

2.   Jha R, Mishra P. Dietary fiber in poultry nutrition and their effects on nutrient utilization, performance, gut health, and on the environment: A review. J Anim Sci Biotechnol. 2021;12(1):1–16.

3.   Fincher GB, Stone B. Chemistry of nonstarch polysaccharides. In: Wrigley C, editor. Encyclopedia of grain science. Amsterdam: Elsevier Academic Press; 2004. p. 206–23.

4.   Fauré R, Courtin CM, Delcour JA, Dumon C, Faulds CB, Fincher GB, Sébastien F, Fry SC, Halila S, Kabel MA, Pouvreau L, Quemener B, Rivet A, Saulnier L, Schols HA, Driguez H, O'Donohue MJ. A brief and informationally rich naming system for oligosaccharide motifs of heteroxylans found in plant cell walls. Aust J Chem. 2009;62(6):533–7.

5.   Izydorczyk MS, Biliaderis CG. Cereal arabinoxylans: Advances in structure and physicochemical properties. Carbohydr Polym. 1995;28(1):33–48.

6.   Chanliaud E, Saulnier L, Thibault JF. Alkaline extraction and characterisation of heteroxylans from maize bran. J Cereal Sci. 1995;21(2):195–203.

7.   Bergmans MEF, Beldman G, Gruppen H, Voragen AGJ. Optimisation of the selective extraction of (glucurono)arabinoxylans from wheat bran: Use of barium and calcium hydroxide solution at elevated temperatures. J Cereal Sci. 1996;23(3):235–45.

8.   Huisman MMH, Schols HA, Voragen AGJ. Glucuronoarabinoxylans from maize kernel cell walls are more complex than those from sorghum kernel cell walls. Carbohydr Polym. 2000;43(3):269–79.

9.   Burton RA, Fincher GB. Evolution and development of cell walls in cereal grains. Front Plant Sci. 2014;5:465.

10. Theander O, Westerlund E, Åman P, Graham H. Plant cell walls and monogastric diets. Anim Feed Sci Technol. 1989;23:205–25.

11. Fontaine AS, Bout S, Barrière Y, Vermerris W. Variation in cell wall composition among forage maize (*Zea mays* L.) inbred lines and its impact on digestibility: Analysis of neutral detergent fiber composition by gyrolysis-gas chromatography-mass spectrometry. J Agric Food Chem. 2003;51(27):8080–7.

12. Harris PJ, Stone B. Chemistry and molecular organization of plant cell walls. In: Himmel ME, editor. Biomass recalcitrance: Deconstructing the plant cell wall for bioenergy. Oxford: Blackwell Publishing Ltd.; 2008. p. 61–93.

13.   Scheller HV, Ulvskov P. Hemicelluloses. Annu Rev Plant Biol. 2010;61:263–89.

14. Gruppen H, Hamer RJ, Voragen AGJ. Water-unextractable cell wall material from wheat flour. 2. Fractionation of alkali-extracted polymers and comparison with water-extractable arabinoxylans. J Cereal Sci. 1992;16(1):53–67.

15. Broxterman SE, Schols HA. Characterisation of pectin-xylan complexes in tomato primary plant cell walls. Carbohydr Polym. 2018;197:269–76.

16. Huisman MMH, Schols HA, Voragen AGJ. Cell wall polysaccharides from soybean (*Glycine max.*) meal. Isolation and characterisation. Carbohydr Polym. 1998;37(1):87–95.

17. Gruppen H, Hamer RJ, Voragen AGJ. Water-unextractable cell wall material from wheat flour. 1. Extraction of polymers with alkali. J Cereal Sci. 1992;16(1):41–51.

18. Murciano Martínez P, Kabel MA, Gruppen H. Delignification outperforms alkaline extraction for xylan fingerprinting of oil palm empty fruit bunch. Carbohydr Polym. 2016;153:356–63.

6

19. Gruppen H, Hamer RJ, Voragen AGJ. Barium hydroxide as a tool to extract pure arabinoxylans from water-insoluble cell wall material of wheat flour. J Cereal Sci. 1991;13(3):275–90.

20. Sun Y, Cheng J. Hydrolysis of lignocellulosic materials for ethanol production: A review. Bioresour Technol. 2002;83(1):1–11.

21. Iiyama K, Lam T, Stone BA. Covalent cross-links in the cell wall. Plant Physiol. 1994;104(2):315–20.

22. Svihus B, Hervik AK. The influence of fibre on gut physiology and feed intake regulation. In: González-Ortiz G, Bedford MR, Knudsen KEB, Courtin CM, Classen HL, editors. The value of fibre. Wageningen: Wageningen Academic Publishers; 2019. p. 127–139.

23. Choct M, Annison G. Anti-nutritive effect of wheat pentosans in broiler chickens: Roles of viscosity and gut microflora. Br Poult Sci. 1992;33(4):821–34.

24. Svihus B, Choct M, Classen HL. Function and nutritional roles of the avian caeca: A review. Worlds Poult Sci J. 2013;69(2):249–64.

25. Pan D, Yu Z. Intestinal microbiome of poultry and its interaction with host and diet. Gut Microbes. 2013;5(1):108–19.

26. Bautil A, Courtin CM. Fibres making up wheat cell walls in the context of broiler diets. In: G. González-Ortiz, Bedford MR, Knudsen KEB, Courtin CM, Classen HL, editors. The value of fibre. Wageningen: Wageningen Academic Publishers; 2019. p. 17–46.

27. Bedford MR. The evolution and application of enzymes in the animal feed industry: the role of data interpretation. Br Poult Sci. 2018;59(5):486–93.

28. Pustjens AM, De Vries S, Schols HA, Gruppen H, Gerrits WJJ, Kabel MA. Understanding carbohydrate structures fermented or resistant to fermentation in broilers fed rapeseed (*Brassica napus*) meal to evaluate the effect of acid treatment and enzyme addition. Poult Sci. 2014;93(4):926–34.

29. Hetland H, Choct M, Svihus B. Role of insoluble non-starch polysaccharides in poultry nutrition. Worlds Poult Sci J. 2004;60(04):415–22.

30. Kouzounis D, Hageman JA, Soares N, Michiels J, Schols HA. Impact of xylanase and glucanase on oligosaccharide formation, carbohydrate fermentation patterns, and nutrient utilization in the gastrointestinal tract of broilers. Animals. 2021;11(5):1285.

31. Kiarie E, Romero LF, Nyachoti CM. The role of added feed enzymes in promoting gut health in swine and poultry. Nutr Res Rev. 2013;26(1):71–88.

32. Kiarie E, Romero LF, Ravindran V. Growth performance, nutrient utilization, and digesta characteristics in broiler chickens fed corn or wheat diets without or with supplemental xylanase. Poult Sci. 2014;93(5):1186–96.

33. Munyaka PM, Nandha NK, Kiarie E, Nyachoti CM, Khafipour E. Impact of combined β-glucanase and xylanase enzymes on growth performance, nutrients utilization and gut microbiota in broiler chickens fed corn or wheat-based diets. Poult Sci. 2016;95(3):528–40.

34. Lærke HN, Arent S, Dalsgaard S, Bach Knudsen KE. Effect of xylanases on ileal viscosity, intestinal fiber modification, and apparent ileal fiber and nutrient digestibility of rye and wheat in growing pigs. J Anim Sci. 2015;93(9):4323–35.

35. Bautil A, Buyse J, Goos P, Bedford MR, Courtin CM. Feed endoxylanase type and dose affect arabinoxylan hydrolysis and fermentation in ageing broilers. Anim Nutr. 2021;7(3):787–800.

36. D. Kouzounis, M.C. Jonathan, N. Soares, M.A. Kabel, H.A. Schols, *In vivo* formation of arabinoxylo-oligosaccharides by dietary endo-xylanase alters arabinoxylan utilization in broilers, Carbohydr Polym. 291 (2022) 119527.

37. Maisonnier S, Gomez J, Carré B. Nutrient digestibility and intestinal viscosities in broiler chickens fed on wheat diets, as compared to maize diets with added guar gum. Br Poult Sci. 2001;42(1):102–10.

38. Bedford MR, Classen HL. Reduction of intestinal viscosity through manipulation of dietary rye and pentosanase concentration is effected through changes in the carbohydrate composition of the intestinal aqueous phase and results in improved growth rate and food conversion efficiency of broiler chicks. J Nutr. 1992;122(3):560–9.

39. Meng X, Slominski BA, Nyachoti CM, Campbell LD, Guenter W. Degradation of cell wall polysaccharides by combinations of carbohydrase enzymes and their effect on nutrient utilization and broiler chicken performance. Poult Sci. 2005;84(1):37–47.

40. Tervilä-Wilo A, Parkkonen T, Morgan A, Hopeakoski-Nurminen M, Poutanen K, Heikkinen P, Autio K. *In vitro* digestion of wheat microstructure with xylanase and cellulase from *Trichoderma reesei*. J Cereal Sci. 1996;24(3):215–25.

41. Le DM, Fojan P, Azem E, Pettersson D, Pedersen NR. Visualization of the anticaging effect of Ronozyme WX xylanase on wheat substrates. Cereal Chem. 2013;90(5):439–44.

42. Meng X, Slominski BA. Nutritive values of corn, soybean meal, canola meal, and peas for broiler chickens as affected by a multicarbohydrase preparation of cell wall degrading enzymes. Poult Sci. 2005;84(8):1242–51.

43. Kim E, Morgan NK, Moss AF, Li L, Ader P, Choct M. Characterisation of undigested components throughout the gastrointestinal tract of broiler chickens fed either a wheat- or maize-based diet. Anim Nutr. 2022;8(1):153–9.

44. Van Erven G, De Visser R, De Waard P, van Berkel WJH, Kabel MA. Uniformly ^{13}C Labeled lignin internal standards for quantitative pyrolysis-GC-MS analysis of grass and wood. ACS Sustain Chem Eng. 2019;7(24):20070–6.

45. van Erven G, De Visser R, Merkx DWH, Strolenberg W, De Gijsel P, Gruppen H, Kabel MA. Quantification of lignin and its structural features in plant biomass using ^{13}C lignin as internal standard for pyrolysis-GC-SIM-MS. Anal Chem. 2017;89(20):10907–16.

46. Englyst HN, Cummings JH. Simplified method for the measurement of total non-starch polysaccharides by gas-liquid chromatography of constituent sugars as alditol acetates. Analyst. 1984;109(7):937.

47. Blumenkrantz N, Asboe-Hansen G. New method for quantitative determination of uronic acids. Anal Biochem. 1973;54(2):484–9.

48. Thibault JF, Robin JP. Automatisation du dosage des acides uroniques par la méthode de carbazol. Application au cas de matières pectiques. Ann Technol Agric. 1975;24:99–110.

49. De Ruiter GA, Schols HA, Voragen AGJ, Rombouts FM. Carbohydrate analysis of water-soluble uronic acid-containing polysaccharides with high-performance anion-exchange chromatography using methanolysis combined with TFA hydrolysis is superior to four other methods. Anal Biochem. 1992;207(1):176–85.

50. Huisman MMH, Schols HA, Voragen AGJ. Enzymatic degradation of cell wall polysaccharides from soybean meal. Carbohydr Polym. 1999;38(4):299–307.

51. Mäki M, Renkonen R. Biosynthesis of 6-deoxyhexose glycans in bacteria. Glycobiology. 2004;14(3):1R-15R.

52. Chateigner-Boutin AL, Lapierre C, Alvarado C, Yoshinaga A, Barron C, Bouchet B, Bakan B, Saulnier L, Devaux MF, Girousse C, Guillon F. Ferulate and lignin cross-links increase in cell walls of wheat grain outer layers during late development. Plant Sci. 2018;276:199–207.

6

53. Vergara P, Ferrando C, Jiménez M, Fernández E, Goñalons E. Factors determining gastrointestinal transit time of several markers in the domestic fowl. Q J Exp Physiol. 1989;74(6):867–74.

54. De Vries S, Kwakkel RP, Pustjens AM, Kabel MA, Hendriks WH, Gerrits WJJ. Separation of digesta fractions complicates estimation of ileal digestibility using marker methods with Cr_2O_3 and cobalt-ethylenediamine tetraacetic acid in broiler chickens. Poult Sci. 2014;93(8):2010–7.

55. Bunzel M, Ralph J, Lu F, Hatfield RD, Steinhart H. Lignins and ferulate−coniferyl alcohol cross-coupling products in cereal grains. J Agric Food Chem. 2004;52(21):6496–502.

56. Yoo CG, Dumitrache A, Muchero W, Natzke J, Akinosho H, Li M, Sykes RW, Brown SD. Significance of lignin S/G ratio in biomass recalcitrance of *Populus trichocarpa* variants for bioethanol production. ACS Sustain Chem Eng. 2018;6(2):2162–8.

57. Nizza A, Dimeo C. Determination of apparent digestibility coefficients in 6-, 12- and 18-week-old ostriches. Br Poult Sci. 2000;41(4):518–20.

58. Mueller WJ. Feasibility of the chromic oxide and the lignin indicator methods for metabolism experiments with chickens. J Nutr. 1956;58(1):29–36.

59. Maes C, Delcour JA. Structural characterisation of water-extractable and water-unextractable arabinoxylans in wheat bran. J Cereal Sci. 2002;35(3):315–26.

60. Saulnier L, Sado P-E, Branlard G, Charmet G, Guillon F. Wheat arabinoxylans: Exploiting variation in amount and composition to develop enhanced varieties. J Cereal Sci. 2007;46(3):261–81.

61. Hakala TK, Liitiä T, Suurnäkki A. Enzyme-aided alkaline extraction of oligosaccharides and polymeric xylan from hardwood kraft pulp. Carbohydr Polym. 2013;93(1):102–8.

62. Valério R, Crespo JG, Galinha CF, Brazinha C. Effect of ultrafiltration operating conditions for separation of ferulic acid from arabinoxylans in corn fibre alkaline extract. Sustain. 2021;13(9):1–16.

63. Kabel MA, van den Borne H, Vincken JP, Voragen AGJ, Schols HA. Structural differences of xylans affect their interaction with cellulose. Carbohydr Polym. 2007;69(1):94–105.

64. Köhnke T, Östlund Å, Brelid H. Adsorption of arabinoxylan on cellulosic surfaces: Influence of degree of substitution and substitution pattern on adsorption characteristics. Biomacromolecules. 2011;12(7):2633–41.

65. Murciano Martínez P, Bakker R, Harmsen P, Gruppen H, Kabel M. Importance of acid or alkali concentration on the removal of xylan and lignin for enzymatic cellulose hydrolysis. Ind Crops Prod. 2015;64:88–96.

Supplementary information

Table S1. Diet composition of wheat-based and maize-based dietary treatments. The data were previously determined and are reported elsewhere (1).

Ingredient (%)	Wheat-based			Maize-based		
	Starter	Grower	Finisher	Starter	Grower	Finisher
Wheat	49.4	58.8	65.9	-	-	-
Maize	10.0	5.0	-	57.3	59.6	59.1
Soybean Meal 48CP[1]	24.4	19.5	17.0	27.2	24.3	24.3
Toasted Soybeans	10.0	10.0	8.0	10.0	10.0	8.0
Soybean Oil	1.4	2.4	4.3	0.6	1.7	3.9
Monocalcium phosphate	1.4	1.3	1.0	1.5	1.4	1.2
Limestone	1.4	1.3	1.1	1.4	1.2	1.1
DL-Methionine	0.4	0.3	0.2	0.4	0.3	0.3
L-Lysine HCl	0.3	0.3	0.3	0.3	0.3	0.2
Salt	0.2	0.2	0.3	0.2	0.2	0.3
Na-Bicarbonate	0.3	0.3	0.2	0.3	0.3	0.2
L-Threonine	0.2	0.1	0.1	0.2	0.1	0.1
L-Valine	0.1	0.1	0.1	0.2	0.1	0.0
Coccidiostat	Sacox[2]	Sacox	-	Sacox	Sacox	-
Premix Article[3]	0.5	0.5	0.5	0.5	0.5	0.5
Diamol[4]	-	-	1.0	-	-	1.0
Total	100.0	100.0	100.0	100.0	100.0	100.0
Analyzed chemical composition (% dry matter)						
Starch[5]	-	-	40.4	-	-	37.4
Crude protein (N x 6.25)	-	-	20.5	-	-	20.7
NSP[6]	-	-	21.0	-	-	18.6
AX[7]	-	-	5.0	-	-	3.4
Analyzed enzyme activity (of enzyme-supplemented diets)						
Xylanase (EPU[8]/kg feed)	-	-	1550	-	-	1740
Cellulase (CU[9]/kg feed)	-	-	240	-	-	190

[1]CP: Crude protein. [2]Provided by Huvepharma NV, Berchem, Belgium. [3] Providing per kg of diet: vitamin A (retinyl acetate), 10000 IU; vitamin D3 (cholecalciferol), 2500 IU; vitamin E (dl-α-tocopherol acetate), 50 mg; vitamin K3 (menadione), 1.5 mg; vitamin B1 (thiamine), 2.0 mg; vitamin B2 (riboflavin), 7.5 mg; niacin, 35 mg; D-pantothenic acid, 12 mg; vitamin B6 (pyridoxine-HCl), 3.5 mg; vitamin B12 (cyanocobalamine), 20 µg; folic acid, 1.0 mg; biotin, 0.2 mg; choline chloride, 460 mg; Fe ($FeSO_4.H_2O$), 80 mg; Cu ($CuSO_4.5H_2O$), 12 mg; Zn (ZnO), 60 mg; Mn (MnO), 85; I ($Ca(IO_3)_2$), 0.8 mg; Co ($Co_2CO_3(OH)_2$), 0.77 mg; Se (Na_2O_3Se), 0.15 mg. [4]Used as acid insoluble ash (AIA) digestibility marker (Franz Bertram GmbH, Hamburg, Germany). [5]Determined according to AOAC Method 996.11 (KOH format). [6]NSP: non-starch polysaccharides; calculated as the difference between Total Carbohydrates (determined according to Englyst and Cummings (1984) and Starch. [7]Calculated as the sum of arabinosyl (Ara) and xylosyl (Xyl) units. [8]Amount of enzyme which releases 0.0083 µmol of reducing sugars (xylose equivalent) per minute from oat spelt xylan at pH 4.7 and 50 °C. [9]Amount of enzyme which releases 0.128 µmol of reducing sugars (glucose equivalents) per minute from barley β-glucan at pH 4.5 and 30 °C.

6

Table S2. Identity and structural classification of lignin-derived pyrolysis products included in the ^{13}C-IS py-GC-HR-MS analysis of WUS samples.

Compound	CAS	Retention time (min)	Structural feature	Sidechain length	M_w [12]C ($g \cdot mol^{-1}$)	Quan ion [12]C [M-e]
guaiacol	90051	10.03	G, unsub.	0	124	124.05188
4-methylguaiacol	93516	12.71	G, methyl	C_α	138	138.06753
4-ethylguaiacol	2785899	14.83	G, misc.	C_β	152	137.05971
4-vinylguaiacol	7786610	16.29	G, vinyl	C_β	150	150.06753
syringol	91101	17.64	S, unsub.	0	154	154.06245
trans-isoeugenol	97541	19.50	G, misc.	C_γ	164	164.08318
4-methylsyringol	6638057	19.86	S, methyl	C_α	168	168.07810
vanillin	121335	19.99	G, C_α-O	C_α	152	151.03897
4-ethylsyringol	14059928	21.58	S, misc.	C_β	182	167.07022
acetovanillone	498022	21.89	G, C_α-O	C_β	166	151.03897
4-vinylsyringol	28343228	22.90	S, vinyl	C_β	180	180.07810
guaiacylacetone	2503460	23.10	G, C_β-O	C_γ	180	137.05971
4-allylsyringol	6627889	23.31	S, misc.	C_γ	194	194.09373
trans-4-propenylsyringol	26624135	25.72	S, misc.	C_γ	194	194.09373
syringaldehyde	134963	26.34	S, C_α-O	C_α	182	182.05736
cis-coniferyl-alcohol	458355	26.42	G, C_γ-O	C_γ	180	137.05971
acetosyringone	2478388	27.76	S, C_α-O	C_β	196	181.04954
trans-coniferyl alcohol	458355	28.11	G, C_γ-O	C_γ	180	137.05971
syringylacetone	19037582	28.68	S, C_β-O	C_γ	210	167.07027
trans-sinapyl alcohol	537337	33.31	S, C_γ-O	C_γ	210	167.07027
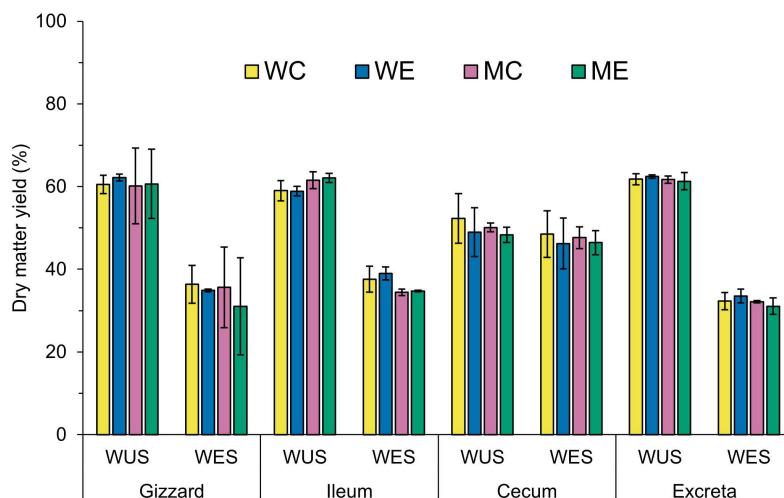
Fig. S1. Dry matter yield (%) after aqueous extraction of digesta from the gizzard, ileum, ceca and excreta corresponding to wheat control (WC), wheat enzyme (WE), maize control (MC) and maize enzyme (ME) diets; WUS: water unextractable solids; WES: water extractable solids. Error bars indicate standard deviation of biological triplicates ($n = 3$).

6

Table S3. Constituent monosaccharide composition (mol %), Ara/Xyl ratio and total carbohydrate (Tot), arabinoxylan (AX: Ara + Xyl) and glucan (Glc) content (% w/w) of WUS obtained from the diet (WUS$_{Feed}$), gizzard (WUS$_{Giz}$), ileum (WUS$_{Ile}$), ceca (WUS$_{Cec}$) and excreta (WUS$_{Exc}$) (n = 3) corresponding to wheat control (WC), wheat enzyme (WE), maize control (MC) and maize enzyme (ME) diets. Standard deviation (n = 3) is given within brackets.

Diet	Constituent monosaccharide composition (mol %)							Ara/Xyl	Carbohydrate content (% w/w)		
	Ara	Xyl	Glc	Gal	Man	Rha	UA		Tot	AX	Glc
WUS$_{Giz}$											
WC	14	22	49	6	3	1	6	0.6	55.3	17.0	29.2
	(2)	(7)	(10)	(<1)	(1)	(<1)	(<1)	(0.1)	(3.2)	(3.6)	(7.3)
WE	16	27	39	7	3	1	7	0.6	48.7	18.4	20.6
	(1)	(2)	(4)	(1)	(<1)	(<1)	(1)	(0.1)	(1.9)	(1.0)	(2.6)
MC	11	15	57	6	2	1	7	0.7	61.9	13.4	37.3
	(2)	(3)	(9)	(2)	(1)	(<1)	(1)	(0.1)	(3.8)	(2.5)	(8.0)
ME	11	16	56	6	2	1	7	0.7	62.7	14.4	36.9
	(2)	(4)	(9)	(1)	(1)	(<1)	(2)	(0.1)	(6.2)	(1.8)	(8.9)
WUS$_{Ile}$											
WC	20	28	28	11	2	1	8	0.7	50.4	21.7	15.3
	(1)	(1)	(3)	(1)	(<1)	(<1)	(1)	(0.0)	(1.6)	(0.9)	(1.7)
WE	21	26	24	13	3	1	10	0.8	48.0	20.3	12.8
	(<1)	(2)	(<1)	(1)	(<1)	(<1)	(<1)	(0.1)	(1.0)	(0.3)	(0.4)
MC	22	20	23	18	2	1	14	1.1	52.3	18.9	12.9
	(<1)	(1)	(1)	(1)	(<1)	(1)	(<1)	(0.1)	(1.2)	(0.1)	(0.8)
ME	21	21	22	17	2	1	14	1.0	52.9	19.5	12.8
	(1)	(2)	(3)	(<1)	(<1)	(<1)	(<1)	(0.1)	(1.8)	(0.1)	(2.1)
WUS$_{Cec}$											
WC	3	9	47	15	2	16	8	0.4	12.3	1.2	6.0
	(<1)	(4)	(6)	(1)	(<1)	(1)	(<1)	(0.1)	(0.9)	(0.4)	(0.6)
WE	2	2	53	16	2	18	7	0.9	12.3	0.4	6.8
	(<1)	(1)	(6)	(3)	(1)	(1)	(2)	(0.2)	(2.9)	(0.1)	(2.3)
MC	1	2	54	14	2	18	8	0.7	9.4	0.3	5.2
	(1)	(1)	(3)	(1)	(<1)	(2)	(1)	(0.2)	(1.2)	(0.2)	(0.7)
ME	1	2	51	16	2	19	9	0.8	9.1	0.2	4.7
	(<1)	(<1)	(7)	(3)	(<1)	(3)	(2)	(0.1)	(1.4)	(0.1)	(1.2)
WUS$_{Exc}$											
WC	19	25	33	11	2	1	8	0.8	51.8	20.0	18.5
	(1)	(1)	(3)	(1)	(<1)	(<1)	(1)	(0.0)	(3.9)	(1.3)	(3.2)
WE	20	24	29	13	2	1	9	0.8	44.5	17.3	14.4
	(1)	(1)	(4)	(1)	(<1)	(<1)	(<1)	(0.0)	(1.9)	(0.3)	(2.0)
MC	21	22	23	16	2	1	13	0.9	49.9	17.0	13.0
	(<1)	(2)	(2)	(<1)	(<1)	(<1)	(1)	(0.1)	(1.0)	(3.6)	(1.4)
ME	21	23	23	15	2	1	14	0.9	49.4	18.4	13.2
	(<1)	(1)	(<1)	(1)	(<1)	(<1)	(1)	(0.0)	(0.8)	(1.0)	(0.9)

Table S4. Lignin content (% w/w) in WUS obtained from the diet (WUS$_{Feed}$), gizzard (WUS$_{Giz}$), ileum (WUS$_{Ile}$), ceca (WUS$_{Cec}$) and excreta (WUS$_{Exc}$) (n = 3) corresponding to wheat control (WC), wheat enzyme (WE), maize control (MC) and maize enzyme (ME) diets, and determined based on lignin-specific pyrolysis products (Table S1) by ^{13}C-IS pyrolysis-GC-MS and excluding H-units.

Diet	Lignin content (% w/w), excluding H–units				
	WUS$_{Feed}$[1]	WUS$_{Giz}$	WUS$_{Ile}$	WUS$_{Cec}$	WUS$_{Exc}$
WC	0.4	5.2	2.8	0.2	1.9
WE	0.5	5.6	3.0	0.2	1.8
MC	0.7	6.4	3.5	0.2	3.1
ME	0.4	7.5	2.7	0.2	2.4
SEM[2]	0.1	0.9	0.4	<0.1	0.3
p value	0.205	0.417	0.577	0.513	0.050

[1]Mean values of analytical triplicates. [2]Standard error of the mean
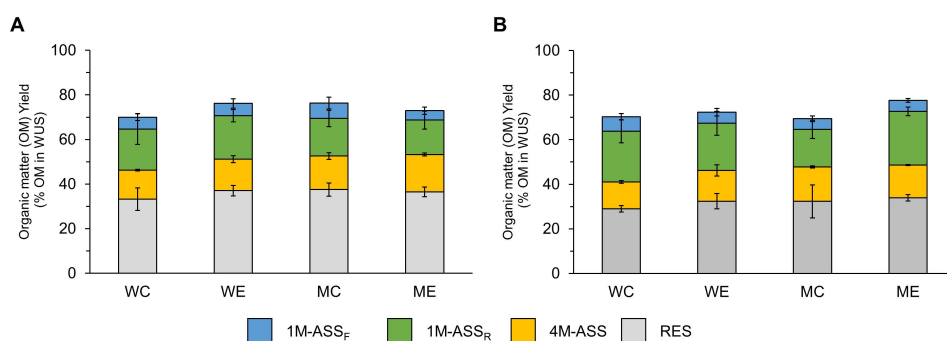
Fig. S2. Organic matter (OM) yield expressed as percentage (%) of OM in WUS recovered in 1M-ASS$_F$, 1M-ASS$_R$, 4M-ASS and RES during sequential alkali extraction of WUS$_{Ile}$ (**A**) and WUS$_{Exc}$ (**B**) corresponding to wheat control (WC), wheat enzyme (WE), maize control (MC) and maize enzyme (ME) diets.

6

Table S5. Glucan recovery in alkali extracts (1M-ASS$_F$, 1M-ASS$_R$, 4M-ASS) and residue (RES) expressed as percentage (%) of Glc units in WUS$_{Ile}$ and WUS$_{Exc}$ corresponding to wheat control (WC), wheat enzyme (WE), maize control (MC) and maize enzyme (ME) diets.

Diet	Glucan recovery (% Glc in WUS)				
WUS$_{Ile}$	**1M-ASS$_{F\_Ile}$**	**1M-ASS$_{R\_Ile}$**	**4M-ASS$_{Ile}$**	**RES$_{Ile}$**	**Losses[1]**
WC	0.7[b]	12.2	7.0	68.2	11.9
WE	0.8[b]	16.2	8.2	87.8	-13.0
MC	1.3[a]	13.5	8.2	94.6	-17.7
ME	1.0[ab]	10.8	7.5	90.7	-10.0
SEM[2]	0.1	2.1	0.4	7.2	7.8
p value	0.017	0.394	0.169	0.118	0.107
WUS$_{Exc}$	**1M-ASS$_{F\_Exc}$**	**1M-ASS$_{R\_Exc}$**	**4M-ASS$_{Exc}$**	**RES$_{Exc}$**	**Losses[1]**
WC	1.0	18.3	3.5	55.2[c]	21.9[a]
WE	1.2	20.2	4.3	72.6[b]	1.7[b]
MC	1.0	10.5	4.7	98.6[a]	-14.9[bc]
ME	1.4	14.0	4.8	95.9[a]	-16.1[c]
SEM	0.2	3.0	0.4	3.8	3.9
p value	0.285	0.185	0.156	<0.001	<0.001

[1]Estimated by the difference between total AX in WUS and the sum of AX recovered in the different fractions. [2]Standard error of the mean, $n = 3$.

Table S6. Constituent monosaccharide composition (mol %) and total carbohydrate content (% w/w, OM basis) of alkali extracts (1M-ASS$_F$, 1M-ASS$_R$, 4M-ASS) and alkali unextractable residue (RES) obtained from WUS$_{Ile}$ corresponding to wheat control (WC), wheat enzyme (WE), maize control (MC) and maize enzyme (ME) diets. Standard deviation (n = 3) is given within brackets.

WUS$_{Ile}$	Diet	Ara	Xyl	Glc	Gal	Man	Rha	UA	Ara/Xyl	Total sugars % OM
1M-ASS$_F$	WC	12	8	31	27	21	1	ND	1.4	8.6
		(1)	(1)	(6)	(2)	(3)	(0)	–	(0.1)	(3.6)
	WE	13	10	26	25	24	1	ND	1.3	9.0
		(0)	(1)	(3)	(1)	(2)	(0	–	(0.1	(3.0)
	MC	7	2	41	28	21	1	ND	3.6	8.3
		(1)	(1)	(0)	(5)	(3)	(0)	–	(0.5)	(1.8)
	ME	8	2	40	24	24	1	ND	3.8	11.6
		(1)	(0)	(0)	(2)	(1)	(<1)	–	(0.3)	(5.0)
1M-ASS$_R$	WC	23	41	18	14	3	1	ND	0.6	65.2
		(3)	(6)	(4)	(2)	(<1)	(1)	–	(0.1)	(14.3)
	WE	23	39	18	16	3	1	ND	0.6	63.5
		(4)	(6)	(4)	(5)	(1)	(1)	–	(0.2)	(14.4)
	MC	27	31	17	20	3	2	ND	0.9	71.3
		(1)	(2)	(2)	(<1)	(<1)	(<1)	–	(<0.1)	(17.5)
	ME	27	29	17	22	4	2	ND	0.9	67.8
		(1)	(<1)	(2)	(1)	(<1)	(<1)	–	(<0.1)	(16.4)
4M-ASS	WC	32	28	13	21	4	2	ND	1.1	69.4
		(<1)	(<1)	(<1)	(1)	(<1)	(<1)	–	(<0.1)	(11.7)
	WE	32	27	13	22	4	3	ND	1.2	74.1
		(<1)	(1)	(1)	(1)	(<1)	(<1)	–	(<0.1)	(12.2)
	MC	32	28	11	24	3	3	ND	1.2	78.5
		(1)	(1)	(1)	(1)	(<1)	(<1)	–	(0.1)	(11.3)
	ME	33	28	11	24	3	3	ND	1.2	78.3
		(<1)	(<1)	(<1)	(<1)	(<1)	(<1)	–	(<0.1)	(11.3)
RES	WC	19	18	50	3	1	<1	9	1.0	59.4
		(1)	(1)	(<1)	(<1)	(<1)	(<1)	0	(0.1)	(2.2)
	WE	19	18	49	4	<1	<1	10	1.1	58.9
		(1)	(2)	(<1)	(1)	(<1)	(<1)	0	(0.1)	(1.5)
	MC	14	15	52	6	0	1	11	1.0	62.7
		(<1)	(2)	(2)	(<1)	(<1)	(<1)	0	(0.2)	(5.6)
	ME	14	16	51	6	1	1	11	0.9	63.5
		(<1)	(<1)	(1)	(1)	(<1)	(<1)	0	(<0.1)	(4.1)

6

Table S7. Constituent monosaccharide composition (mol %) and total carbohydrate content (% w/w, OM basis) of alkali extracts (1M-ASS$_F$, 1M-ASS$_R$, 4M-ASS) and alkali unextractable residue (RES) obtained from WUS$_{Exc}$ corresponding to wheat control (WC), wheat enzyme (WE), maize control (MC) and maize enzyme (ME) diets. Standard deviation (n = 3) is given within brackets.

WUS$_{Exc}$	Diet	Ara	Xyl	Glc	Gal	Man	Rha	UA	Ara/Xyl	Total sugars % OM
1M-ASS$_F$	WC	11	7	42	21	18	1	ND	1.4	7.7
		(1)	(1)	(6)	(2)	(2)	(<1)	–	(<0.1)	(2.6)
	WE	11	8	37	21	21	1	ND	1.3	11.4
		(1)	(<1)	(4)	(3)	(1)	(<1)	–	(0.1)	(3.8)
	MC	8	2	41	22	26	1	ND	4.1	11.1
		(<1)	(<1)	(2)	(1)	(1)	(<1)	–	(0.8)	(2.6)
	ME	9	2	41	21	25	1	ND	3.7	8.9
		(<1)	(<1)	(3)	(2)	(2)	(<1)	–	(0.4)	(4.0)
1M-ASS$_R$	WC	20	35	30	13	2	1	ND	0.6	53.8
		(2)	(9)	(4)	(3)	(<1)	(<1)	–	(0.2)	(17.0)
	WE	23	31	26	17	3	1	ND	0.8	61.4
		(4)	(5)	(5)	(4)	(1)	(<1)	–	(0.2)	(16.1)
	MC	28	30	18	20	3	2	ND	0.9	55.7
		(1)	(1)	(2)	(1)	(<1)	(<1)	–	(<0.1)	(16.6)
	ME	27	30	19	19	3	1	ND	0.9	39.9
		(1)	(30	(5)	(1)	(<1)	(<1)	–	(0.1)	(12.0)
4M-ASS	WC	32	28	14	18	3	3	ND	1.1	41.8
		(<1)	(1)	(<1)	(1)	(<1)	(1)	–	(<0.1)	(8.9)
	WE	31	27	16	19	4	3	ND	1.2	67.6
		(1)	(1)	(1)	(1)	(<1)	(<1)	–	(0.1)	(3.0)
	MC	33	28	11	22	3	3	ND	1.2	85.6
		(<1)	(2)	(<1)	(1)	(<1)	(1)	–	(0.1)	(0.8)
	ME	33	30	11	21	2	3	ND	1.1	88.5
		(1)	(2)	(<1)	(1)	(<1)	(<1)	–	(0.1)	(6.2)
RES	WC	18	18	52	3	<1	<1	9	1.0	61.0
		(1)	(1)	(<1)	(<1)	(<1)	(<1)	(<1)	(<0.1)	(2.1)
	WE	19	18	51	3	<1	<1	9	1.0	60.2
		(<1)	(1)	(<1)	(<1)	(<1)	(<1)	(<1)	(<0.1)	(4.9
	MC	13	17	54	5	<1	1	11	0.8	64.7)
		(<1)	(1)	(1)	(10	(<1)	(<1)	(1)	(<0.1)	(2.7)
	ME	13	17	55	4	1	1	11	0.8	66.0
		(<1)	(<1)	(1)	(<1)	(<1)	(<1)	(<1)	(<0.1)	(6.6)

Supplementary information references

1.   Kouzounis D, Hageman JA, Soares N, Michiels J, Schols HA. Impact of xylanase and glucanase on oligosaccharide formation, carbohydrate fermentation patterns, and nutrient utilization in the gastrointestinal tract of broilers. Animals. 2021;11(5):1285.

Chapter

7

General Discussion

1 General discussion outline

In this chapter, the outcomes of the experimental work presented in **Chapters 2-6** are discussed in context of recent literature findings and literature presented in **Chapter 1**. The aim of this thesis research was to elucidate, at a molecular level, the impact of dietary non starch polysaccharide (NSP)-active enzymes on the fate and fermentability of NSP in the broiler gastrointestinal tract (GIT). The main findings of the research are discussed in four subsections: (i) Application of advanced analytical techniques to characterize *in vivo* generated arabinoxylo-oligosaccharides (AXOS), (ii) The significance of AXOS release by endo-xylanase *in vivo*, (iii) Looking beyond the prebiotic effect: nutrient de-encapsulation by NSPases, (iv) The future role of NSP and NSPases in animal nutrition.

2 Application of advanced analytical techniques to characterize *in vivo* generated AXOS

2.1 Oligosaccharide screening by MALDI-TOF-MS

As outlined in **Chapter 1**, until the start of this thesis research, direct evidence of AX degradation by dietary xylanase taking place during feed digestion was lacking. In this research (**Chapter 2**), arabinoxylan (AX) degradation by dietary endo-xylanase taking place in the upper GIT was substantiated for the first time, by the recognition of AX-derived oligosaccharides having a DP of 5-26 by MALDI-TOF-MS. At the time of submission of our findings for publication, Lin & Olukosi (2021) reported the presence of DP 3-6 xylo-oligosaccharides (XOS) by MALDI-TOF-MS, in the broiler jejunum (1). In their study, sample clean up followed by permethylation was used to improve the signal of oligosaccharides. In comparison, we demonstrate that minimum sample preparation and short analysis time make MALDI-TOF-MS a powerful tool for oligosaccharide screening in animal digesta. Therefore, MALDI-TOF-MS can be used to strengthen NSP characterization in digesta samples next to sugar composition analysis. The present findings add to the already wide range of MALDI-TOF-MS applications regarding the analysis of oligosaccharides in complex matrices without the need of elaborate sample pre-treatment. Such complex matrices include beer, industrial fermentation slurry, lab scale fermentation broth and xylan digests by termite hindgut homogenate (2–5). In spite of being a powerful screening method, MALDI-TOF-MS cannot provide in-depth structural analysis of isomeric oligosaccharides. In addition, quantification by MALDI-TOF-MS is riddled with serious limitations especially when analytes are present in complex samples (6–10), such as animal digesta. Consequently, novel sample clean-up and LC-MS approaches for the comprehensive oligosaccharide analysis in complex digesta matrices were cautiously developed and elaborated in **Chapter 4, 5**.

2.2 Unambiguous AXOS characterization in digesta

In **Chapter 4**, we introduced a strategy to identify individual AXOS in enzymatic digests of arabinoxylan (AX) by HILIC-MS^n analysis, preceded by oligosaccharide reduction. The utter aim was to implement this technique for the identification and structural characterization of AXOS formed *in vivo* (**Chapter 5**), as exemplified in Fig 1. AXOS could be clearly detected in digesta by MALDI-TOF-MS (Fig. 1A; **Chapter 2**), but their precise structure could not be further investigated. The same AXOS were amply resolved and characterized by HILIC-MS^n (Fig. 1B; **Chapter 5**). Moreover, by using the newly developed strategy, unknown (A)XOS were identified despite the absence of standards (**Chapter 4**). Overall, the detailed AXOS characterization obtained by HILIC-MS^n showcased the importance of implementing a robust and sophisticated technique for digesta analysis.
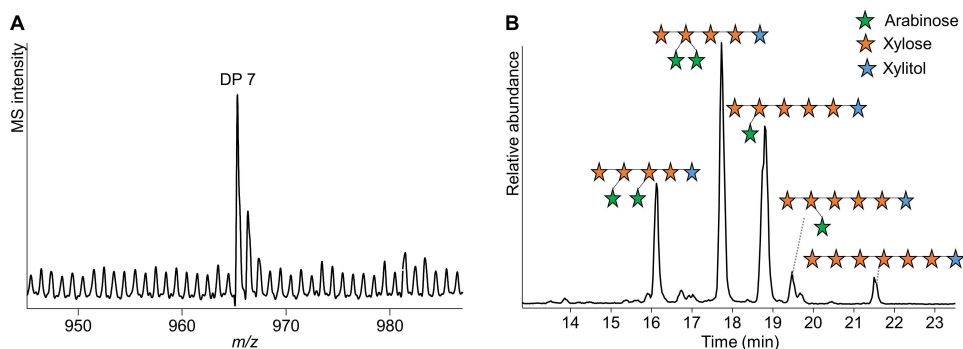
Fig. 1. Part of a MALDI-TOF mass spectrum (**A**) of digesta from the broiler ileum showing DP 7 ([M + Na]$^+$) pentose oligosaccharide(s) as one peak (**Chapter 2**). HILIC-MS ion extracted chromatogram (**B**) of the same sample after SPE (**Chapter 5**), resolving the presence of five isomeric (NaBH$_4$-reduced) DP 7 (A)XOS ([M − H]$^-$).

The applicability of the current HILIC-MS^n strategy for the analysis of a wide range of AXOS isomers was established by the clear relationship between oligosaccharide structure and elution time in HILIC (Fig. 2). Groups of (A)XOS sharing structural features (number, position, linkage type of Ara substituents) presented linear relationships between DP and retention time (RT). This relationship can now be further used for the identification of (unknown) (A)XOS present in mixtures. It should further be noted that NaBH$_4$ reduction was crucial for (A)XOS identification by the new HILIC-MS^n strategy (**Chapter 4**). In particular, reduction helped distinguishing fragments from the reducing (Y/Z fragment ions) or non-reducing ends (B/C fragment ions) (11). Interestingly, reduced AXOS presented different MS^2 spectra than underivatized ones, mainly documented by the low intensity of C ions. The same behavior has been previously observed for cello-oligosaccharides, galacto-oligosaccharides and *O*−linked mucin oligosaccharides (12–15).

	Slope	Intercept	R²
Multiple Single	3.9	-11.1	1.00
Terminal, single *O*-3	3.4	-6.0	1.00
Double	4.2	-11.5	0.99
Internal *O*-3	3.7	-6.9	1.00
Internal *O*-2	3.7	-6.2	1.00
Linear	3.6	-3.6	1.00
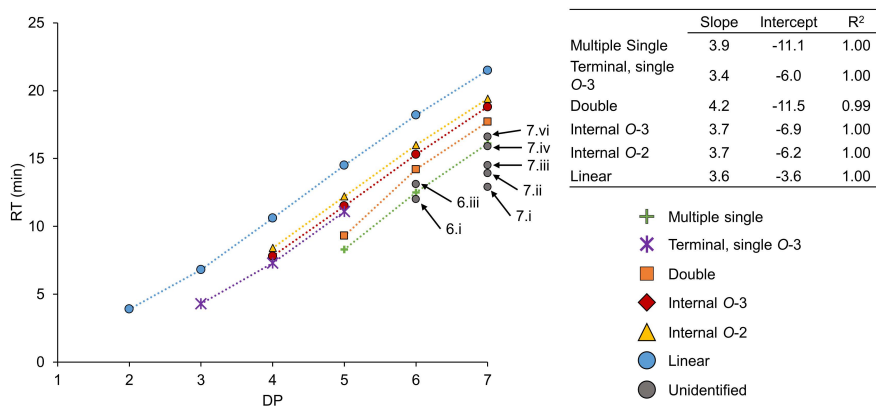
Fig. 2. Overview of the elution pattern of $NaBH_4$-reduced AXOS isomers (DP 2-7) identified in **Chapter 4**. Identified AXOS were grouped according to the presence of: multiple single substitutions (✚), single *O*-3-linked Ara at the non-reducing terminal Xyl (✳), double *O*-2,3-linked Ara (■), single *O*-3-linked Ara at an internal Xyl residue (◆), single *O*-2-linked Ara at an internal Xyl residue (△). Linear XOS (●) and unidentified AXOS (●) are also displayed. Unidentified DP 6,7 AXOS were labelled according to their elution order (i-vi). RT (min) is the HILIC-MS^n retention time in minutes.

To put our developed strategy for $NaBH_4$-reduced (A)XOS analysis into a broader context, it was compared with other LC-MS-based approaches used in the analysis of AXOS (Table 1) and other glycans (10,11,15–20). It can be seen that early LC-MS studies used reverse phase (RP) and normal phase (NP) chromatography for AXOS separation, followed by positive ion mode (PI) MS analysis. However, HILIC and porous-graphitized carbon chromatography (PGC) are the preferred separation modes for glycan analysis in recent studies (10,12,14,19–21). In particular, HILIC offers better separation and MS compatibility for glycan analysis compared to RP (C18) and other NP modes (16,22). Furthermore, oligosaccharide MS analysis in negative ion mode (NI) appears more commonly in the recent literature, due its ability to provide more structural information compared to PI (16,22,23). Utilization of MS^2 and MS^3 dimensions are crucial for the detailed AXOS characterization (15,19), as confirmed in the present study (**Chapter 4**).

The distinct MS fragmentation patterns of reduced oligosaccharides distinguished the MS-based identification developed in this thesis (**Chapter 4**) from previously published methods for AXOS analysis (15,19,20,24). Previous studies based the identification of underivatized AXOS in NI on the presence or absence of unique ions resulting from double cleavages (15,23,24). However, reduced AXOS generated diagnostic fragment ions whose relative abundance ratios in both MS^2 and MS^3 were indicative of oligosaccharide structure.

Table 1. Comparison of the different LC-MS methods reported in literature for AXOS identification. Literature references indicated between brackets.

LC	RP[1] (C18)	NP[2]	HILIC	HILIC	HILIC
Ion Mode	Positive	Positive	Negative	Negative	Negative
Ionization	ESI	MALDI[3]	ESI	ESI	ESI
MS[n] dimension(s)	2-4	2	2	2-3	2-3
Derivatization	Per-methylation	Reductive amination	TEMPO, Fenton oxidation	None	NaBH$_4$-reduction
Substrate	Xylanase digest from switchgrass	Xylanase digest from wheat AX	(A)XOS standards & xylanase digest from wheat AX	(A)XOS standards	(A)XOS standards & xylanase digest from wheat AX
Outcome	Separation and identification of DP 3-9 AXOS	Separation and identification of DP 4-8 AXOS	Characterization of oxidized (A)XOS	MS-based identification between DP 3-6 isomers	Separation and identification of DP 3-7 AXOS
Main limitations	Not optimal LC and MS conditions for glycan analysis	Identification based on unique fragments	Poor LC resolution, limited DP identification	Identification based on unique ions & previous studies	More standards required for identification of complex AXOS
	(19)	(10)	(20)	(15)	This thesis (Chapter 4)

[1]Reverse phase. [2]Normal phase. [3]Offline coupling

Overall, the present study contributes to an increasing volume of research focusing on oligosaccharide analysis by HILIC-MS[n] (12,15,20,21,25,26) and solidifies this technique for AXOS analysis. Finally, the strategy presented in **Chapter 4** can be further developed in future research. For instance, the current spectral library (**Chapter 4**) can be expanded by AXOS originating from AXs with different Ara-substitution patterns than wheat AX (e.g., maize, rice, sorghum) (27–32). Next to AXOS, the present HILIC-MS[n] approach can be applied to identify heteroxylo-oligosaccharides substituted by more complex side chains (e.g., xylosyl units and oligomeric arabinosyl side chains) or by acetyl, *O*-methyl-glucuronosyl, feruloyl and galactosyl substituents (27,30–33). The present work provides experimental evidence regarding the influence of reduction on oligosaccharide MS fragmentation patterns, in line with previous research (12,13), but cannot explain this behavior. Therefore, more fundamental research should be carried out to elucidate the underlying mechanism. This way, the fragmentation of reduced oligosaccharides could be predicted and theoretical differences between isomers could be modelled, resulting in more systematic structural characterization. All the above will contribute to the robustness of this method, making it applicable for the structural characterization and sequencing of various polysaccharides as well as for studying the mode of action of several carbohydrate-active enzymes. As a critical reflection, it should be noted that, although semi-quantification of reduced AXOS is facilitated by baseline HILIC separation (**Chapter 4**), absolute quantification of glycans still depends on the use of standards and fluorescent labels (16,34–36).

7

2.3   AXOS extraction from digesta

Analysis of *in vivo* formed AXOS could not be directly performed by our newly developed HILIC-MS^n method due to the complexity of the digesta matrix. To address this issue, we successfully isolated AX and AXOS species from broiler digesta using RP C18 solid phase extraction (SPE). At the same time, maltodextrins, fructans and raffinose oligosaccharides were removed by SPE, after their enzymatic degradation to monosaccharides (**Chapter 5**). Overall, AXOS isolation by SPE enabled their unambiguous monitoring by HPSEC-RI, HPAEC-PAD and eventually, their identification by HILIC-MS^n.

Oligosaccharide purification by SPE is mainly performed with two types of chromatography packings: the aforementioned RP C18 and non-porous graphitized carbon (nPGC) (37). In our research, both nPGC and RP C18 were tested to separate monosaccharides (i.e., glucose) from (A)XOS and AX. Both packings were successful in removing Glc with water and completely recovering AXOS by elution with increasing solvent strength (C18: 30% methanol, nPGC: 40% acetonitrile). Similar observations were described by Jonathan et al. (2017) regarding the separation of neutral AXOS with RP C18-SPE from fermented corn stover, and by Redmond and Packer (1999) for the Glc removal with water and elution with water-ACN solution of oligosaccharides by nPGC (3,38). An advantage of nPGC over RP C18 was the elution of DP 2-4 XOS together with AXOS. In contrast, small XOS were removed together with glucose in the water elution step from the C18-SPE. Still, C18-SPE was able to recover ~50% of polymeric AX loaded in the column and to completely recover AXOS (**Chapter 5**). On the contrary, polymeric AX could not be eluted from the nPGC packing and was insoluble in 40% ACN. Consequently, RP C18 was selected for SPE, as presented in **Chapter 5**.

Replacing RP C18 cartridges with nPGC ones could be viewed as an alternative approach to the one described in **Chapter 5** in order to isolate both AXOS and XOS from animal digesta. In such case, soluble polymers could be precipitated in 70-80% ethanol, while the oligosaccharides (~ DP <12) that remain in solution (3,27,39,40), could be further isolated from salts and monosaccharides by nPGC-SPE. Graded ethanol precipitation was previously used by Lærke et al. (2015) to indirectly estimate oligosaccharide release by dietary endo-xylanase in the ileum of pigs (41). However, addition of an extra fractionation step can result in an unfeasible, tedious procedure and in considerable sample loss. Therefore, isolation protocols as the one in **Chapter 5** that enable the comparison between treatments (e.g. control vs. enzyme-supplemented diet) should ultimately be preferred.

2.4   Toward AXOS quantification *in vivo*

In addition to (A)XOS detailed identification, monitoring (A)XOS fate throughout the GIT in a quantitative manner by using digestibility markers is also highly important to investigate (A)XOS biofunctionality. Acid insoluble ash (AIA) is a commonly used marker, that was currently added to the diet to monitor the digestibility and hindgut recovery of the main feed fraction (**Chapter 2**), and was

used to estimate the recovery of water-extractable and water-unextractable AX populations in the ileum and excreta (**Chapter 5**). Nevertheless, a limitation of this approach was that AX recovery could only be based on its structural units (i.e., arabinosyl and xylosyl) after acid hydrolysis, as commonly performed, which means that most structural information is lost. Therefore, (individual) AXOS content and recovery could not yet be defined.

The use of markers is intricate due to digesta heterogeneity, different transit of soluble and insoluble feed fractions and occurrence of reflux throughout the GIT (42–44). In particular, soluble compounds can demonstrate different transit in the GIT than insoluble ones. Consequently, the use of a soluble marker could improve monitoring of the transit of *in vivo* released AXOS (42). Even more so, using soluble markers that can be quantitatively recovered from SPE phases used for oligosaccharide isolation, such as polyethylene glycol (45), can be foreseen advantageous to fully integrate advanced analysis of both qualitative and quantitative determination of carbohydrates in animal digesta.

3   The significance of AXOS release by endo-xylanase *in vivo*

3.1   AXOS formation in the upper GIT

In this thesis, we unambiguously demonstrated the ability of a dietary GH11 endo-xylanase to form AXOS of varying structure throughout the upper GIT of broilers (**Chapter 2,5**). Moreover, we provided solid evidence regarding the beneficial impact of enzyme supplementation for animal growth, nutrient digestion and hindgut fermentation (**Chapter 2,3**). Based on our findings, we argue that the magnitude of AXOS release by endo-xylanase during feed digestion is significant, and can positively impact broiler health. This conclusion was based on the structural determination of (A)XOS achieved by various analytical techniques (MALDI-TOF-MS, HPSEC, HPAEC, HILIC-MS^n) and was combined with the quantitative, marker-based determination of the extent of AX/AXOS utilization in the GIT (**Chapter 2,5**).

To further investigate the magnitude of AXOS release by dietary endo-xylanase, additional *in vitro* experiments were carried out (Box 1) using the same enzymes as used *in vivo*. Hereto, endo-xylanase preparation also containing endo-glucanase side-activity (HX) was added to isolated cell wall material from wheat (Fig. 3, 6) and maize (Fig. 7). AX/AXOS released (solubilized) under conditions mimicking digestion in the upper GIT of poultry were identified and quantified. The data obtained for wheat (Fig. 3, 6) was compared with the observations made *in vivo* for the gizzard and ileum (**Chapter 5**).

Box 1: *In vitro* digestion study of alcohol insoluble solids (AIS) from wheat and maize

Materials
Alcohol insoluble solids (AIS) were prepared by incubating whole wheat and maize grains with starch- and protein-degrading enzymes, followed by NSP precipitation in 70% ethanol. The enzymes used were a commercially available GH11 endo-xylanase (HX) and a pure GH7 endo-glucanase (Cel7).

***In vitro* digestion protocol**
AIS (100 mg) was incubated without (Unt) or with the addition of HX, Cel7 and their combination under conditions mimicking the broiler digestive tract. Each enzyme was added at 0.125 $\mu g_{protein}$/mL, and the final volume was 10 mL. In brief, samples were incubated for the first 60 min under gastric conditions (stomach - ST: pH 3.2, 40 ºC), followed by small intestine conditions (SI: pH 6.5, 40 ºC) for a total digestion time of 480 min. Digestive enzymes were omitted as they did not impact xylanase activity (Fig. 3B). Aliquots of soluble material were removed at 30, 60 90, 120, 240 and 480 min and were analyzed for sugar composition (TFA hydrolsysis followed by HPAEC analysis), and oligosaccharides (HPAEC and MALDI-TOF-MS).

Under the present experimental *in vitro* conditions, GH11 endo-xylanase (HX) released ~16% AX/AXOS during the gastric phase (ST: 60 min) from wheat AIS. Almost the same amount of AX was solubilized in Untr, when no enzyme was added (~14%; Fig. 3A). The low pH during gastric phase (pH is 3.2) decreased endo-xylanase activity (Fig. 3B). This was expected as fungal GH11 endo-xylanases typically present pH optima around pH 5.0, while their activity is considerably reduced at lower pH values (46). This marginal AX solubilization observed *in vitro* under gastric conditions was in agreement with soluble AX depolymerization and marginal insoluble AX release observed *in vivo* in the gizzard (avian stomach) (**Chapter 5**). Hence, both approaches advocate that endo-xylanase mainly depolymerized soluble AX in the gizzard, while exhibited limited action towards insoluble, cell-wall associated AX. The present findings are in agreement with recent studies reporting that wheat cell wall degradation by endo-xylanase *in vivo,* as visualized by auto-fluorescence microscopy, occurred in the broiler crop and gizzard (47,48). All the above-mentioned findings concur that AX degradation by endo-xylanase, albeit limited, begins in the early stages of feed digestion.

HX activity toward AX profoundly increased under conditions mimicking the small intestine (SI) (Fig. 3A). Approximately ~25% and ~30% total AX was solubilized in the first 30 min (90 min total) and at the end of *in vitro* digestion (480 min total), respectively, in the presence of HX. In contrast, Untr sample presented 14-15% soluble AX in SI, similar to ST. In particular, HX released AXOS and DP 2 and DP 3 XOS (Fig. 3C), while the addition of endo-glucanase (Cel7) did not induce further AX solubilization. The action and possible implications of endo-glucanase for broilers shall be elaborated further in the discussion (see 4.1). Overall, this *in vitro* study confirmed the ability of the GH11 endo-xylanase (HX) used in the current animal study (**Chapter 2, 3, 5**) to release AXOS under conditions simulating the upper GIT. More importantly, the same endo-xylanase presented comparable extent of AX release *in vivo* (**Chapter 5**) and *in vitro* (Fig. 3D), which represented ~25% of the initial AX in both cases.
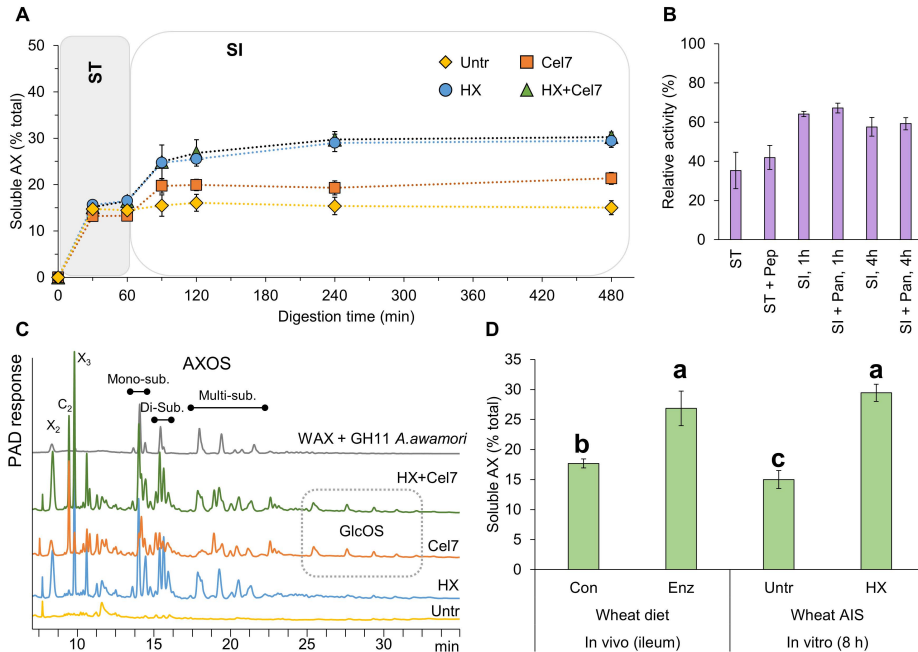
Fig. 3. AX solubilization (**A**) from wheat AIS during *in vitro* digestion without (Untr: ◇) or with the addition of endo-xylanase HX (●), endo-glucanase Cel7 (■) and HX & Cel7 (▲). Wheat arabinoxylan (WAX) hydrolysis by HX (**B**): reducing sugars release under stomach (ST) and small intestine (SI) conditions without or with addition of pepsin (ST) or pancreatin (PA), expressed as percentage (%) of the amount of reducing sugars released during WAX hydrolysis at pH 5.5, 40 ºC for 1 and 4 h. HPAEC-PAD elution patterns (**C**) of oligosaccharides released at the end of *in vitro* AIS digestion (8 h). Soluble AX (**D**) expressed as i) *in vivo:* marker-based AX (Ara + Xyl, % total AX consumed) recovery in the broiler ileum for control diet (Con) and endo-xylanase & endo-glucanase supplemented diet (Enz) reported in **Chapter 5**. ii) *in vitro*: AX % of total AX in AIS that was released at the end of *in vitro* digestion (8 h) without (Untr) and with endo-xylanase addition (HX).

Nevertheless, comparison of *in vivo* and *in vitro* studies does not always result in similar observations (Table 2). Recent *in vivo* broiler studies demonstrated that GH11 endo-xylanase supplementation in wheat diets increased soluble AX in the ileum by up to 30% compared to the corresponding control diets (49,50). In contrast, far more extensive degradation of wheat whole grains (WG) by xylanases has been reported *in vitro*, under conditions mimicking digestion (51–55). For instance, enzyme action *in vitro* increased AX solubilization by 19-250% compared to corresponding control treatments (Table 2). The high hydrolysis degree observed *in vitro* can be mainly attributed to the use of closer to optimum conditions (pH, T) for fungal endo-xylanases, prolonged incubation (2-16 h) and higher enzyme dosing compared to *in vivo* studies (56). Still, there are also examples of *in vitro* studies where the differences in released AX between untreated and xylanase-treated wheat are closer to *in vivo* observations (Table 2).

This appeared to be the case when dosing and hydrolysis times were more representative of the *in vivo* conditions.

Table 2. Relative arabinoxylan (AX) solubilization upon xylanase treatment documented in broilers (*in vivo*) or under *in vitro* digestive conditions. The effect of the enzyme is expressed as the relative change in values for soluble AX compared to the corresponding control treatments (no enzyme added).

			Dosage			Rel.	
Substrate (wheat)		**Xylanase**	**Xyn[1]**	**Gluc[2]**	**Units**	**change (%)**	**Ref**
In vivo studies: soluble AX in ileum (marker basis)							
Diet		GH11	100 (0.3)[9]	100 (0.5)[9]	mg_{prep}/kg[6]	43	This thesis
Diet		GH11	10-1000	-	mg_{prep}/kg	13-30	(49)
Diet		GH11	200	-	mg_{prep}/kg	28	(50)
Conditions	**Time (h)**	*In vitro* studies: soluble AX					
Digestive[3]	0-8	AIS GH11	12.5[10]	12.5[10]	mg_{prot}/kg[7]	6-96	This thesis
40 ºC	4	WG[4] GH11	1	-	mg_{prot}/kg	92	(51)
Digestive	2	WG N.S.[5]	1.2-12	15-150	mg_{prot}/kg	67-250	(53)
45 ºC, pH 5.2	16	WG N.S.	10	10	mg_{prep}/kg	36-43	(54)
Digestive (TIM1)	6	WG GH11 GH10	0.13	-	$\mu L/kg$[8]	40	(52)
Digestive	5	WG N.S.	2	2	mL/kg[8]	19	(57)

[1]Endo-xylanase dosage. [2]Endo-glucanase dosage. [3]Protocols involving a gastric and small intestinal phase. [4]Milled whole grains. [5]Not specified. [6]mg preparation per kg substrate, when protein content not provided. [7]mg protein per kg substrate. [8]Protein content or activity units not provided. [9]corresponding mg_{prot}/kg. [10]dosage was estimated to be 4-10 times higher than the one used during the *in vivo* study (Chapter 2).

Optimization of *in vitro* procedures will offer scientists a reliable platform to perform experiments with different combinations of NSP-active enzymes, and can thus help minimizing the number of animals being sacrificed for scientific purposes. In addition, *in vitro* digestion models like the one used in this study can contribute to the design of novel feed enzymes. Finally, the present work provides clear answers on the so far reported lack of evidence regarding AXOS formation *in vivo* (56,58). The unambiguous elucidation of the ability of dietary endo-xylanase to form AXOS *in vivo* sheds new light on the potential prebiotic effect of NSPases.

3.2 Influence of AXOS formation on hindgut fermentation

AX fermentation in broilers is governed by cereal type

The findings of **Chapter 2** and **3** clearly demonstrated that cereal type is a crucial factor determining the baseline AX fermentability in the broiler hindgut. For instance, the apparent lack of AX fermentation observed for maize diets (**Chapter 2**) was attributed to the more complex structure and lower solubility of maize AX compared to wheat AX (29,30,59–65). Therefore, AX degradability, as determined by its botanical origin, will greatly impact its role during feed digestion as well as

the ability of supplemented enzymes to work. This relationship became more evident in **Chapter 3**, by the comparison of microbiota composition in the ceca of wheat-fed and maize-fed broilers. The abundance of NSP- and AX-fermenting bacteria of the Clostridia class was higher in the wheat diets, than in the maize diets, under the current experimental conditions. An overview of the main findings described in **Chapters 2, 3, 5** and **6** is presented in Fig. 4, to better illustrate the influence of cereal on AX fermentation.
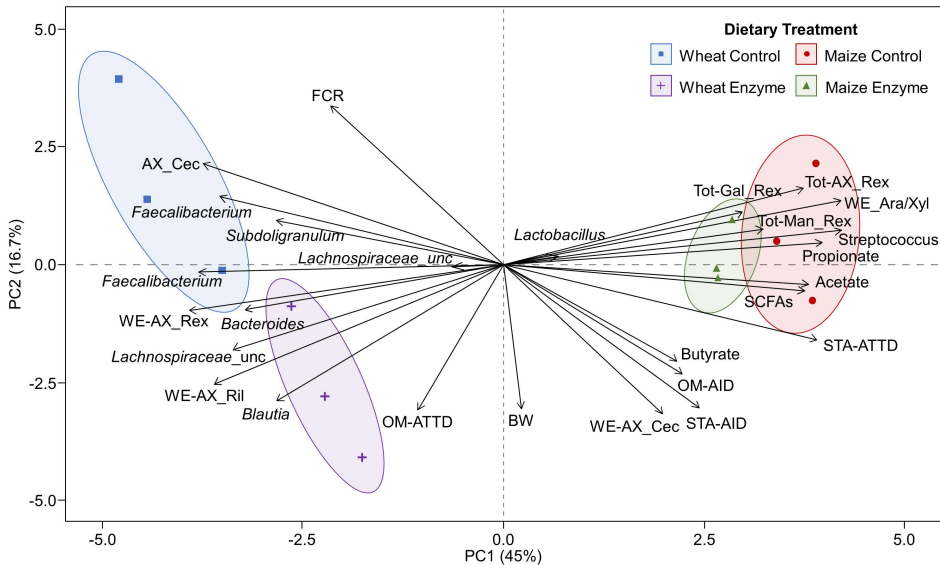
Fig. 4. Principal component analysis (PCA) biplot of wheat control (blue), wheat enzyme (purple), maize control (red), and maize enzyme (green) dietary treatments. The scores were plotted for PC1 and PC2. The amount of variance explained by each PC is shown in parentheses. The data set used was obtained from: **Chapter 2**: body weight (BW), feed conversion ratio (FCR), apparent ileal digestibility (AID) and apparent total tract digestibility (ATTD) of organic matter (OM) and starch (STA), apparent ileal (Ril) and apparent total tract (Rex) recovery of total AX, galactosyl (Gal) and mannosyl (Man) units, total AX content (% w/w) in the ceca, acetate, butyrate, propionate and total short-chain fatty acids (SCFAs) contents (% w/w) in the ceca (66), **Chapter 3:** relative abundance (%) of representative bacteria genera present in the ceca: *Lactobacillus*, *Blautia*, *Subdoligranulum*, *Bacteroides*, two *Faecalibacterium* and two uncultured Lachnospiraceae genera), **Chapter 5, 6:** water extractable AX (WE-AX) Ril and Rex and Ara/Xyl ratio of WE-AX.

Wheat and maize diets were clearly separated in the biplot (Fig. 4), demonstrating the higher content of water-extractable AX (WE-AX) in the ileum (WE-AX_Ril) and excreta (WE-AX_Rex) for wheat diets coincided with higher abundance of *Blautia*, *Bacteroides*, *Faecalibacterium*, *Subdoligranulum* and an uncultured Lachnospiraceae genera. Consequently, the higher provision of fermentable AX in wheat diets is considered important for enhanced hindgut fermentation in broilers, as demonstrated by the lower AX total tract recovery (Tot-AX_Rex) of these diets. Additionally, differences in short chain fatty acids (SCFAs) contents and

composition demonstrate that a differentiated fermentation occurs in the ceca of broilers fed wheat and maize diets (**Chapter 2**). Interestingly, despite lower AX fermentation occurring in the ceca, the maize diets presented higher SCFAs contents than wheat diets (**Chapter 2**). Variation of SCFAs contents between wheat and maize diets has been previously documented in literature, suggesting that AX alone cannot account for the entirety of cecal fermentation (67–70). Co-fermentation of Man and Gal-containing NSP appeared to proceed differently for wheat and maize diets (**Chapter 2**, Fig. 4), while the high fructan content in wheat was expected to have contributed to a different microbial ecology and fermentation (**Chapter 2, 3, 5**). Moreover, fermentation of undigested nutrients (e.g., protein) may also have contributed to SCFAs formation (71). In spite of these differences, our study and several other recent studies, do demonstrate the prevalence of AX for hindgut fermentation in broilers fed cereal-based diets (68,72,73). A systematic evaluation and side-by-side comparison of carbohydrate fermentation in broilers fed different cereals (e.g., wheat, maize, barley, oats, sorghum) during their full growth period is necessary to put the contribution of AX and other NSP into perspective.

Relevance of AXOS chemical structure for in vivo fermentation

Improved AX fermentation upon AXOS release by endo-xylanase supplementation in the wheat diet (**Chapter 2**) further impacted the cecal microbiota composition (**Chapter 3**). Our findings (i.e., Wheat Enzyme diet (Fig. 4)) pointed that dietary endo-xylanase stimulated the growth of important players involved in AX, AXOS and XOS fermentation (72–81). Such benefited microbiota were currently found to be members of *Blautia*, *Bacteroides* and uncultured Lachnospiraceae genera. This was well in line with previous studies reporting that endo-xylanase stimulated the growth of Clostridia such as Ruminonocaceae and Lachnospiraceae, next to Bacteroidetes, *Lactobacillus* and *Bifidobacterium* (72,73,75). The positive impact of AXOS and XOS provision for cecal ecology is further explained by the higher abundance in the broiler ceca of genes encoding exo-acting and debranching enzymes (β-xylosidases, arabinofuranosidases) compared to endo-xylanases (80).

Interestingly, structurally different AXOS and XOS have been shown to be fermented differently by gut microbiota, resulting in different SCFAs profiles (2,77). AXOS, feruloylated AXOS and acetylated, *O*-methyl-glucuronylated, and linear XOS were differently fermented by individual bacteria as well as bacterial consortia from human feces (2,77,79,82,83). In specific, *Bifidobacterium* and *Bacteroides* spp. have been shown to prefer DP 2-4 XOS over AXOS (60,79). The preference of bifidobacteria for small XOS over AXOS and polymeric AX could partly explain the lack of bifidobacteria detection in the present study (**Chapter 3**). Endo-xylanase was currently only supplemented in the finisher period and the *in vivo* AXOS formation seemed to mainly stimulate already developed AX/AXOS-fermenting communities (Fig. 4). The importance of such communities for SCFAs formation and optimal gut function in ageing broilers might have been overlooked in favor of more well characterized beneficial bacteria.

In this view, the observation that endo-xylanase released *in vivo* AXOS with relatively low substitution degree (**Chapter 5**) helped us to better understand the xylanase-mediated improvements regarding cecal fermentation. For example, identified DP 5-7 AXOS were substituted by one or two arabinosyl units. Hence, taking into consideration the pronounced fermentability of simple (A)XOS as demonstrated *in vitro* (2,59,82), we expect that these relatively simple AXOS did stimulate cecal fermentation. Moreover, as lower recovery (based on AX structural units; see 2.4) of the same structures of AXOS was found in excreta compared to the ileum (**Chapter 5**), most likely, no preferential utilization of specific structures occurred, in line with the low degree of AXOS substitution. Still, it is quite plausible that AXOS present in excreta cannot be considered as proxy for unfermentable structures, due to digesta reflux (42,84).

3.3   Role of AXOS in promoting animal growth

The beneficial impact of enzyme supplementation in wheat diet was highlighted by the increase in broiler weight and decrease in feed conversion ratio (Fig. 4) (**Chapter 2**). This impact of enzyme supplementation most likely resulted from two metabolic processes: improved nutrient digestion in the small intestine and stimulation of beneficial bacteria by pronounced cecal AX fermentation.

The improvement in nutrient digestion has been widely attributed to the ability of endo-xylanase to reduce digesta viscosity (56,85,86). Depolymerization of soluble AX to AXOS began in the gizzard (**Chapter 5**), thus preceding nutrient digestion in the small intestine (**Chapter 5**). Therefore, it was anticipated that the increased starch and protein digestibility currently observed (**Chapter 2**), was at least partly due to digesta viscosity reduction by endo-xylanase. In addition, the degradation of insoluble AX, as determined by the increased recovery of water-extractable AX in the ileum (WE-AX-Ril) (**Chapter 5**, Fig. 4), and its implications in nutrient de-encapsulation shall be further elaborated in Section 4.

Next to promoting nutrient digestion, the current research showed that improved animal growth upon enzyme supplementation also coincided with pronounced AX fermentation for the enzyme-supplemented wheat diet. NSP metabolism in the hindgut has been reported to provide ~3.5% of the required energy in broilers, while it can contribute up to 11-30% in pigs (87,88). Therefore, a potentially higher energy provision in the form of SCFAs due to endo-xylanase supplementation cannot fully explain the improved broiler performance currently observed (Box 2) (**Chapter 2**). Torok and co-workers (2011) identified that members of the phyla Firmicutes and Bacteroidetes were associated with improved broiler performance (89). Furthermore, there is an increasing volume of studies reporting that the increase in SCFAs content upon supplementation of AXOS, XOS and xylanase coincided with improved animal performance (50,67,72,74,75,90).

<div style="border:1px solid black;padding:10px;background:#e0e0e0;">

Box 2: Theoretical calculation of the amount of energy provision by fermentable AX in the ceca

1. *Assumption: The total amount of DM present in the broiler ileum is ~ 10 g* (91)

2. AX content in the ileum is 16.5% w/w → 1.6 g. Of that, 19% is soluble for Wheat Control (Con) and 27% for Wheat Enzyme (Enz) → 0.3 g and 0.4 g respectively (**Chapter 5**)

3. This translates to 2300–2600 µmoles soluble AX (measured as pentosyl units (Mw = 132 g/mol)) entering the ceca. *The total amount of DM present in the ceca is ~1.6 g* (91).

Therefore 1400-1600 µmoles/g AX are fermented in the ceca. The total SCFA content in the ceca was found to be 240-340 µmoles/g (**Chapter 2**). This means that the SCFA amount measured in the ceca accounts for 17-30% of the theoretical maximum AX amount entering the ceca.

4. The daily feed intake is 126 g (**Chapter 2**) and the metabolizable energy is 12.5 MJ/kg (**Chapter 3**) → 1.6 MJ energy is consumed daily.

5. NSP provide 2.8 MJ/kg ingested (87) and the AX and NSP content in diet is 5% and 21%, respectively (**Chapter 2**).

Based on these calculations, AX fermentation accounted for 1% of the metabolizable energy, and accounted for ~25% of the energy provided in the form of SCFAs by NSP fermentation.

</div>

Overall, xylanase-mediated improvements in nutrient digestion, as documented in **Chapter 2**, suggest that *in vivo* AX degradation to AXOS by endo-xylanase can instigate a response far greater than the output of SCFAs in terms of energy. Additionally, improved animal performance due to dietary interventions could be a result of a holistic amelioration of microbial ecology and intestinal physiology rather than a strict increase in energy output (Box 2). For instance, the measurable increase in SCFAs formation (Box 2) currently observed, may be linked with improved enterocyte growth, improved mineral absorption and better control of the pH that has been previously proposed to reduce growth of pathogenic bacteria (78,92,93). Finally, it is highlighted that the structural analysis of released AXOS currently achieved, greatly improves our understanding of the ability of endo-xylanase to promote animal growth via a prebiotic mechanism.

4   Looking beyond the prebiotic effect: nutrient de-encapsulation by NSPases

As introduced in 3.3, NSPase-mediated improvements in nutrient digestion primarily observed for wheat diets, coincided with improved animal growth (**Chapter 2**). Improved nutrient digestion has been attributed to reduction in digesta viscosity as well as to nutrient de-encapsulation due to enzyme-mediated hydrolysis of insoluble cereal cell walls (56). It was, therefore, hypothesized that cell wall matrix degradation by NSPases *in vivo* would not only release NSP in aqueous medium, but it will additionally loosen the cell wall architecture, resulting in improved NSP extractability by alkali. This hypothesis was investigated in **Chapter 6**. Moreover, enzyme-mediated nutrient de-encapsulation was hypothesized to increase digestion rate of starch *in vitro*.

4.1 Impact of NSPases on the cell wall matrix

In contrast to our hypothesis, enzyme supplementation did not improve the alkali extractability of AX and other NSP from digesta (**Chapter 6**). This demonstrated that the impact of NSPase supplementation on the structure of insoluble cell walls is principally explained *in vivo* by the xylanase-driven release of AXOS (**Chapter 5**). The overall impact of enzyme on the distribution of all AX species present in the ileum and excreta into water-extractable, alkali-extractable and alkali-unextractable populations was determined by combining the observations made in **Chapter 5 and 6** (Fig. 5).
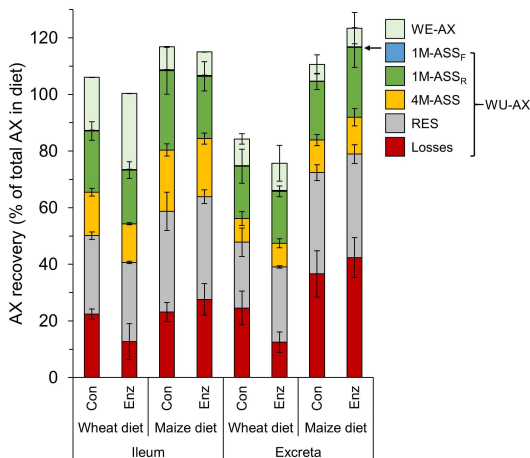
Fig. 5. Marker-based recovery of water-extractable AX (WE-AX, □) and water-unextractable AX (WU-AX) in the ileum and excreta, expressed as percentage (%) of the total AX present in the control diets (Con) and enzyme-supplemented diets (Enz). WU-AX was sequentially extracted with 1 M NaOH (extract was further fractionated to populations below 3.5 kDa ($1M\text{-}ASS_F$, ■) or above 3.5 kDa ($1M\text{-}ASS_R$, ■)) and 4 M NaOH (4M-ASS, ■). Unextractable AX was determined in RES, ■. Losses (■) during alkali extraction are presented as well.

The main difference in AX extractability between wheat control diet (Con) and wheat diet supplemented with enzymes (Enz) was already noticeable from the higher proportion of water-extractable AX (WE-AX) in the ileum for wheat Enz compared to wheat Con (Fig. 5). However, enzyme supplementation did not further increase alkali extractability of AX, as indicated by the similar proportions of insoluble, alkali extractable AX being recovered for both wheat Con and Enz diets under the current experimental conditions (**Chapter 6**). The lack of improvement in alkali extractability suggested that alkali-labile associations between AX molecules and between AX and lignin (ferulate, diferulate cross-links) or AX and cellulose (hydrogen bonds) were not affected by enzymatic cell wall degradation (94,95). Similar to our study, no impact on alkali extractability of NSP was previously observed upon xylanase treatment of hardwood pulp (96). Another *in vivo* study also reported that pectinase supplementation in maize-rapeseed meal diet did not impact NSP extractability by alkali in broilers (97). The overall absence of differences in AX extractability from digesta for maize Con and maize Enz (Fig. 5) further corroborated that low AX solubility was responsible for the low fermentability observed in **Chapter 2** and previous studies (67,98). Finally, no

effect of enzymes was observed regarding the alkali extractability of maize AX (Fig. 5).
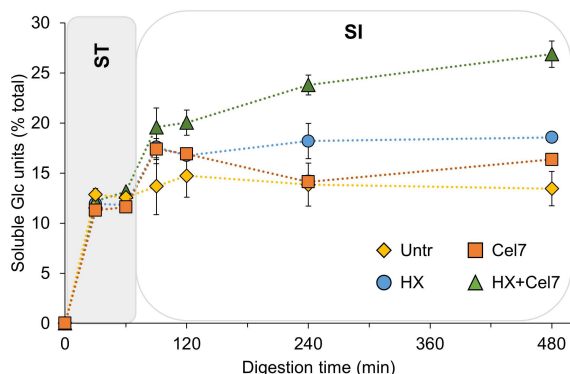
Fig. 6. Glucan (Glc equivalents) solubilization from wheat AIS during *in vitro* digestion without (Untr: ◇) or with the addition of HX (●), Cel7 (■) and HX & Cel7 (▲).

The potential impact of endo-xylanase and endo-glucanase on cell wall degradation beyond AXOS release was further studied *in vitro* (Box 1 Fig. 3,6). Despite its known side-activity towards xylan (99), Cel7 did not result in more AX being released when used together with HX (Fig. 3). This further indicates that AX solubilization from wheat is driven by endo-xylanase. Still, Cel7 was able to release Glc units from insoluble cell walls that coincided with oligosaccharide release (Fig. 3; GlcOS), especially when combined with HX and after prolonged incubation (> 4 h). The low contribution of glucanase in the degradation of wheat grains *in vivo* (**Chapter 2, 6**) seems to be linked to the slow action of Cel7 observed *in vitro*. Limited endo-glucanase action was partly explained by the low β-glucan and cellulose contents of wheat (100) and may further explain the low impact of enzyme supplementation in NSP extractability by alkali from wheat diets (**Chapter 6**).

4.2 Maize cell wall degradation by endo-xylanase and endo-glucanase

Although endo-xylanase supplementation benefited broilers fed the wheat diet via a prebiotic mechanism, this was not apparent for broilers fed the maize diet (**Chapter 2, 3, 6**). The main reasons indicated for this difference are maize AX recalcitrance to GH11 endo-xylanase and low maize AX fermentability in broilers (**Chapter 2**). Still, numerical improvements in broiler performance and starch digestibility upon enzyme addition observed in **Chapter 2** could result from a positive, albeit subtle effect of NSPase inclusion in the maize diet. Enzyme supplementation was not expected to influence animal performance through viscosity reduction (**Chapter 1**) for maize diets, as endo-xylanase was previously found not to reduce the already low digesta viscosity observed (101,102). In light of the low impact of enzyme supplementation on maize NSP degradation observed

in vivo (**Chapter 2,6**), further evidence of endo-xylanase and endo-glucanase action on maize cell wall was sought *in vitro* (Fig. 7).
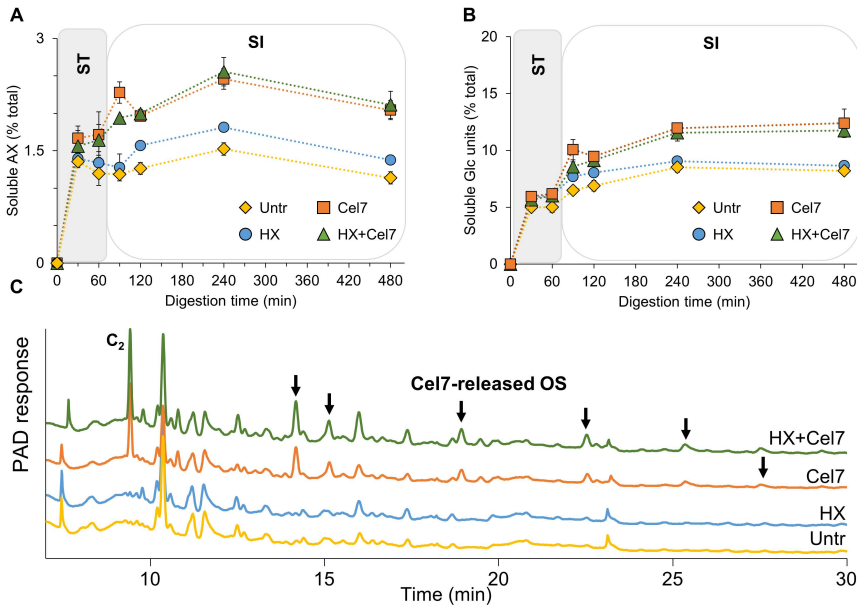
Fig. 7. AX (**A**) and glucan (Glc equivalents) (**B**) solubilization from maize AIS during *in vitro* digestion without (Untr: ◇) or with the addition of HX (●), Cel7 (■) and HX & Cel7 (▲). HPAEC-PAD chromatograms (**C**) of oligosaccharides released at the end of *in vitro* AIS digestion (8 h), C_2:cellobiose.

As expected from the *in vivo* results (Fig. 5), AX solubility was particularly low for maize AIS, (~1.5%). Still, slight AX release was observed upon enzyme addition. Clearly, HX impact on AX hydrolysis and AXOS release was far less pronounced for maize compared to wheat AIS (Fig. 3). Interestingly, for maize AIS, Cel7 appeared to be driving AX solubilization, even when used in combination with HX. For instance, ~2% AX was released by Cel7 and HX & Cel7, whereas 1.6% AX was released by HX alone. Next to AX, Cel7 released Glc (Fig. 7B), Man and Gal residues (data not shown) from maize AIS, which coincided with release of cellobiose and larger oligosaccharides (Fig. 7 C). The present findings suggest that the added glucanase might have a larger role in maize cell wall degradation than so far anticipated. A possible explanation could be that endo-glucanase increases the xylan accessibility for the endo-xylanases, which has also been suggested for lignocellulose degradation in general (103,104).

Interestingly, the recalcitrance of maize AX towards xylanases is further displayed by inconsistent findings in animal studies. For example, xylanase and glucanase addition was found to improve nutrient digestibility or animal performance when broilers were fed with energy-deficient maize diets, while no difference was found when fed with maize diets of adequate energy content (105–107). In addition, no

effect of enzyme supplementation in animal performance and NSP utilization was observed for maize-fed pigs (108).

However, several studies reported that the addition of maize distiller's dried grains with solubles (mDDGS) in maize diets coincided with improved broiler performance by dietary xylanase (with or without glucanase) (69,70,98,102,105,109–112). It should be noted that mDDGS is a byproduct generated after fermentation of maize for bioethanol production (65,113,114). As a consequence of (bio)processing, the AX populations present in mDDGS are more soluble and less-substituted compared to native maize AX (65,113). The more soluble and low substituted AX in mDDGS was shown to be degradable by endo-xylanase alone, whereas the hydrolysis of complex AX from maize kernel required the action of debranching enzymes (e.g., arabinofuranosidase, glucuronidase) as well (29,65).

In several other studies, xylanase was supplemented in maize diets together with amylase or proteases, but all appropriate control treatments were not reported (112,115–117). Consequently, improvements in starch digestibility and animal performance could not be solely attributed to endo-xylanase action. Such approach further confounds specific conclusions on xylanase efficacy in maize diets.

Overall, the effect of xylanase supplementation in maize diets for increased animal performance is not always easy to conclude on. Indeed, only three studies report that xylanase supplementation to (native) maize diets led to significant improvements in animal performance (67,73,118). Remarkably, these three studies all report improvements in SCFAs formation and beneficial microbiota growth. Two of those studies used a commercial preparation from *Trichoderma reesei* containing mainly, but not exclusively, endo-xylanase, whereas the third study used a genetically modified, acid-tolerant GH10 endo-xylanase (67,73,118,119). Based on these findings, it is tempting to speculate that other types of endo-xylanases than the GH11 used in our research, in collaboration with accessory xylan degrading enzymes and/or cellulases (29,104,120), might open up the way for maize AX degradation in broilers and consequently improve animal performance. It is, therefore, essential to study in detail the biochemical parameters of dietary endo-xylanases in order to elucidate their mode of action required to improve maize NSP degradation during feed digestion.

4.3 Implications of nutrient de-encapsulation for animal growth

In our efforts to determine the potential de-encapsulating effect of dietary enzymes, it was hypothesized that NSPase action will increase starch digestion rate *in vitro* (Box 3, Fig. 8). Overall, wheat starch was digested faster and to a more complete extent compared to maize starch, in accordance to previous *in vitro* studies (121,122). In relation with the hypothesis mentioned, HX and Cel7 addition did not clearly alter the digestion rate either in wheat or in maize. It could be argued, however, that a slight improvement for starch digestion was achieved for maize upon NSPase addition (Fig. 8). These results show that the link between cell

wall degradation by dietary enzymes and starch digestion is rather weak, if present.

Box 3: *In vitro* starch digestion for wheat and maize whole grains

Materials See Box 1.

Methods

Approximately 1000 mg milled (0.5 mm) whole grains was incubated with or without HX and Cel7 combination (each enzyme was added at 0.125 μg$_{protein}$/mL, and the final volume was 30 mL), under *in vitro* digestive conditions. Gastric digestion was carried out by the addition of pepsin at pH 3.2 40 °C for 60 min. Next, the pH value of the mixture was increased at pH 6.5 and pancreatin was added to simulate the small intestine conditions, and the incubation proceeded for 480 min in total. Aliquots were removed at 15, 30, 45, 60, 90, 120, 240 and 420 min (time in small intestine). Supernatant solution was separated by centrifugation, heated at 99 °C for 15 min, and upon cooling incubated with amyloglucosidase to convert soluble starch degradation products to glucose (Glc). Glc release from starch was quantified by HPAEC-PAD.

Starch hydrolysis was determined using the Chapman-Richards model, as modified by van Kempen et al. (2007) (122):

$$Starch\ hydrolysis\ \%\ = Plateau \times (1 - e^{\frac{-Kplateau}{Plateau}*t})^{\frac{Cplateau}{Plateau}+1}$$

Where:

Starch hydrolysis (%): hydrolyzed starch (Glc) expressed as percentage (%) of total starch, **Plateau:** Maximum amount of starch released (% of total starch), **K$_{plateau}$:** Starch hydrolysis rate (%/min), corrected for plateau effects, **C$_{plateau}$:** Shape parameter of *in vitro* digestion, corrected for plateau effects, **t:** digestion time (min)

Our findings are in contrast to previous studies demonstrating that xylanase and glucanase addition released protein and starch from wheat grains *in vitro* (53,123). Others have recently questioned the validity of the cell wall de-caging effect of NSPases as well, in recent papers (56,102). In particular, the lack of proper experimental design as well as the difficulty to separate the effect of nutrient encapsulation from that of viscosity during feed digestion makes it difficult to draw meaningful conclusions (124,125). On the contrary, there are both *in vitro* and *in vivo* studies arguing that intact cell walls do limit nutrient digestion in cereal diets (126,127). As such, endo-xylanase was previously shown to improve Glc release *in vitro* from wheat grains with relatively large particle size (~1 mm) (52). However, feed particles entering the small intestine of broilers are much smaller (< 0.5 mm) due to extensive grinding in the gizzard (128,129). Therefore, the similar *in vitro* starch digestion presently observed for finely ground grains (0.5 mm) with or without NSPases suggested that dietary enzymes may only exert limited impact on nutrient de-encapsulation in broilers.

7
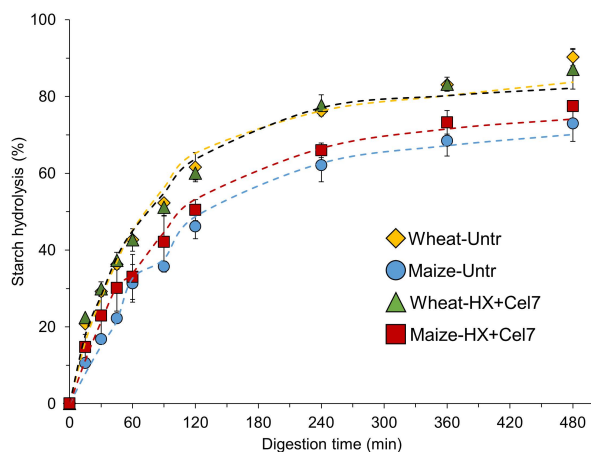
Fig. 8. Starch hydrolysis (% of total starch) during *in vitro* digestion under small intestine conditions of wheat whole grain without (Wheat-Untr: ◇) or with HX and Cel7 addition (Wheat-HX+Cel7: ▲), and maize whole grain without (Maize-Unt: ●) or with HX and Cel7 addition (Maize-HX+Cel7: ■). Theoretical models (dotted lines) were fitted to the data. Error bars indicate standard deviation ($n = 3$).

In this research, it was hypothesized that enzyme supplementation in cereal diets would improve animal performance through several mechanisms. Our findings strongly demonstrate the ability of endo-xylanase supplementation in wheat diet to release AXOS *in vivo* (**Chapter 2, 5**), thus instigating a prebiotic response (**Chapter 2, 3, 5**). Improved hindgut fermentation is demonstrated to have greatly contributed to gut health and animal performance alongside increased nutrient digestion (**Chapter 2**) via an expected decrease in digesta viscosity. The hypothesis that endo-xylanase and endo-glucanase to promote digestion by nutrient de-encapsulation was not validated (**Chapter 6**, Fig. 5, 6 and 8). However, the ability of dietary enzymes to degrade cell wall NSP was demonstrated for both wheat and maize diets (Fig. 6,7) and is expected to be highly relevant considering the trend in animal nutrition to shift to more high-fiber diets, as will be discussed next.

5   The future role of NSP and NSPases in animal nutrition

5.1   Improving NSP utilization across the board

In response to the continuous confrontation with the impact of climate change in our daily lives, stakeholders are tasked with mitigating the environmental impact of food production whilst keeping the impact on business activity and consumer demands to a minimum. In that context, replacement of meat-derived protein with more sustainable plant-based foods has been in the spotlight of food innovation in the past decade. However, cereal grains and vegetables still play a major role in human and animal nutrition. For example, the demand of wheat is projected to exceed global production in 2021-2022 (130). Therefore, knowledge and research on how to improve nutrient and fiber utilization from staple plant products is still of great consideration, especially during a period of rising energy cost and geopolitical instability.

Overall, the limited grain supply and the direct competition with their use as food by an increasing human population means that animal nutrition has to rely more and more on fiber-rich side-streams (131–133). Upcycling of such byproducts presents the potential to lower the production costs and the environmental impact of animal farming (134,135). This trend looks quite promising for pigs as fermentation of more than 70% of dietary NSP can contribute to 11-30% their energy requirements (88,108).The lower energy contribution of NSP in broilers suggests that greater improvements in fiber fermentation are required in this field (87,133,135). In addition to using alternative ingredients, eradication of antibiotics and promotion of intestinal health of livestock is crucial, in line with the One Health concept (133,136). In that context, the ability of specific and tailored NSPase preparations to improve NSP fermentation and promote gut health via a prebiotic mechanism whilst mitigating the anti-nutritive influence of NSP in the small intestine is expected to increase their importance as feed ingredients.

5.2   Hoatzin: tropical weirdo or digestive trailblazer?

Although fiber fermentation is limited in broilers, this is not the case for all birds (137). For example, ostriches obtain up to 76% of their energy through fiber fermentation, compared to ~3.5% measured in broilers (87,138). However, there is an even more intriguing adaptation of the avian GIT to utilize fibers as main nutrients, namely the GIT of the hoatzin (137). The hoatzin is a folivore native to the Orinoco basin and the Amazon rainforest, that presents a uniquely large crop populated by the phyla Firmicutes and Bacteroidetes, which are known to contain members able to ferment hemicellulose (139,140). Consequently, the main part of microbial fermentation of fiber mainly occurs in the upper GIT, as observed in ruminants (140). This unique GIT physiology is an interesting specimen that can provide further insight on fiber utilization by birds. For example, studying in detail the microbiota composition colonizing the hoatzin GIT can increase our understanding about the interactions between diet and microbiota able to improve fiber fermentation in poultry.

5.3   Improving cell wall degradation by NSPases: more enzymes needed?

The increasing interest in the inclusion of high-fiber agricultural byproducts in animal diets suggests that the role of NSPases will become even more important in the future. Therefore, the combination of pre-treatments and NSPase formulations aiming at improving NSP degradability *in vivo* has been a topic of scientific research and debate (54,56,97,141,142).

For instance, application of pectolytic enzymes can improve the fermentability of pectin-rich feedstock (54,97). Systematic *in vitro* and *in vivo* studies are required to establish the significance of such additional activities for livestock (124,142). Still, AX prevalence in high-fiber cereal byproducts means that xylanases shall maintain their leading role. Nevertheless, *in vivo* xylanase efficacy under digestive

conditions could be further explored, aiming at maximizing the beneficial effect of xylanases on animal growth. For that, investigation of acid-tolerant enzymes able to further degrade insoluble AX is of great interest (143). Furthermore, xylanases with carbohydrate binding domains that facilitate the attachment to insoluble substrates could be highly relevant for improving AXOS release *in vivo* (144,145). Moreover, research of novel endo-xylanase members within GH10 and GH11 families and beyond, that can exhibit higher tolerance toward heteroxylan substitutions is ongoing by our group in collaboration with Westerdijk Fungal Biodiversity Institute, Utrecht.

Additionally, the added value of AX debranching enzymes (**Chapter 1**) has not been clearly demonstrated in animal studies yet. For instance, AX debranching by arabinofuranosidases may enhance endo-xylanase action, but the release of less diverse oligosaccharides may disturb the balance between beneficial microbiota (59,77,142). Still, the targeted removal of acetyl, 4-*O*-methyl-glucuronoyl and feruloyl decorations can unlock the utilization of complex structures, especially in maize. Overall, the comprehensive investigation of carbohydrate structures, and their role *in vivo*, is necessary in order to harness the full potential of dietary NSPases. The high-end analytical techniques as well as the isolation and *in vitro* digestion procedures currently developed can greatly contribute to such research.

6   References

1.   Lin Y, Olukosi OA. Qualitative and quantitative profiles of jejunal oligosaccharides and cecal short-chain fatty acids in broiler chickens receiving different dietary levels of fiber, protein and exogenous enzymes. J Sci Food Agric. 2021;101(12):5190-5201

2.   Kabel MA, Kortenoeven L, Schols HA, Voragen AGJ. *In vitro* fermentability of differently substituted xylo-oligosaccharides. J Agric Food Chem. 2002;50(21):6205–10.

3.   Jonathan MC, DeMartini J, Van Stigt Thans S, Hommes R, Kabel MA. Characterisation of non-degraded oligosaccharides in enzymatically hydrolysed and fermented, dilute ammonia-pretreated corn stover for ethanol production. Biotechnol Biofuels. 2017;10(1):112.

4.   Brasseur C, Bauwens J, Tarayre C, Mattéotti C, Thonart P, Destain J, Francis F, Haubruge E, Portetelle D. MALDI-TOF MS analysis of cellodextrins and xylo-oligosaccharides produced by hindgut homogenates of *Reticulitermes santonensis*. Molecules. 2014;19(4):4578–94.

5.   Ling L, Jiang L, Chen Q, Zhao B, Li Y, Guo X. Rapid and accurate profiling of oligosaccharides in beer by using a reactive matrix via MALDI-TOF MS. Food Chem. 2021;340:128208.

6.   Wang CC, Lai YH, Ou YM, Chang HT, Wang YS. Critical factors determining the quantification capability of matrix-assisted laser desorption/ionization-time-of-flight mass spectrometry. Philos Trans R Soc A. 2016;374:20150371.

7.   Szájli E, Fehér T, Medzihradszky KF. Investigating the quantitative nature of MALDI-TOF MS. Mol Cell Proteomics. 2008;7(12):2410–8.

8.   Harvey DJ. Analysis of carbohydrates and glycoconjugates by matrix-assisted laser desorption/ionization mass spectrometry: An update for 2015–2016. Mass Spectrom Rev. 2021;40(4):408–565.

9.   Kabel MA, Schols HA, Voragen AGJ. Mass determination of oligosaccharides by matrix-assisted laser desorption/ionization time-of-flight mass spectrometry following HPLC, assisted by on-line desalting and automated sample handling. Carbohydr Polym. 2001;44(2):161–5.

10. Maslen SL, Goubet F, Adam A, Dupree P, Stephens E. Structure elucidation of arabinoxylan isomers by normal phase HPLC-MALDI-TOF/TOF-MS/MS. Carbohydr Res. 2007;342(5):724–35.

11. Domon B, Costello CE. A systematic nomenclature for carbohydrate fragmentations in FAB-MS/MS spectra of glycoconjugates. Glycoconj J. 1988;5(4):397–409.

12. Sun P, Frommhagen M, Kleine Haar M, van Erven G, Bakx EJ, van Berkel WJH, Kabel MA. Mass spectrometric fragmentation patterns discriminate C1- and C4-oxidised cello-oligosaccharides from their non-oxidised and reduced forms. Carbohydr Polym. 2020;234:115917.

13. Doohan RA, Hayes CA, Harhen B, Karlsson NG. Negative Ion CID Fragmentation of *O*-linked oligosaccharide aldoses—charge induced and charge remote fragmentation. J Am Soc Mass Spectrom. 2011;22(6):s13361-011-0102–3.

14. Logtenberg MJ, Donners KMH, Vink JCM, Van Leeuwen SS, De Waard P, De Vos P, Schols HA. Touching the high complexity of prebiotic Vivinal galacto-oligosaccharides using porous graphitic carbon ultra-high-performance liquid chromatography coupled to mass spectrometry. J Agric Food Chem. 2020;68(29):7800–8.

15. Juvonen M, Kotiranta M, Jokela J, Tuomainen P, Tenkanen M. Identification and structural analysis of cereal arabinoxylan-derived oligosaccharides by negative ionization HILIC-MS/MS. Food Chem. 2019;275:176–85.

16. Nagy G, Peng T, Pohl NLB. Recent liquid chromatographic approaches and developments for the separation and purification of carbohydrates. Anal Methods. 2017;9(24):3579–93.

17. Wang J, Zhao J, Nie S, Xie M, Li S. Mass spectrometry for structural elucidation and sequencing of carbohydrates. TrAC - Trends Anal Chem. 2021;144:116436.

18. Kailemia MJ, Ruhaak LR, Lebrilla CB, Amster IJ. Oligosaccharide analysis by mass spectrometry: A review of recent developments. Anal Chem. 2014;86(1):196–212.

19. Bowman M, Dien B, O'Bryan P, Sarath G, Cotta M. Comparative analysis of end point enzymatic digests of arabino-xylan isolated from switchgrass (*Panicum virgatum* L) of varying maturities using LC-MS[n]. Metabolites. 2012; 19;2(4):959–82.

20. Demuth T, Boulos S, Nyström L. Structural investigation of oxidized arabinoxylan oligosaccharides by negative ionization HILIC-qToF-MS. Analyst. 2020;145(20):6691–704.

21. Leijdekkers AGM, Sanders MG, Schols HA, Gruppen H. Characterizing plant cell wall derived oligosaccharides using hydrophilic interaction chromatography with mass spectrometry detection. J Chromatogr A. 2011;1218(51):9227–35.

22. Kiely LJ, Hickey RM. Characterization and analysis of food-sourced carbohydrates. In: Davey GP, editor. Glycosylation, vol 2370. New York, NY: Humana; 2022. p. 67–95.

23. Harvey DJ. Negative ion mass spectrometry for the analysis of N-linked glycans. Mass Spectrom Rev. 2020;39(5–6):586–679.

24. Quéméner B, Ordaz-Ortiz JJ, Saulnier L. Structural characterization of underivatized arabino-xylo-oligosaccharides by negative-ion electrospray mass spectrometry. Carbohydr Res. 2006;341(11):1834–47.

25. Remoroza CA, Mak TD, De Leoz MLA, Mirokhin YA, Stein SE. Creating a mass spectral reference library for oligosaccharides in human milk. Anal Chem. 2018;90(15):8977–88.

26. Hernández-Hernández O, Calvillo I, Lebrón-Aguilar R, Moreno FJ, Sanz ML. Hydrophilic interaction liquid chromatography coupled to mass spectrometry for the characterization of prebiotic galactooligosaccharides. J Chromatogr A. 2012;1220:57–67.

27. Izydorczyk MS, Biliaderis CG. Cereal arabinoxylans: Advances in structure and physicochemical properties. Carbohydr Polym. 1995;28(1):33–48.

28. Gruppen H, Kormelink FJM, Voragen AGJ. Water-unextractable cell wall material from wheat flour. 3. A structural model for arabinoxylans. J Cereal Sci. 1993;18(2):111–28.

29. Huisman MMH, Schols HA, Voragen AGJ. Glucuronoarabinoxylans from maize kernel cell walls are more complex than those from sorghum kernel cell walls. Carbohydr Polym. 2000;43(3):269–79.

30. Saulnier L, Marot C, Chanliaud E, Thibault JF. Cell wall polysaccharide interactions in maize bran. Carbohydr Polym. 1995;26(4):279–87.

31. Verbruggen MA, Spronk BA, Schols HA, Beldman G, Voragen AGJ, Thomas JR, Kamerling JP, Vliegenthart JFG. Structures of enzymically derived oligosaccharides from sorghum glucuronoarabinoxylan. Carbohydr Res. 1998;306(1–2):265–74.

32. Vinkx CJA, Delcour JA. Rye (*Secale cereale* L.) arabinoxylans: A critical review. J Cereal Sci. 1996;24(1):1–14.

33. Saulnier L, Peneau N, Thibault J-F. Variability in grain extract viscosity and water-soluble arabinoxylan content in wheat. J Cereal Sci. 1995;22(3):259–64.

34. Meriö-Talvio H, Dou J, Vuorinen T, Pitkänen L. Fast HILIC method for separation and quantification of non-volatile aromatic compounds and monosaccharides from willow (*Salix* sp.) bark extract. Appl Sci. 2021;11(9).

35. Pismennõi D, Kiritsenko V, Marhivka J, Kütt ML, Vilu R. Development and optimisation of HILIC-LC-MS method for determination of carbohydrates in fermentation samples. Molecules. 2021;26(12):3669.

36. An Z, Zhang Z, Zhang X, Yang H, Lu H, Liu M, et al. Oligosaccharide mapping analysis by HILIC-ESI-HCD-MS/MS for structural elucidation of fucoidan from sea cucumber *Holothuria floridana*. Carbohydr Polym. 2022;275:118694.

37. Sanz ML, Martínez-Castro I. Recent developments in sample preparation for chromatographic analysis of carbohydrates. J Chromatogr A. 2007;1153(1–2):74–89.

38. Redmond JW, Packer NH. The use of solid-phase extraction with graphitised carbon for the fractionation and purification of sugars. Carbohydr Res. 1999;319(1–4):74–9.

39. Yan X. Short-chain polysaccharide analysis in ethanol-water solutions. J AOAC Int. 2017;100(4):1134–6.

40. Balto AS, Lapis TJ, Silver RK, Ferreira AJ, Beaudry CM, Lim J, Penner, MH. On the use of differential solubility in aqueous ethanol solutions to narrow the DP range of food-grade starch hydrolysis products. Food Chem. 2016;197:872–80.

41. Lærke HN, Arent S, Dalsgaard S, Bach Knudsen KE. Effect of xylanases on ileal viscosity, intestinal fiber modification, and apparent ileal fiber and nutrient digestibility of rye and wheat in growing pigs. J Anim Sci. 2015;93(9):4323–35.

42. De Vries S, Kwakkel RP, Pustjens AM, Kabel MA, Hendriks WH, Gerrits WJJ. Separation of digesta fractions complicates estimation of ileal digestibility using marker methods with Cr_2O_3 and cobalt-ethylenediamine tetraacetic acid in broiler chickens. Poult Sci. 2014;93(8):2010–7.

43. De Vries S, Gerrits WJ., Vries D. The use of tracers or markers in digestion studies. In: Moughan PJ, Hendriks WH, editors. Feed Evaluation Science. Wageningen: Wageningen Academic Publishers; 2018. p. 275–94.

44. Sacranie A, Svihus B, Denstadli V, Moen B, Iji PA, Choct M. The effect of insoluble fiber and intermittent feeding on gizzard development, gut motility, and performance of broiler chickens. Poult Sci. 2012;91(3):693–700.

45. Loret S, Nollevaux G, Remacle R, Klimek M, Barakat I, Deloyer P, Grandfils C, Dandrifosse G. Analysis of PEG 400 and 4000 in urine for gut permeability assessment using solid phase extraction and gel permeation chromatography with refractometric detection. J Chromatogr B. 2004;805(2):195–202.

46. Paës G, Berrin JG, Beaugrand J. GH11 xylanases: Structure/function/properties relationships and applications. Biotechnol Adv. 2012;30(3):564–92.

47. Matthiesen CF, Pettersson D, Smith A, Pedersen NR, Storm AC. Exogenous xylanase improves broiler production efficiency by increasing proximal small intestine digestion of crude protein and starch in wheat-based diets of various viscosities. Anim Feed Sci Technol. 2021;272:114739.

48. Gonzalez-Ortiz G, Sola-Oriol D, Martinez-Mora M, Perez JF, Bedford MR. Response of broiler chickens fed wheat-based diets to xylanase supplementation. Poult Sci. 2017;96(8):2776–85.

49. Bautil A, Buyse J, Goos P, Bedford MR, Courtin CM. Feed endoxylanase type and dose affect arabinoxylan hydrolysis and fermentation in ageing broilers. Anim Nutr. 2021;7(3):787–800.

50. Craig AD, Khattak F, Hastie P, Bedford MR, Olukosi OA. Xylanase and xylo- oligosaccharide prebiotic improve the growth performance and concentration of potentially prebiotic oligosaccharides in the ileum of broiler chickens. Br Poult Sci. 2020;61(1):70–8.

51. Ravn JL, Martens HJ, Pettersson D, Pedersen NR. A commercial GH 11 xylanase mediates xylan solubilisation and degradation in wheat, rye and barley as demonstrated by microscopy techniques and wet chemistry methods. Anim Feed Sci Technol. 2016;219:216–25.

7

52. Tervilä-Wilo A, Parkkonen T, Morgan A, Hopeakoski-Nurminen M, Poutanen K, Heikkinen P, Autio K. *In vitro* digestion of wheat microstructure with xylanase and cellulase from *Trichoderma reesei*. J Cereal Sci. 1996;24(3):215–25.

53. Meng X, Slominski BA, Nyachoti CM, Campbell LD, Guenter W. Degradation of cell wall polysaccharides by combinations of carbohydrase enzymes and their effect on nutrient utilization and broiler chicken performance. Poult Sci. 2005;84(1):37–47.

54. Lafond M, Bouza B, Eyrichine S, Rouffineau F, Saulnier L, Giardina T, Bonnin E, Preynat A. *In vitro* gastrointestinal digestion study of two wheat cultivars and evaluation of xylanase supplementation. J Anim Sci Biotechnol. 2015;6:5.

55. Vangsøe CT, Nørskov NP, Devaux MF, Bonnin E, Bach Knudsen KE. Carbohydrase complexes rich in xylanases and arabinofuranosidases affect the autofluorescence signal and liberate phenolic acids from the cell wall matrix in wheat, maize, and rice bran: An *in vitro* digestion study. J Agric Food Chem. 2020;68(37):9878–87.

56. Vangsøe CT, Bonnin E, Joseph-Aime M, Saulnier L, Neugnot-Roux V, Bach Knudsen KE. Improving the digestibility of cereal fractions of wheat, maize, and rice by a carbohydrase complex rich in xylanases and arabinofuranosidases: An *in vitro* digestion study. J Sci Food Agric. 2021;101:1910–9.

57. Bedford MR. The evolution and application of enzymes in the animal feed industry: the role of data interpretation. Br Poult Sci. 2018;59(5):486–93.

58. Bedford MR, Apajalahti JH. The role of feed enzymes in maintaining poultry intestinal health. J Sci Food Agric. 2021;11670.

59. Lei Z, Shao Y, Yin X, Yin D, Guo Y, Yuan J. Combination of xylanase and debranching enzymes specific to wheat arabinoxylan improve the growth performance and gut health of broilers. J Agric Food Chem. 2016;64(24):4932–42.

60. Mendis M, Martens EC, Simsek S. How fine structural differences of xylooligosaccharides and arabinoxylooligosaccharides regulate differential growth of *Bacteroides* species. J Agric Food Chem. 2018;66(31):8398–405.

61. Rose DJ, Patterson JA, Hamaker BR. Structural differences among alkali-soluble arabinoxylans from maize (*Zea mays*), rice (*Oryza sativa*), and wheat (*Triticum aestivum*) brans influence human fecal fermentation profiles. J Agric Food Chem. 2010;58(1):493–9.

62. Rumpagaporn P, Reuhs BL, Kaur A, Patterson JA, Keshavarzian A, Hamaker BR. Structural features of soluble cereal arabinoxylan fibers associated with a slow rate of *in vitro* fermentation by human fecal microbiota. Carbohydr Polym. 2015;130:191–7.

63. Beaugrand J, Chambat G, Wong VWKK, Goubet F, Rémond C, Paës G, Benamrouche S, Debeire P, O'Donohue M, Chabbert B. Impact and efficiency of GH10 and GH11 thermostable endoxylanases on wheat bran and alkali-extractable arabinoxylans. Carbohydr Res. 2004;339(15):2529–40.

64. Courtin CM, Delcour JA. Relative activity of endoxylanases towards water-extractable and water-unextractable arabinoxylan. J Cereal Sci. 2001;33(3):301–12.

65. Pedersen MB, Dalsgaard S, Arent S, Lorentsen R, Bach Knudsen KE, Yu S, Lærke, HN. Xylanase and protease increase solubilization of non-starch polysaccharides and nutrient release of corn- and wheat distillers dried grains with solubles. Biochem Eng J. 2015;98:99–106.

66. Masey-O'Neill H V., Singh M, Cowieson AJ. Effects of exogenous xylanase on performance, nutrient digestibility, volatile fatty acid production and digestive tract thermal profiles of broilers fed on wheat- or maize-based diet. Br Poult Sci. 2014;55(3):351–9.

67. Nguyen HT, Bedford MR, Wu S-B, Morgan NK. Soluble non-starch polysaccharide modulates broiler gastrointestinal tract environment. Poult Sci. 2021;101183.

68. Sanchez J, Barbut S, Patterson R, Kiarie EG. Impact of fiber on growth, plasma, gastrointestinal and excreta attributes in broiler chickens and turkey poults fed corn- or wheat-based diets with or without multienzyme supplement. Poult Sci. 2021;100(8).

69. McCafferty KW, Bedford MR, Kerr BJ, Dozier WA. Effects of age and supplemental xylanase in corn- and wheat-based diets on cecal volatile fatty acid concentrations of broilers. Poult Sci. 2019;98(10):4787–800.

70. Qaisrani SN, Van Krimpen MM, Kwakkel RP, Verstegen MWA, Hendriks WH. Dietary factors affecting hindgut protein fermentation in broilers: A review. Worlds Poult Sci J. 2015;71(1):139–60.

71. Singh AK, Mandal RK, Bedford MR, Jha R. Xylanase improves growth performance, enhances cecal short-chain fatty acids production, and increases the relative abundance of fiber fermenting cecal microbiota in broilers. Anim Feed Sci Technol. 2021;277:114956.

72. Wang J, Cao H, Bao C, Liu Y, Dong B, Wang C, Shang Z, Cao Y, Liu S. Effects of xylanase in corn- or wheat-based diets on cecal microbiota of broilers. Front Microbiol. 2021;12:757066.

73. Kouzounis D, Hageman JA, Soares N, Michiels J, Schols HA. Impact of xylanase and glucanase on oligosaccharide formation, carbohydrate fermentation patterns, and nutrient utilization in the gastrointestinal tract of broilers. Animals. 2021;11(5):1285.

74. Morgan NK, Keerqin C, Wallace A, Wu SB, Choct M. Effect of arabinoxylo-oligosaccharides and arabinoxylans on net energy and nutrient utilization in broilers. Anim Nutr. 2019;5(1):56–62.

75. Ribeiro T, Cardoso V, Ferreira LMA, Lordelo MMS, Coelho E, Moreira ASP, Coimbra MA, Bedford MR, Fontes CMGA. Xylo-oligosaccharides display a prebiotic activity when used to supplement wheat or corn-based diets for broilers. Poult Sci. 2018;97(12):4330–41.

76. Liu X, Mao B, Gu J, Wu J, Cui S, Wang G, Zhao J, Zhang H, Chen W. *Blautia*—a new functional genus with potential probiotic properties? Gut Microbes. 2021;13(1):e1875796.

77. Broekaert WF, Courtin CM, Verbeke K, van de Wiele T, Verstraete W, Delcour JA. Prebiotic and other health-related effects of cereal-derived arabinoxylans, arabinoxylan-oligosaccharides, and xylooligosaccharides. Crit Rev Food Sci Nutr. 2011;51(2):178–94.

78. Pan D, Yu Z. Intestinal microbiome of poultry and its interaction with host and diet. Gut Microbes. 2013;5(1):108–19.

79. van Laere KMJ, Hartemink R, Bosveld M, Schols HA, Voragen AGJ. Fermentation of plant cell wall derived polysaccharides and their corresponding oligosaccharides by intestinal bacteria. J Agric Food Chem. 2000;48(5):1644–52.

80. Sergeant MJ, Constantinidou C, Cogan TA, Bedford MR, Penn CW, Pallen MJ. Extensive microbial and functional diversity within the chicken cecal microbiome. PLoS One. 2014;9(3):e91941.

81. Grootaert C, Delcour JA, Courtin CM, Broekaert WF, Verstraete W, Van de Wiele T. Microbial metabolism and prebiotic potency of arabinoxylan oligosaccharides in the human intestine. Trends Food Sci Technol. 2007;18(2):64–71.

82. Mendis M, Martens EC, Simsek S. How fine structural differences of xylooligosaccharides and arabinoxylooligosaccharides regulate differential growth of *Bacteroides* species. J Agric Food Chem. 2018;66(31):8398–405.

83. Snelders J, Olaerts H, Dornez E, Van de Wiele T, Aura AM, Vanhaecke L, Delcour JA, Courtin CM. Structural features and feruloylation modulate the fermentability and evolution of antioxidant properties of arabinoxylanoligosaccharides during *in vitro* fermentation by human gut derived microbiota. J Funct Foods. 2014;10:1–12.

84. Duke GE. Relationship of cecal and colonic motility to diet, habitat, and cecal anatomy in several avian species. J Exp Zool. 1989;252(3 S):38–47.

7

85. Bedford MR, Classen HL. Reduction of intestinal viscosity through manipulation of dietary rye and pentosanase concentration is effected through changes in the carbohydrate composition of the intestinal aqueous phase and results in improved growth rate and food conversion efficiency of broiler chicks. J Nutr. 1992;122(3):560–9.

86. Choct M, Annison G. The inhibition of nutrient digestion by wheat pentosans. Br J Nutr. 1992;67(1):123–32.

87. Jamroz D, Jakobsen K, Bach Knudsen KE, Wiliczkiewicz A, Orda J. Digestibility and energy value of non-starch polysaccharides in young chickens, ducks and geese, fed diets containing high amounts of barley. Comp Biochem Physiol Part A Mol Integr Physiol. 2002;131(3):657–68.

88. Bergman EN. Energy contributions of volatile fatty acids from the gastrointestinal tract in various species. Physiol Rev. 1990;70(2):567–90.

89. Torok VA, Hughes RJ, Mikkelsen LL, Perez-Maldonado R, Balding K, MacAlpine R, Percy NJ, Ophel-Keller K. Identification and characterization of potential performance-related gut microbiotas in broiler chickens across various feeding trials. Appl Environ Microbiol. 2011;77(17):5868–78.

90. Courtin CM, Swennen K, Broekaert WF, Swennen Q, Buyse J, Decuypere E, Michiels CW, De Ketelaere B, Delcour JA. Effects of dietary inclusion of xylooligo- saccharides, arabinoxylooligosaccha- rides and soluble arabinoxylan on the microbial composition of caecal contents of chickens. J Sci Food Agric. 2008;88(14):2517–22.

91. Papa CM. Lower gut contents of broiler chickens withdrawn from feed and held in cages. Poult Sci. 1991;70(2):375–80.

92. Jha R, Mishra P. Dietary fiber in poultry nutrition and their effects on nutrient utilization, performance, gut health, and on the environment: A review. J Anim Sci Biotechnol. 2021;12:51.

93. Pourabedin M, Zhao X. Prebiotics and gut microbiota in chickens. FEMS Microbiol Lett. 2015;362(15):1–8.

94. Iiyama K, Lam T, Stone BA. Covalent cross-links in the cell wall. Plant Physiol. 1994;104(2):315–20.

95. Harris PJ, Stone B. Chemistry and molecular organization of plant cell walls. In: Himmel ME, editor. Biomass recalcitrance: Deconstructing the plant cell wall for bioenergy. Oxford: Blackwell Publishing Ltd.; 2008. p. 61–93.

96. Hakala TK, Liitiä T, Suurnäkki A. Enzyme-aided alkaline extraction of oligosaccharides and polymeric xylan from hardwood kraft pulp. Carbohydr Polym. 2013;93(1):102–8.

97. Pustjens AM, De Vries S, Schols HA, Gruppen H, Gerrits WJJ, Kabel MA. Understanding carbohydrate structures fermented or resistant to fermentation in broilers fed rapeseed (*Brassica napus*) meal to evaluate the effect of acid treatment and enzyme addition. Poult Sci. 2014;93(4):926–34.

98. Munyaka PM, Nandha NK, Kiarie E, Nyachoti CM, Khafipour E. Impact of combined β-glucanase and xylanase enzymes on growth performance, nutrients utilization and gut microbiota in broiler chickens fed corn or wheat-based diets. Poult Sci. 2016;95(3):528–40.

99. Vlasenko E, Schülein M, Cherry J, Xu F. Substrate specificity of family 5, 6, 7, 9, 12, and 45 endoglucanases. Bioresour Technol. 2010;101(7):2405–11.

100. Bach Knudsen KE. Fiber and nonstarch polysaccharide content and variation in common crops used in broiler diets. Poult Sci. 2014;93(9):2380–93.

101. Maisonnier S, Gomez J, Carré B. Nutrient digestibility and intestinal viscosities in broiler chickens fed on wheat diets, as compared to maize diets with added guar gum. Br Poult Sci. 2001;42(1):102–10.

102. Khadem A, Lourenço M, Delezie E, Maertens L, Goderis A, Mombaerts R, Höfte M, Eeckhaut V, Van Immerseel F, Janssens GPJ. Does release of encapsulated nutrients have an important role in the efficacy of xylanase in broilers? Poult Sci. 2016;95(5):1066–76.

103. Bajaj P, Mahajan R. Cellulase and xylanase synergism in industrial biotechnology. Appl Microbiol Biotechnol. 2019;103(21–22):8711–24.

104. Song HT, Gao Y, Yang YM, Xiao WJ, Liu SH, Xia WC, Liu ZL, Yi L, Jiang ZB. Synergistic effect of cellulase and xylanase during hydrolysis of natural lignocellulosic substrates. Bioresour Technol. 2016;219:710–5.

105. Singh A, O'Neill HVM, Ghosh TK, Bedford MR, Haldar S. Effects of xylanase supplementation on performance, total volatile fatty acids and selected bacterial population in caeca, metabolic indices and peptide YY concentrations in serum of broiler chickens fed energy restricted maize-soybean based diets. Anim Feed Sci Technol. 2012;177(3–4):194–203.

106. Nusairat B, Wang JJ. The effect of a modified GH11 xylanase on live performance, gut health, and *Clostridium perfringens* excretion of broilers fed corn-soy diets. Front Vet Sci. 2021;8(June):678536.

107. Cowieson AJ, Bedford MR, Ravindran V. Interactions between xylanase and glucanase in maize-soy-based diets for broilers. Br Poult Sci. 2010;51(2):246–57.

108. Abelilla JJ, Stein HH. Degradation of dietary fiber in the stomach, small intestine, and large intestine of growing pigs fed corn-or wheat-based diets without or with microbial xylanase. J Anim Sci. 2019;97(1):338–52.

109. Ravn JL, Glitsø V, Pettersson D, Ducatelle R, Van Immerseel F, Pedersen NR. Combined endo-β-1,4-xylanase and α-L-arabinofuranosidase increases butyrate concentration during broiler cecal fermentation of maize glucurono-arabinoxylan. Anim Feed Sci Technol. 2018. p. 159–69.

110. Kiarie E, Romero LF, Ravindran V. Growth performance, nutrient utilization, and digesta characteristics in broiler chickens fed corn or wheat diets without or with supplemental xylanase. Poult Sci. 2014;93(5):1186–96.

111. Cowieson AJ. Factors that affect the nutritional value of maize for broilers. Anim Feed Sci Technol. 2005;119(3–4):293–305.

112. Wealleans AL, Walsh MC, Romero LF, Ravindran V. Comparative effects of two multi-enzyme combinations and a *Bacillus* probiotic on growth performance, digestibility of energy and nutrients, disappearance of non-starch polysaccharides, and gut microflora in broiler chickens. Poult Sci. 2017;96(12):4287–97.

113. Pedersen MB, Dalsgaard S, Knudsen KEB, Yu S, Lærke HN. Compositional profile and variation of Distillers Dried Grains with Solubles from various origins with focus on non-starch polysaccharides. Anim Feed Sci Technol. 2014;197:130–41.

114. Pecka-Kielb E, Zachwieja A, Mista D, Zawadzki W, Zielak-Steciwko A. Use of corn dried distillers grains (DDGS) in feeding of ruminants. In: Jacob-Lopes E, Zepka LQ, editors. Frontiers in bioenergy and biofuels. London: InTechOpen; 2017. p. 137–44.

115. Stefanello C, Vieira SL, Santiago GO, Kindlein L, Sorbara JOB, Cowieson AJ. Starch digestibility, energy utilization, and growth performance of broilers fed corn-soybean basal diets supplemented with enzymes. Poult Sci. 2015;94(10):2472–9.

116. Romero LF, Sands JS, Indrakumar SE, Plumstead PW, Dalsgaard S, Ravindran V. Contribution of protein, starch, and fat to the apparent ileal digestible energy of corn- and wheat-based broiler diets in response to exogenous xylanase and amylase without or with protease. Poult Sci. 2014;93(10):2501–13.

7

117. Giacobbo FCN, Eyng C, Nunes R V., de Souza C, Teixeira L V., Pilla R, Suchodolski JS, Bortoluzzi C. Influence of enzyme supplementation in the diets of broiler chickens formulated with different corn hybrids dried at various temperatures. Animals. 2021;11(3):643.

118. Singh AK, Mishra B, Bedford MR, Jha R. Effects of supplemental xylanase and xylooligosaccharides on production performance and gut health variables of broiler chickens. J Anim Sci Biotechnol. 2021;12:98.

119. Rychen G, Aquilina G, Azimonti G, Bampidis V, Bastos M de L, Bories G, Chesson A, Cocconcelli PS, Flachowsky G, Gropp J, Kolar B, Kouba M, López-Alonso M, López Puente S, Mantovani A, Mayo B, Ramos F, Saarela M, Villa RE, Wallace RJ, Wester P, Brantom P, Dierick NA, Anguita M. Safety and efficacy of ECONASE ® XT (endo-1,4-β-xylanase) as a feed additive for pigs for fattening. EFSA J. 2018;16(3):4–10.

120. Van Gool MP, Toth K, Schols HA, Szakacs G, Gruppen H. Performance of hemicellulolytic enzymes in culture supernatants from a wide range of fungi on insoluble wheat straw and corn fiber fractions. Bioresour Technol. 2012;114:523–8.

121. Martens BMJ, Gerrits WJJ, Bruininx EMAM, Schols HA. Amylopectin structure and crystallinity explains variation in digestion kinetics of starches across botanic sources in an *in vitro* pig model. J Anim Sci Biotechnol. 2018;9:91.

122. van Kempen T, Pujol S, Tibble S, Balfagon A. *In vitro* characterization of starch digestion and its implications for pigs. In: Wiseman J, Varley MA, McOrist S, Kemp B, editors. Paradigms in pig science. Nottingham: Nottingham University Press; 2007. p. 515–25.

123. Le DM, Fojan P, Azem E, Pettersson D, Pedersen NR. Visualization of the anticaging effect of Ronozyme WX xylanase on wheat substrates. Cereal Chem. 2013;90(5):439–44.

124. O'Neill HVM, Smith JA, Bedford MR. Multicarbohydrase enzymes for non-ruminants. Asian-Australasian J Anim Sci. 2014;27(2):290–301.

125. Baker JT, Duarte ME, Holanda DM, Kim SW. Friend or foe? Impacts of dietary xylans, xylooligosaccharides, and xylanases on intestinal health and growth performance of monogastric animals. Animals. 2021;11(3):609.

126. Bhattarai RR, Dhital S, Mense A, Gidley MJ, Shi YC. Intact cellular structure in cereal endosperm limits starch digestion *in vitro*. Food Hydrocoll. 2018;81:139–48.

127. Martens BMJ, Flécher T, De Vries S, Schols HA, Bruininx EMAM, Gerrits WJJ. Starch digestion kinetics and mechanisms of hydrolysing enzymes in growing pigs fed processed and native cereal-based diets. Br J Nutr. 2019;121(10):1124–36.

128. Svihus B. The gizzard: Function, influence of diet structure and effects on nutrient availability. Worlds Poult Sci J. 2011;67(2):207–23.

129. Amerah AM, Lentle RG, Ravindran V. Influence of feed form on gizzard morphology and particle size spectra of duodenal digesta in broiler chickens. J Poult Sci. 2007;44(2):175–81.

130. Food and Agriculture Organization of the United Nations. Food outlook – Biannual report on global food markets [Internet]. Food Outlook. Rome: FAO; 2021 [cited 2022 Feb 10]. Available from: https://www.fao.org/documents/card/en/c/cb4479en

131. Mottet A, Tempio G. Global poultry production: Current state and future outlook and challenges. Worlds Poult Sci J. 2017;73(2):245–56.

132. Giller KE, Delaune T, Silva JV, Descheemaeker K, van de Ven G, Schut AGT, van Wijk M, Hammond J, Hochman Z, Taulya G, Chikowo R, Narayanan S, Kishore A, Bresciani F, Teixeira HM, Andersson JA, van Ittersum MK. The future of farming: Who will produce our food? Food Secur. 2021;13(5):1073–99.

133. Ravindran V, Abdollahi MR. Nutrition and digestive physiology of the broiler chick: State of the art and outlook. Animals. 2021;11(10):2795.

134. Chuang WY, Lin LJ, Shih H Der, Shy YM, Chang SC, Lee TT. The potential utilization of high-fiber agricultural by-products as monogastric animal feed and feed additives: A review. Animals. 2021;11(7):2098.

135. Babatunde OO, Park CS, Adeola O. Nutritional potentials of atypical feed ingredients for broiler chickens and pigs. Animals. 2021;11(5):1196.

136. Saettone V, Biasato I, Radice E, Schiavone A, Bergero D, Meineri G. State-of-the-art of the nutritional alternatives to the use of antibiotics in humans and monogastric animals. Animals. 2020;10(12):2199.

137. Klasing KC. Poultry nutrition: A comparative approach. J Appl Poult Res. 2005;14(2):426–36.

138. Swart D, Hayes JP. Fermentative digestion in the ostrich (*Struthio camelus var. domesticus*), a large avian species that utilizes cellulose. S Afr J Anim Sci. 1993;23(5–6):127–35.

139. Godoy-Vitorino F, Ley RE, Gao Z, Pei Z, Ortiz-Zuazaga H, Pericchi LR, Garcia-Amado MA, Michelangeli F, Blaser MJ, Gordon JI, Domínguez-Bello MG. Bacterial community in the crop of the hoatzin, a neotropical folivorous flying bird. Appl Environ Microbiol. 2008;74(19):5905–12.

140. Grajal A. Structure and function of the digestive tract of the hoatzin (*Opisthocomus hoazin*): A folivorous bird with foregut fermentation. Auk. 1995;112(1):20–8.

141. Long C, Rösch C, de Vries S, Schols H, Venema K. Cellulase and alkaline treatment improve intestinal microbial degradation of recalcitrant fibers of rapeseed meal in pigs. J Agric Food Chem. 2020;68(39):11011–25.

142. Bedford MR. Future prospects for non-starch polysaccharide degrading enzymes development in monogastric nutrition. In: González-Ortiz G, Bedford MR, Knudsen KEB, Courtin CM, Classen HL, editors. The value of fibre. Wageningen: Wageningen Academic Publishers; 2019. p. 372–83.

143. Van Gool MP. Targeted discovery and functional characterisation of complex-xylan degrading enzymes (Doctoral Thesis). Wageningen University; 2012.

144. Van Gool MP, van Muiswinkel GCJ, Hinz SWA, Schols HA, Sinitsyn AP, Gruppen H. Two novel GH11 endo-xylanases from *Myceliophthora thermophila* C1 act differently toward soluble and insoluble xylans. Enzyme Microb Technol. 2013;53(1):25–32.

145. Hoffmam ZB, Zanphorlin LM, Cota J, Diogo JA, Almeida GB, Damásio ARL, Squina F, Murakami MT, Ruller R. Xylan-specific carbohydrate-binding module belonging to family 6 enhances the catalytic performance of a GH11 endo-xylanase. N Biotechnol. 2016;33(4):467–72.

7

Summary

The aim of this thesis was to elucidate the impact of dietary non-starch polysaccharide (NSP)-active enzymes on NSP fate and fermentability in the broiler gastrointestinal tract (GIT) at a molecular level.

In Chapter 1, a bibliographic overview of main cereal grain components and their implications for digestion and hindgut fermentation in broilers is introduced. In particular, cereal grain NSP such as arabinoxylan (AX) can increase viscosity, thereby hindering nutrient digestion in the small intestine. In spite of their negative influence in the small intestine, NSP can promote the growth and metabolism of beneficial microbiota in the hindgut. NSP-active enzymes are supplemented to the feed in order to offset the negative impact of NSP and to promote NSP utilization in the hindgut, with the utter aim of their supplementation to improve animal performance. Still, the action of NSP-active enzymes (e.g., xylanase, glucanase) in the gastrointestinal tract and their ability to form oligosaccharides with prebiotic potential has not been fully understood.

In Chapter 2, the impact of the combined xylanase and glucanase supplementation in wheat and maize diets on NSP fermentation, nutrient digestion and broiler growth is described. It is shown that for wheat diets, enzyme action improved starch and protein digestibility. More importantly, formation of arabinoxylo-oligosaccharides (AXOS) by dietary xylanase was observed in the ileum. This coincided with improved AX utilization and pronounced short chain fatty acids (SCFAs) formation in the hindgut. Ultimately, the enzyme-mediated improvements in nutrient digestion and AX fermentation for wheat diets, coincided with improved animal growth. The more complex NSP structure and high nutrient digestibility observed for maize diets compared to the wheat diets, possibly, resulted in less pronounced effect of enzyme addition in the maize diet.

In Chapter 3, the impact of cereal type and enzyme supplementation on bacterial ecology and fermentation is discussed. The comparison of microbiota composition in the ceca of broilers fed wheat or maize diets (with and without xylanase/glucanase supplementation) demonstrated that cereal type had a tremendous influence on cecal microflora. In this respect, the higher AX fermentability found for the wheat diets coincided with the proliferation of NSP-fermenting bacteria, mainly belonging to *Blautia*, *Faecalibacterium*, *Subdoligranulum* and uncultured Lachnospiraceae genera. Enzyme supplementation in the wheat diet was shown to modulate bacterial communities of close phylogenetic proximity, and was most likely attributed to pronounced fermentation upon AXOS release, as documented in Chapter 2.

In Chapter 4, a novel analytical strategy to characterize AXOS is described. Here, AX was digested by endo-xylanases, and the resulting AXOS mixtures were subjected to reduction by $NaBH_4$, and then analyzed by HILIC-MS^n. AXOS debranching by well characterized arabinofuranosidases was applied to assist the elucidation of oligosaccharide substitution patterns. Overall, (reduced) structural isomers having the same degree of polymerization (DP) were successfully

separated by HILIC and presented distinct MS^2 and MS^3 fragmentation patterns. Consequently, individual AXOS could be discerned based on both their elution and fragmentation behavior. This approach paved the way for the straightforward characterization of AXOS in complex (digesta) matrices, as described in Chapter 5.

In Chapter 5, the formation of AXOS by endo-xylanase *in vivo* along the gastrointestinal tract is followed in detail, for broilers fed wheat diet (i.e., from Chapter 2). Here, soluble AX and AXOS fractions were extracted from digesta by aqueous extraction, and subsequently isolated from other soluble carbohydrates by solid phase extraction (SPE). It was shown that AX degradation to AXOS began in the gizzard and proceeded in the small intestine, where endo-xylanase degraded both soluble and insoluble AX. Analysis of ileal digesta and excreta by using the strategy developed in Chapter 4 revealed that AXOS formed *in vivo* by endo-xylanase presented a low degree of branching. Consequently, it was concluded that higher amounts of more easily fermentable substrates (XOS/AXOS) were present and utilized in the hindgut upon xylanase supplementation, further confirming the beneficial impact of enzyme supplementation for microbial fermentation and animal growth (Chapter 2, 3).

In Chapter 6, the fate of insoluble fibers (NSP & lignin) that are the main fiber fraction in feed along the broiler GIT is described in more detail. In particular, it was observed that a lignin-rich fiber fraction accumulated in the gizzard, while the main (insoluble) AX-rich fraction transited to the ileum. NSP extraction by alkali released approximately 30-40% of total insoluble AX. Xylanase/glucanase supplementation did not improve AX extractability by alkali, suggesting that apart from releasing AXOS (Chapter 5), enzyme action had limited additional effect on the structure of insoluble NSP.

In Chapter 7, the main findings of this thesis are being discussed. Firstly, the progress in oligosaccharide analysis in digesta currently achieved throughout Chapters 2, 4, 5, and its relevance for future research, is highlighted. Next, the observations from Chapters 2, 3, 5, combined with additional data from *in vitro* experiments, unambiguously demonstrated the significance of AXOS *in vivo* formation by endo-xylanase for hindgut fermentation and animal growth. Lastly, the observations from Chapter 2, 5, 6 and those from *in vitro* experiments (i.e., additional data) were combined to address the recalcitrance of maize NSP observed *in vivo*. Finally, the relevance of nutrient de-encapsulation by dietary enzymes for improved digestion in the small intestine is being discussed as well as future implications of dietary enzyme supplementation.

Acknowledgements

I would like to extent my thanks to Xinxin, Adiphol and Ronald from Westerdijk Fungal Biodiversity Institute. I really enjoyed our collaboration that gave me the opportunity to learn so many new things about my beloved endo-xylanases.

Now a word for my wonderful paranymphs! Peicheng, you do appear a lot in my acknowledgements; as a lab mate, co-author, paranymph, but above all, as a true friend. I remember you were quite shy in the beginning, but we managed to build a great connection, bit by bit. Thank you for all the nice discussions (scientific & other) and for your kindness!

Katharina, I could never have imagined after briefly meeting you in Waterhouse back in 2014, that you would become such a dear friend to me. Thank you for all the endless discussions in the lab and funny times outside of it. I am a huge fan of your art (labels of vials, meeting logos) and music taste. I would also like to extend my thanks to Xi and Lukas for our awesome dinners together; serving the deer was definitely the highlight!

Fleur, Zixuan, Amber and Mart, thank you for your hard work and valuable contribution to my project. It has been a pleasure and big responsibility for me to be your thesis supervisor. I hope you learned as much from me as I did from you.

I also want to thank all FCH technicians. First and foremost, Margaret; thank you so much for your continuous help, especially with the chromatography systems. I really learned a lot with you! Peter, it was an honor to be the Dumas sous-chef with you. Thank you for helping with GC instruments and EFB practicals, and I really appreciate the calmness by which you dealt with my clumsiness. Edwin, thank you so much for the MS discussions. Rene, thank you for helping with several instruments and for giving me a reason to practice my Italian ;). Mark, thank you very much for the insightful introduction for UPLC and discussions for SPE. Wouter, it was a pleasure working with you and I really appreciate your constant engagement.

Jolanda, thank you so much for being the beating heart of FCH. I truly appreciate your help with the administrative tasks and I want you to know that I am really doing my best to fill MyProjects on time!!

Jean-Paul, thank you very much for our discussions and support, which definitely improved my morale and provided me with valuable scientific insight. I hope I was also able to motivate you to exercise a bit more after your injury.

Yuxi, Claire, Moheb, Maud, Dazhi, Gijs V, Lorenz, Romy and Cas, thank you for being such amazing office mates! I enjoyed our scientific talks and chit chat the same. To the ones remaining, good luck with Lorenz!

Margaret, Katharina, Peicheng, Dazhi, Krishna, Pim and Dounia thank you for being such great lab mates!! Suzanne, Bianca, Matthias and Hugo, thank you for showing me the ropes in the lab and for our nice talks.

friendship and laughs in Utrecht. Panagiotis, I am grateful for the amazing guitar lessons, that helped me to blow off some steam and be more creative, especially during COVID-19.

Σταθάρα, Παλιέ, Κωνσταντινό, Μάικ, Στέις! Μου λείπετε πάρα πολύ αδερφάκια μου. Κάθε φορά που βρισκόμασταν έπερνα δύναμη για τους επόμενους μήνες μακριά από την Ελλάδα. Παρόλο που σας πήρε κάποια χρόνια να καταλάβετε οτι κάνω διδακτορικό και ακόμα δεν με έχετε επισκεφτεί, ποτέ δεν αμφέβαλα για τη φιλία μας. Σας βλέπω που κάνετε παιδιά και μεγαλώνετε και σας χαίρομαι. Ελπίζω κάποια στιγμή στο όχι και τόσο μακρινό μέλλον να τα λέμε πιο συχνά. Άλκη φιλαράκο, σ'ευχαριστώ πολύ για το φανταστικό εξώφυλλο και χαίρομαι κάθε φορά που τα λέμε.

Αυτή η διατριβή είναι αφιερωμένη στην οικογένειά μου, την οποία αγαπάω όσο τίποτα στον κόσμο. Μαμά, μπαμπά σας ευχαριστώ για όλα όσα μου έχετε προσφέρει και συνεχίζετε να μου προσφέρετε. Δε θα τα κατάφερνα χωρίς εσάς. Ίσως να μην σας το δείχνω όσο θα έπρεπε, αλλά μου λείπετε τρομερά. Θεία, σ'ευχαριστώ για τη θετική ενέργεια που μου έστελνες συνέχεια. Τη χρειάστηκα πολύ περισσότερο απ' όσο είχα φανταστεί. Γιαγιά, δε μπόρεσα να σε αποχαιρετήσω όπως θα 'θελα, όμως ξέρω οτι με βλέπεις από ψηλά κάθε μέρα όπως οδηγάω.

Finalmente mi koalcito hermoso, mi Lili. La verdad es que no existen las palabras para describir todo lo que me has dado y todo lo que siento por ti. Asi que ni voy a intentar hacerlo en estas paginas. Lo único que puedo hacer es darte las gracias, gracias y mil gracias por aguantarme. Sólo tú sabes cómo lo lograste. Aunque no sepa lo que nos depara el futuro, estoy feliz de que lo vaya a descubrir contigo. Te amo.

Dimitris Kouzounis

Δημήτρης

About the author

Curriculum vitae

Dimitrios (Dimitris) Kouzounis was born on November 28th, 1990 in Thessaloniki, Greece. In 2008, he started his bachelor's degree in Agriculture with specialization in Food Science and Technology at the Aristotle University of Thessaloniki. During his study, he was an Erasmus exchange student at Universidad Politecnica de Valencia (2012) and Wageningen University (2014). His bachelor study was completed with a BSc thesis on the replacement of animal fat by oleogels in sausages and an internship at E.G. Passias S.A.. In 2014, he started his master's degree in Food Technology, with specialization in Ingredient Functionality at Wageningen University. He performed his MSc thesis at the Laboratory of Food Chemistry on the effect of Maillard induced glycation and aggregation on *in vitro* protein digestion. In 2016, he obtained his master's degree, after carrying out his internship at Danone Nutricia Research, Utrecht, where he worked on the functionality of dairy proteins. In 2017, he started working as a researcher at the Laboratory of Food Chemistry and continued as a PhD candidate on the same project, under the supervision of prof. dr. Henk A. Schols and dr. ir. Mirjam A. Kabel. This project was a collaboration with Huvepharma NV. The results of his PhD research are presented in this thesis. Dimitris is currently working as a postdoctoral researcher at the Laboratory of Food Chemistry, Wageningen University and Research.

Contact: dimitris_kouzounis@hotmail.com

List of publications

Kouzounis D, Jonathan MC, Soares N, Kabel MA, Schols HA. *In vivo* formation of arabinoxylo-oligosaccharides by dietary endo-xylanase alters arabinoxylan utilization in broilers. Carbohydr Polym. 2022;291:119527.

Kouzounis D, Kers JG, Soares N, Smidt H, Kabel MA, Schols HA. Cereal type and combined xylanase/glucanase supplementation influence the cecal microbiota composition in broilers. J Anim Sci Biotechnol. 2022;13(1):51.

Kouzounis D, Sun P, Bakx EJ, Schols HA, Kabel MA. Strategy to identify reduced arabinoxylo-oligosaccharides by HILIC-MS^n. Carbohydr Polym. 2022;289:119415.

Kouzounis D, Hageman JA, Soares N, Michiels J, Schols HA. Impact of xylanase and glucanase on oligosaccharide formation, carbohydrate fermentation patterns, and nutrient utilization in the gastrointestinal tract of broilers. Animals. 2021;11(5):1285.

Kouzounis D, Lazaridou A, Katsanidis E. Partial replacement of animal fat by oleogels structured with monoglycerides and phytosterols in frankfurter sausages. Meat Sci. 2017;130:38–46.

Li X, **Kouzounis D**, Kabel MA, de Vries RP. GH10 and GH11 endoxylanases in *Penicillium subrubescens* : Comparative characterization and synergy with GH51, GH54, GH62 α-L-arabinofuranosidases from the same fungus. N Biotechnol. 2022;70:84–92.

Li X, **Kouzounis D,** Kabel MA, de Vries RP, Dilokpimol A. Glycoside Hydrolase family 30 harbors fungal subfamilies with distinct polysaccharide specificities. N Biotechnol. 2022;67:32–41.

Sun P, Laurent CVFP, Scheiblbrandner S, Frommhagen M, **Kouzounis D**, Sanders MG, van Berkel, WJH, Ludwig R, Kabel MA. Configuration of active site segments in lytic polysaccharide monooxygenases steers oxidative xyloglucan degradation. Biotechnol Biofuels. 2020;13(1):1–19.

Overview of completed training activities

Discipline specific activities

Courses

Summer School Glycosciences[a]	VLAG / GBB, Wageningen, 2018
Advanced Food Analysis[a]	VLAG, Wageningen, 2019
Masterclass Applied Biocatalysis	VLAG, Wageningen, 2019
Chemometrics	VLAG, Wageningen, 2019
Online Lectures	VLAG, Online, 2020
XI Hands-on Course in Ultrafast Sample Treatment for Proteomics	BIOSCOPE research group, Online, 2020

Conferences and seminars

Digestion Kinetics in Pigs	WIAS, Wageningen, 2019
Nutrient Digestion and Feed Intake in Pigs	WIAS, Wageningen, 2019
5th IMEKO FOODS Metrology For Sustainable Food Production	IMEKO, Online, 2020
7th International Polysaccharide Conference[b]	EPNOE, Nantes, 2021
World Poultry Congress Seminars[a]	WPSA France Online, 2021

General courses

Introduction to R	VLAG, Wageningen, 2019
Applied Statistics	VLAG, Wageningen, 2019
Mixed Linear Models	PE&RC, Online, 2020
Rmarkdown	VLAG, Wageningen, 2020
Scientific Writing	WGS, Online, 2020
Career Perspectives	VLAG, Online, 2020
Philosophy and Ethics of Food Science and Technology	VLAG, Online, 2020

Optional

Preparation of research proposal	FCH, Wageningen, 2018
PhD study tour to Italy/Austria[a,b]	FCH, 2018
Weekly group meetings	FCH, 2018-2022
PhD lunch presentations	FCH, 2018-2022
Last stretch of the PhD programme	WGS, Wageningen, 2020
PhD study tour to Netherlands[a,b]	FCH, 2022

[a] Poster presentation. [b] Oral presentation.
Abbreviations: VLAG, Graduate School for Advanced Studies in Food Technology, Agrobiotechnology, Nutrition and Health Science; IMEKO, International Measurement Confederation; WIAS, Wageningen Institute of Animal Sciences; EPNOE, European Polysaccharide network of Excellence; WPSA, World's Poultry Science Association; PE&RC, Graduate School for Production Ecology and Resource Conservation; WGS; Wageningen Graduate Schools, FCH; Laboratory of Food Chemistry, Wageningen University and Research.